2008

Reconstruction of Peace River Flood Frequency and Magnitude for the Past ~600 Years from Oxbow Lake Sediments, Peace-Athabasca Delta, Canada

Suzanne Jarvis
Wilfrid Laurier University

Your file Votre référence
ISBN: 978-0-494-46144-0
Our file Notre référence
ISBN: 978-0-494-46144-0

Reconstruction of Peace River Flood Frequency and Magnitude for the Past ~ 600 Years from Oxbow Lake Sediments, Peace-Athabasca Delta, Canada

By

Suzanne Jarvis

Honours Bachelor of Science, University of Winnipeg, 2004

THESIS
Submitted to the Department of Geography and Environmental Studies
in partial fulfillment of the requirements
for the Master of Science degree
Wilfrid Laurier University
Waterloo, Ontario, Canada
2008

ABSTRACT

Ice-jam flooding in the Peace-Athabasca Delta (PAD) is an important hydrological process for the replenishment of shallow perched basins that support a highly productive northern ecosystem. The PAD is also used by nearby First Nations communities for traditional lifestyle occupations such as hunting and trapping. Previous research on laminated sediments collected from two oxbow lakes periodically connected to major Peace River distributaries has resulted in a 300-year record of flood frequency. In an effort to extend this record and broaden the understanding of the relationships among climate variability, Peace River hydrology, and delta hydroecology, a series of vibracores and gravity cores were collected at sites proximal, intermediate, and distal to the inlet of each oxbow lake (PAD 54 and PAD 15).

Remarkably consistent patterns of strongly varying flood frequency and magnitude are reconstructed for the past ~600 years using stratigraphic observations and the development of a facies model for PAD 54 and PAD 15, magnetic susceptibility measurements from two cores collected from PAD 15 (proximal and distal sites), and organic carbon and nitrogen elemental and stable isotope records from one sediment core from PAD 15 (distal site). The sediment chronologies, constrained using cesium-137 (^{137}Cs) and radiocarbon dating (^{14}C), suggest that Peace River flood frequency and magnitude were substantially greater during late medieval times (AD ~1418-1595) when compared to the intervals AD ~1595-1720, AD ~1720-1900, and AD ~1900-2005. This is largely indicated by relatively coarse-grained sediments in the lower portions of vibracores, and highly variable and overall higher magnetic susceptibility values and C/N ratios.

The distinct shift from high flood frequency and magnitude at the end of medieval times (AD ~1595) to extended periods of relatively low flood frequency and magnitude during AD ~1595 to ~1720 is indicated by an abrupt shift from generally coarse-grained sediments (fine to coarse sand and pebbles) to generally massive and/or thick beds of fine-grained sediments (light grey clay and silt), and magnetic susceptibility values and C/N ratios with relatively low variability. During AD ~1720 to ~1900, the nature of the sediments (alternating light and dark grey clay and silt laminations) suggests oscillating energy conditions. This is consistent with magnetic susceptibility and C/N records during this time interval, which exhibit somewhat greater frequency variability than during AD ~1595 to ~1720. Sediments deposited since AD ~1900 also consist of alternating light and dark grey clay and silt laminations. However, the C/N and $\delta^{13}C_{org}$ records clearly indicate declining values over this interval, suggesting a decline in flood frequency.

The distinct shift to reduced flood frequency and magnitude at the end of medieval times is also reflected by a substantial reduction in river floodwater influence and a substantial increase in evaporation inferred from the isotopic record ($\delta^{18}O$) of two basins (PAD 5 and PAD 12) in the northern Peace sector of the PAD. The diatom records from sites in low-lying areas of the Peace (PAD 9) and Athabasca (PAD 31) sectors reflect different hydrological conditions over similar time periods. During medieval times (AD ~1418 to ~1595), when Peace River flood frequency and magnitude were relatively high, diatom assemblages in these low-lying sites indicate these basins were hydrologically closed. During the interval AD ~1595 to ~1720, the diatom assemblages indicate that these sites were generally open-drainage basins, likely because of relatively high water

levels in Lake Athabasca, whose outflow also flooded into PAD 12. During AD ~1900 to 2005, the diatom records indicate that these two lakes largely returned to closed-drainage basin conditions.

Earlier and/or more rapid snowmelt in the eastern Rocky Mountains during medieval times may have produced conditions conducive to more frequent and more severe spring ice-jam events along the Peace River during AD ~1418 to ~1595. Expansion of glaciers and a late and/or protracted snowmelt under cooler conditions of the Little Ice Age (LIA) may have created conditions less conducive to ice-jams along the Peace River, particularly during AD ~1595 to ~1720. Sustained snowmelt run-off throughout the summer months may have contributed to relatively high water levels of Lake Athabasca and frequent flooding of low-lying lake basins (PAD 9 and PAD 31) during this interval. Although during AD ~1900 to 2005, climatic conditions in the Columbia Icefield region appear to be returning to those similar to medieval times, Peace River flood frequency has continued to decline. This is likely due to declining alpine snowpack depths and receding alpine glaciers, which have created conditions that are not favourable for ice-jam development. If these conditions persist into the future, Peace River flood frequency will likely continue to decline.

ACKNOWLEDGEMENTS

I sincerely thank Brent Wolfe for a great opportunity to take part in this research project. His guidance and dedication to this research has made it a valuable experience, both personally and academically. I would also like to thank John Johnston, whose knowledge, experience, and enthusiasm for my project carried me in times when I was less than enthusiastic. I would also like to extend my thanks to Tom Edwards and Roland Hall for their advice, ideas, and encouragement.

Assistance during field work provided by Brent Wolfe, John Johnston, Tom Edwards, Roland Hall, Johan Wiklund, and Mike Morin of Wood Buffalo Helicopters was essential. Vibracoring equipment for field work was used courtesy of Dr. Tim Fisher, from the University of Toledo. Magnetic susceptibility measurements were taken using equipment in the Paleoecology Laboratory at the University of Carleton, courtesy of Dr. Mike Pisaric. Thank-you to Bill Mark and the University of Waterloo Environmental Isotope Laboratory for carbon and nitrogen analyses.

Financial assistance was provided by various agencies and organizations including the NSERC Northern Research Chair and Post Graduate Scholarship Programs, the NSERC Collaborative Research and Development (CRD) Grant, the Royal Canadian Geographical Society, the Canadian Northern Studies Trust, the Association of Canadian Universities for Northern Research, the Northern Scientific Training Program, the Premier's Research Excellence Award, the Canada Foundation for Innovation, BC Hydro, and Wood Buffalo National Park.

I would like to thank my family for their support. A special thank-you to Steve St. Onge from the bottom of my heart. There is no way to express how important your encouragement and support have been to me throughout this process.

I would like to thank Bronwyn Brock and Paige Harms for their assistance with laboratory work, but more importantly for making me laugh when things didn't seem so funny.

Several other friends have helped in various capacities along the way including Cherie Mongeon, Scott Brown, Dianne Pawlowski, and Michelle Zurbrigg. A special thank-you goes to Danielle Solondz for Wilf's monday night pitchers and pizza, and of course, wing sauce.

TABLE OF CONTENTS

LIST OF TABLES

LIST OF FIGURES

INTRODUCTION

Role of River Hydrology in Northern Ecosystems

Hydrological conditions are the primary controller of ecosystem-level processes and play a dominant role in northern regions (Prowse and Culp 2003). Many of the north-flowing rivers in North America have origins in the temperate latitudes much farther south, therefore conditions in the headwaters can greatly affect the hydrology and ecology of Arctic regions (Schindler and Smol 2006). All of the major rivers in the western prairie provinces originate in the Rockies, with deep winter snowpacks and melting glaciers maintaining river and groundwater supplies (Schindler and Donahue 2006). Overall, summer flows in major rivers of the western prairie provinces have been declining in the late 20th century, by as much as 20-85%, when compared to the early 20th century (Schindler and Donahue 2006). In particular, summer river flows in tributaries of the Mackenzie River (Athabasca, Peace, Oldman and Slave rivers) have declined by 20% to 60% since the early- to mid-20th century (Schindler and Smol 2006, Schindler and Donahue 2006). Declining annual streamflow trends over the 20th century are most apparent in rivers draining into the Arctic Ocean and Hudson Bay (Rood et al. 2005). In addition, hydrometric data from 1970 to 2000 show an earlier onset of the spring freshet in the Mackenzie River basin, which has been mainly attributed to the observed warmer temperatures of the late winter and spring periods (Aziz and Burn 2006).

Increasing emphasis in water science research is being placed on the linkages between hydrology and ecosystem structure and function, and ecological vulnerability to hydrological changes (Hannah et al. 2007). Declines in stream flow will affect riverine

and riparian ecosystems in a variety of ways. Changing patterns of erosion, transport, and deposition of alluvial sediments will alter channel patterns and floodplain characteristics, and subsequently wildlife and vegetation habitat (Rood et al. 2005). Changes in flow regime could also alter the structure of aquatic and riparian communities by altering ice break-up intensities (Rouse et al. 1997). For north-flowing rivers, thinner ice covers, smaller temperature gradients between southern and northern portions of the basins, and reduced spring flood peaks could lead to reduced ice-jamming. A decrease in disturbance caused by fewer ice-jams could potentially decrease the richness of biological communities. In addition, because of a deeper active layer, a longer unfrozen period, and increased active layer storage capacity, peak flows associated with snowmelt and rainfall events would be similar or lower than at present (Rouse et al. 1997). The longer ice-free season in lakes could lead to a higher amount of stress on cold-water organisms because of lower oxygen concentrations in the water column (Rouse et al. 1997). Likely the most significant effect from warming would be the thawing of ground ice, resulting in massive slumping, and affecting drainage patterns, sediment loads in rivers and lakes, and subsequently aquatic ecosystems (Rouse et al. 1997). With increasing demands on water resources and concerns regarding climate change in northern regions, a better understanding of the effects of climate variability on changes in hydrological processes and northern ecosystems is needed (Déry and Wood 2005).

Background of the Peace-Athabasca Delta

The Peace-Athabasca Delta (PAD), located in northern Alberta, is one of the largest freshwater inland deltas in the world (Figure 1, PAD-TS 1996). It was designated a

Wetland of International Importance by the Ramsar Convention in 1982, and a United Nations Educational, Scientific, and Cultural Organization (UNESCO) World Heritage Site in 1983. Approximately 80% of the delta lies within the boundaries of Wood Buffalo National Park and contains over 1,200 km^2 of sedge meadow, one of the largest undisturbed grasslands in North America (Prowse and Lalonde 1996). Several hundred perched basins provide habitat for a variety of flora and are critical in supporting migratory birds, wood bison, and muskrat populations (PAD-TS 1996, Timoney et al. 1997). The delta is located at the convergence of the four main North American flyways (Pacific, Central, Mississippi, and Atlantic) and is particularly important for duck populations when there is drought on the prairies (PAD-PG 1973, Prowse and Lalonde 1996). These birds are of international significance because they follow the flyways to many points in Canada, the United States, Mexico, and some parts of Central and South America (PAD-PG 1973). Open delta areas and perched basins are important for bison herds as sedge meadows and reed grasses compose 70% of bison annual diet and 100% of their winter diet (Carbyn et al. 1993). Several of the channels provide a means of transportation for local residents and many lake basins support muskrat populations that are of particular importance to local First Nation communities for traditional hunting and trapping (PAD-PG 1973).

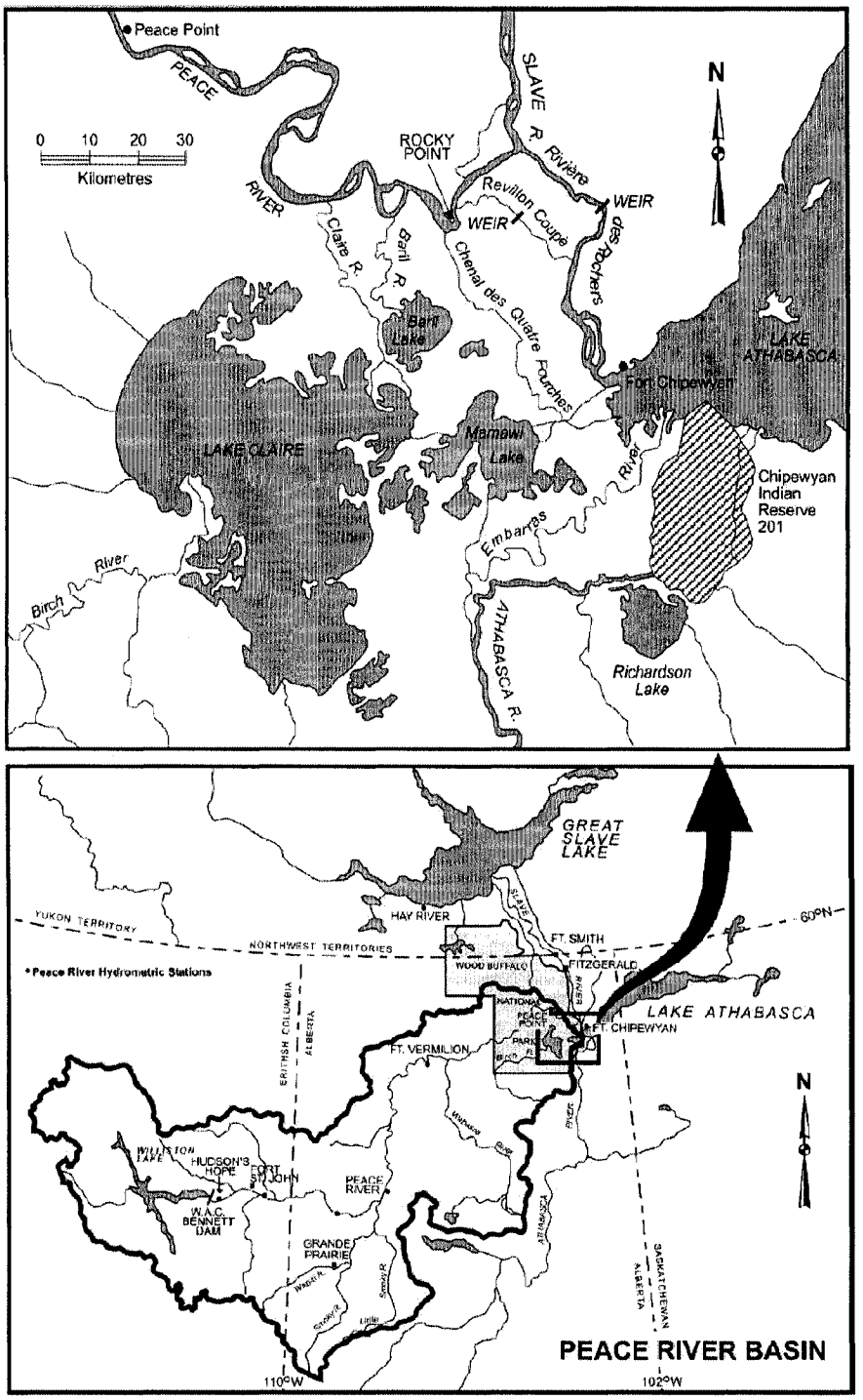

Figure 1: The PAD is located in northeastern Alberta. The Peace River drainage basin is outlined, Wood Buffalo National Park is shaded, and the PAD is outlined with a box and expanded above (from Leconte et al. 2006, p. 4218).

Frequent river flooding is an important hydrological process for the replenishment of shallow perched basins in the PAD. In the absence of significant ice-jam flooding, water in the PAD normally drains northwards to the Peace River, and eventually into Great Slave Lake via the Slave River. When significant ice-jam flooding occurs along the Peace River, river stages may become elevated relative to that of Lake Athabasca, causing the three main tributaries of the Peace River (Chenal des Quatre Fourches, the Revillon Coupé, and the Rivière des Rochers, Figure 2) to reverse flow and act as distributaries. Under these conditions water flows southward, and may inundate significant portions of the PAD as last occurred in 1996 and 1997 (Prowse and Conly 1998). Demuth et al. (1996) identified three likely ice-jam lodgement sites along the lower Peace River and the PAD, including 1) near the confluence of the Peace and Slave rivers at the mouth of Rivière des Rochers 2) Rocky Point, near the confluence of the Peace River and Chenal des Quatre Fourches, and 3) at the upstream end of Moose Island (Figure 2).

The importance of ice-jam flooding to riverine ecology in northern environments was generally not a focus of many studies until the 1980s and 1990s (Prowse and Culp 2003). Prowse and Lalonde (1996) published one of the first studies highlighting the importance of Peace River ice-jam events to the flooding of perched basins, particularly in the northern sector of the PAD. A historically high open-water flood in 1990 failed to replenish many of the perched basins. Following this event, a historical analysis of hydrometric records revealed that the major peak-water levels had been produced at the time of ice break-up, which was closely related to the downstream tributary runoff rather than waters originating in the headwater region above the point of Peace River regulation.

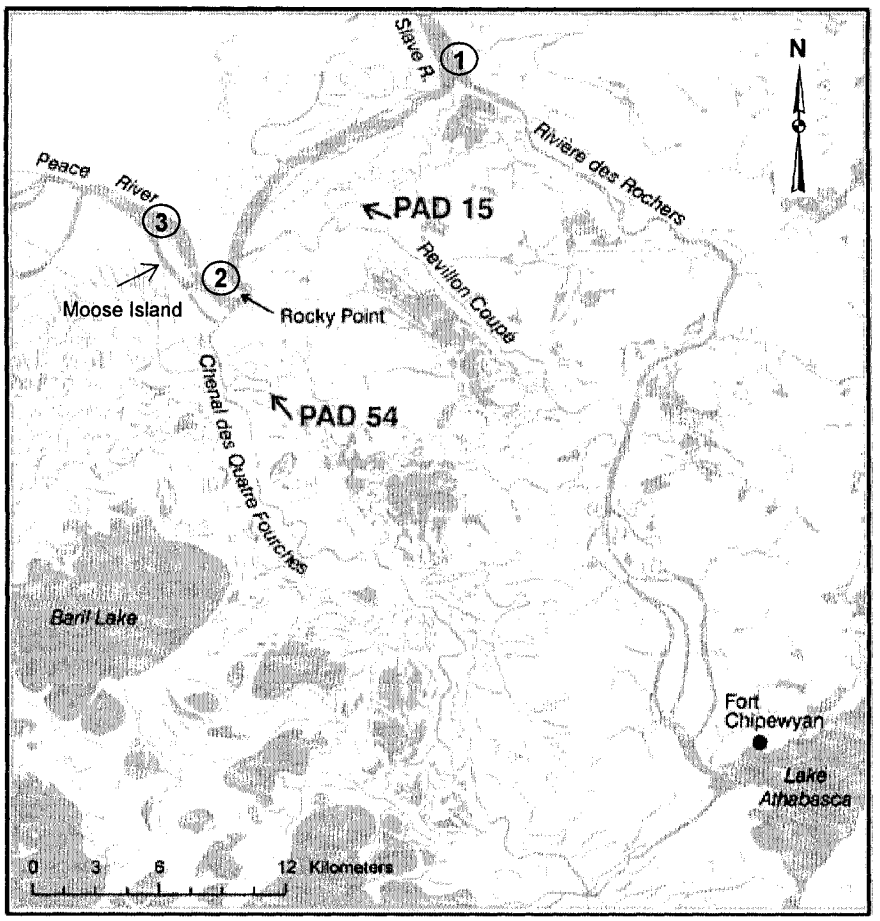

Figure 2: A map of the northeastern portion of the PAD showing the three channels that normally flow from Lake Athabasca to the Peace River and periodically act as distributaries of the Peace River during ice-jam events. Three locations where ice-jams are likely to occur are noted (1-3). The oxbow lakes labelled PAD 54 and PAD 15 are the focus of this thesis.

However, the development of delta management strategies has been hampered by poor knowledge of the hydro-ecological processes that control biodiversity in the delta and how they relate to the ice regime (Beltaos 2003).

In the last 35 years, the PAD has been at the centre of controversy, in large part due to the construction and operation of the WAC Bennett Dam on the Peace River near Hudson Hope in British Columbia, over 1,100 km upstream of the delta (Figure 1). The filling of the Williston Reservoir took place between 1968 and 1971. Natural low flow conditions on the Peace River and absence of flooding in the PAD coincided with a temporary significant reduction in stream flow with the storage of 41 x 10^9 m^3 of water in the reservoir (Prowse et al. 2002). Substantial changes in the landscape, vegetation, and wildlife of the PAD occurred during this 4-year interval (PAD-PG 1973, Townsend 1975). A second period of apparent prolonged drying in the PAD began in 1975 and continued to 1996, a year in which a large ice-jam event on the Peace River flooded many of the perched basins.

Largely because of mounting public concern, a series of investigations was initiated by various government bodies, stakeholders, and researchers. The focus of these investigations was to study and mitigate the perceived negative impacts of the WAC Bennett Dam on the delta and surrounding settlements (PAD-PG 1973, PAD-IC 1987, PAD-TS 1996, NRBS 1996). Research findings of the PAD-PG (1973) led to the construction of weirs to artificially raise water levels at various locations in the delta. Although these weirs had restored peak summer water levels on the delta, the water levels were still not adequate for the replenishment of many of the shallow perched basins. The PAD-TS (1996) and the NRBS (1997) shifted focus, incorporating studies to gain a better understanding of how the combined impacts of flow regulation and climate variability affected the hydroecology of the delta. These studies resulted in a variety of recommendations such as maintaining dam releases during the spring break-up period to

complement downstream tributary runoff and the use of artificial ice-jams to flood individual perched basins.

Several other studies have been undertaken involving modelling ice thickness, strength, and roughness and various heat fluxes that control ice freeze-up and break-up conditions (Prowse and Conly 1998, Prowse and Beltaos 2002, Beltaos 2003, Beltaos et al. 2006a) in an effort to address the gaps in knowledge of ice-related processes in the PAD and other cold regions. Unfortunately, these models are generally not applicable to multiple reaches in the same river, or in different fluvial systems. In addition, these studies usually require detailed records of past events, which are limited (Beltaos 2003). Several other studies have focused solely on the PAD, modelling various ice conditions and flow regimes in relation to climate by considering scenarios from several general circulation models (Beltaos and Burrell 2003, Beltaos et al. 2006b, Pietroniro et al. 2006, Toth et al. 2006). Unfortunately, many of these studies lack field observations, owing to difficulties in obtaining measurements during ice break-up. Additional focus has been placed on declining snowpack conditions in the major tributaries of the Peace River (Peters and Prowse 2006) and its relationship to changing winter atmospheric patterns (Romolo et al. 2006a, 2006b) in order to predict future hydroecological conditions in the PAD. Results have shown that increases in temperature during the ice-cover season reduced snow-pack depths and altered the intensity and duration of the snowmelt period, making conditions less conducive to ice-jam flooding. Substantial work still needs to be done on other phenomena such as the magnitude and frequency of low flows and floods, ice mechanics, meteorology, hydrology, and hydraulics (Prowse and Beltaos 2002).

Until recently, a combination of climate change and river regulation was thought to be the major driver of perceived recent drying trends in the PAD. One of the main limitations that has hampered hydroecological research in the delta to date is the lack of long-term records (Timoney 2002, Timoney and Marsh 2004). Effective management of any type of ecosystem requires long-term environmental data to gain knowledge of baseline conditions and natural variability in order to predict possible future scenarios (Smol 1992). A relevant temporal context for long-term studies in the PAD might be as many as ~1000 years, allowing sufficient time for variation in climate, hydrologic and deltaic processes, fire regime, human activities, and succession to be expressed (Timoney 2002). Detecting changes in the hydrologic regime that might be a result of climate change (or river regulation) is complicated by the variability and randomness inherent in all hydrologic variables (Burn 1994). Lake sediments provide information regarding background reference conditions and act as an archive of lake histories, often with a relatively high temporal resolution. Paleolimnological studies allow researchers and stakeholders to determine how a system has changed through time and in relation to changing anthropogenic and natural influences (Smol 2008).

Paleo-environmental research in the PAD was initiated in 2000, and included isotope dendroclimatological studies in the headwater region of the Athabasca and Smoky Rivers (Edwards et al. 2008). The isotopic dendroclimatology investigations were aimed at providing a framework for the long-term climate history of western Canada and runoff generation in the rivers feeding the Peace-Athabasca Delta. The records were developed from carbon and oxygen isotope analyses of a composite tree ring chronology from the eastern Rocky Mountains in the headwaters of the Athabasca River. The 1100-year

record indicates that from AD ~935 to ~1530, atmosphere conditions were relatively warm and humid. The driest period occurred during the early 1700s, corresponding to the peak of the Little Ice Age (Edwards et al. 2008), followed by a less severe dry period during the mid-1800s. Relatively warm and moist conditions, similar to those prior to AD ~1530, occurred from the mid-1800s to the mid-twentieth century, followed by progressive declines in relative humidity (Edwards et al. 2008).

The climate reconstructions from the Athabasca River headwater region and paleolimnological analysis of lakes in the Peace Sector of the PAD are compatible over the last ~300 years. Paleolimnological evidence suggests that the PAD has experienced multi-decadal wet and dry periods in the last 3 centuries (Hall et al. 2004, Wolfe et al. 2005, 2006). Sediment records from lakes in the Peace sector (PAD 54, PAD 15, and PAD 5) show evidence indicative of low water levels and/or periods of desiccation during the 1700s (Wolfe et al. 2005, 2006, Figure 3). The increase in relative humidity during the late 1800s and early 1900s is consistent with a shift towards the abundance of open-drainage indicator diatoms in the restricted- and closed-drainage basins. From ~1940 to present, these lakes appear to have shifted towards restricted- and closed-drainage conditions as evidenced by the abundance of closed-drainage indicator diatoms (Hall et al. 2004, Wolfe et al. 2005). It is important to note that in the absence of flooding, water persists in many basins due to the undulating landscape and the nature of many of the catchments in the Peace sector (Wolfe et al. 2008, Yi et al. 2008). Bedrock outcrops and forested shorelines tend to accumulate sufficient amounts of snow to offset the effects of evaporation. Thus, the northeastern Peace sector of the PAD is relatively resilient to the changing flood regime of the Peace River.

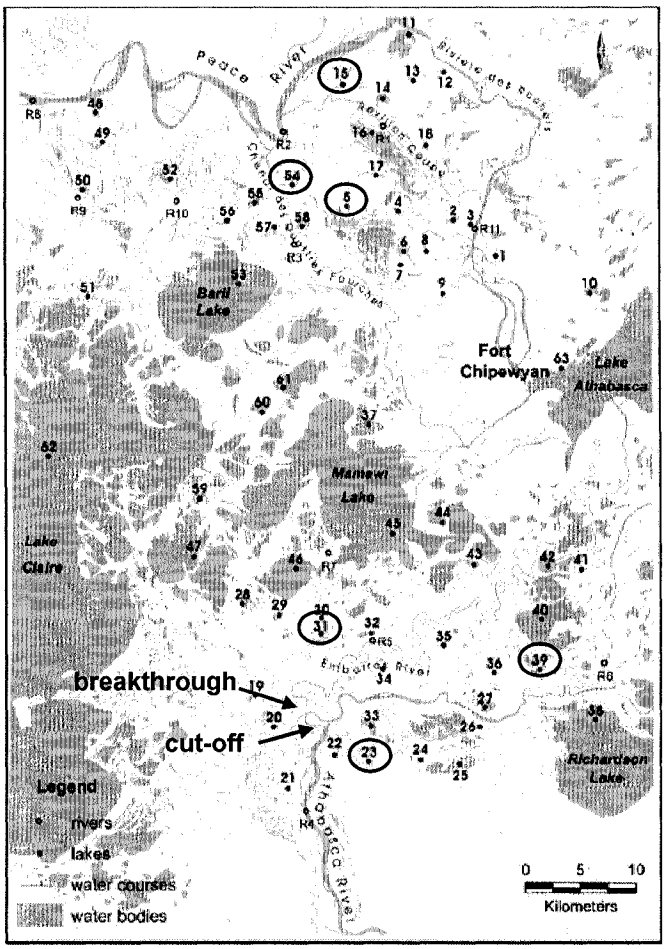

Figure 3: Map of the PAD with circles showing PAD 5 and study sites PAD 54 and PAD 15 in the Peace sector, and PAD 23, PAD 31 and PAD 39 in the Athabasca sector. The arrows indicate the Athabasca River meander cut-off (1972) and the location of the Embarras Breakthrough (1982).

Lakes in the Athabasca sector are also compatible with the climate reconstruction in the Athabasca River headwater region, although recent hydroecological shifts are largely driven by geomorphic changes (Wolfe et al. 2008). The Embarras Breakthrough (occurred naturally in 1982) diverted flow of the Embarras River (~58%) from Lake Athabasca northwest to Mamawi Lake (De Boer et al. 1994). This has resulted in increased susceptibility to floodwaters inundating PAD 31 and decreased flood susceptibility of PAD 39 along the main channel of the Athabasca River. Paleolimnological records suggest that PAD 23 (Figure 3) was less responsive to climatic conditions during the early- to mid-1900s because of the strong influence of Athabasca River floodwaters. However, PAD 23 also shows increasingly drier conditions post-1970, which closely corresponds to the artificial excavation and deepening of the Athabasca River meander cut-off in 1972 designed to prevent the Athabasca River meander from eroding to the Embarras River channel (PAD-PG 1973). This has reduced the frequency of ice-jam floods that reach PAD 23 (Wolfe et al. 2008). It is important to note that the Athabasca sector seems to be more sensitive to periods with no flooding because its relatively flat landscape likely does not effectively capture and transfer adequate amounts of snow to generate runoff and offset the effects of evaporation (Wolfe et al. 2008, Yi et al. 2008). In addition to climatic and geomorphic drivers, the drying trends observed at PAD 23 and PAD 39 are possibly being intensified by decreasing Athabasca River discharge in the latter half of the 20th century (Schindler and Donahue 2006, Wolfe et al. 2008).

Previous Research on PAD Oxbow Lake Sediments

In March of 2001, sediment cores were collected from one site at each of two oxbow lakes (PAD 54 and PAD 15) several hundred metres away from their respective inlets (Wolfe et al. 2006, Figure 2). These lakes were chosen because of their periodic connection to distributaries of the Peace River during high water events, like those induced by ice-jams. The cores were collected using a 10 cm diameter Russian peat corer and extension rods. Each time the corer was deployed it collected a 1 metre section of sediment. A series of overlapping sections was collected to ensure a continuous sediment sequence. Two surface sediment cores were also collected at each site using a Glew (1989) gravity corer, which reduces the disturbance to water-laden upper sediments. Research questions addressed by Wolfe et al. (2006) included: 1) Had flood frequency in the PAD declined since river regulation began in 1968? and 2) Had prolonged multi-decadal intervals (≥20 years) without significant flooding occurred prior to regulation of the Peace River (similar to the 1975 to 1995 dry interval)?

The sediment cores consisted largely of silty clay and clayey silt with alternating light and dark grey laminations. Although ^{210}Pb dating techniques were unsuccessful due to rapid sedimentation rates, a well-defined ^{137}Cs peak and an Accelerator Mass Spectrometry (AMS) ^{14}C determined macrofossil age at PAD 15 rendered weakly-constrained geochronologies spanning the last 180 and 300 years for PAD 54 and PAD 15, respectively (Wolfe et al. 2006). A suite of physical (grain size, mineralogy, magnetic susceptibility) and chemical (organic C and total N content, C/N weight ratios, and bulk organic $\delta^{13}C$) approaches used by Wolfe et al. (2006) revealed a consistent record of fluctuating energy conditions in both PAD 54 and PAD 15. Deposits that had a

high magnetic susceptibility were positively correlated with mean and median grain size, quartz and total feldspar content, and inversely correlated with carbon and nitrogen content. These trends were interpreted as being high energy events, characterized by the influx of coarse-grained quartz and feldspar and magnetic-rich detrital material, and reduced lake productivity. Light bands, interpreted as non-flood deposits, were positively correlated with fine-grained material that had little magnetic material. The light bands also had lower C/N ratios, relatively high C and N content, and depleted $\delta^{13}C$ values, likely due to internal carbon recycling in the water column (Wolfe et al. 2006).

Magnetic susceptibility was used as the key tool to reconstruct flood frequency and magnitude. Flood frequency was observed to be relatively low during the 1700s, relatively high during the late 1800s and early 1900s, and in decline during the 20th century (Figure 4). Results showed that extended multi-decadal low flood frequency intervals, similar to that of 1975 to 1995, had occurred prior to Peace River regulation (indicated with arrows in Figure 4). In both PAD 54 and PAD 15 a multi-decadal (35 years) low flood frequency interval occurred in the mid-1800s. The longer record at PAD 15 indicated several periods with no flooding including AD ~1813 to ~1839 and AD ~1705 to ~1786. These results suggest that variable flood frequency and magnitude is a natural feature of the system. Although the work of Wolfe et al. (2006) extended the flood history record developed by others (Timoney et al. 1997, 2002) and placed the last 35 years in a longer-term perspective, it was not sufficiently long to fully evaluate the relationship between Peace River hydrology, flood frequency, and climate variability. A long-term perspective (~1000 years) is necessary in order to identify the relationship between ice-jam flood frequency and climatic variability (Wolfe et al. 2006).

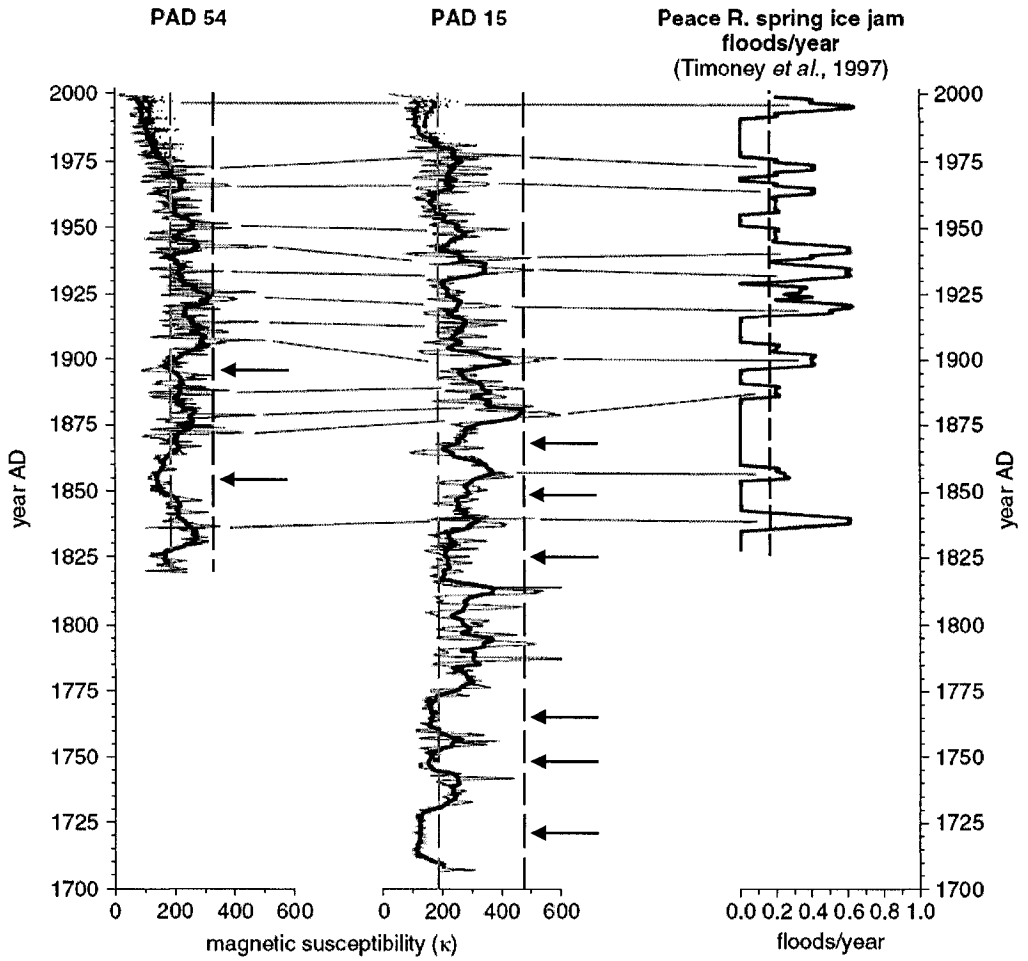

Figure 4: Magnetic susceptibility records for PAD 54 and PAD 15 (Wolfe et al. 2006) and the flood frequency records based on historical records and Traditional Knowledge gathered by Timoney et al. (1997). The vertical hatched lines in the plots of PAD 54 and PAD 15 represent the discharge required for the sill elevation threshold to be reached. The dark vertical hatched lines in the graphs of PAD 54 and PAD 15 represent the discharge of the 1974 ice-jam flood event. The hatched line on the historical and Traditional Knowledge graph illustrates the long term flood frequency average (modified from Wolfe et al. 2006, p. 4149). Extended dry periods are shown with arrows.

Research Objectives

The main objectives of this research are to extend the existing 300-year flood history record of Wolfe et al. (2006) by several hundred years and gain a better understanding of the relationship between Peace River hydrology and climate variability. This timeframe encompasses late medieval times, the Little Ice Age (LIA) and post-LIA. The research questions that are directly addressed include 1) What is the relationship between flood frequency and magnitude and climate variability at the PAD study sites 54 and 15? 2) What hydrological factors may have influenced the frequency of ice-jam events along the Peace River under different climate regimes? and 3) How does the behaviour of the Peace River and the flood histories of PAD 54 and PAD 15 compare with the hydroecological histories of other basins in the central and southern portions of the PAD? The paleohydrological information gained regarding riverine responses within the delta to varying climatic conditions will assist in the development of improved ecosystem management strategies that will account for the natural variability river discharge characteristics and accompanying hydroecological responses in the Peace-Athabasca Delta.

SITE DESCRIPTION

The Peace River Drainage Basin

The Peace River originates in the eastern Rocky Mountains of northeastern British Columbia with the headwaters generated by alpine snowpacks and glacial meltwater (Figure 1). It drains an area of approximately 293,000 km^2, bypassing the PAD except at times of significant ice-jamming, and subsequently flows northward through the Slave River and Mackenzie rivers; the latter discharging into the Arctic Ocean. River morphology is largely determined by a combination of the local geological formations and sediment supply, as well as in-channel flow and tributary inputs (Prowse et al. 2002). The upper portion of the channel (upstream of the Smoky River) is roughly 450 to 500 m wide. The river has incised more than 200 m into the Alberta Plateau, which is underlain by Cretaceous sedimentary rock (Prowse et al. 2002). Downstream of the town of Peace River, the river channel is characterized as partly entrenched and confined with irregular meanders. The channel width increases to 650 m at Fort Vermillion. Contrary to upstream reaches of the Peace River, lower reaches of the river are incised 20 to 25 m into glacial Lake McConnell sediments (Craig 1965, Smith 1994). As the river incised these sediments, it wandered away from its preglacial channel pattern and cut into bedrock, creating small rapids and waterfalls. The current channel is weakly sinuous with split channels and island complexes, and is in some areas greater than 1500 m wide (Prowse et al. 2002).

Headwaters of the Peace River above Hudson Hope are located primarily in the high elevation alpine regions of the Rockies, with snowmelt occurring in June, well after break-up downstream. The five major tributaries (Smoky, Wabasca, Beaton, Halfway,

and Pine Rivers) between Hudson's Hope and Peace Point have a combined catchment area of 55% of the total contributing area (Prowse and Conly 1998). However, downstream tributary input at break-up is dominated by the Smoky and Wabasca Rivers (Prowse and Conly 1998). Together they comprise about 40% of the catchment area between Hudson's Hope and the PAD and are composed of foothills and lowland plains that experience the earliest spring snowmelt. Almost all of the Smoky River lies below 900 m and is incising into the Alberta plateau, and all of the Wabasca River lies below 600 m. Of these two tributaries, the Smoky River contributes a greater percentage of flow and enters the Peace River just upstream of the town of Peace River and is considered to be the main tributary trigger for dynamic break-up events in the vicinity of the PAD (Prowse et al. 2006). The Smoky River is sinuous with irregular meanders, islands and bar formations. This is the source of much of the sediment load of the Peace River, with the fine-grained sediment affecting much of the channel patterns downstream (Prowse et al 2002). The Beaton, Halfway, and Pine rivers drain higher elevations that experience later spring snowmelt and therefore only contribute a relatively small amount of spring flow to the Peace River. Their main contributions generally arrive after break-up has occurred in the PAD (Prowse and Conly 1998).

The Peace-Athabasca Delta

The Peace-Athabasca Delta (59°N and112°W) lies at the confluence of the Peace, Athabasca, and Birch rivers in northeastern Alberta. The delta began forming ~10,000 years ago in Glacial Lake McConnell (Craig 1965, Smith 1994). Isostatic rebound and sedimentation have led to the development of three deltas at the western end of Lake

Athabasca that currently have surface areas of 1,680, 1,970, and 170 km^2 (Peace, Athabasca, and Birch deltas, respectively, PAD-PG 1973). In total, the PAD occupies an area of just under 3,900 km^2. The majority of the area is occupied by three large shallow lakes (Claire, Mamawi, and Baril, from less than 1 to 3 m deep), which are connected to Lake Athabasca and other small basins by numerous active and inactive channels (Prowse and Conly 2002). Lake Athabasca and the other numerous lake basins and channels in the PAD are connected to the Peace River by three main channels: the Rivière des Rochers, Revillon Coupé, and Chenal des Quatre Fourches.

After the last deglaciation, the Peace Delta experienced rapid growth and formed levees that channelled the largest portion of Peace River flow into the Slave River. This delta is considered to be essentially inactive with the exception of large flood stages typically generated by ice-jam events (Peters et al. 2006). The Athabasca and Birch deltas are actively extending into the shallow, central lakes and Lake Athabasca with very fine- to medium-grained sands deposited in the active and semi-active portions (Stanley Associated Engineering Ltd. 1982). Overall, the highest clay concentrations are found in the Peace Delta and the lowest clay concentrations are found in the Athabasca Delta (Stanley Associated Engineering Ltd. 1982). With the exceptions of levees and islands created by outcrops of the Canadian Shield in the northeast portion of the delta, relief rarely exceeds 1 m above the surface of the major delta lakes (Prowse and Lalonde 1996).

The PAD contains one of the largest undisturbed grassland areas of North America, with over 1,200 km^2 of sedge (*Carex atherodes*) and reed (*Calamagrostis spp.*) grasses (Prowse and Conly 2002). Willow (*Salix spp.*) borders the slightly elevated areas along distributaries and fringes of meadows and marshes (Prowse and Conly 2002). Generally,

tree and shrub growth increases towards the margins of the grasslands, with spruce (*Picea spp.*) and poplar (*Populus spp.*) species present. White spruce (*Picea glauca*), jack pine (*Pinus banksiana*), and white birch (*Betula papyrifera*) are common in areas of the northeastern portion of the PAD, where the Canadian Shield is near the surface or exposed (Prowse and Conly 2002). The numerous shallow open ponds are dominated by pondweed (*Potamogetan spp.*), duckweed (*Lemna spp.*), common bladderwort (*Utricularia vulgaris* L.), and coon's tail (*Ceratophylum demersum* L.), while water horsetail (*Equisetum fluviatile*) is commonly found along the rivers (Timoney 2002).

A host of migratory birds and waterfowl use the delta and arrive mainly via the Central and Mississippi Flyways (Prowse and Conly 2002). The delta is of particular importance during years when there is drought on the prairies, especially for migrating duck populations (PAD-IC 1987). Instead of stopping in the Canadian prairies to forage, they will continue to travel northwest to the delta. Some migratory birds, such as tundra swans, lesser snow geese, and Canada geese, will use the PAD as a staging area before traveling to and returning from nesting grounds in the arctic or other areas (Prowse and Conly 2002). Staging birds prefer to use the mud flats, immature meadow, emergent and meadow shorelines of the largest delta lakes, especially lakes Mamawi and Claire (PAD-PG 1973). Breeding birds settle mainly along the shorelines of the perched basins, with some use of stream channels and marshes (PAD-PG 1973).

Muskrat pelts are the most important traditional source of income for residents of the delta (Prowse and Conly 2002). Muskrat survive best in marshes having several feet of water and an abundance of emergent and submergent vegetation (PAD-PG 1973). However, muskrat habitat selection is based on water depth rather than on vegetation type

as the availability of suitable plant species is linked to seasonal water regimes (Prowse and Conly 2002). Moose also provide a valuable source of income for local residents, although they do not play a major role in the ecology of the delta. They tend to favour areas that are periodically disturbed by events such as fire and flooding, where a mixture of early successional vegetation and mature stands survive (PAD-PG 1973). Hybrid wood bison play a larger ecological role and are found throughout the lower Peace River area. Sedge meadows and reed grasses comprise 70% of their annual diet and 100% of their winter diet, applying significant grazing pressure on the open grasslands (Carbyn et al. 1993, Prowse and Conly 2002).

Climate

The PAD is located within the Slave River lowlands of the Boreal Plain ecoregion and the discontinuous permafrost zone (Ecoregions Working Group 1989). It is classified as having a sub-humid mid-boreal ecoclimate (Ecoregions Working Group 1989), characterized by short cool summers and long cold winters. Based on 1971–2000 climate normals (Environment Canada weather station 3072658, Fort Chipewyan), mean annual air temperature is 1.9°C, mean January air temperature is -23.2°C, and mean July air temperature is 16.7°C. Annual precipitation averages 391.9 mm, with approximately 59% falling as rain during the May–September period. Water levels and channel networks are typically highest during the spring and summer but recede during the late fall and winter with water primarily lost by evapotranspiration from May to September. Mean annual lake evaporation calculated from class-A pan measurements at Fort Smith, NWT, 145 km to the north, is 525 mm (AES 1993). The quantity of regional groundwater

flow from the nearby Birch and Caribou Mountains is relatively small because soft marine shale, having very low permeability, extends from the bed of the Peace River to the mountains (Nielsen 1972, Peters et al. 2006). In addition, because of the low relative relief, relict permafrost, and the low permeability of Glacial Lake McConnell silty-clay deposits, groundwater flow within the PAD is thought to be negligible (Nielsen 1972, Peters 2003).

Lake Hydrology

Prowse and Lalonde (1996) identified the need for a detailed water balance model for perched basins in the PAD in order to understand the relative importance of water fluxes such as overbank flooding, precipitation, groundwater, evaporation, and evapotranspiration. A number of water balance studies have been completed using field measurements and remote sensing techniques on specific basins (Pietroniro et al. 1999, Peters et al. 2006, Töyrä et al. 2001). However, analysis of water isotope tracers ($\delta^{18}O$, $\delta^{2}H$) allows a rapid and effective assessment of water balances (and identification of key hydrological processes) of many water bodies at a single point in time, and does not require intensive field work.

Using an isotopic approach and building on previous hydrological studies (PAD-PG 1973), Wolfe et al. (2007) classified 57 basins in the PAD into four categories (open-, restricted-, closed-drainage basins, and rainfall-influenced basins). Basins in open-, restricted-, and closed-drainage classes gain water from precipitation and catchment runoff, and lose water through evaporation and outflow. However, the relative importance of individual processes can vary significantly among basins, depending on the

geomorphology, frequency of river connection, variations in local runoff generation, and hydroclimate (Wolfe et al. 2007). In open-drainage basins river flow is dominant, whereas in closed-drainage basins, a combination of precipitation, runoff, and evaporation influences the water balance, except during times of overland flooding. Intermediate to these two basin categories is restricted-drainage basins, which are intermittently connected to rivers at times of relatively high water levels. Based on additional water chemistry information, a fourth category was identified as rainfall-influenced basins (Zmax <50 cm). These basins are situated near large open-drainage lakes that occupy the central portion of the delta and are likely prone to extensive or complete desiccation over the growing season, resulting in high concentrations of ions. Remobilization of ions following a rain event and rewetting of these basins may contribute to conductivities and concentrations of ions that are significantly higher than other basins, regardless of their hydrological classification, including similar rainfall-influenced basins that are deeper (Zmax > 50 cm).

Oxbow Lakes PAD 54 and PAD 15

PAD 54 (local name: Horseshoe Slough) is a 6-metre deep oxbow lake with a surface area of about 18 ha and is located adjacent to the Chenal des Quatre Fourches, approximately 4 km south of the Peace River (Figure 2). This oxbow is currently a hydrologically-closed basin but is occasionally connected to the river by a small channel across a levee with an elevation of 209.92 metres above sea level (Wolfe et al. 2006). This lake was selected for paleolimnological analyses because it was likely to provide a highly sensitive record of flood events and overbank flow from the Chenal des Quatre

Fourches. It is also important to note that this distributary connects with the Peace River immediately upstream of Rocky Point, where ice-jams frequently develop (Prowse and Lalonde 1996, Figure 2).

PAD 15 (local name: Pete's Creek), is a 4-m deep oxbow lake formed by a meander cut-off (~16 ha surface area) from the Revillon Coupé, a major distributary of the Peace River during ice-jam flood events. This basin is currently hydrologically closed except for the intermittent connections during high water events on the river. The precise sill elevation of this lake is not known but it is likely slightly higher than at PAD 54 because field observations indicated that in 2001 only PAD 54 was flooded, while in 2003 both oxbows were inundated with turbid, isotopically-depleted river water (Wolfe et al. 2006).

METHODOLOGY

Field Work

In March of 2005, oxbow lakes PAD 54 and 15 were revisited and sampled using monopod vibracoring techniques described by Fisher (2004). An initial hole was made in the ice using an ice auger and the water depth was measured. The monopod was then erected and secured to the lake ice using several ice screws and three guidelines with ratchet tighteners. The core tubing was arranged on the ice, connected together with couplers, and the piston and cable was run through all the tubes. The piston was used to reduce compaction, acting in a similar manner to the plunger in a syringe. The piston was placed at the base of the bottom tube and secured by cable to the monopod. Core catchers, used to prevent sediment from being lost at the base of the core during recovery, were then attached. The core tubing was then erected using two ropes guided by a pulley system at the top of the monopod mast. A vibrahead, typically used to remove air bubbles before cement hardens, was attached to the core tube and powered using a generator. The vibrations liquefied a thin film of sediment on the inside of the core tube, thereby reducing friction and allowed the core tube to penetrate through the sediment. Cores were recovered using a winch attached to a hoist frame assembled after coring was complete. Figure 5 illustrates the vibracore monopod setup prior to coring. Advantages of using this type of coring device compared to previous attempts at these sites include the retrieval of a continuous sediment record, increased penetration, and the ability to recover different types of sediment.

Figure 5: The vibracoring apparatus.

Cores were collected at sites that were proximal, intermediate and distal to the inlet of each oxbow (Figure 6). In addition, a gravity corer (Glew 1989) was used to collect the uppermost sediments, which have high water content and are often susceptible to disturbance (i.e. compaction) using the vibracore technique. The gravity cores were sectioned into half-centimetre intervals at the field station. The vibracores were cut into manageable sections (1-2 m in length) before transportation and stored at 4°C at the University of Waterloo.

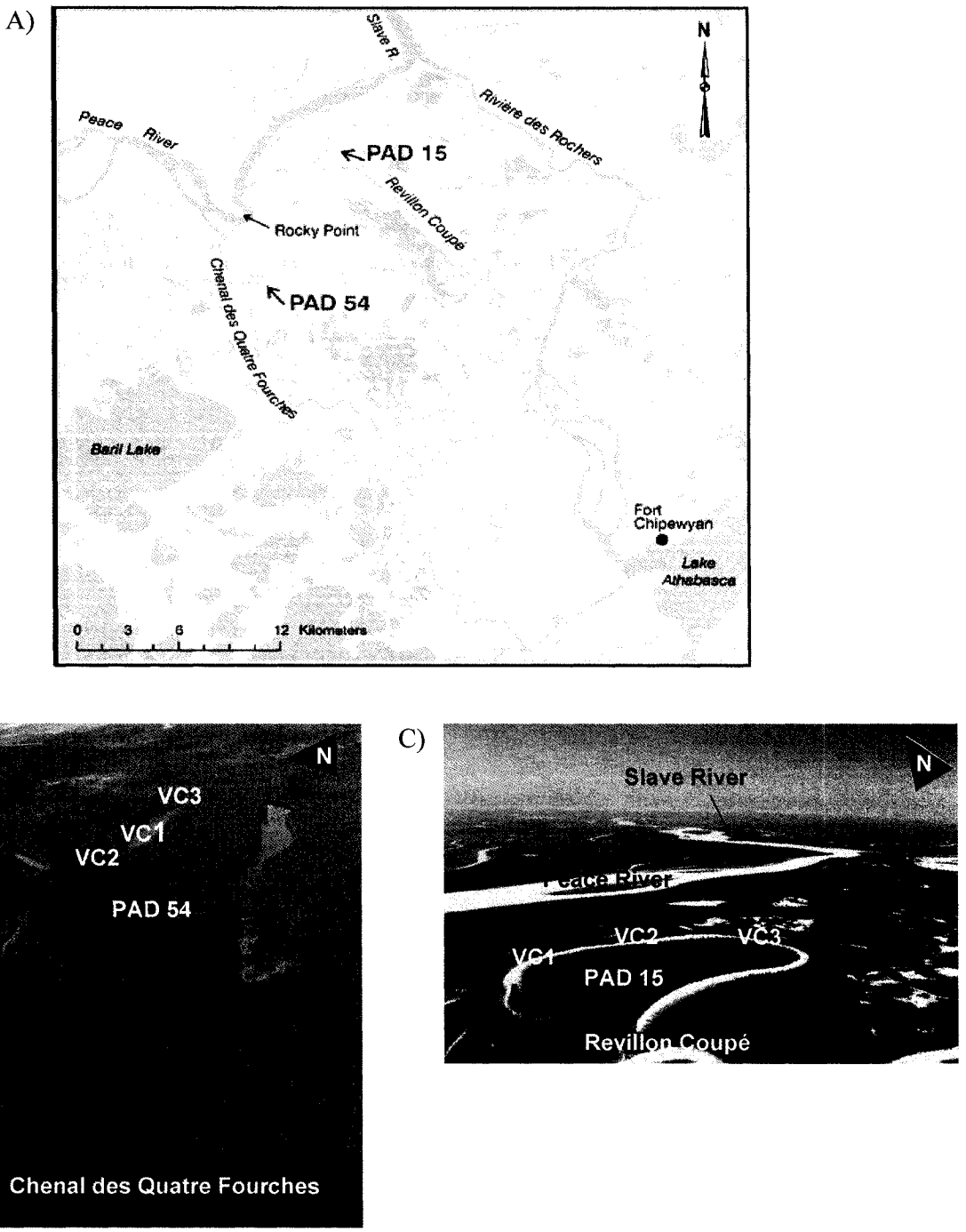

Figure 6: A) The two oxbow lakes that are periodically flooded during Peace River ice-jam events B) A photo of PAD 54, locally known as Horseshoe Slough, showing the three coring sites, and C) A photo of PAD 15, locally known as Pete's Creek, showing the three coring sites.

Core Splitting and Stratigraphic Descriptions

A core splitting table was constructed from spruce plywood for stratigraphic documentation and photographing purposes (A in Figure 7). The table was approximately 2 m in length and constructed to accommodate the longest core section with ample extra length for maneuverability. The table contained a holder for whole core sections prior to splitting, as well as a holder to anchor the core sections in place during the core splitting procedure. The adjacent flat working surface, wide enough to accommodate the two equal halves, had a scale showing 10 cm intervals with 5 cm midpoints for measuring stratigraphic features. The table was then coated with varathane to seal the wood and prevent staining and moisture penetration from wet sediment. Each core section was placed in the core splitting holder and secured with wedges so that it did not move while being cut. Paraffin wax was rubbed on the core tube to reduce the amount of aluminum shavings produced from cutting the tube. A circular saw with a 24-tooth carbide blade was used to cut the irrigation tubing. The saw blade was adjusted to only cut the tubing, minimizing penetration into the sediment. Once one side of the tubing was cut in a single, smooth motion, all visible fragments of aluminum were removed. The cut was taped shut with duct tape to minimize sediment and water loss and then rotated 180°. The other side of the core tubing was then cut with the saw and the tape was removed. Ten-pound stainless steel trolling line was run through the middle of the core tube to split the core into two halves. The core was carefully pulled apart, often with the help of a trowel and/or a large kitchen knife in sections that were particularly moist.

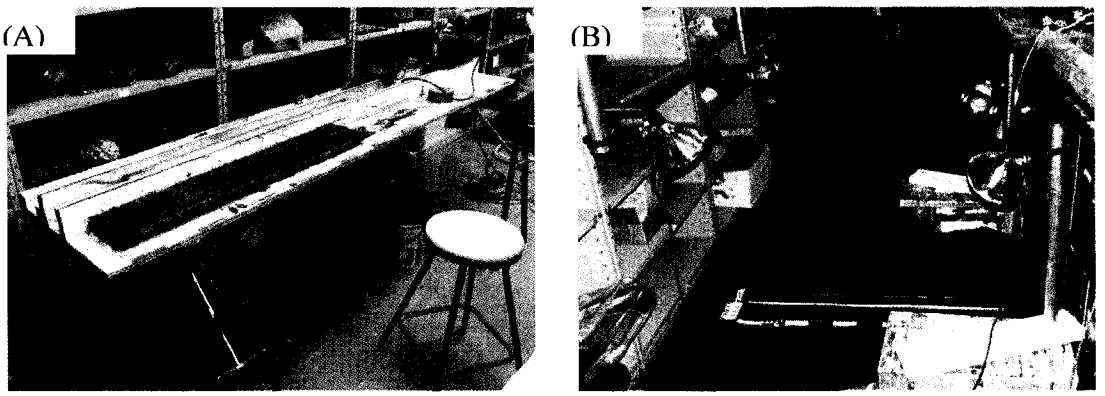

Figure 7: A) The core splitting table constructed out of spruce plywood and B) the table and lights used for photographing cores after they were split open.

Each core section was visually described, noting sedimentary structures, grain size, colour, bed thickness, and the presence of wood and macrofossils for potential radiocarbon dating. Sediment compaction and rodding have been important concerns in past studies that have used the vibracoring technique (Fisher and Souch 1998, Fisher 2004). Though the piston was designed to minimize these occurrences, sediment compaction was calculated as the difference between the penetrated core tube length and the length of sediment retrieved in the core tube. The percentage recovery was calculated by the following formula:

% core recovery = (retrieved sediment length/penetrated core tube length) * 100.

Because the core tube length was not consistently recorded in the field, sediment compaction could only be calculated for cores VC1 and VC2 from PAD 54 (see core descriptions in the results section).

Once the cores were described they were arranged on the light table (B in Figure 7). The light table was constructed for the purpose of photographing the cores using consistent lighting and positioning. It was built using plywood, and a series of 2x4" and 2x2" boards. The table was able to fit 5 split core halves at a time, with a maximum length of 110 cm. A sheet of black felt was placed over the table to obtain the correct exposure and contrast for photographing. Four lamps containing 250 W incandescent lights were positioned around the light table and all fluorescent room lighting was turned off. Pictures of entire core sections, as well as every 20 cm were taken maintaining a consistent distance from the light table as well as a consistent camera lens zoom. The functions used on the camera (Sony Digital Camera DSC-F828) included auto-focus, default metering mode, aperture priority mode, an ISO (sensitivity of the image to light) of 300, and an exposure bracket of ±0.3. The cores were then wrapped in 12.7 cm diameter, 4 mm thick polytubing to retain moisture and prevent contamination. One core half was reserved as an archive while the other half was designated for laboratory analyses.

With the consideration of results from previous research and the visual examination of stratigraphic sequences in the vibracore, it was determined that the core recovered from the distal site (VC3) at PAD 15 (Figure 3) likely contained the longest flood frequency record. This is largely because lower portions of the vibracore contained well-defined laminated clay and silt that was not found in any other sediment core, either from current research or previous research by Wolfe et al. (2006). Because this site was furthest away from the inlet it likely had a lower sedimentation rate relative to other sites, and thus was considered likely to provide the longest sediment record. In addition, a massive sediment

interval immediately above well-defined clay and silt laminations in the vibracore was similar to the massive light grey interval observed near the bottom of the Russian core sequence from approximately 357 cm to 400 cm sediment depth taken in 2001 (Wolfe et al. 2006). Therefore this core was selected for detailed analyses. Individual bed thicknesses of clay and silt beds were measured in VC3 prior to being sectioned into 0.5 cm intervals using a paint scraper cut to the shape of the core tube.

Sediment Chronology

Lead-210 (^{210}Pb) and Cesium-137 (^{137}Cs)

One of the most common methods for dating recent sediments (younger than ~150 years) is using ^{210}Pb, a radioactive isotope in the Uranium-238 (^{238}U) decay series. In addition, the peak ^{137}Cs concentration associated with above-ground nuclear bomb testing during the late 1950s and early 1960s can be used as a stratigraphic indicator (Appleby 2001). The radioactive isotopes ^{210}Pb and ^{137}Cs were measured at the University of Waterloo Environmental Change Research laboratory (WATER) using a gamma spectrometer, which counts gamma particles produced by a decay event and identifies radioisotopes producing each gamma particle (Appleby 2001, Jarvis et al. 2006).

Up to 5 g of wet sediment was weighed, freeze-dried, placed in plastic test tubes, compacted to remove pockets of air, sealed with epoxy, and measured following methods discussed in Jarvis et al. (2006). Initial ^{210}Pb and ^{137}Cs activity profiles were generated using a sample every 5 cm in the 41 cm gravity core from the distal site at PAD 15. Once the ^{137}Cs peak was determined to occur below 30 cm, additional ^{210}Pb and ^{137}Cs measurements were obtained using a sample from every 0.5 cm from 30 cm to the base

(41 cm) of the gravity core. In addition, ^{210}Pb and ^{137}Cs measurements were completed every 0.5 cm from 30 cm to 50 cm of the vibracore (VC3). When it was determined that the ^{137}Cs peak did not occur in this interval of the vibracore (VC3), additional ^{210}Pb and ^{137}Cs measurements were obtained every 0.5 cm from 0 cm to 20 cm in the vibracore (VC3).

Radiocarbon Dating (^{14}C)

Radiocarbon (^{14}C) has a half-life of 5,568 years and is generally applied for age-dating back to ~40,000 to 50,000 years. However, the most recent few hundred years are associated with high uncertainties because of varying atmospheric ^{14}C content, the release of "old carbon" from fossil fuel combustion, and the increase of ^{14}C production during nuclear bomb testing (Björk and Wohlfarth 2001). Lake sediments usually contain telmatic and limnic plant and animal debris that can be collected with the objective of obtaining age control on sedimentary sequences by dating selected portions (Björk and Wohlfarth 2001). In previous research by Wolfe et al. (2006) dark-coloured beds in oxbow lake sediments were found to be contaminated with "old carbon", likely originating from reworked bitumen. Therefore, light-coloured beds were selected in this study from the base of PAD 15 VC3 (from 403 cm to 418 cm and 508 cm to 528 cm) for bulk organic sediment ^{14}C dating. Because these sediments were relatively inorganic (<10% dry weight), several beds were combined to ensure there was a sufficient amount of carbon. The samples were freeze-dried, weighed, and submitted to Beta Analytic, Inc (Miami, Florida). The sediments were then pretreated using their standard acid washing procedures and measured using accelerator mass spectrometry (AMS). Three additional

wood samples were selected from the vibracore at the proximal site at PAD 15 (VC1) at 564.5 cm, 605 cm, and 632.5 cm. These samples were also freeze-dried, weighed, and sent to Beta Analytic, Inc. All wood samples were pretreated using their standard acid-alkali-acid procedures. The samples collected at 564.5 cm and 632.5 cm were measured using AMS and the remaining sample was measured using conventional ^{14}C dating methods because of its greater carbon content.

Magnetic Susceptibility (κ)

Magnetic susceptibility (κ) is a non-destructive and cost-effective proxy that can be measured on virtually any material, and complements many other environmental analyses (Thompson et al. 1980, Thompson and Oldfield 1986). Magnetic susceptibility is the ratio between the strength of the magnetization (A m^{-1}) to a magnetic field of ~80 (A m^{-1}), or the ability of a sample of sediment to magnetize to a weak magnetic field created by the sensor (Dearing 1999). Specifically, this tool has proven to be a sensitive proxy for fluctuating energy conditions in PAD 15 and PAD 54 (Wolfe et al. 2006). Therefore, volume-specific magnetic susceptibility (κ) was measured at the Paleoecology Laboratory at Carleton University on contiguous 0.5 cm intervals sampled from vibracores VC1 (proximal) and VC3 (distal) and the corresponding gravity cores at PAD 15. The samples were allowed to equilibrate to room temperature prior to measurement. A Bartington Instrument MS2B dual frequency sensor was used to measure discrete 1 cm^3 samples of wet sediment and was interfaced with MULTISUS software. The samples were placed in a low frequency, low intensity, alternating magnetic field produced by the sensor. Because the samples had relatively weak magnetic properties,

the sensor was operated at a low frequency range of 0.1 (or 0.465 kHz ±1%). Each sample measurement was automatically corrected by measuring the magnetic susceptibility of air before and after each sample. The correction uses the following simple calculation:

κ (corrected) = sample κ – {{first air κ + second air)/2}

At approximately every 10 cm a sample was measured multiple times to assess analytical precision of the equipment. The time between measuring cycles was kept as short and constant as possible to minimize any possible sources of sensor drift. The automatically corrected output was digitally displayed in dimensionless SI (standard international) 10^{-5} units, logged into a MULTISUS spreadsheet, and subsequently imported into Microsoft Excel. The z-score is a dimensionless quantity that indicates how many standard deviations a value is above or below the mean and allows the comparison between data sets with different means and distributions (Khazanie 1996). The z-score for each measurement was calculated using the following formula:

$$z - score \equiv \frac{(\chi - \mu)}{\sigma},$$

where χ is the raw magnetic susceptibility value of a given sample, μ is the average magnetic susceptibility of the entire core, and σ is the standard deviation of the magnetic susceptibility for the entire core.

Organic Carbon and Nitrogen Elemental and Stable Isotope Geochemistry

Organic matter forms part of the paleolimnological record contained in lake sediments. Detailed histories of carbon and nitrogen cycling at local scales can be reconstructed from the amounts and isotopic compositions of organic matter in lake sediments (Meyers and Ishiwatari 1993, Meyers 1997). Previous studies (Brown et al. 2000, Bierman et al. 1997, Wolfe et al. 2006) have shown that carbon and nitrogen geochemistry is a useful proxy for identifying flood events in lake sediments. In anticipation of similar results, 0.5 cm interval samples from PAD 15 VC3 and the associated gravity core that were measured for magnetic susceptibility were also used for organic carbon and nitrogen elemental and stable isotope analyses. The samples were pretreated with 10 % by volume HCl at 60 °C for two hours to remove carbonate minerals and shells. The samples were then rinsed with deionized water (DI) until the pH of DI water was reached. The samples were freeze-dried, weighed, and measured on an elemental analyzer interfaced with a continuous flow isotope ratio mass spectrometer at the University of Waterloo Environmental Isotope Laboratory (UWEILAB). Carbon and nitrogen stable isotope results are expressed as δ values, or deviations in per mil (‰) from the Vienna-PeeDee Belemnite (VPDB) standard and the atmosphere (AIR), respectively, using the following formula:

$$\delta_{sample} = [R_{sample}/R_{standard}-1]*10^3 ,$$

where R refers to the $^{13}C/^{12}C$ or $^{15}N/^{14}N$ in the sample and the standard.

Repeat analyses were performed every 10 cm on one sample to assess the analytical uncertainty. Analytical uncertainty is calculated as change (±) in permil (‰) of the initial measurement from the repeat. The analytical uncertainties for $\delta^{13}C_{org}$ and $\delta^{15}N$, based on replicate analyses, are ± 0.08 ‰ and ± 0.07 ‰, respectively.

RESULTS

Core Descriptions

Seven gravity cores (20 cm to 41 cm long) and 6 vibracores (471 cm to 733 cm long) were recovered from 3 sites in each of the two oxbows, PAD 54 and PAD 15. Table 1 shows the lengths and locations of the sediment cores recovered at each site. The general characteristics of the gravity core sediments were obtained in the field by visual examination through the clear plastic core tubes. Characteristics of the gravity core sediments (such as colour, texture, and presence/absence of plant material) were also described during sectioning of the sediment into 0.5 cm intervals at the field station. The gravity core sediments consist of black organic matter and plant fragments, generally 1-2 cm thick at the top of the cores, and light and dark grey laminated clay and silt.

Vibracore sediments are described in more detail (according to sedimentary structures, grain size, colour, bed thickness, bed contacts, and successions) because the cores were cut vertically and were not sampled until visual observations were completed. There are no obvious organic structures such as borings, burrows, tracks, and trails in any of the vibracores. There is also no visible organic matter at the top of any of the vibracores. All of the cores consist of primary (formed during or shortly after deposition) inorganic structures including planar laminated silt and clay, and massive deposits of fine- to coarse-grained sand and pebbles. The lower sediments in all of the cores generally consist of larger grain sizes (silt to coarse sand) with planar bed contacts. The upper roughly 200 cm to 350 cm of sediments in each vibracore consist of alternating dark (beds ranging from <0.5 cm to 8 cm thick) and light grey (beds ranging from <0.5 cm to

Table 1: Length (in cm) of the gravity cores and vibracores recovered from each site.

Coring Site	Proximal	Intermediate	Distal
PAD 54	VC2	VC1	VC3
Vibracore	469.0	537.0	660.5
Gravity Core	34.0	31.5 and 25.5	20.0
Coordinates	N 0466601	N 0466829	N 0467234
(NAD 83)	E 6525748	E 6525655	E 6525590
PAD 15	VC1	VC2	VC3
Vibracore	733.5	693.0	530.0
Gravity Core	22.5	24.0	41.0
Coordinates	N 0471101	N0471538	N0471759
(NAD 83)	E 6534635	E 6534635	E6534442

15 cm thick) laminated clay and silt. The dark grey beds generally have sharp planar lower and gradational upper bed contacts.

Visual observations for each core in PAD 54 and PAD 15 are described in the following paragraphs and compared in the subsequent Discussion. Observations begin at the base of each core and progress up-core. The water-laden modern sediments near the sediment-water interface are missing and/or compacted in many of the vibracores (e.g. see the chronology of the distal site in the results section). This is a function of the vibracoring technique that may be related to the initial set-up of the core tube at depth and the correct position of the piston and piston cable. If the piston was placed too high in the tube and/or the piston cable was not taut, the effectiveness of the piston would be minimized during initial penetration (i.e. failure to act like a rubber stopper in a syringe) and the tube may have initially ploughed through the surface sediments. The upper sediments (0.5 m to 2.5 m) in all of the cores had significant draping along the sides of

the core tubes, which may be attributed to the rigid nature of the core catchers during coring and the fine-grained nature of the sediment. Figure 8 illustrates the draping of sediments along the sides of a core tube and disturbance caused by the rigid core catchers when the core tube was rotated during coring to achieve greater depths of penetration.

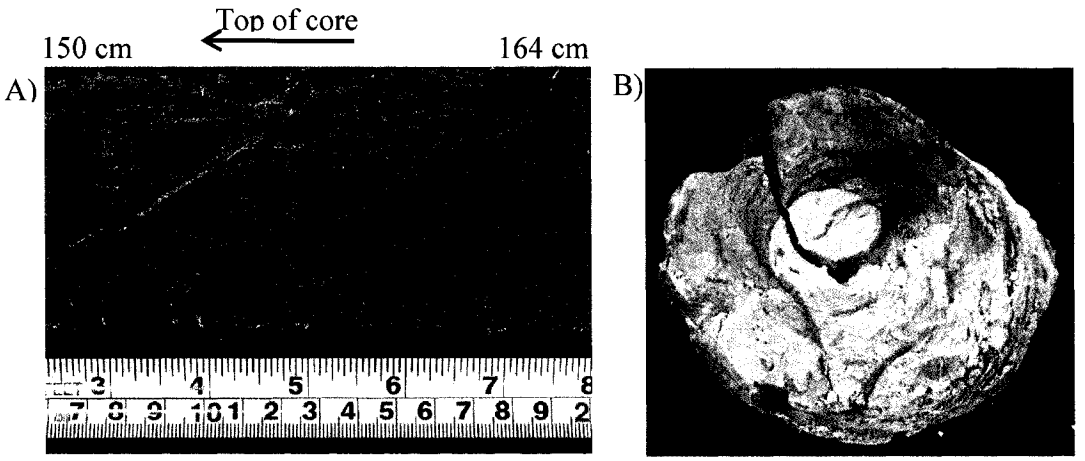

Figure 8: A) vibracore collected from the intermediate site at PAD 54 (VC1) showing draping along the sides of the core tube from the core catchers and B) top view (230.5cm) of a dried portion of core from the distal core at PAD 54 (VC3), showing disturbance caused by the core catchers when the core tube was rotated during collection.

In the left-hand plot of each figure describing vibracore stratigraphy below, the letters along the x-axis c, s, fs, ms, cs, and p refer to the visually estimated grain sizes clay, silt, fine sand, medium sand, coarse sand, and pebbles, respectively. The width of each stratigraphic unit reflects grain size. The two adjacent plots refer to the ranges of bed thicknesses of dark and light laminated clay and silt beds. The right-hand plot refers to the number of "sets" of dark and light grey clay and silt beds that are grouped (Figure 9).

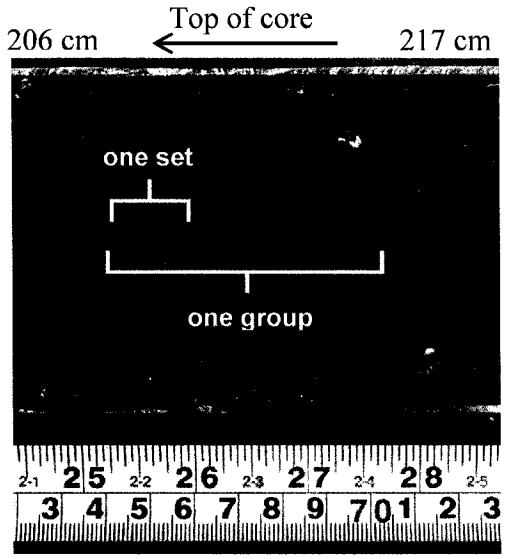

Figure 9: The term "set" refers to a light grey bed and a relatively thin dark grey bed. The term group refers to the number of sets of dark and light grey clay and silt beds that are separated by a relatively thick dark grey bed. The photograph is from the vibracore at the distal site of PAD 54 (VC3).

The term "set" refers to a relatively thin dark grey bed and a relatively thick light grey bed. The term "group" refers to a similarly appearing sequence of alternating dark and light grey clay and silt beds having similar bed thicknesses and/or bed contacts. Each of these groups is generally separated by a relatively thick dark grey bed. Roman numerals in each figure refer to different units, or segments of the vibracores having similar physical characteristics. Detailed digital photographs of all of the vibracores can be found in Appendix A on the accompanying compact disc.

PAD 54 VC2 (Proximal core)

The length of recovered sediment collected from the proximal site in PAD 54 is 490 cm. The total core tube length used to collect sediment was 501 cm, resulting in 11 cm of

sediment compaction, or a percent retrieval of 97.8%. However, approximately 21 cm was lost from the base of the core immediately after recovery leaving 469 cm of sediment. Significant freezing-thawing and/or wet-drying cycles occurred prior to core splitting because between recovery, shipping, and storage, the sediment expanded causing the caps at either end to pop off of the first section of the core (0-57 cm). The ends of section 2 (57-156 cm) were sealed with duct tape instead of plastic end caps, causing the sediments near the ends of the core tube to dry out during shipping and storage. Disturbance is visible from the base of the core to 356 cm (Figure 10). Sedimentological characteristics were difficult to distinguish in the upper 90 cm of sediment because of significant sediment draping along the sides of the core tube due to the vibracoring technique.

This core contains primary inorganic sedimentary structures such as massive and laminated sediments. The lower 113 cm contains relatively coarse-grained sediment, while the upper 356 cm contains fine-grained clay and silt. The stratigraphic profile is shown in Figure 11. Unit I, from the base of the core to 356 cm, consists of silt and fine sand, and is relatively coarse compared to the overlying sediments. Unit II, from 356 cm to 306 cm consists of dark grey clay and silt. Laminations are visible but because of the sediment disturbance, bed thickness and groupings are not measured from 356 cm to 306 cm (Figure 10). From 306 cm to 283.5 cm (unit III) the sediment is massive light grey clay and silt. Both the upper and lower contacts of unit III are gradational.

Unit IV, from 283.5 cm to the top of the core, consists of clay and silt and has been divided into subunits according to bed thickness, bed contacts, and sediment sequences. From 283.5 cm to 256 cm (subunit IVa), the clay and silt beds are characterized by dark

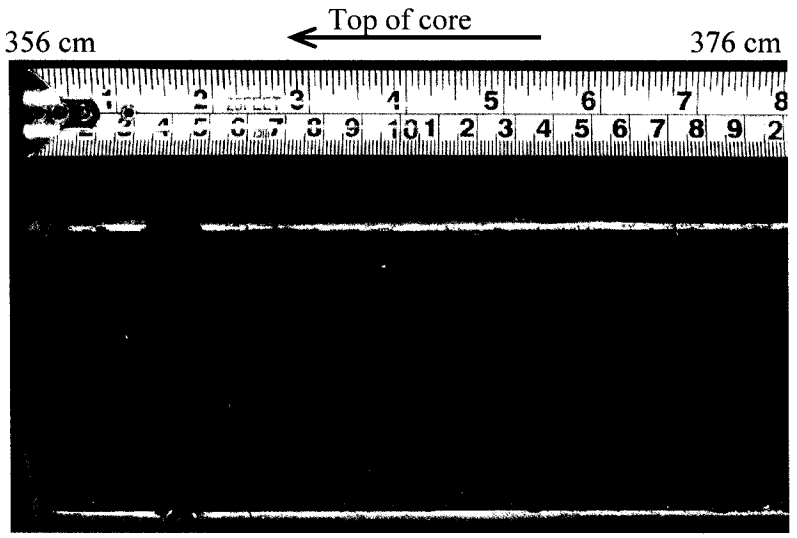

Figure 10: Sediment disturbance near the base of PAD 54 VC2 (proximal site).

grey beds ranging in thickness from 1.5 cm to 2 cm and light grey beds are significantly thicker, ranging from 5.5 cm to 9 cm. These beds are not grouped as in the upper 256 cm. From 256 cm to 216 cm (subunit IVb), dark grey clay and silt laminations range in thickness from 0.5 cm to 1 cm, while light grey beds range in thickness from 0.5 cm to 1.5 cm. Clay and silt beds are in groups of 2 to 3. In subunit IVc, from 216 cm to 189 cm, the dark grey beds are thicker, ranging from 0.3 cm to 2 cm thick. Light grey bed thickness ranges from 0.5 cm to 1 cm. This subunit also has groups of 3 to 5 light and dark grey beds. In the subunit IVd, from 189 cm to 118 cm, dark grey beds range in thickness from 0.5 cm to 5 cm and light grey beds range in thickness from 0.5 cm to 1.5 cm. Beds are grouped in sets of 3 to 5. In subunit IVe, from 118 cm to 90 cm, dark grey bed thickness ranges from 0.5 cm to 1 cm and light grey bed thickness ranges from 1 cm to 1.5 cm. Dark and light grey beds also occur in groups of 2 to 3. Lastly, from 90 cm

to the top of the core (subunit IVf), the dark grey beds range in thickness from 1 cm to 2 cm. The light grey beds are similar, ranging in thickness from 0.5 cm to 2 cm. Dark and light grey beds occur in groups of 2 to 3. Overall, the lower contacts of the dark grey beds are sharp and the upper contacts are gradational in the upper 256 cm.

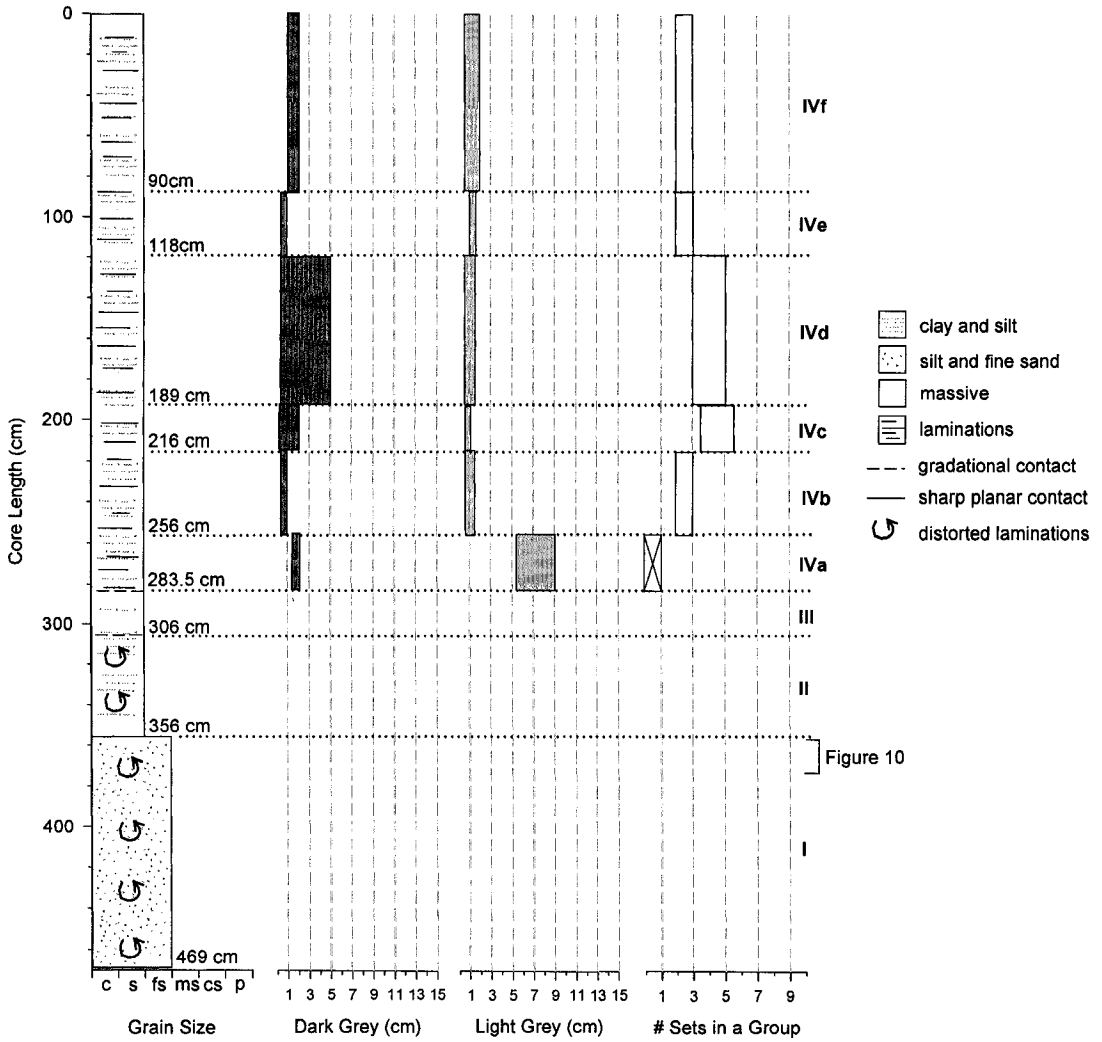

Figure 11: PAD 54 VC2 (proximal site) sedimentological structures, estimated grain size, the range of bed thicknesses of dark and light grey alternating clay beds, and the number of sets of dark and light grey clay and silt beds in a group. The box containing the x in the right-hand plot indicates that the beds were not grouped in this subunit.

PAD 54 VC1 (Intermediate core)

The length of core recovered from the intermediate site (VC1) is 537 cm. The total length of core tube used is 544 cm. Therefore, there is 7 cm of sediment compaction, or 98.7% core retrieval. This core is also disturbed by the vibracoring technique in the upper 300 cm and particularly in the top 20 cm, but it is not as severe as in PAD 54 VC2. This vibracore contains primary inorganic structures such as laminated and massive sediments. PAD 54 VC2 contains fine-grained alternating dark and light grey laminated clay and silt, from the base of the core (537 cm) to 428 cm, which is overlain by 68 cm of coarse-grained sand. The upper 360 cm consist of alternating dark and light grey laminated clay and silt.

The stratigraphic profile is graphically represented in Figure 12. Unit I, from the base of the core (537 cm) to 428 cm, contains clay and silt. Although these sediments are laminated, the colour changes are generally not as obvious as in the upper portions of this core and PAD 54 VC2 (see photographs from PAD 54 VC2 from 537 cm to 428 cm in Appendix A). Dark grey beds range in thickness from 0.1 cm to 1.5 cm, while light grey beds range in thickness from 0.1 cm to 10 cm. This sequence is interrupted by a black deposit, from 525.5 cm to 525 cm, that has a sharp irregular upper contact and a gradational lower contact (Figure 13). There are two well-defined, very light grey beds from 507.7 cm to 507 cm and 493 cm to 492.5 cm (Figure 14). A second black deposit is visible from 473 cm to 472.5 cm. In unit I, the clay and silt beds are grouped into sets of 1 to 10 beds. This range of sets in this subunit is unlike those of other units and subunits in this core and other cores from both PAD 54 and PAD 15. Unit II (428 cm to 360 cm) consists of a massive fine- to medium-grained sand deposit. Although there are faint

colour changes, there are no visible sedimentary structures. The lower contact of this sediment bed is notably sharp while the upper contact is diffuse (Figure 15).

From 360 cm to the top of the core (unit III), the sediment consists of alternating dark and light grey laminated clay and is divided in subunits (a-f). In subunit IIIa, from 360 cm to 232.5 cm, dark grey beds range in thickness from only 0.5 cm to 2 cm, while light grey beds range in thickness from 0.5 cm to 10 cm. The dark grey beds have sharp planar lower contacts and diffuse upper contacts. The clay and silt beds are in groups of 3 to 5. In subunit IIIb, from 232.5 cm to 184 cm, dark grey beds range in thickness from 0.5 cm to 3 cm, and light grey beds range in thickness from 1 cm to 2 cm. The dark grey beds also have sharp planar lower contacts and gradational upper contacts in this unit. The beds are generally grouped in sets of 2 to 5. From 184 cm to 144 cm (subunit IIIc), the dark grey beds have a wider range of bed thicknesses, from 0.5 cm to 8 cm. The light grey beds range in thickness from 0.5 cm to 1.5 cm. The dark grey beds have sharp lower contacts and diffuse upper contacts. The beds are grouped in sets of 3 to 5. In subunit IIId, from 144 cm to 100 cm, the dark grey beds range in thickness from 0.5 cm to 3 cm and light grey beds range in thickness from 1 cm to 2 cm. The beds occur in groups of 2 to 4. Subunit IIIe, from 100 cm to 72.5 cm, consists of dark grey beds ranging in thickness from 0.3 cm to 0.5 cm, and light grey beds ranging in thickness from 0.5 cm to 1 cm. The beds are not grouped and simply alternate. Subunit IIIf is defined from 72.5 cm to the top of the core. The dark and light grey beds both range in thickness from 0.5 cm to 2 cm. The beds are grouped into sets of 2 to 3. In subunits IIId to IIIf, the upper and lower contacts of the dark grey beds are generally diffuse.

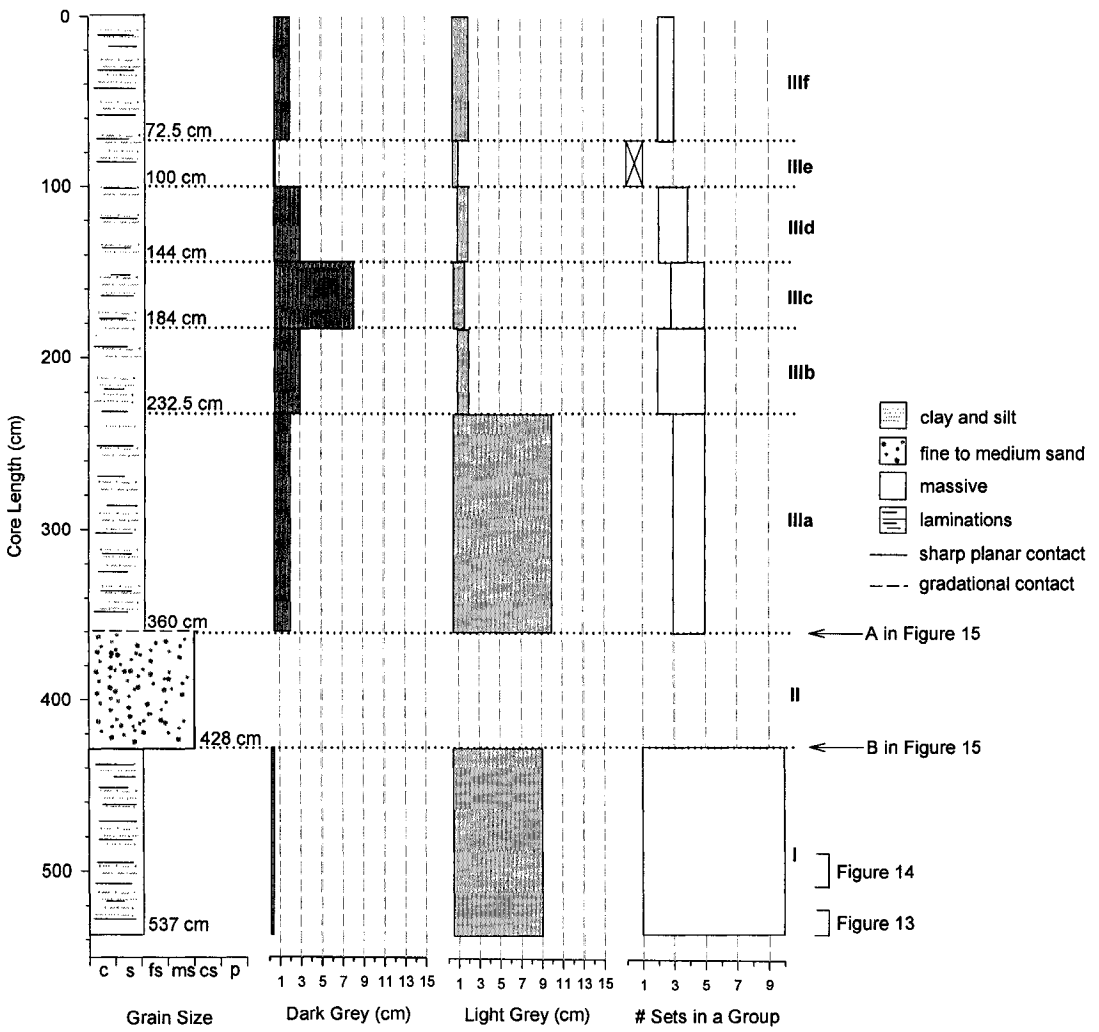

Figure 12: PAD 54 VC1 (intermediate site) sedimentological structures, estimated grain size, the range of bed thicknesses of dark and light grey alternating clay and silt beds, and the number of sets of dark and light grey clay and silt beds in a group. Note that the box in the right-hand plot containing an x indicates that the beds were not grouped in that subunit.

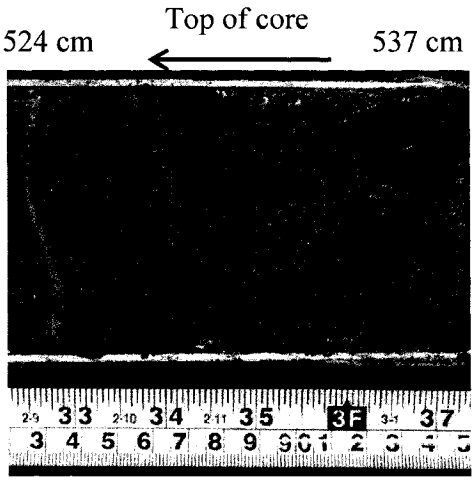

Figure 13: Irregular contact in unit I of PAD 54 VC1 (intermediate site).

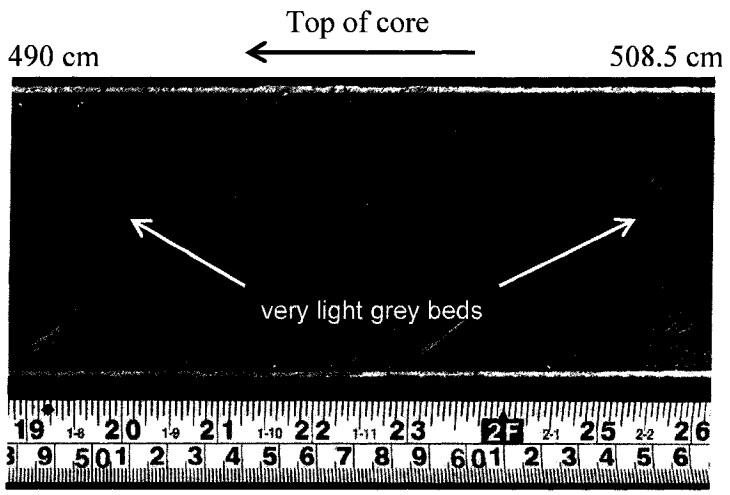

Figure 14: Well-defined, very light grey clay beds in unit I of PAD 54 VC1 (intermediate site).

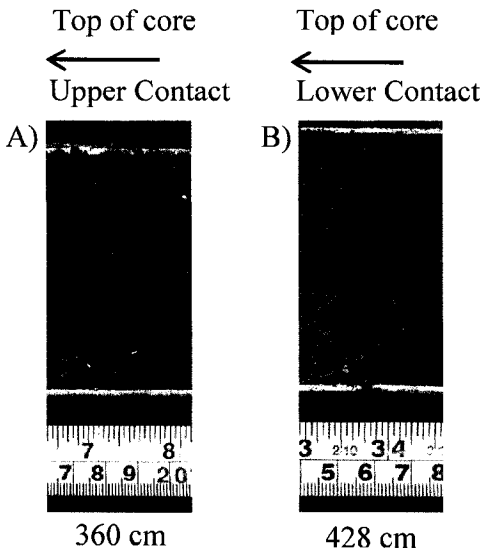

Figure 15: A) Diffuse upper and B) sharp lower contacts of the sandy deposit in unit II in PAD 54 VC1 (intermediate site).

PAD 54 VC3 (Distal core)

The sediment recovered from the distal site at PAD 54 is 660.5 cm long. Sediment compaction cannot be calculated at this site because the core tube length was not measured prior to cutting the core into sections for shipment from the field. However, it is reasonable to assume that compaction is similar to other cores from this site (7 cm to 10 cm, or approximately 98% core recovery). The bottom of the first section (0 cm to 100 cm) and the top of the second section (100 cm to 232 cm) of the core had been sealed with duct tape and not plastic end caps, causing the sediment to dry out, crack, and expand. The third section of this core (from 232 cm to 332 cm) was also in poor condition because during transport or storage, the cap came off of the top of the core tube, causing the upper 10 cm (232 cm to 332 cm) to dry out and crack. There is significant sediment draping in the upper 150 cm because of the vibracoring technique.

Similar to the other two cores in this site, this vibracore contains generally coarser-grained material (660.5 cm to 288.5 cm) overlain by alternating dark and light grey laminated clay and silt (288.5 cm to top of core).

The stratigraphic profile of PAD 54 VC3 is represented in Figure 16. Unit I, from the base of the core (660.5 cm) to 629.5 cm, consists of silt and fine sand with thin discontinuous black lenses (from 649.5 cm to 629.5 cm, Figure 17). From 629.5 cm to 620.5 cm (unit II) sediments consist of a fine- to medium-grained sand deposit with relatively small clay rip-up clasts (long axes 1 cm to 3 cm, short axes 0.5 cm, Figure 18). Unit III, from 620.5 cm to 484.5 cm, consists generally of massive silt and fine sand with thin discontinuous black lenses (513 cm to 484.5 cm, Figure 19). Unit IV contains fine- to medium-grained sand with several relatively large clay rip-up clasts from 484.5 cm to 464.5 cm (long axes from 1 cm to 4 cm, short axes from 0.5 cm to 1.5 cm, Figure 20) and a coarse sand deposit from 464.5 cm to 462.5 cm with sharp planar upper and lower contacts. Unit V, from 464.5 cm to 422.5 cm, contains light grey clay and silt from 464.5 cm to 440.5 cm, dark grey clay and silt from 440.5 cm to 428.5 cm, and light grey clay and silt from 428.5 cm to 422.5 cm. The dark grey clay and silt deposit has a gradational upper contact and a sharp irregular lower contact. As in PAD 54 VC1, there is a massive sandy deposit from 422.5 cm to 288.5 cm (unit VI) with a sharp planar lower contact and a diffuse upper contact. At a depth of 389.5 cm, there is black material that is possibly organic. In addition, unit VI contains an oblong clay rip-up clast (long axis 4.5 cm, short axis 3 cm), from 368 cm to 363.5 cm, with two smaller clasts above it (long axes 0.6 cm, short axes 0.3 cm, Figure 21).

From 288.5 cm to the top of the core, the stratigraphic units are less variable in sedimentary structure and grain size and consist of alternating light and dark grey clay and silt laminations. Unit (VII) has been divided into 2 subunits according to bed thickness, bed contacts, and sediment sequences. Unit VIIa, from 288.5 cm to 146.5 cm, has dark grey beds ranging from 0.5 cm to 1 cm thick, and light grey beds ranging from 1 cm to 3.5 cm thick. Dark grey beds in this zone generally have diffuse upper and lower contacts. There are three sharp irregular clay and silt bed contacts at 201.5 cm, 194 cm, and 193 cm (Figure 22). These are similar in shape to the contact observed in unit I of PAD 54 VC1 (525 cm, Figure 13). The beds are in groups of 3 to 5 in this subunit. In subunit VIIb, from 146.5 cm to the top of the core, the dark grey beds range in thickness from 0.5 cm to 2 cm and the light grey beds range in thickness from 0.5 cm to 1 cm. The dark grey beds generally have sharp lower contacts and diffuse upper contacts. The beds occur in groups of 3 to 5 in this unit.

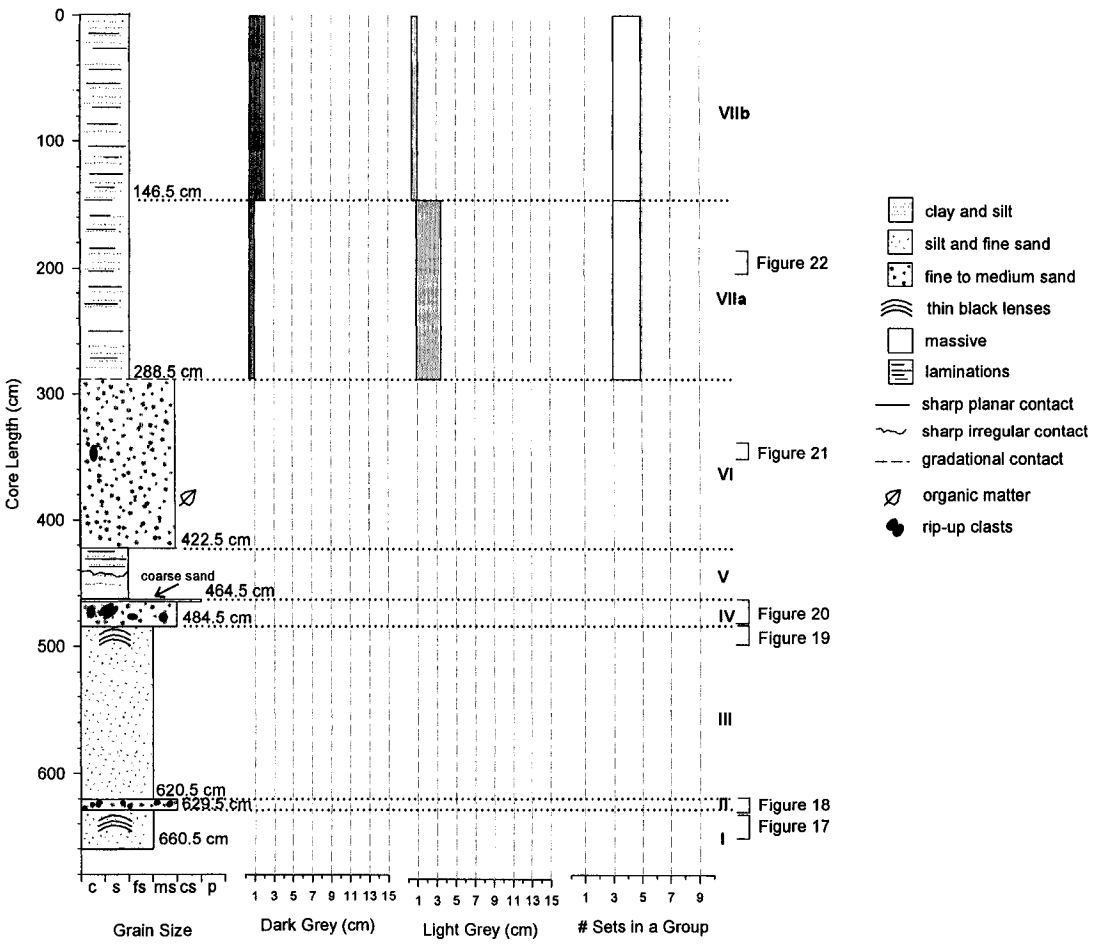

Figure 16: PAD 54 VC3 (distal site) sedimentological structures, estimated grain size, the range of bed thicknesses of dark and light grey alternating clay and silt beds, and the number of sets of dark and light grey clay and silt beds in each group. Note that the symbols for thin black lenses, organic matter, and rip-up clasts are not to scale.

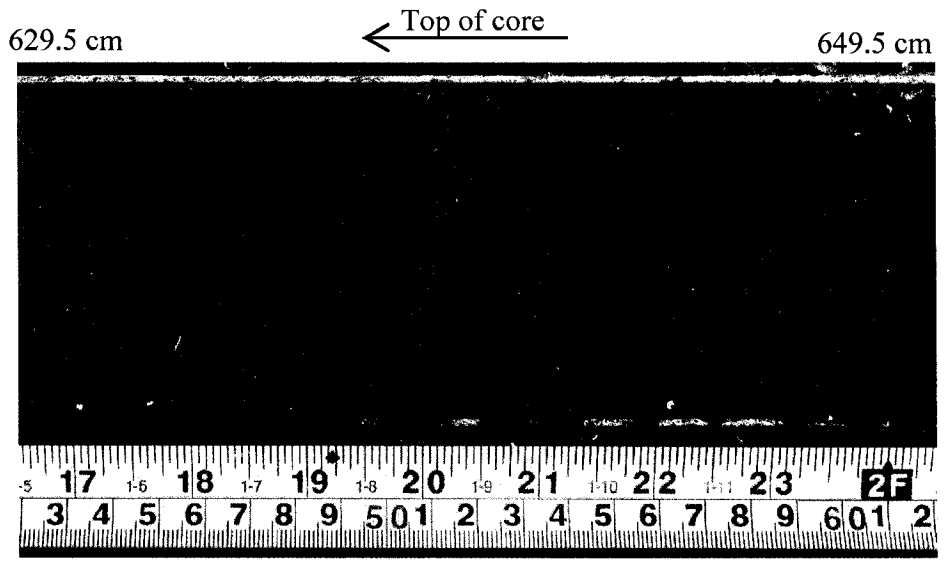

Figure 17: Thin discontinuous black lenses in PAD 54 VC3 (distal site).

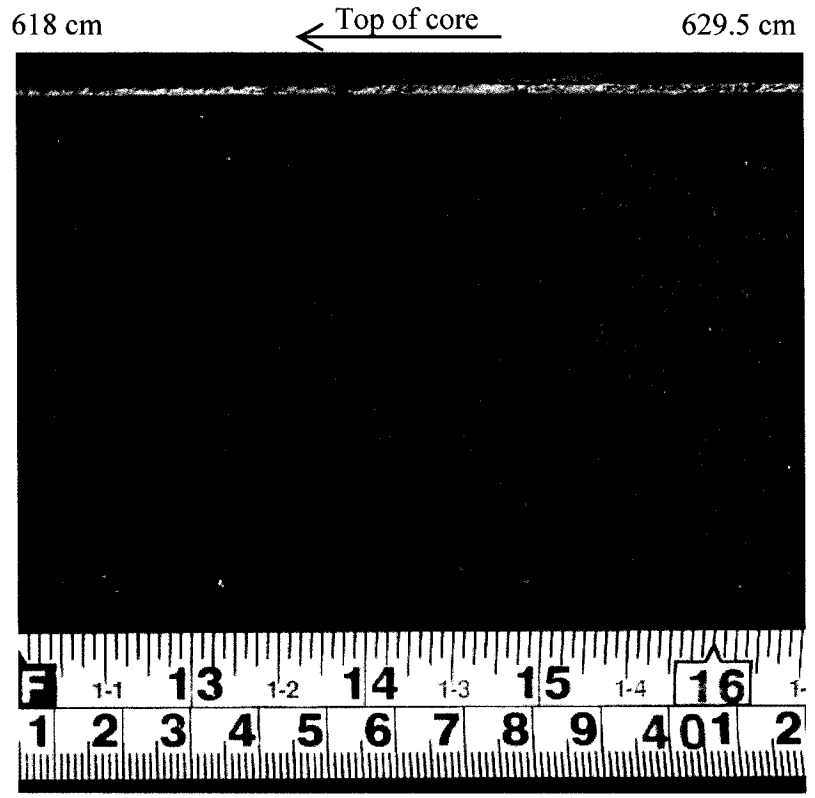

Figure 18: Relatively small rip-up clasts in PAD 54 VC3 (distal site).

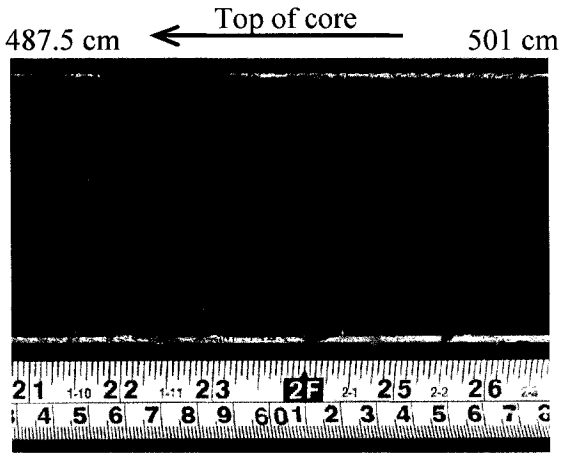

Figure 19: Thin discontinuous black lenses in PAD 54 VC3 (distal site).

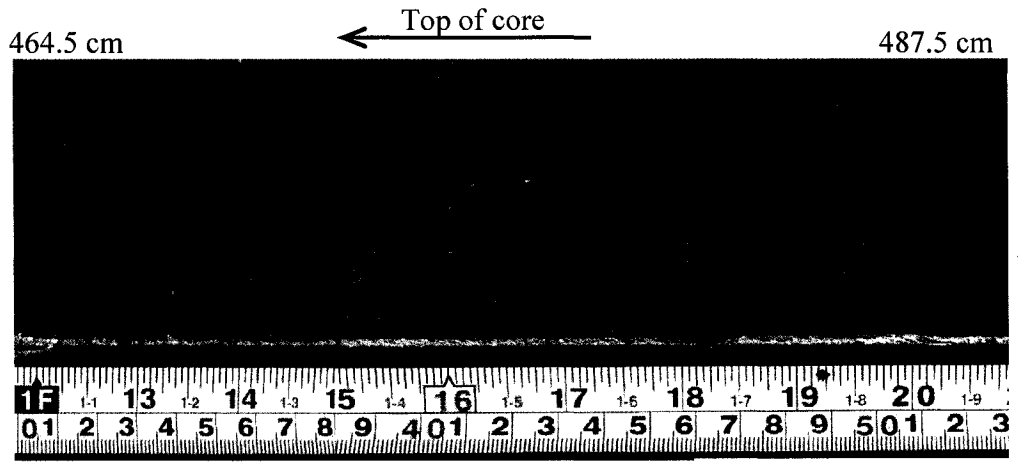

Figure 20: Relatively large rip-up clasts in PAD 54 VC3 (distal site).

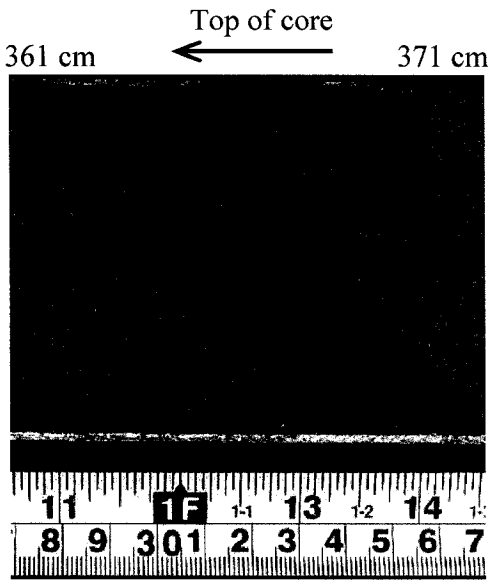

Figure 21: Rip-up clasts in PAD 54 VC3 (distal site).

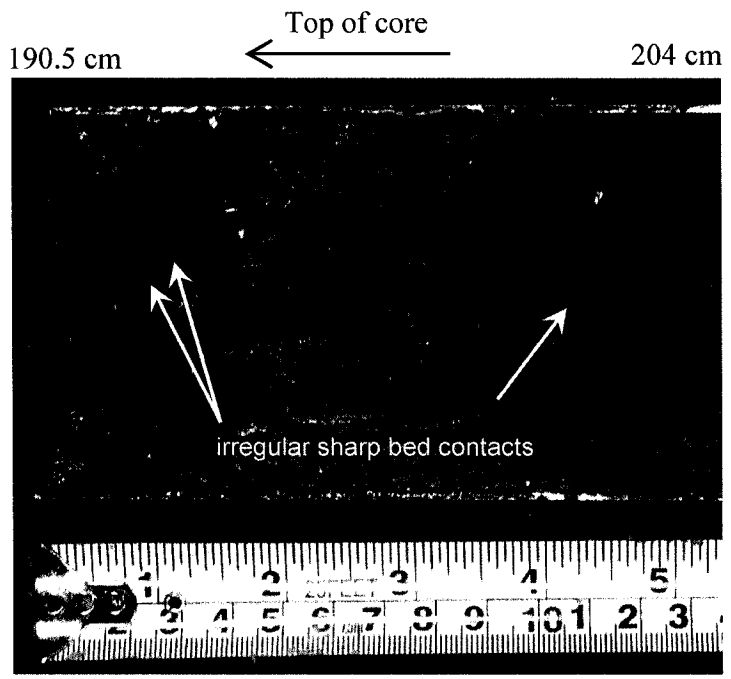

Figure 22: The sharp irregular contacts in PAD 54 VC3 (distal site).

PAD 15 VC1 (Proximal core)

The sediment recovered from PAD 15 VC1 is 733 cm long. No field measurements are available to calculate core compaction or % core retrieval. Methane escaped from the hole that had been augered in the ice and several amphipods were visible. The sediment was extremely moist, with the sound of moving water audible before core sections were split from 341 cm to 0 cm. Water flowed out of the core tube after the first cut was made with the circular saw. There is also significant sediment draping in the upper 200 cm due to vibracoring. This core contains primary inorganic sedimentary structures such as laminated and massive sediments. Similar to all of the cores collected in PAD 54, the lower portion of the core (733 cm to 370 cm) generally consists of coarse-grained sediments including coarse sand and pebbles, and is overlain by fine-grained clay and silt deposits. This core has the coarsest sediment of all of the cores collected from both PAD 54 and PAD 15. In addition, VC1 contains significantly higher amounts of organic matter in the lower stratigraphic units when compared to all the other cores from PAD 54 and PAD 15.

Figure 23 illustrates the stratigraphic details in PAD 15 VC1. Unit I, from the base of the core (733 cm) to 710.5 cm, consists of laminated clay and silt. From 716.5 cm to 710.5 cm, there is a very light grey clay and silt deposit that is similar in colour to the two very light grey deposits found in PAD 54 VC1 at 507.7 cm to 507 cm and 493 cm to 492.5 cm (Figure 14). In general, the laminations are visible but disturbed, likely due to rigid core catchers at the base of the tube. The dark grey beds are 0.5 cm to 1 cm thick, and light grey beds are 0.5 cm to 2 cm thick. Beds are grouped in sets of 2 to 4. The upper contact of this unit is irregular. Unit II, from 710.5 cm to 594.5 cm, contains silt

and fine sand, and several other features including coarse sand and pebbles from 700.5 cm to 697.5 cm, and clay and silt beds from 654 cm to 653.5 cm, 646 cm to 644 cm, 631.5 cm to 626.5 cm, and 617.5 cm to 613.5 cm. A notably large branch with bark still remaining occurs from 610 cm to 604.5 cm. Small fragments of woody debris are visible 712.5 cm to 711.5 cm, 694 cm to 693.5 cm, 672 cm to 671 cm, 662 cm to 661 cm, 652 cm to 651.5 cm, and 635 cm to 632.5 cm. The grain size increases to medium- to coarse-grained sand from 594.5 cm to 567 cm in unit III, with a thin clay deposit from 581.5 cm to 578 cm. From 567 cm to 370 cm (unit IV), there is massive silt and fine sand. Faint colour changes are visible but there are no apparent sedimentary structures. In addition, there is a tree branch at 564.5 cm (diameter is 1.5 cm, no bark). There are thin black lenses from 562 cm to 551 cm and 536 cm to 529.5 cm. In addition, there are thin clay and silt laminations from 520 cm to 512 cm, with each bed being 0.2 cm to 0.5 cm thick (Figure 24). Grain size increases from 540.5 cm to 537 cm, with fine- to medium-grained sand overlain by a 0.5 cm clay and silt bed.

As previously stated, the upper 370 cm consist of clay and silt. From 370 cm to 339.5 cm, unit V, the sediment is massive and dark grey. There are no visible sedimentary structures or colour changes. The upper and lower bed contacts of unit V are gradational. Unit VI, from 339.5 cm to the top of the core, has been divided into subunits according to bed thickness, bed contacts, and sediment sequences. In subunit IVa (339.5 cm to 218.5 cm), dark grey beds range in thickness from 0.5 cm to 1.5 cm, and the light beds range in thickness from 1.5 cm to 8 cm. These beds are in groups of 3 to 6. The upper and lower contacts in this subunit are generally gradational. However, some of the relatively thick dark grey beds had sharp lower contacts and gradational upper contacts. From 326 cm to

305 cm, the sediments were significantly disturbed during core splitting and are therefore difficult to visually describe. Laminations can be seen above and below the disturbed portion and the dominant colour is light grey. From 218 cm to 131.5 cm (subunit VIb), the dark grey beds range in thickness from 0.5 cm to 5 cm, and the light grey beds range in thickness from 0.5 cm to 2 cm. These beds are in groups of 2 to 7. Unit VIc, from 131.5 cm to the top of the core, contains dark grey beds ranging from 0.5 cm to 3 cm thick, and light grey beds ranging from 0.3 cm to 1 cm thick. The beds are grouped in sets of 3 to 6. The dark grey beds in unit VIb and VIc have sharp lower contacts and diffuse upper contacts.

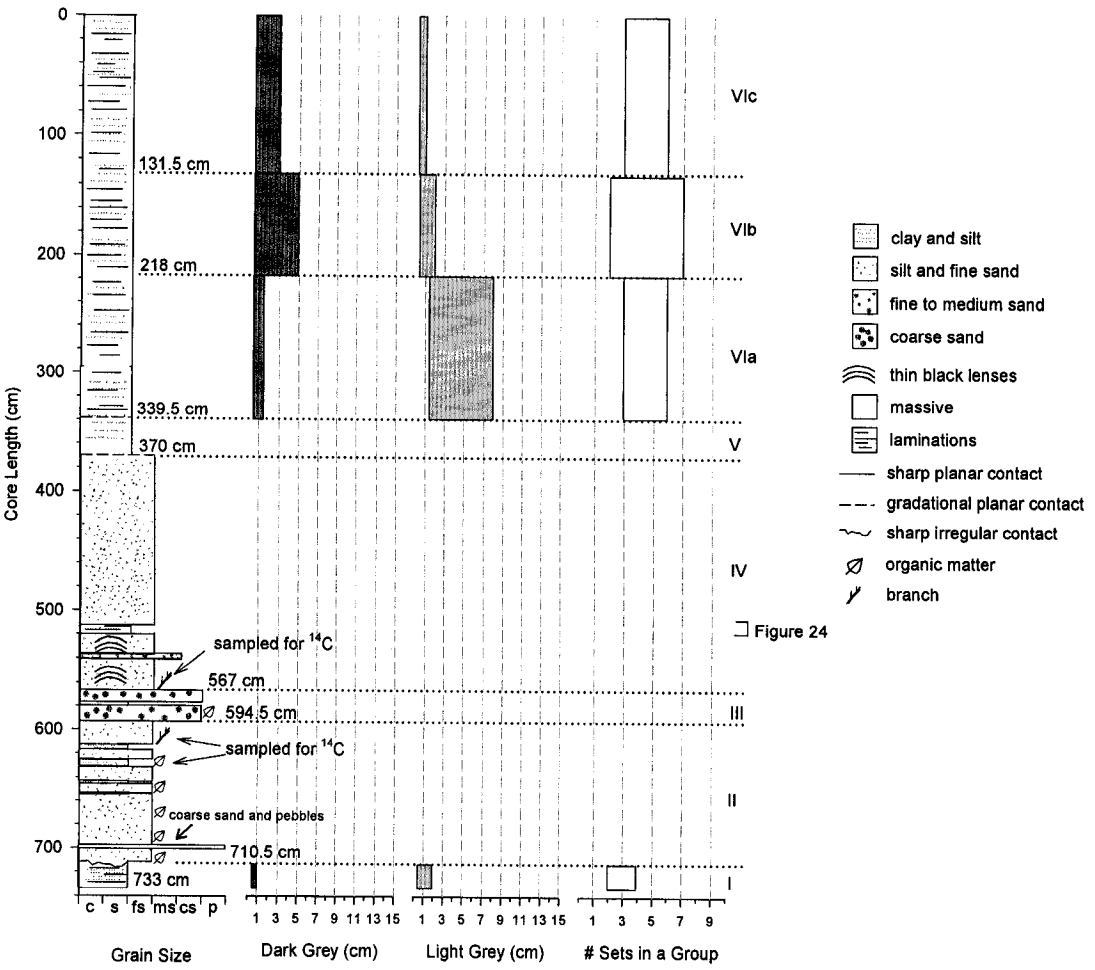

Figure 23: PAD 15 VC1 (proximal site) sedimentological structures, estimated grain size, the range of bed thicknesses of dark and light grey alternating clay and silt beds, and the number of sets of dark and light grey clay and silt beds in each group. Note that symbols for thin black lenses, organic matter, and branches are not to scale.

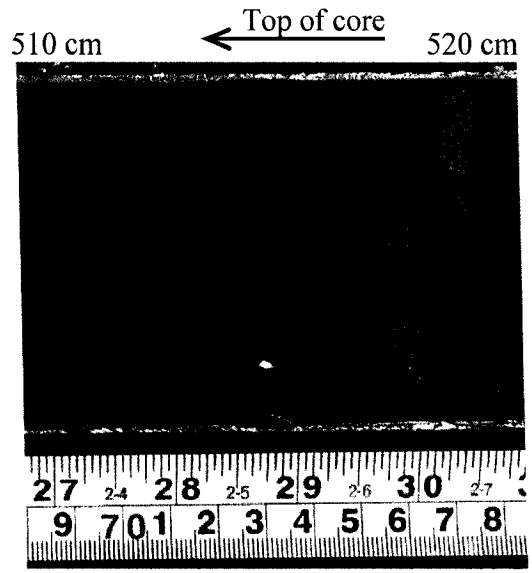

Figure 24: Clay and silt laminations in PAD 15 VC1 (proximal site) in unit IV.

PAD 15 VC2 (Intermediate core)

The core recovered from the intermediate site at PAD 15 is 693 cm long. Similar to PAD 15 VC1, this core seemed to be saturated, with water flowing out of the core tube as it was turned 180° during splitting of the upper 337 cm. Challenges encountered during core splitting caused a great amount to disturbance to the upper 150 cm of sediment. There is also significant draping in the upper 200 cm of core. This core contains primary inorganic laminated and massive sedimentary structures. The lower 322 cm of coarser-grained sediment (sand) is overlain by 371 cm of fine-grained sediment (clay and silt). In portions where the clay and silt are laminated, the bed contacts are generally diffuse, and the bed thicknesses of both the dark and light grey clay laminations are thinner than in other cores from both PAD 54 and PAD 15.

The stratigraphic profile is shown in Figure 25. Unit I, from the base of the core (693 cm) to 502 cm, consists of generally massive silt and fine sand with several other features. There are thin deposits of laminated silt and clay from 683.5 cm to 678.5 cm and 595.5 cm to 594.5 cm. Grain size increases to fine to medium sand from 545.5 cm to 541 cm. In addition, there is organic debris from 590 cm to 589 cm, 581 cm to 580.5 cm, 546 cm to 545.5 cm, 542.5 cm to 542 cm, 529 cm to 527 cm, and 525 cm to 524 cm, and several black lenses from 578 cm to 549 cm. Unit II, from 502 cm to 424 cm, consists of clay and silt. There are slightly finer-grained laminated clay and silt beds from 502 cm to 493 cm, 479 cm to 469 cm, and 464 cm to 461 cm (Figure 26). The upper and lower contacts of these clay and silt beds are generally diffuse. From 447.5 cm to 445.5 cm, thin discontinuous black lenses are visible. There is also organic debris from 486 cm to 485 cm. In unit III, from 424 cm to 409 cm, the sediment is fine-grained massive clay and silt. These sediments are slightly less gritty when compared to the clay and silt deposit in unit II, suggesting that there is a relatively higher amount of clay or less silt. In unit IV, from 409 cm to 371 cm, the sediment consists of massive silt and fine sand. Both the upper and lower bed contacts are sharp. In addition, there are thin black lenses from 409 cm to 405 cm.

In unit V, from 371 cm to 196 cm, the sediment is dark grey and massive. Within this massive deposit there are light grey clay and silt deposits that are slightly less gritty than adjacent sediment. They occur from 371 cm to 370 cm, 323 cm to 320.5 cm, 259 cm to 256 cm, and 242.5 cm to 240.5 cm. These deposits generally have sharp upper contacts and diffuse lower contacts. Unit VI (from 196 cm to the top of the core) is laminated and divided into subunits according to bed thickness, bed contacts, and laminae sequences.

This unit is generally less gritty than underlying sediments, suggesting that it contains more clay or relatively less silt. From 196.5 cm to 80.5 cm (subunit VIa), the dark grey beds are relatively thin, ranging in thickness from 0.5 cm to 1.5 cm and the light grey beds are thicker, ranging in thickness from 1 cm to 4 cm. From 173 cm to 163 cm there is a black organic deposit. All of the bed contacts within the upper sediments are diffuse. In unit VIb, from 80.5 cm to the top of the core, dark grey beds range in thickness from 0.5 cm to 2 cm, and light grey beds range in thickness from 0.3 cm to 1 cm. The beds in both of these subunits occur grouped in sets of 2 to 3.

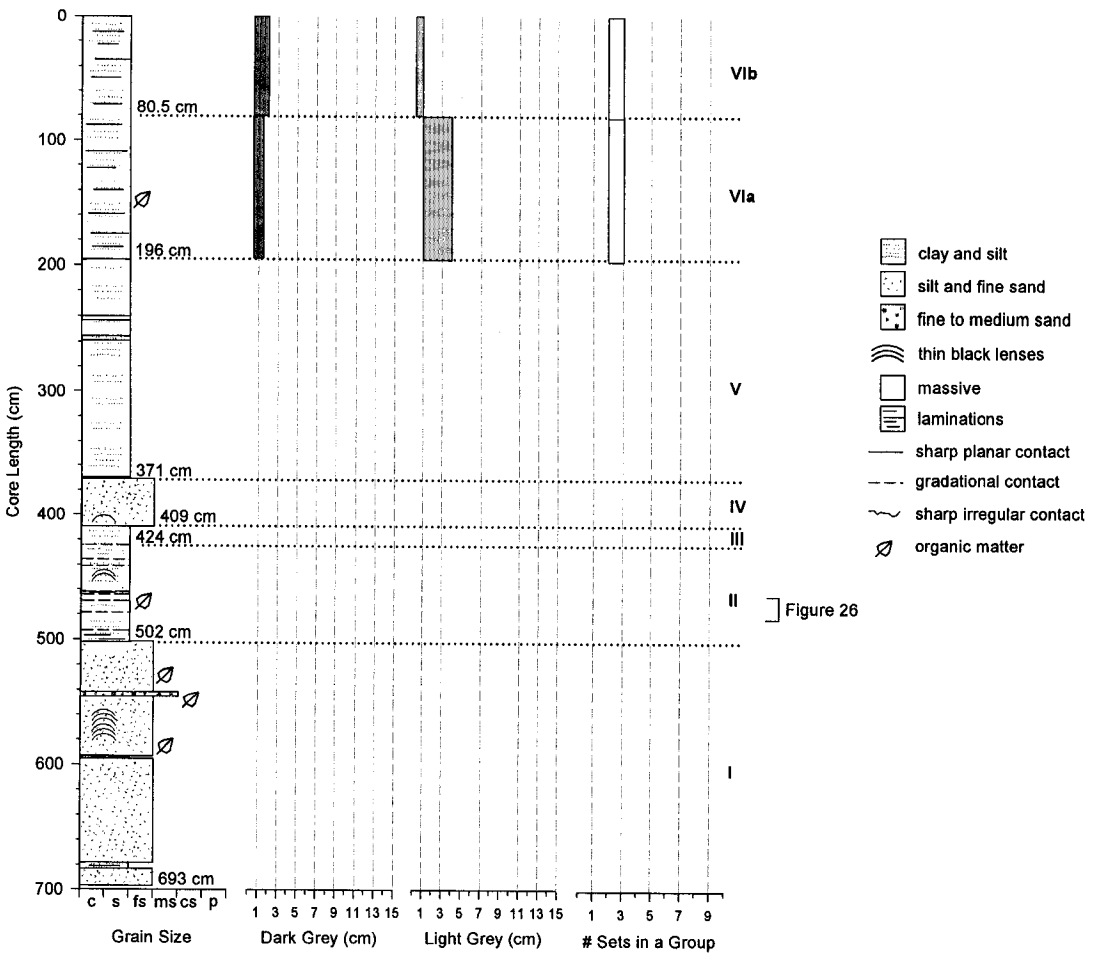

Figure 25: PAD 15 VC2 (intermediate site) sedimentological structures, estimated grain size, the range of bed thicknesses of dark and light grey alternating clay and silt beds, and the number of sets of dark and light grey clay and silt beds in each group. Note that symbols for thin black lenses and organic matter are not to scale.

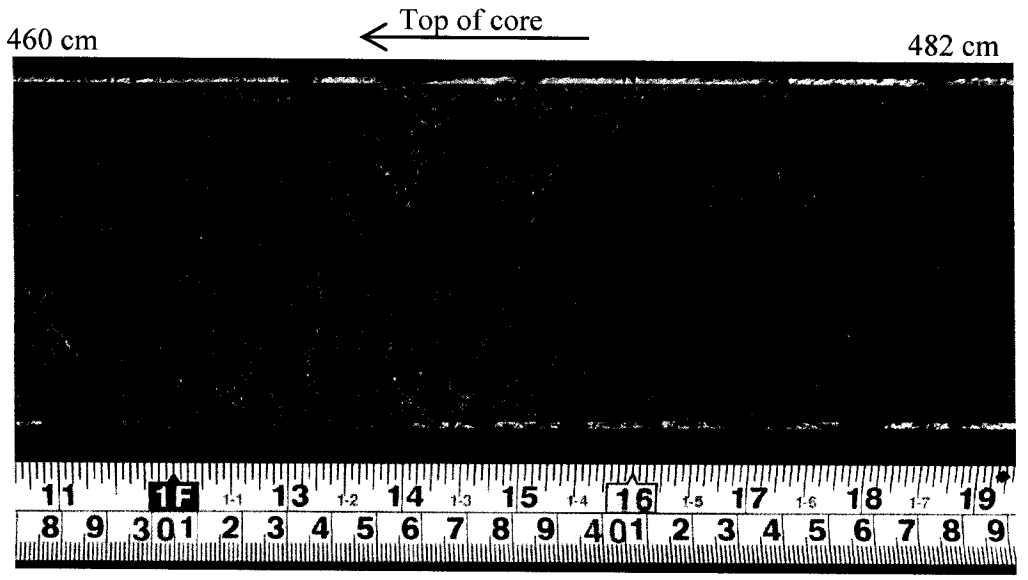

Figure 26: Laminated clay and silt beds with diffuse upper and lower contacts in PAD 15 VC2 (intermediate site).

PAD 15 VC3 (Distal core)

The sediment recovered from PAD 15 VC3 is 530 cm long. Core compaction could not directly be estimated from field notes as the core tube was not measured prior to shipment and stratigraphic documentation (see chronology of the distal site in the results section for estimates of offset between the gravity core and vibracore). As in VC1 (proximal site) and VC2 (intermediate site) of PAD 15, water came flowing out of the core tube in the upper 329 cm as the core tube was being cut and rotated 180°. The two halves of the first section (from 0 cm to 129 cm) were difficult to separate because of the high water content holding the sediment together. There is also evidence of gas bubbles in the upper 329 cm and significant sediment draping in the upper 361.5 cm due to the coring technique. This core contains primary inorganic sediment structures (laminations and massive sediments). Overall, the beds are consistently thinner than beds from any of

the cores from PAD 54 and PAD 15. Unlike other cores from PAD 54 and PAD 15, it consists entirely of clay and silt. In addition, from the base of the core to 350 cm, the clay laminations are well-defined, and the lower contacts of the dark grey beds are consistently sharp, while the upper contacts are generally diffuse (Figure 27). These well-defined laminations are not observed in any of the other cores from PAD 54 and PAD 15.

Figure 28 shows the sedimentological characteristics of PAD 15 VC3. Unit I, from the base of the core (530 cm) to 350 cm, contains unique, well-defined clay and silt laminations and has been divided into subunits (Ia to Ig), according to bed thickness, bed contacts, and laminae sequences. Subunit Ia, from the base of the core (530 cm) to 509 cm, consists of dark grey beds from 0.2 cm to 2.5 cm thick and light grey beds from 0.1 cm to 0.5 cm thick. The beds are grouped in sets of 4 to 6. In subunit Ib, from 509 cm to 494 cm, there is a thick dark grey deposit with 3 highly distorted light grey beds that are only 0.2 cm thick (Figure 29). In subunit Ic, from 494 cm to 479 cm, the dark grey beds are relatively thin, ranging from 0.1 cm to 1 cm thick, and the light grey beds remain relatively consistent, 0.4 cm to 0.6 cm thick. From 479 cm to 456.5 cm, subunit Id, the dark grey beds are relatively thick, ranging from 0.5 cm to 4 cm, and light grey beds are 0.4 cm to 0.6 cm thick. The beds in subunits Ic and Id are not grouped. Subunit Ie, from 456.5 cm to 403 cm, has both dark and light grey beds that range in thickness from 0.4 cm to 1 cm. This subunit has groups of 2 to 4 beds. Subunit If, from 403 cm to 388.5 cm, contains dark grey beds ranging from 0.1 cm to 1 cm thick and light grey beds that are from 0.3 cm to 1 cm thick. The beds are grouped in sets of 2 to 3. Subunit Ig, from

388.5 cm to 350 cm, consists of dark grey beds from 0.5 cm to 3 cm thick, and light grey beds from 0.3 cm to 0.5 cm thick. The beds are not grouped.

Unit II, from 350 cm to 312 cm, consists of a massive dark grey clay and silt bed with no visible bedding structures (Figure 30). Unit III is divided into subunits according to bed thickness, bed contacts, and laminae sequences. Subunit IIIa, from 312 cm to 189.5 cm, contains dark grey beds ranging in thickness from 0.5 cm to 1.5 cm, and relatively thick light grey beds ranging in thickness from 1.5 cm to 15 cm. Most of the light grey beds are 5 cm thick or greater. The thick light grey beds are separated by 1 to 2 relatively thin dark grey beds. The lower contacts of the dark grey beds are sharp and the upper contacts are diffuse. The light grey beds in this subunit are the thickest of any subunit/unit in all of the cores from PAD 54 and PAD 15, and are shown in Figure 31. Subunit IIIb, from 189.5 cm to 177 cm, consists of dark grey beds ranging from 0.5 cm to 1.5 cm thick and light grey beds ranging from 0.5 cm to 2 cm thick. The dark grey beds have sharp lower contacts and diffuse upper contacts. In subunit IIIc, from 177 cm to 148.5 cm, the dark grey beds range in thickness from 0.2 cm to 1.5 cm, and light grey beds range in thickness from 0.2 cm to 1 cm. The upper and lower bed contacts are diffuse. In addition, there is an organic deposit from 149.5 cm to 148.5 cm. The beds are thicker in subunit IIId, from 148.5 cm to 130.5 cm, with dark grey beds 0.4 cm to 4 cm thick, and the light grey beds 2.5 cm to 4.5 cm thick. The lower contacts of the dark grey beds are sharp and the upper contacts are diffuse. In subunit IIIe, from 130.5 cm to the top of the core, the beds are relatively thin and of consistent thickness, with dark and light grey beds ranging in thickness from 0.2 cm to 1 cm. The upper and lower bed contacts are diffuse. The beds from subunits IIIb to IIIe are not grouped.

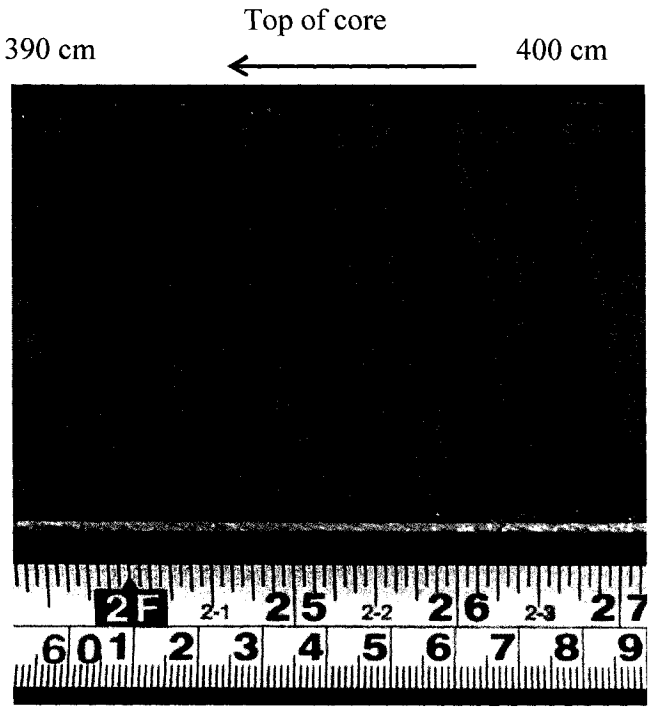

Figure 27: Well-defined clay and silt laminations unique to PAD 15 VC3 (distal site).

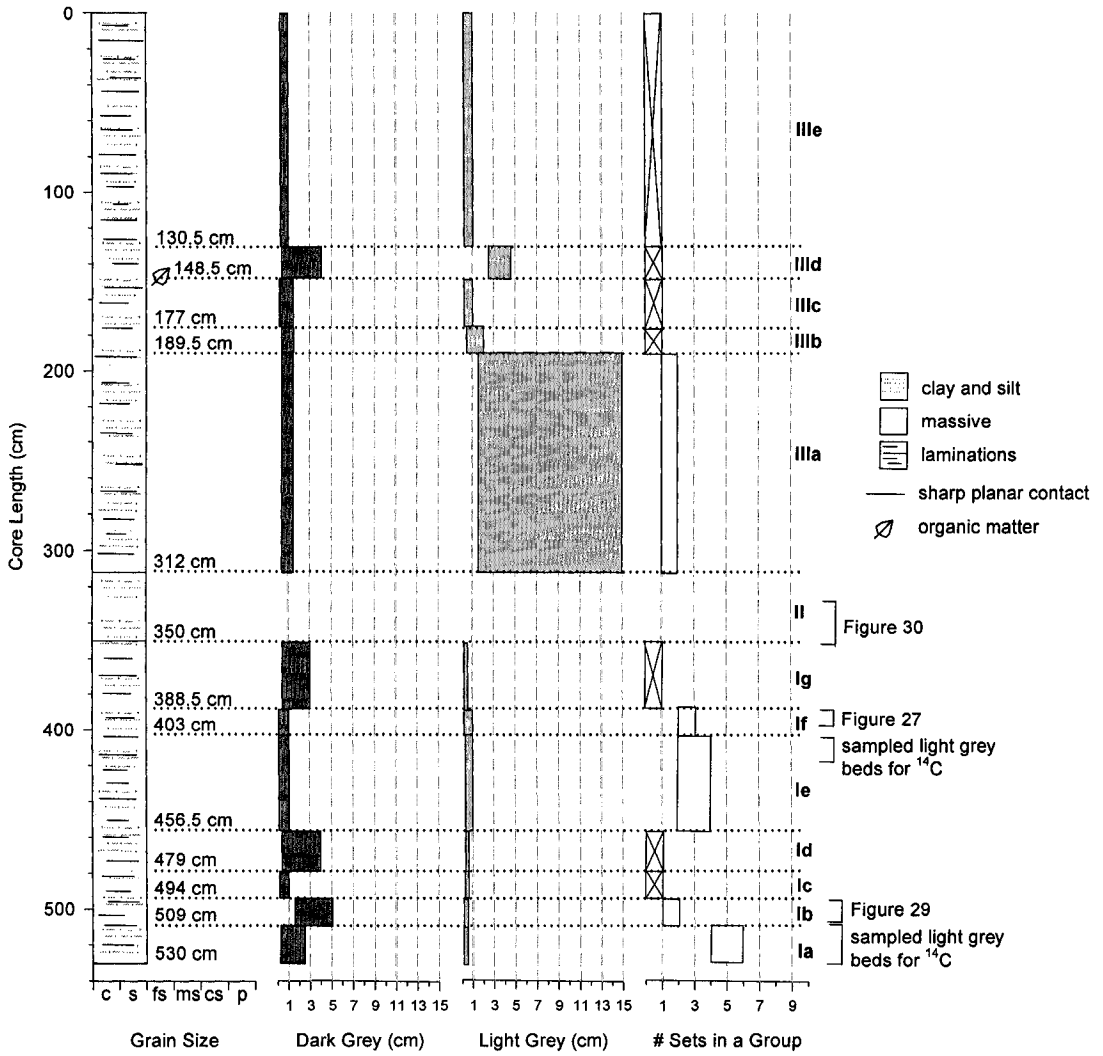

Figure 28: PAD 15 VC3 (distal site) sedimentological structures, estimated grain size, the range of bed thicknesses of dark and light grey alternating clay and silt beds, and the number of sets of dark and light grey clay and silt beds in each group. Boxes that contain an x indicate subunits that are not grouped. Note that the organic matter symbol is not to scale.

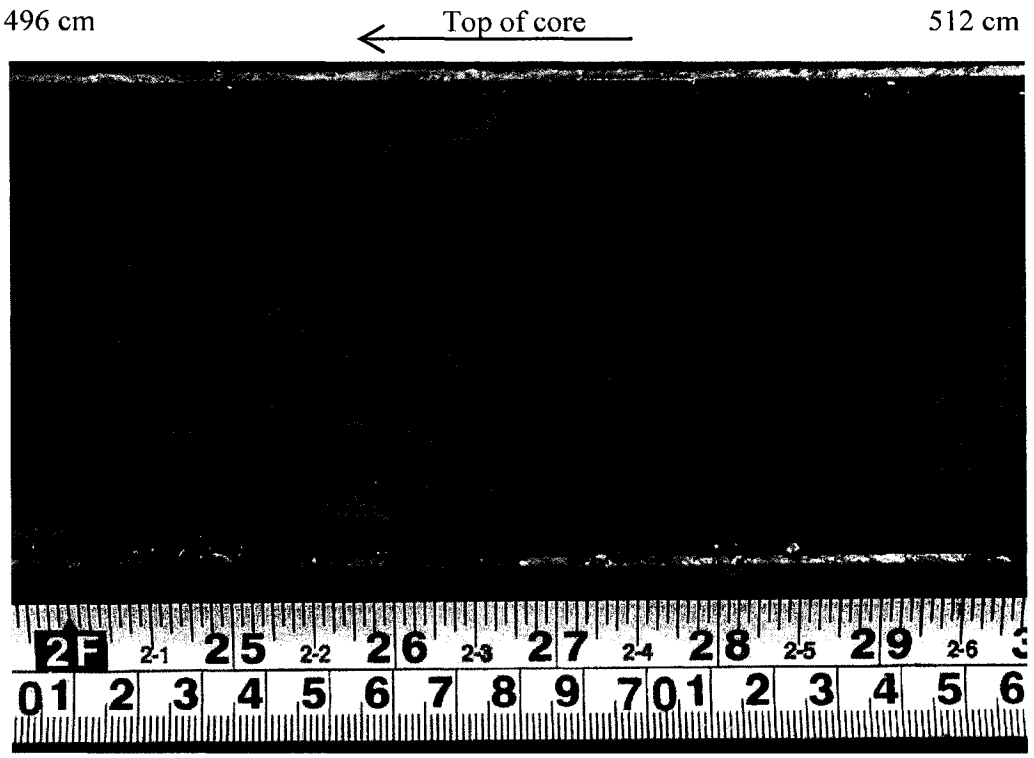

Figure 29: Distorted thin clay and silt laminations in subunit Ib of PAD 15 VC3 (distal site).

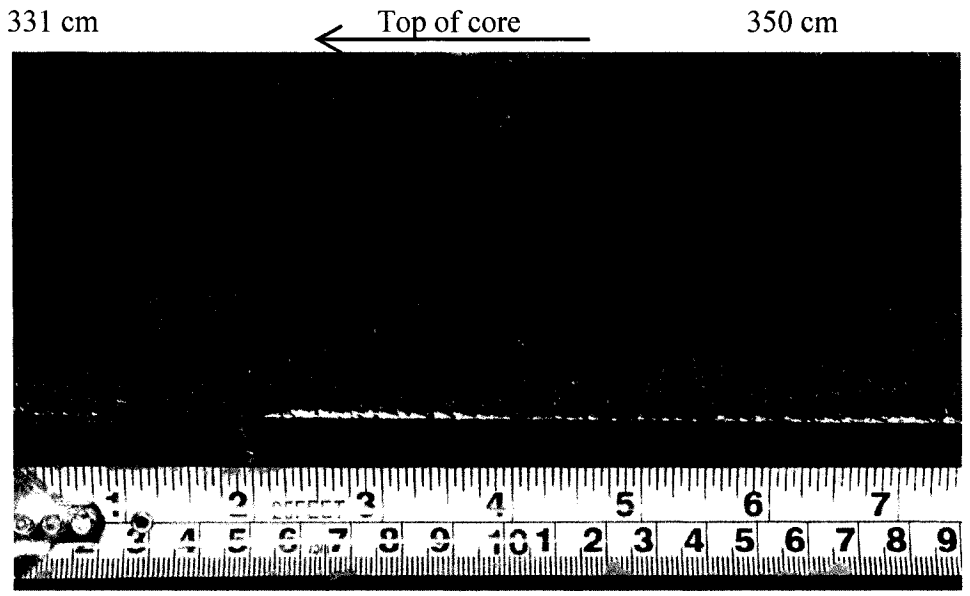

Figure 30: Dark grey massive bed in PAD 15 VC3 (distal site).

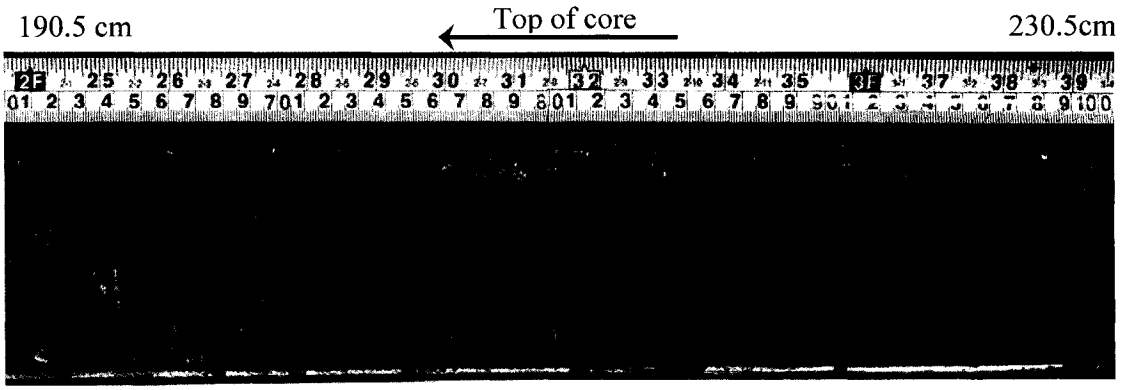

Figure 31: The relatively thick light grey beds in PAD 15 VC3 (distal site) subunit IIIa.

Sediment Chronology and Magnetic Susceptibility

Chronology of PAD 15 VC3 (Distal Site)

The ^{210}Pb profiles for the gravity core and vibracore sediments for PAD 15 VC3 are shown in Figure 32. An ideal ^{210}Pb activity profile would have a smooth curve, with logarithmically decreasing ^{210}Pb activity through time until it approached background (Appleby 2001). In this case, the total ^{210}Pb remained relatively constant with increasing core depth, with an average total ^{210}Pb activity of 0.0472 Bq/g and a range of 0.0292 Bq/g to 0.1073 Bq/g (Appendix B). These values are similar to supported ^{210}Pb measured in other lakes in the PAD by Hall et al. (2004). The concentrations of total ^{210}Pb and supported ^{210}Pb are thus equivalent, indicating that a high sedimentation rate in the oxbow is likely diluting the unsupported ^{210}Pb activity, which negates the use of ^{210}Pb-based dating models. Although similar results could also indicate bioturbation or physical sediment mixing, the intact sediment laminations indicate otherwise. These results are similar to the ^{210}Pb activity (0.0296 Bq/g to 0.1171 Bq/g) previously measured on lake sediments from PAD 15 by Wolfe et al. (2006).

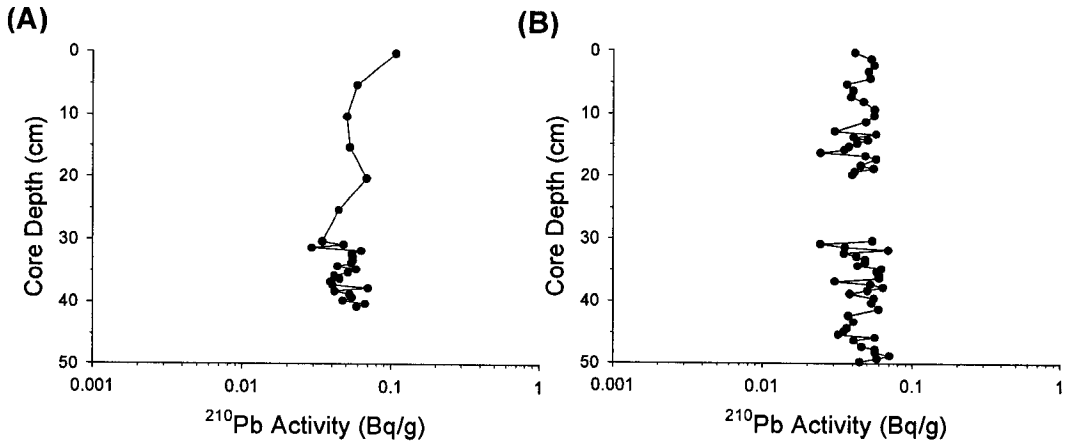

Figure 32: Total ^{210}Pb activity of (A) the gravity core and (B) the vibracore from PAD 15 VC3 (distal site). Only 0 cm to 20 cm and 30 cm to 50 cm were measured in the vibracore, once it was determined that ^{210}Pb dating techniques were not applicable, in order to isolate the ^{137}Cs peak.

In contrast, a well-defined ^{137}Cs peak was found in both the gravity core and the vibracore and interpreted to represent peak atmospheric fallout in AD 1964 (Figure 33, Appendix B). The ^{137}Cs peak was located at 37.75 cm in the gravity core from PAD 15 (distal site). The corresponding ^{137}Cs peak was isolated at 13.75 cm in the vibracore from PAD 15 VC3 (distal site). As a result, the measured vibracore depth was adjusted by shifting the core down 24 cm. Thus, 13.75 cm depth in the vibracore was adjusted to 37.75 cm, the equivalent depth of the ^{137}Cs peak in the gravity core. The offset of the ^{137}Cs peak in the vibracore is likely due to sediment compaction and/or possible sediment rodding during either the positioning of the vibracore tube at the sediment-water interface or during penetration of the vibracore tube. An accurate calculated starting depth in the loose organic sediment or the piston cable not being taut may have caused some of the sediment to be lost. The minor peaks in the gravity core

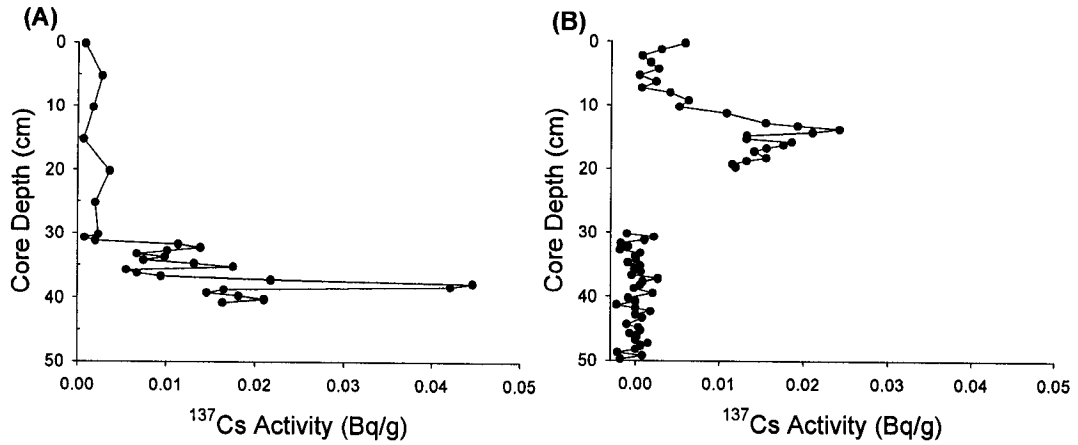

Figure 33: The ^{137}Cs peaks of (A) the gravity core and (B) the vibracore from PAD 15 VC3 (distal site). Only 0 cm to 20 cm and 30 cm to 50 cm were measured in the vibracore in order to isolate the ^{137}Cs peak.

^{137}Cs profile may reflect the input of reworked sediment from post-1964 flood events. ^{137}Cs has been found to be mobile in sediments that are rich in organic content and poor in clay (Longmore 1982, Foster et al. 2006). However, it is unlikely that ^{137}Cs is mobile in this case because the sediment consists of relatively inorganic clay and silt and the interpreted 1964 peak is well-defined.

To obtain chronological control for down-core sediments, two bulk sediment samples of light grey beds from PAD 15 VC3 (distal site) were submitted for ^{14}C dating. The ages of these bulk sediment samples are greater than 20,000 years old (Table 2, Appendix C). At this time the region was covered by the Laurentide Ice Sheet during the most recent glacial maximum in the Wisconsinan glaciation, and the PAD had yet to form (Smith 1994). Therefore, it is likely that the sediment has been contaminated by old

Table 2: Results of bulk sediment samples submitted for radiocarbon dating reported with 1 sigma standard deviation.

Lab Number	Sample	Adjusted Core Depth (+24cm)	Reported Age (^{14}C yr BP)
PAD 15 VC3			
beta-225393	Bulk sediment (light beds only)	427-442	22530±140
beta-225394	Bulk sediment (light beds only)	532-552	22040±130

Note: These ^{14}C yr BP ages could not be calibrated because they exceed the upper range (250 years to ~20,000 years) for radiocarbon age calibration (IntCal04: Calibration Issue of Radiocarbon 46 (3) 2004).

carbon originating from upstream and related to erosion of tar sands by the Wabasca and Peace rivers (Mossop 1980, NRBS 1996, Wolfe et al. 2006). Given the absence of other datable material, a constant sedimentation rate of 0.92 cm/year, based on the 1964 ^{137}Cs peak, was applied to the entire core to establish a preliminary chronology. This resulted in a basal date of AD ~1404 (Figure 34).

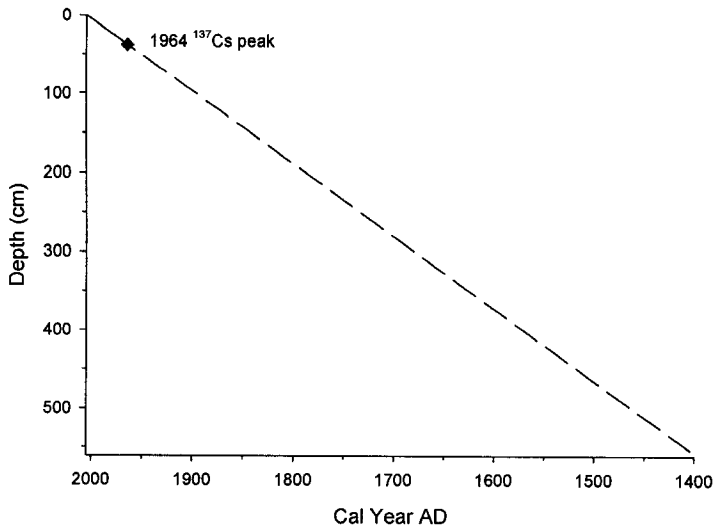

Figure 34: The preliminary linear age-depth profile for the distal site PAD 15 (VC3). Using an average sedimentation rate (0.92 cm/yr) based on the ^{137}Cs peak of 1964, the basal date of this core is AD ~1404.

Magnetic Susceptibility of PAD 15 VC3 (Distal Core)

The magnetic susceptibility profiles of the entire vibracore and gravity core from the distal site (VC3) in PAD 15 are shown in Figure 35, according to both age and core depth. Magnetic susceptibility values have been highly variable over the last approximately 600 years (AD ~1404 to 2005). From AD ~1404 to ~1595 (zone 1), the magnetic susceptibility z-scores are significantly more variable when compared to the entire profile, and are also as a whole, higher than in subsequent zones. The z-scores in this zone range from -0.77 to 3.89. There is a notable large peak in magnetic susceptibility, with the maximum values occurring at AD ~1445. In addition, a smaller peak with maximum values occurring at AD ~1590 corresponds to a shift from highly variable magnetic susceptibility values and generally higher magnetic susceptibility measurements overall to relatively less variable, low magnetic susceptibility values. A transitional period, from AD ~1595 to ~1720 (zone 2), exhibits three distinct troughs (AD

~1595 to ~1625, AD ~1625 to ~1675, and AD ~1675 to ~1720) ranging from ~30 to ~50 years. These three troughs encompass extended periods when compared to other troughs in the profile and have z-scores ranging from -1.21 to 1.02. Furthermore, the magnetic susceptibility z-scores also show an overall decreasing trend over the entire time period. Zone 3 (AD ~1720 to ~1900) also contains three troughs from AD ~1750 to ~1781, AD ~1787 to ~1820, and AD ~1829 to ~1846, with several other smaller troughs. However, this zone is punctuated with periodic increases in magnetic susceptibility values when compared to zones 1 and 2. Z-scores in this zone range from -1.23 to 0.59. For the last roughly 100 years (~1900 to 2005, zone 4), the magnetic susceptibility values appear to be relatively stable with z-scores ranging from -1.43 to -0.62.

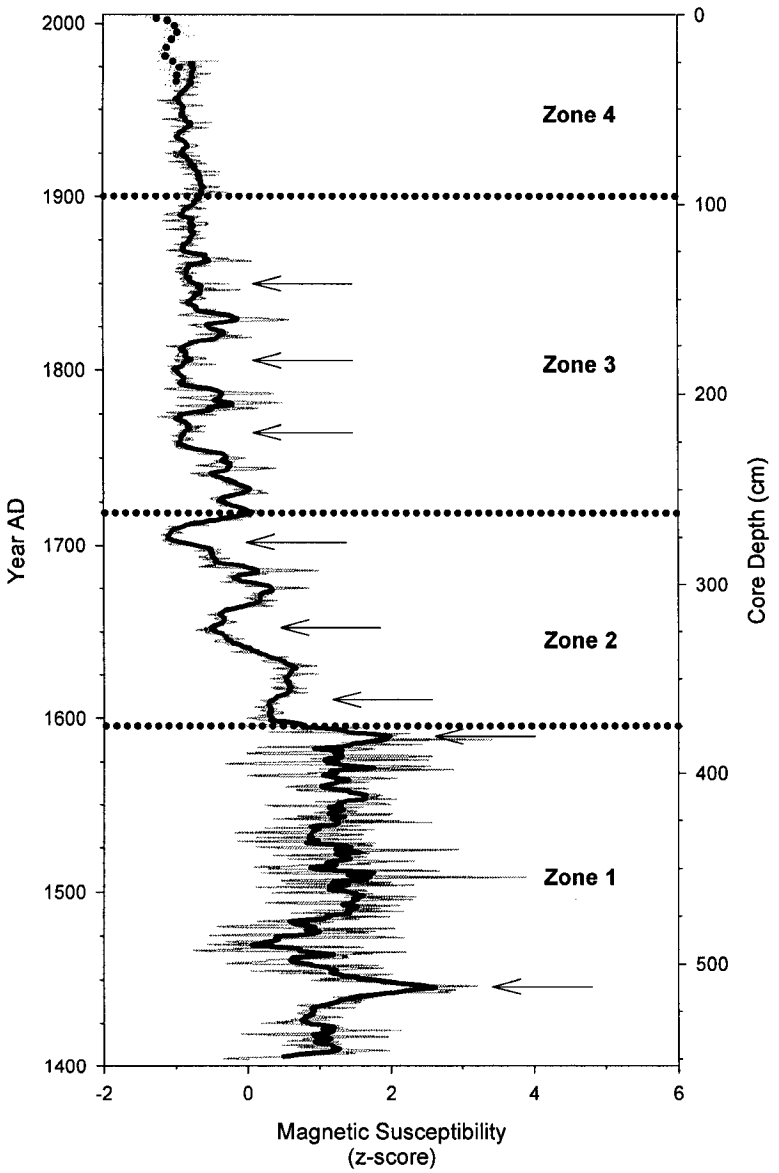

Figure 35: The magnetic susceptibility profiles of the gravity core and vibracore from PAD 15 VC3 (distal site). The preliminary chronology has been calculated using an average sedimentation rate of 0.92 cm/year. The solid and dashed grey lines represent the z-scores of the vibracore and gravity core, respectively. The solid and dashed black lines represent the 5-year running means. Arrows indicate peaks and troughs discussed in text.

Chronology of PAD 15 VC1 (Proximal Site)

Magnetic susceptibility measurements are frequently used for core-to-core correlations by matching similar patterns (Thompson and Oldfield 1986). For this purpose, magnetic susceptibility was measured on 0.5 cm intervals of the gravity core and vibracore from the proximal site at PAD 15 (VC1). Unfortunately, no distinct similarities could clearly be defined between the magnetic susceptibility of the gravity core and the upper sediments of the vibracore. Given that the ^{137}Cs peak was isolated at 37.75 cm in the gravity core from the distal site and the gravity core from the proximal site was only 24 cm long, it is highly unlikely that the gravity core from the proximal site contains a ^{137}Cs peak. With no other methods of core alignment available at the proximal site, it was assumed that the vibracore was offset by 24 cm as well. Thus, 24 cm were added to the depth of the vibracore at the proximal site.

The magnetic susceptibility profiles for the distal site (VC3) and the proximal site (VC1) share several similar patterns (Figure 36). The most notable similarity is the abrupt shift from highly variable and overall higher magnetic susceptibility values in the lower portions of each core (zone 1 in VC3 at the distal site, and from 757 cm to 392 cm in VC1 at the proximal site) to generally lower magnetic susceptibility values in upper portions of both cores (zones 2, 3, and 4 in VC3 at the distal site, and from 392 cm to the top of VC1 at the proximal site). The second similarity is the three distinct troughs that occur from AD ~1595 to ~1720 at the distal site (zone 2 in VC3) and from 392 cm to 326 cm at the proximal site (VC1), although the amplitude of the troughs is not as pronounced in the vibracore from the proximal site (VC1). The magnetic susceptibility patterns in

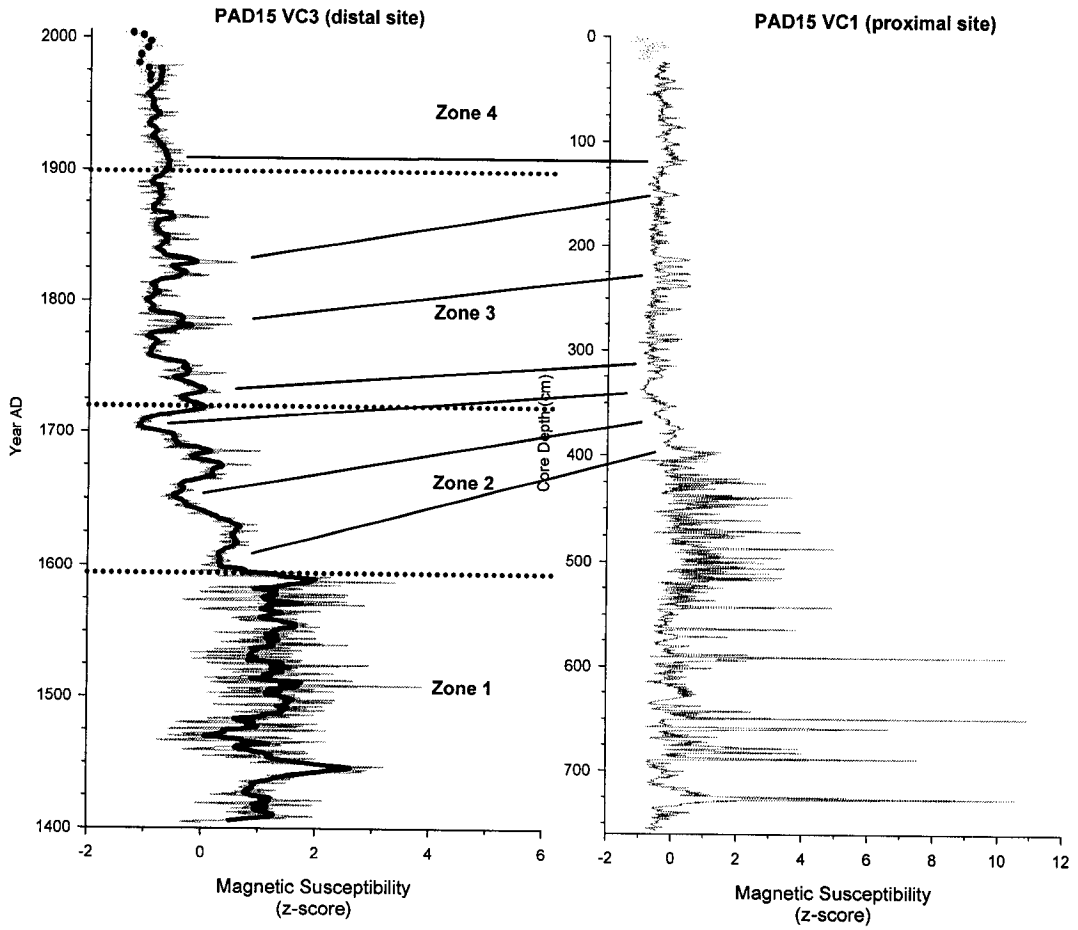

Figure 36: The magnetic susceptibility profiles of PAD 15 VC3 (distal site, shown on left) and PAD 15 VC1 (proximal site, shown on right). The distal site (VC3) magnetic susceptibility is plotted according to age, with the solid black line representing the 5-year running mean, and the proximal site (VC1) is plotted according to depth. Solid black lines are drawn to show several similarities between the cores.

zone 3 in VC3 (distal site) can be matched to similar patterns in VC1 (proximal site) from 326 cm to 200 cm. The relatively stable values evident from AD ~1900 to 2005 in the distal site (VC3) are similar to the relatively stable values seen at the proximal site (VC1) from 210 cm to the top of the core.

Because the vibracores were collected from the same oxbow lake basin and the magnetic susceptibility profiles of these two vibracores have several similar features, it is assumed that these sediments were deposited during similar time periods. The distinct shift from relatively high variability and generally high magnetic susceptibility values to relatively low variability and generally low magnetic susceptibility values in both cores is a key characteristic that can be used as a chronological marker. The date of the distinct shift at AD ~1595 in VC3 (353.25 cm depth) corresponds to 392 cm depth in VC1. Calculating the average sedimentation rate from 0 cm to 392 cm in VC1 produces a value of 0.95 cm/year. Although there is approximately 676 m distance between VC1 and VC3, the proximal site (VC1) appears to have a remarkably similar sedimentation rate (0.95 cm/yr) to that of VC3 (0.92 cm/yr), the distal site. In addition, this shift in magnetic susceptibility coincides with a decrease in grain size from silt and fine sand to clay and silt at 392 cm in VC1 (proximal site) and a shift from the unique clay and silt laminations found in VC3 (distal site, Figure 27) at AD ~1595 to clay and silt laminations common to the upper sediments of all of the cores from both oxbows.

A second sedimentation rate was calculated in VC1 (proximal site) from the base of the core (757 cm) to 392 cm using additional ^{14}C results of wood samples. Three wood samples (two branches and a sample of woody debris) from the vibracore collected at the proximal site (VC1) were analysed for ^{14}C dating (Appendix C). Photographs of these samples are shown in Figure 37, and the results are shown in Table 3. Because wood fragments are relatively resistant to erosion and are often transported they can be a part of several depositional cycles (Björk and Wohlfarth 2001), the results are therefore considered with caution. Two of the three ^{14}C results are similar (AD 1420 to 1490 and

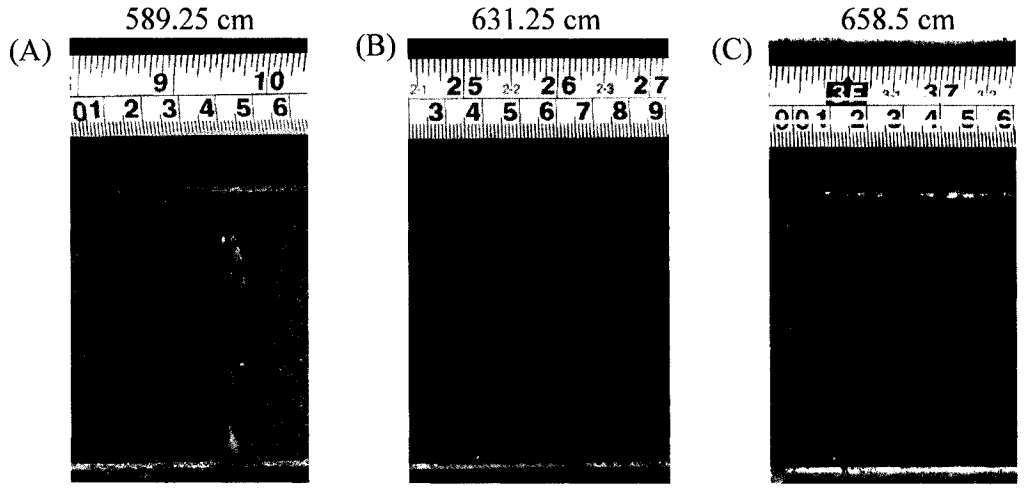

Figure 37: Photographs of samples submitted for radiocarbon dating (A) beta-229807, (B) beta- 229808, and (C) beta-229809. The mid-point depths of each sample are shown above each photograph.

Table 3: Results of wood samples submitted for radiocarbon dating with 2 sigma standard deviations (95% probability) from PAD 15 VC1 (proximal site). Calibrated results were calculated using IntCal04 (IntCal04: Calibration Issue of Radiocarbon 46(3) 2004) and Talma and Vogel (1993).

Sample Photograph	Lab Number	Material	Core Depth (adjusted +24 cm)	Reported Age (^{14}C yr BP)	Calibrated Age (year AD)
PAD 15 VC1					
A	beta-229807	Branch	588.5-590.0	440±40	1420 to 1490
B	beta-229808	Branch	629.0-633.5	270±50	1480 to 1680
C	beta-229809	Wood fragments	656.5-660.5	1590±40	390 to 560

AD 1480 to 1680, sample photographs A and B in Figure 37, respectively), while the third sample (the deepest, sample photograph C in Figure 37) appears to be comparatively old (390 to 560 Cal yr AD). This sample is unlike the others in that it consists of wood fragments. Figure 38 shows that the calibrated age range of this sample is also an outlier. Although the sediment depths of the two bottom samples (B and C) are 27.25 cm apart and the upper two samples (A and B) are 42 cm apart, the upper two samples are closer in age, and have 10 years of overlap at the 95% probability interval. If the upper limit for the age range of the wood fragments (AD 560) was used in chronological calculations, it would result in a sedimentation rate of 0.26 cm/year and a basal age of AD ~201 (Figure 38). This sedimentation rate is over 3.5 times lower than the sedimentation rate in the upper portions of this core (0.95 cm/year) and is highly unlikely because the lower portion contains generally massive coarser-grained (sand) sediment, indicating relatively high energy conditions and suggests that the sedimentation rate may be relatively high. This sample has likely been involved in multiple redepositional cycles because it consisted of relatively thin fragments of wood that would be readily transported, including during low energy events.

Sample B has some remaining bark (unlike A and C in Figure 37) and is also the largest sample. The relatively good preservation of this sample suggests that it may be an intrusion, whereby relatively young wood is forced into relatively old sediment. This phenomenon can occur during high energy conditions associated with ice-jam events. With further consideration of the condition of the samples and the ^{14}C results, sample A in Figure 37 and Table 3 was used in chronological calculations. This sample consists of a wood branch without bark. It has a calibrated ^{14}C date range of AD 1420 to 1490

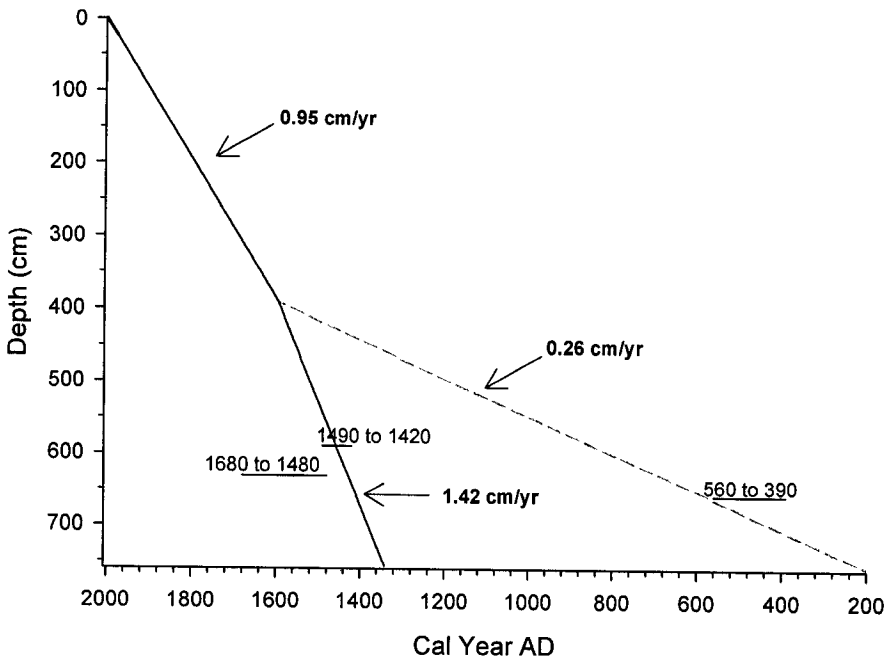

Figure 38: Linear age-depth model for the proximal site at PAD 15 (VC1) derived from the 1964 ^{137}Cs peak in VC3 (distal site) and stratigraphic correlations between VC1 (proximal site) and VC3 (distal site) using magnetic susceptibility. The grey dashed line represents the age-depth profile if a date of AD 560 was used. The solid black line is the most probable age model deduced in the text for the lower portion of PAD 15 VC1. The calibrated ^{14}C date ranges are given as 2 sigma standard deviations (95% probability) with the IntCAL04 radiocarbon calibration curve (IntCal04: Calibration Issue of Radiocarbon 46(3) 2004 and Talma and Vogel 1993).

(95% probability using IntCAL04 and Talma and Vogel 1993). The midpoint of this age range was used in chronological calculations as a conservative estimate of average sedimentation in the lower strata of the proximal core (VC1). This resulted in a sedimentation rate of 1.42 cm/yr and a basal date of AD ~1343 (Figure 38).

Additional Chronological Development Within PAD 15

Both magnetic susceptibility profiles for VC1 (proximal site) and VC3 (distal site) are plotted by age in Figure 39. There are still clear inconsistencies between the two cores. Firstly, the large individual peaks in magnetic susceptibility plotted near the base of the proximal core (VC1) are not evident in the distal core (large peak z-score values in VC1 labelled on Figure 39). Because there is greater chronological control (^{14}C date) in the lower portion of the proximal core (VC1) when compared to the distal core (VC3), the magnetic susceptibility z-score trends were used to re-evaluate and refine the chronology of the lower strata in the distal core (VC3). The date of AD ~1457 for the peak with a z-score of 10.2269 in VC1 (proximal site) was transposed onto the notable large peak near the base of PAD 15 VC3 (distal site, shown by the dashed black line in Figure 39), changing the date from AD ~1445 to AD ~1457. To accommodate this adjustment, the sedimentation rate from the base of the core to AD ~1595 in VC3 (distal site) only slightly increased from 0.92 cm/year to 0.99 cm/year, and resulted in a corrected basal age of AD ~1418. Thus, VC3 (distal site) is assumed to contain two slightly different average sedimentation rates. From AD ~1418 to ~1595 the average sedimentation rate is 0.99 cm/yr, and from AD ~1595 to 2005 the average sedimentation rate is 0.92 cm/year (Figure 40). This minor adjustment in the estimate of the average sedimentation rate is consistent with the stratigraphy of the core collected from distal site (VC3) at PAD 15. The core consists entirely of clay and silt, suggesting that a large change in sedimentation rate was unlikely.

The three distinct troughs in zone 2 of both cores do not correspond by age (shown by

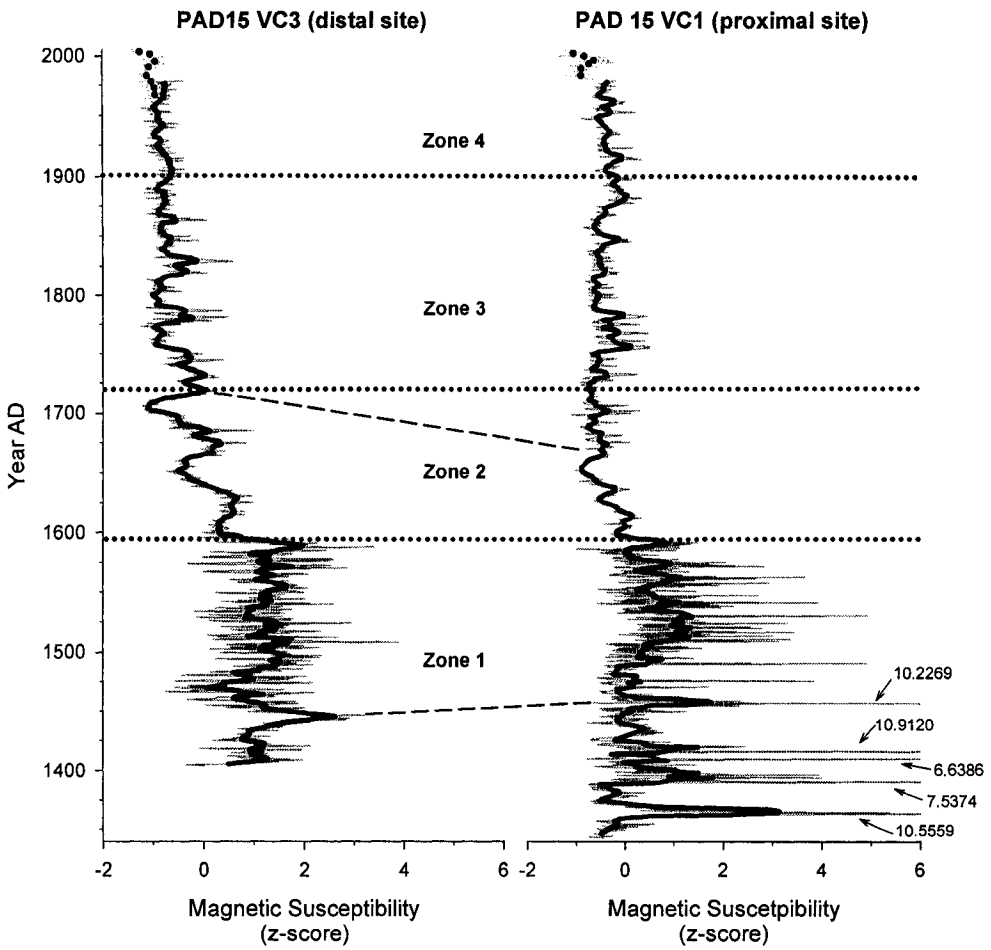

Figure 39: Magnetic susceptibility profiles for the PAD 15 VC3 (distal site, shown on left) and PAD 15 VC1 (proximal site, shown on right). The grey line represents the z-score of magnetic susceptibility measurements, while the black line represents the 5-year running mean of the z-score of magnetic susceptibility measurements. Note that the values are given where the x-axis of the profile for the proximal site (VC1) has been truncated to show both cores at the same scale.

the dashed black line in Figure 39). At the distal site (VC3) the three troughs occur from AD ~1595 to ~1720, while at the proximal site (VC1) the three troughs occur from AD ~1595 to ~1663, resulting in a difference of 57 years. Because there is chronological

control in the upper strata of VC3 (distal site, 1964 ^{137}Cs peak), the chronology of the upper portion of the proximal site (VC1) was adjusted. The date of AD ~1595 for the significant shift in magnetic susceptibility values remained the same. However, the date at the end of the last of the three troughs in magnetic susceptibility at the distal site (VC3), AD ~1720 (262 cm depth), was transposed onto the proximal core, changing the date from AD ~1663 (326 cm depth) to AD ~1720. Consequently, the proximal site has 3 different average sedimentation rates, as shown by the age-depth profile in Figure 41. From AD ~1343 to ~1595, the sedimentation rate is 1.42 cm/year, from AD ~1595 to ~1720 the sedimentation rate is 0.53 cm/year, and from AD ~1720 to 2005 the sedimentation rate is 1.14 cm/year. Figure 42 shows the magnetic susceptibility profiles for both cores with the adjusted, final chronologies, and the resultant similar trends in magnetic susceptibility (Appendix D).

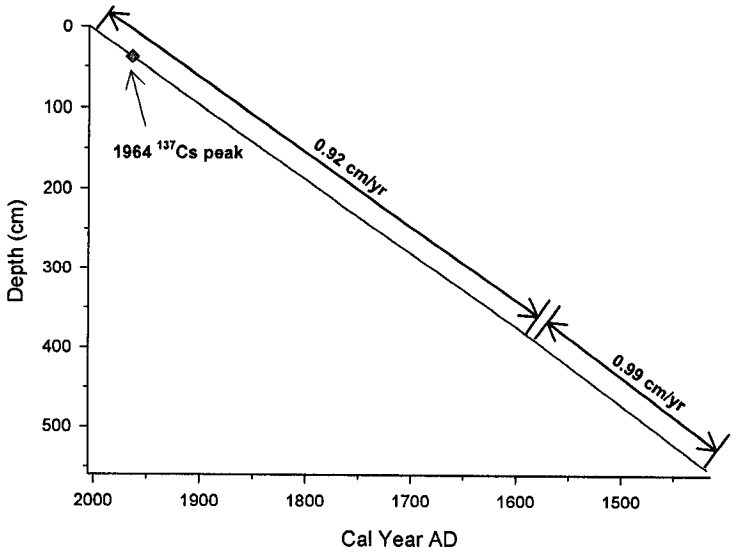

Figure 40: The adjusted age-depth profile for the distal site at PAD 15 (VC3). The sedimentation rates are based in the 1964 ^{137}Cs peak and similar trends in magnetic susceptibility z-scores between PAD 15 VC1 (proximal site) and VC3 (distal site). The slight increase in sedimentation rate is hardly perceptible. The corrected basal date of the core is AD ~1418.

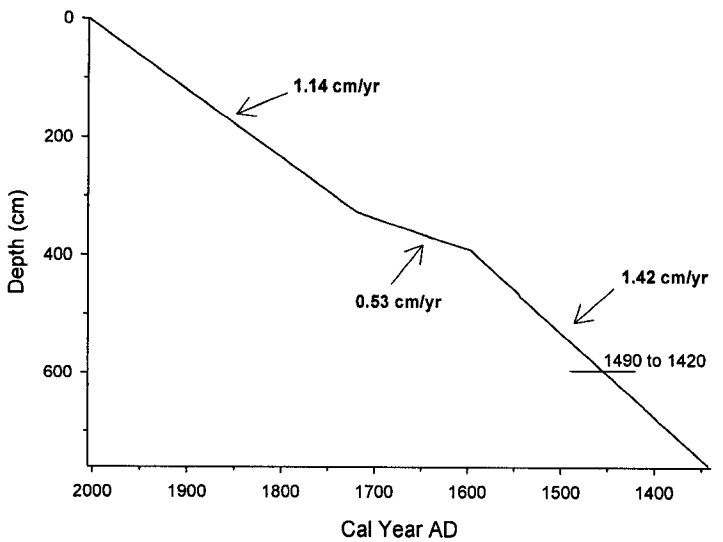

Figure 41: Final age-depth profile for the proximal site at PAD 15 (VC1). Note the variable sedimentation rate is based on core-to-core correlations of magnetic susceptibility measurements and one ^{14}C date from Table 3. The radiocarbon date range is the calibrated using the INCAL04 radiocarbon calibration curve (IntCal04: Calibration Issue of Radiocarbon 46(3) 2004) and Talma and Vogel (1993). The basal date is AD ~1343.

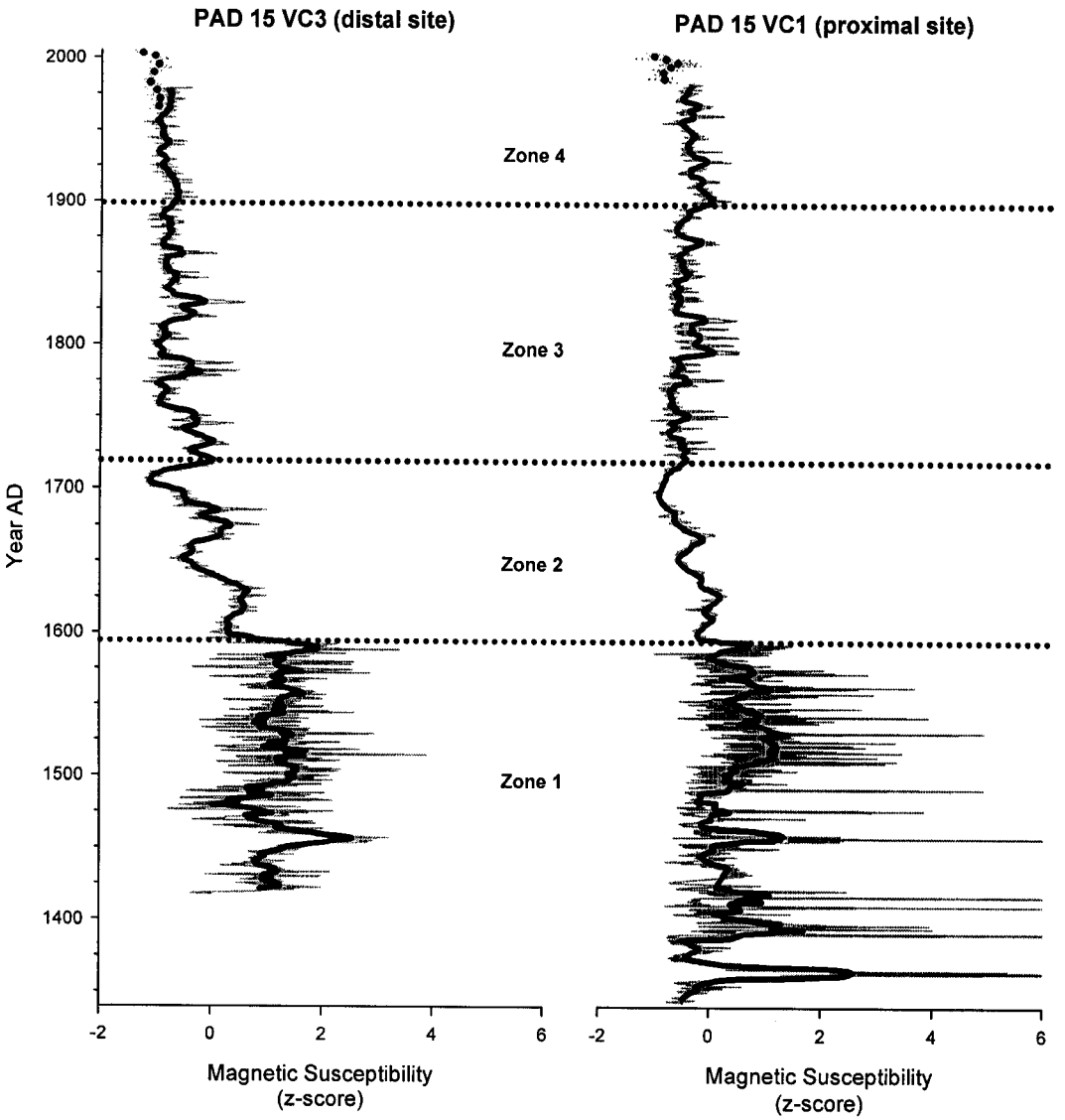

Figure 42: Magnetic susceptibility z-score profiles for the distal (VC3: left) and proximal (VC1: right) sites at PAD 15 versus the final chronologies. Note that the x-axis of the profile for the proximal site has been truncated to show both profiles at the same scale.

These linear age-depth models provide the best approximation of the average sedimentation rates given the available data. The chronologies are likely overestimating periods when there was little flooding and sedimentation rates were relatively low, and

underestimating periods during flooding when sedimentation rates were relatively high. Although over short periods of time this chronology may not be accurate, it does provide long-term, conservative estimates of sediment age. The sedimentation rates in zone 1 of both cores are likely highly variable over short time periods given the variable stratigraphy, particularly in VC1 (proximal site, stratigraphy shown in Figure 23, page 58).

When comparing the sedimentation rates for PAD 15 VC1 (proximal) and VC3 (distal) there is still a remaining inconsistency. It was expected that the sedimentation rate at the proximal site (VC1) would be higher than the sedimentation rate at the distal site (VC3) because of the greater supply of sediment near the inlet. From the top of the core to AD ~1720 (zones 3 and 4 in Figure 42) in VC1 (proximal site) the sedimentation rate (1.14 cm/yr) is somewhat higher than the sedimentation rate of VC3 (distal site, 0.92 cm/yr). However, from AD ~1595 to ~1720 in VC1 (proximal site, zone 2 in Figure 40), the sedimentation rate is 0.55 cm/yr, which is roughly 1.5 times lower than the sedimentation rate at VC3 (distal site). This would appear to be inconsistent with the relative locations of the cores to the inlet and source of sediment, and difficult to explain without obtaining many more cores to examine the spatial distribution of sedimentation in the basin.

Organic Carbon and Nitrogen Elemental and Stable Isotope Geochemistry

Measurements of bulk organic carbon (C_{org}%) and nitrogen (N%) content and carbon ($\delta^{13}C_{org}$) and nitrogen ($\delta^{15}N$) isotope composition are often used as indicators of carbon and nitrogen cycling processes in lakes (Meyers and Teranes 2001). The elemental and

stable isotope stratigraphy for PAD 15 VC3 (distal) is shown in Figure 43 (Appendix E). For the entire sediment sequence (AD ~1418 to 2005), C_{org} values range from 0.28 % to 3.57 % and N values range from 0.03 % to 0.43 %, indicating that these sediments are mainly inorganic. Overall, C_{org} and N content gradually increase up-core. $\delta^{13}C_{org}$ composition generally remains relatively constant with the exception of the period from AD ~1418 to ~1496 and the decrease from AD ~1900 to 2005. The $\delta^{15}N$ profile generally shows more variability than the $\delta^{13}C_{org}$ profile. $\delta^{13}C_{org}$ ranges from -30.19 ‰ to -15.74 ‰ and $\delta^{15}N$ ranges from 0.88 ‰ to 5.62 ‰. The C/N ratios (ranging from 8.76 to 18.77) generally increase until AD ~1600, and then generally decrease to the top of the core. These profiles have been divided into zones consistent with the magnetic susceptibility profiles and are discussed in more detail below.

Zone 1, (from AD ~1418 to ~1595) contains C_{org} ranging from 0.3 % to 1.8 %, N ranging from 0.03 % to 0.1 %, $\delta^{13}C_{org}$ ranging from -30.2 ‰ to -15.7 ‰, $\delta^{15}N$ ranging from 1.3 ‰ to 3.8 ‰, and C/N ratios ranging from 9.1 to 18.8. Although this zone contains the lowest C_{org} and N content, the values are generally more variable when compared to overlying sediments. Zone 1 also contains the widest range, and the most depleted and enriched $\delta^{13}C_{org}$ compositions. The $\delta^{15}N$ composition is generally higher when compared to all of the other zones. The highest C/N ratios also occur in this zone when compared to all overlying sediments. It is important to note that although the sediment in zone 1 contains relatively high $\delta^{13}C_{org}$ and C/N values, they are restricted to a relatively small portion near the base of the core, from AD ~1418 to ~1496. Overall, the $\delta^{13}C_{org}$ composition is consistent with zones 2 and 3 and the C/N ratios are relatively low when compared to zone 2.

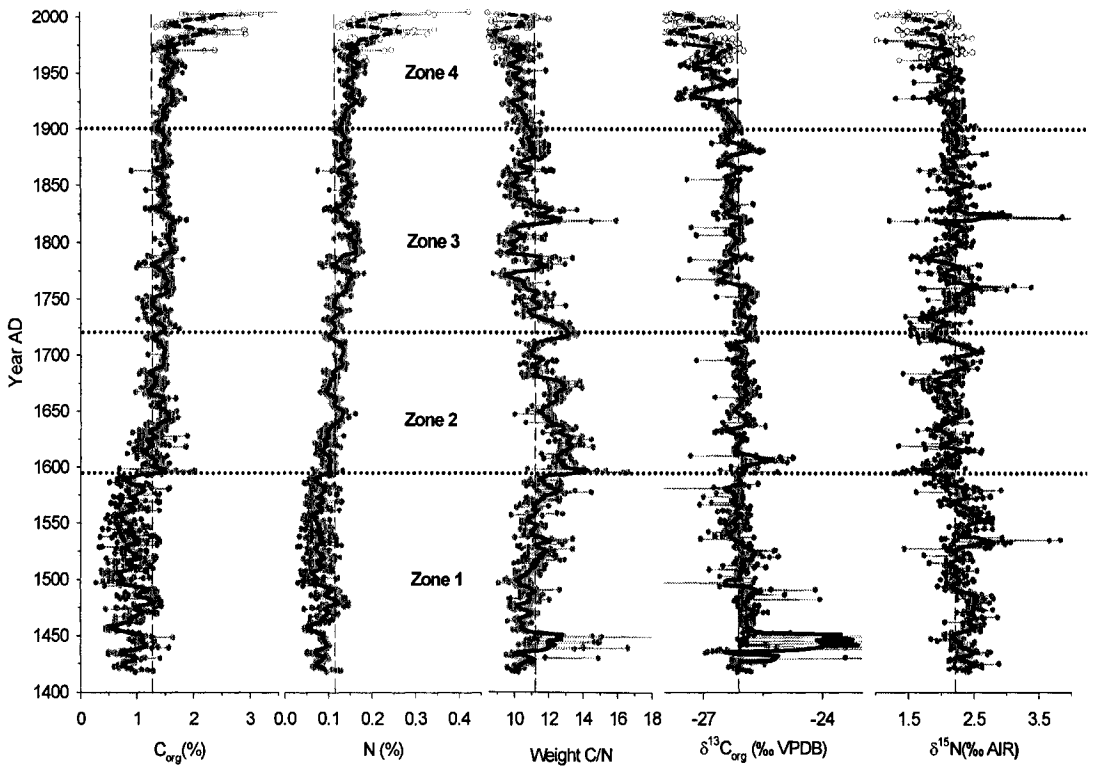

Figure 43: Geochemical stratigraphy of PAD 15 VC3 (distal site). The dashed and solid black lines are the 5 year running means of the gravity core and the vibracore, respectively. The vertical dashed lines are the overall mean of each profile.

In Zone 2 (from AD ~1595 to ~1720), C_{org} and N content increases slightly compared to zone 1, with values ranging from 0.7 % to 2.0 % and 0.06 % to 0.2 %, respectively. The $\delta^{13}C_{org}$ and $\delta^{15}N$ compositions have narrower ranges of -27.3 ‰ to -24.7 ‰ and 1.4 ‰ to 2.6 ‰, respectively. However, the $\delta^{13}C_{org}$ composition remains stable overall, and the $\delta^{15}N$ is slightly lower when compared to zone 1. The C/N ratio range narrows to values ranging from 10.0 to 16.6. However, the C/N ratio is generally higher than in zone 1.

In Zone 3 (from AD ~1720 to ~1900), C_{org} and N content remain relatively stable when compared to zone 2, with values ranging from 0.9 % to 1.9 % and from 0.08 % to 0.2 %, respectively. $\delta^{13}C_{org}$ and $\delta^{15}N$ have still narrower ranges when compared to zones 1 and 2, with values ranging from -27.6 ‰ to -25.6 ‰ and 1.2 ‰ to 5.6 ‰ respectively. Although when compared to zone 2, the C/N ratio range widens somewhat to values from 8.8 to 15.9, the ratios also generally decrease. This zone contains the lowest C/N values of the entire core, but the overall average (10.9) is slightly higher than zone 4 (10.5).

Zone 4 (from ~1900 to 2005) contains sediments having the highest organic matter content, with C_{org} content ranging from 1.3 % to 3.6 % and N content ranging from 0.1 % to 0.4 %. $\delta^{13}C_{org}$ and $\delta^{15}N$ have slightly higher ranges of values of -28.8 ‰ to -25.5 ‰ and 1.2 ‰ to 2.7 ‰, respectively, when compared to zone 3. There is a clear decrease in $\delta^{13}C_{org}$ composition from AD ~1900 to 2005 and only a slight decrease in $\delta^{15}N$ over the same time period. The C/N ratio range narrows relative to zone 3, with values ranging from 8.4 to 12.3. The C/N ratio also shows steadily decreasing values from AD ~1900 to 2005.

DISCUSSION

Sedimentological History of Oxbow Lakes PAD 54 and PAD 15

Core-to-Core Correlation

Initially, the cores were fixed to a lake ice-atmosphere datum to investigate a possible gradient change in the water-sediment interface between core sites. Visual core-to-core comparisons were problematic because of the extremely high horizontal exaggeration (1 cm = 3000 cm) when compared to the vertical exaggeration (1 cm = 42 cm). Because the slopes between the cores within each oxbow were found to be insignificant (values ranging from only 0.03° to 0.69°), the water depths were removed and each core was plotted with the sediment-water interface as the datum in both PAD 54 and PAD 15. The horizontal relationship between the cores was maintained in each of the following figures (Figures 44 and 45).

Stratigraphic Relations within PAD 54

Several consistent trends can be noted among the cores from PAD 54, shown in Figure 44. A prominent core-to-core correlation among all three cores in this oxbow lake is the shift from generally sand, silt, and clay to silt and clay (indicated with arrows in Figure 44). This occurs from units I to II at the proximal site (VC2, 356 cm depth), from unit II to subunit IIIa in the intermediate core (VC1, 360 cm depth), and from unit VI to subunit VIIa in the distal core (VC3, 288.5 cm depth). Unit I in the proximal core (VC2) may correspond to unit II in the intermediate core (VC1), based on the relatively large grain sizes in these units. In turn, unit I in the intermediate core (VC1) likely

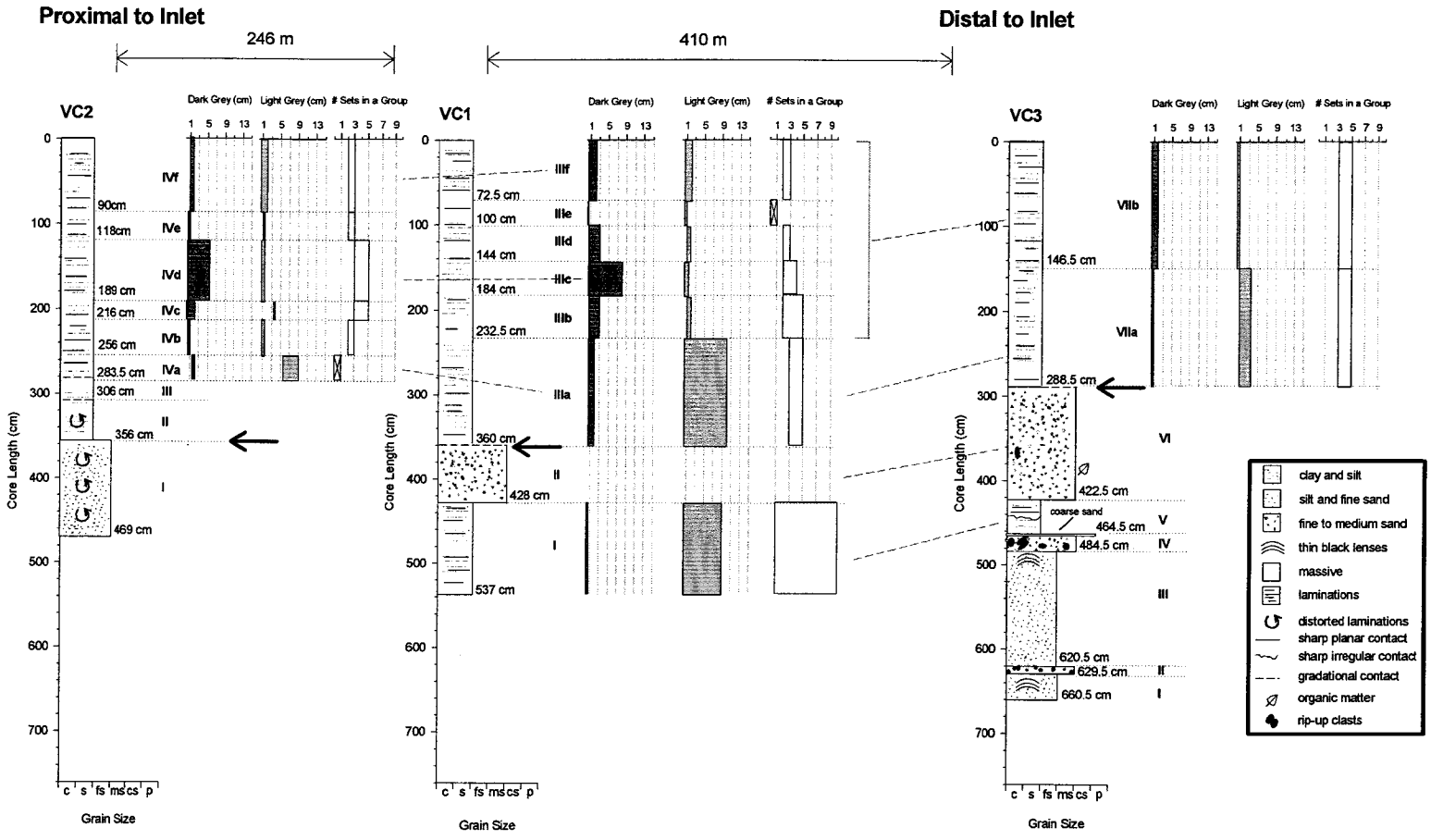

Figure 44: Stratigraphic profiles of the sediment cores from PAD 54. The sediment-water interface is designated as 0 cm. Dashed lines correlate similar features in the cores. The solid black arrows represent the shift from generally sand, silt, and clay to silt and clay.

corresponds to unit V in the distal core (VC3), based on the clay and silt grain sizes and the overlying relatively coarse-grained material in both cores.

General trends in dark grey bed thickness are apparent between the proximal (VC2) and intermediate sites (VC1). For example, subunit IVa in the proximal site (VC2) likely corresponds to subunit IIIa in the intermediate site (VC1) based on the similar relative bed thicknesses ranges of both the dark and light grey clay and silt beds and stratigraphic position. The dark grey beds in subunit IVa in VC2 (proximal site) and subunit IIIa in VC1 (intermediate site) are relatively thin and have narrow bed thickness ranges, while the light grey beds are relatively thick and have relatively wide bed thickness ranges. Subunit IVd of VC2 (proximal site), having the maximum range of dark grey bed thicknesses (0.5 cm to 5 cm) of unit IV, likely corresponds to the maximum range of dark grey bed thickness (0.5 cm to 8 cm) in the intermediate core (VC1), subunit IIIc. The number of sets of beds in a group (refer to Figure 9, page 40) in these two subunits are also similar, with subunit IVd in the proximal core (VC2) having sets of 3 to 5, and the intermediate core (VC1) having 2 to 4 sets in a group. Subunit IVf in the proximal core (VC2) likely corresponds to subunit IIIf in the intermediate core (VC1), because these represent the youngest sediments in both cores. The clay and silt beds of both of these subunits also share the same number of sets in a group (2 to 3).

The relationship of clay and silt beds between the intermediate (VC1) and distal (VC3) cores is less clear and may be related to visual observations of the cores or due to the distance between the distal (VC3) and the intermediate (VC1) sites being over 1.5 times that of the distance between the proximal (VC2) and intermediate sites (VC2). However, both the light and dark grey clay and silt beds are thinnest at the distal site

(VC3) when compared to the other cores and correspond to declining energy conditions as distance increases from the sediment source. Subunit IIIa in the intermediate core (VC1) likely corresponds to subunit VIIa in the distal core (VC3). Both of these subunits overly fine to medium sand. They also contain relatively thin dark grey beds and relatively narrow dark grey bed thickness ranges, as well as relatively thick light grey beds. The clay and silt beds in subunits IIIa in VC1 (intermediate site) and VIIa in VC3 (distal core) are also both grouped into sets of 3 to 5. Subunits IIIb to IIIf in the intermediate site (VC1) may correspond to subunit VIIb in the distal core (VC3) as these are the uppermost subunits in each core and were likely deposited over similar time intervals.

Stratigraphic Relations within PAD 15

The core depths at the proximal and distal sites at PAD 15 (Figure 45) have been adjusted by an additional 24 cm to account for the missing and/or compacted upper sediments in each vibracore (see Chronology and Magnetic Susceptibility section). Although it was noted that the top 24 cm of the gravity cores at each of the sites contained laminated clay and silt, the dark and light grey bed thicknesses were not measured as the sediment was extruded from the core tubes and sectioned into 0.5 cm intervals in the field.

Several sedimentological characteristics can be noted in the stratigraphic profiles from PAD 15 (Figure 45). The shift from generally sand, silt, and clay to silt and clay in PAD 54 (indicated by arrows in Figure 44) also occurs in PAD 15 at the proximal (VC1; 394 cm depth) and intermediate (VC2; 371 cm depth) sites (indicated by arrows in Figure

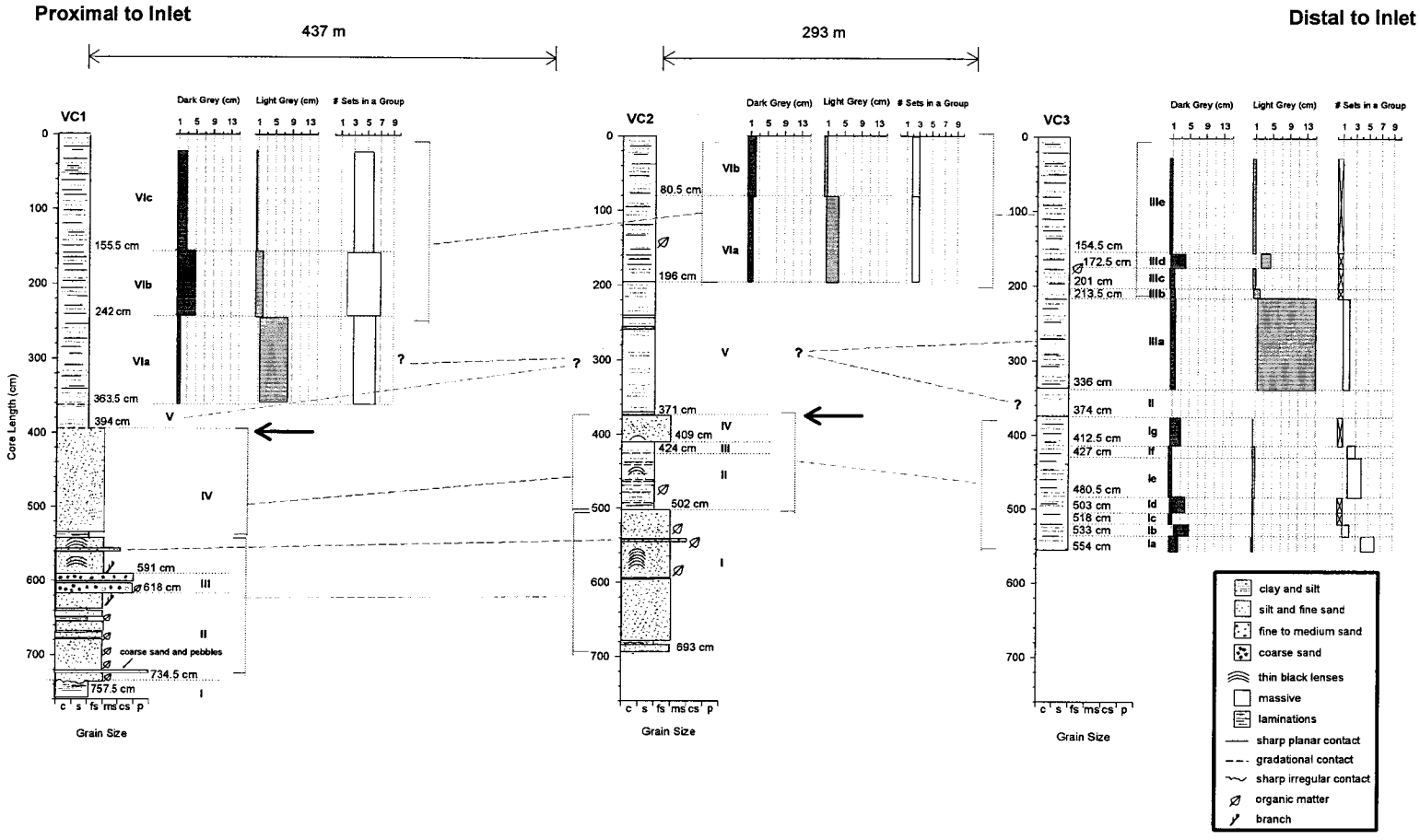

Figure 45: Stratigraphic profiles of the sediment cores from PAD 15. The sediment-water interface is designated as 0 cm. Dashed lines correlate similar features in the cores. The solid black arrows represent the shift from generally sand, silt, and clay to silt and clay.

45). In addition, the shift from the uniquely well-defined clay and silt laminations at the distal site (VC3) to those common to all the cores from both oxbows may have occurred during the same time period as the shift from sand, silt, and clay, to silt and clay at the proximal (VC1) and intermediate (VC2) sites at PAD 15. Because the clay and silt laminations are uniquely well-defined (Figure 27, page 66) in all of the subunits of unit I at the distal site of PAD 15 (VC3), the depositional process presumably was different from that which deposited the clay and silt laminations observed in all of the upper strata of all of the cores from both lakes. The sharp bed contacts of the well-defined laminations are consistent with distal sediments during relatively high influxes of energy, and are thus correlated to the relatively large grain size deposits in the proximal (VC1) and intermediate (VC2) cores from PAD 15.

Several additional tentative correlations can be made among the cores at PAD 15. Unit I in VC1 (proximal site) does not appear to correlate with the lower units in VC2 (intermediate site). However, unit II, III, and a portion of unit IV (from 591 cm to 544 cm) in VC1 (proximal site) may be correlated to unit I in VC2 (intermediate site) because of similar grain sizes and the relative abundance of organic deposits in both cores. In addition, the fine- to medium-grained sand deposit in unit IV in VC1 (proximal site) may be correlated to the fine- to medium-grained sand deposit in unit IV of VC2 (intermediate site) because they are both of similar thickness and grain sizes. A portion or all of unit IV in the proximal site (VC1) may be correlated to units II, III, and IV in the intermediate core (VC2). Although unit IV in VC1 (proximal site) contains mainly fine- to medium-grained sand and units II and III in VC2 (intermediate site) contain varying amounts of clay and silt, the similar upper contacts and shift to generally clay and silt (as indicated

by the arrows in Figure 45) at the top of unit IV in both cores suggest that these units may be correlated. VC3 (distal site) is the only core to consist entirely of clay and silt. A tentative correlation may be drawn between units II, III, and IV of VC2 (intermediate site) and unit I of VC3 (distal site) because of the relatively high clay and silt content in unit II of the VC2 (intermediate site).

Core-to-core correlations are less clear in the upper massive and laminated clay and silt sediments from the cores collected from PAD 15, but several trends can be noted. A massive clay and silt deposit occurs in all three cores (unit V in VC1 and VC2, the proximal and intermediate cores respectively, and unit II in VC3, the distal core). Unit V in VC2 (intermediate site) is notably thicker than in any of the other correlated units from PAD 15. This unit may not be massive, but contain laminations that were not observed. Thus, unit V in VC2 (intermediate site) could also be correlated to subunit VIa of VC1 (proximal site, light grey bed thickness ranges from 1.5 cm to 8 cm) and subunit IIIa of VC3 (distal site, light grey bed thickness ranges from 1.5 cm to 15 cm), which have notably thick light grey beds.

Subunits VIb and VIc in VC1 (proximal core) likely correlate to subunits VIa and VIb in VC2 (intermediate core). Although the dark grey bed thickness decreases from subunit VIb to subunit VIc in VC1 (proximal site) and increases from subunit VIa to subunit VIb, the light grey bed thickness trends are consistent between the two subunits of each core. In turn, subunits VIa and VIb in VC2 (intermediate site) are likely correlated to subunits IIIb to IIIe in VC3 (distal site). This is based on the relatively thin light grey bed thicknesses in these subunits when compared to subunit IIIa in VC3 (distal site). In general, the range of bed groupings decreases with increasing distance from the

inlet, with the distal site only having sets in some of the subunits grouped. This is likely because the dark grey bed thicknesses decrease with distance from the inlet, making the groupings more difficult to distinguish.

Interpreting Sedimentological Evidence from PAD 54 and PAD 15

A facies analysis was performed on the cores collected from oxbow lakes PAD 54 and PAD 15. In general, the term facies is used to describe a set of characteristics of a stratigraphic unit, such as lithology, composition, colour, physical, chemical, and biological sedimentary structures, and fossil content (Walker 1992). Because each facies is defined by a set of discrete characteristics, it can be used to identify a depositional process. Individual facies can be grouped together to form facies associations, or groups of facies that are considered to be environmentally related (Walker 1992). In turn, these facies associations can be compared to a facies model, or a previously established summary of a given environment based on a combination of modern and ancient environments, to interpret the depositional environment (Walker 1992).

Figures 44 and 45 in the previous sections highlighted similar stratigraphic features, and units and subunits with similar characteristics. These units and subunits are henceforth referred to as facies and subfacies, respectively, as the sediments contained therein share similar lithology, colour, and sedimentary structures, and are indicative of depositional processes, environments, and systems. Several general similarities can be noted between the cores collected from oxbow lakes PAD 54 and PAD 15. For example, both of the oxbow lakes generally contain fining-upward successions. The shift from generally sand, silt and clay to silt and clay (shown by the arrows in Figures 44 and 45) is

a prominent characteristic in all of the cores (with the exception of PAD 15 VC3, the distal core) and likely occurred during the same time period in both oxbows. This suggests overall declining energy conditions in both oxbows over time.

The facies and subfacies from PAD 54 and PAD 15 have been grouped into four general facies associations (A, B, C, and D in Figures 46 and 47). Facies association A includes medium to coarse-grained sand and pebbles and abundant organic debris. These deposits are consistent with high energy conditions and are interpreted as likely being deposited prior to the neck of the meander being cut-off, when the oxbows were part of the main river channels. Facies association B consists of relatively coarse-grained sediments (fine to medium sand) that require relatively high energy conditions to be entrained and transported as bed load or suspended load into the oxbow. This suggests a depositional environment with high flood frequency and magnitude. The well-defined laminated clay and silt found in the lower sediments of the distal core (VC3) was also included in this facies association based on the core-to-core correlations outlined in the previous section and the characteristics of these sediments, which are distinct from the laminated clay and silt in the upper sediments. Facies association C consists of massive grey clay and silt deposits. These sediments are interpreted as being deposited largely from suspension during periods with relatively low energy conditions, created by infrequent or absence of flooding. Facies association D consists of alternating light and dark grey laminated clay and silt beds, and is interpreted as being deposited during oscillating energy conditions, with relatively low flood frequency and occasional moderate flooding.

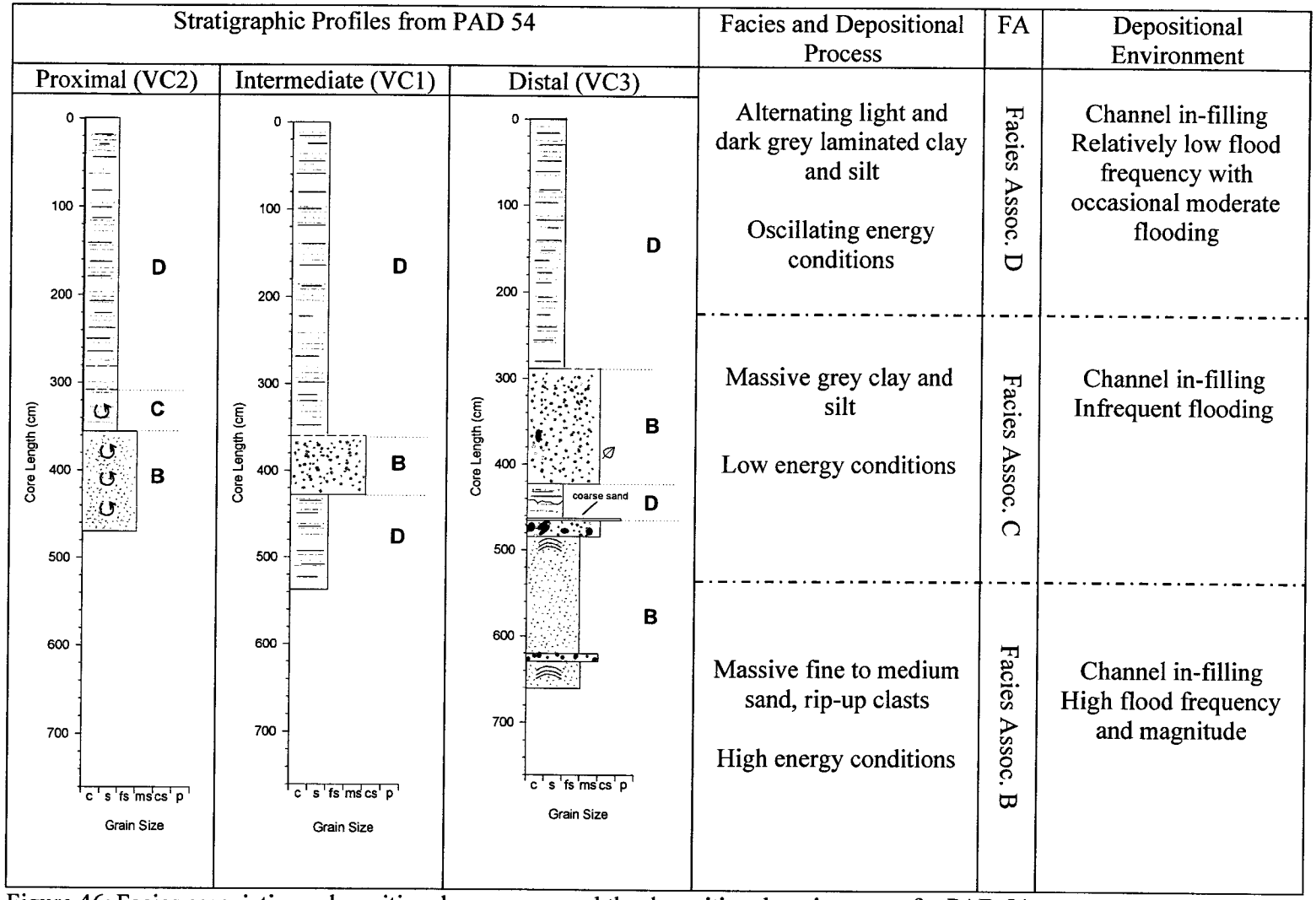

Figure 46: Facies associations, depositional processes, and the depositional environment for PAD 54.

Stratigraphic Profiles from PAD 15			Facies and Depositional Process	FA	Depositional Environment
Proximal (VC1)	Intermediate (VC2)	Distal (VC3)			
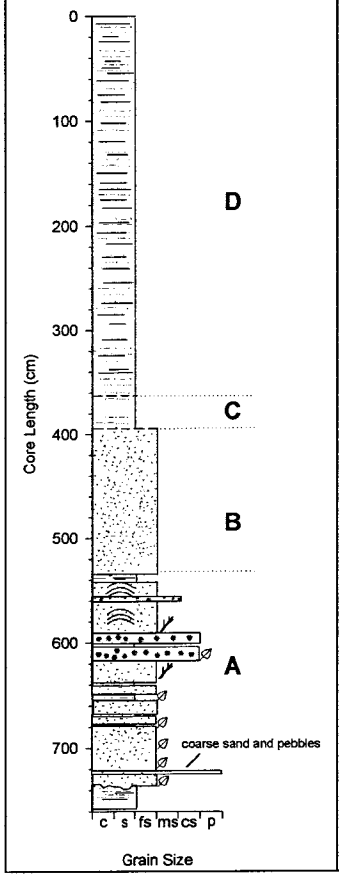	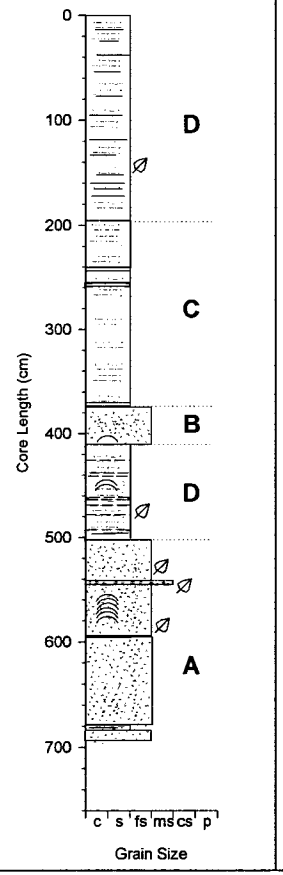	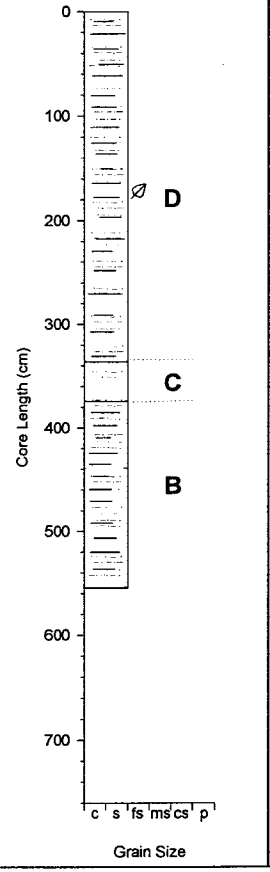	Alternating light and dark laminated clay and silt Oscillating energy conditions	Facies Assoc. D	Channel in-filling Relatively low flood frequency with occasional moderate flooding
			Massive grey clay and silt Low energy conditions	Facies Assoc. C	Channel in-filling Infrequent flooding
			Well-defined laminated clay and silt Massive fine to medium sand High Energy Conditions	Facies Assoc. B	Channel in-filling High flood frequency and magnitude
			Medium to coarse sand, pebbles, abundant organic debris Persistent high energy conditions	Facies Assoc. A	Active meandering river channel

Figure 47: Facies associations, depositional processes, and the depositional environment for PAD 15.

The facies model above generally shows an abrupt shift from coarse-grained (mainly sand) sediment deposition to relatively fine-grained sediment (clay and silt) deposition during fluctuating energy conditions. Although fining-upward sequences are generally a characteristic of sequences from a meandering river system as it actively accretes laterally (Boggs 2006), none of the cores contain any of the main features included in facies models of meandering river systems and fluvial environments (as outlined by Collinson 1978, Miall 1992, Boggs 2006, and Stow 2005), such as ripples, dunes, antidunes, cross-bedding, and imbrication. However, it appears that a portion of the sediment sequence prior to when the river meander was cut off and the oxbow lake was created is captured in the proximal (VC1) and intermediate (VC2) cores of PAD 15, based on the large grain sizes (pebbles and coarse sand) and the abundance of organic debris (refer to the heading "Magnetic Susceptibility and Stratigraphic Records" on page 106, and Figure 51 on page 108 for further details). The erosion, transport, and deposition of the clay and silt rip-up clasts in the lower strata of the distal core (VC3) at PAD 54, designated as facies association B, likely required a significant burst of energy and flood waters because of the nature of the strong cohesion of fine-grained sediment, rather than being an indication that the meander had not yet been cut-off and was still conducting the main flow of the channel. The source of these rip-up clasts is likely local (from floodplain, oxbow, or near channel sediments), because the individual clasts are susceptible to erosion.

A detailed examination of individual beds of all of the laminated clay and silt deposits in all of the cores from both PAD 54 and PAD 15 revealed that dark grey beds generally have sharp lower contacts and diffuse upper contacts (Figure 48). During core

sectioning at the field station, the dark grey beds were also noted as consisting of coarser-grained material when compared to the light grey beds. An initial input of sediment during high energy conditions likely created the sharp lower contact and caused the relatively coarse-grained material to settle out more rapidly from suspension. As energy conditions decreased, the relatively fine-grained material settled out gradually from suspension, creating a diffuse upper contact. This suggests that the dark grey beds are flood deposits, while light grey beds are deposited during periods when there is no flooding and is consistent with the findings of Wolfe et al. (2006).

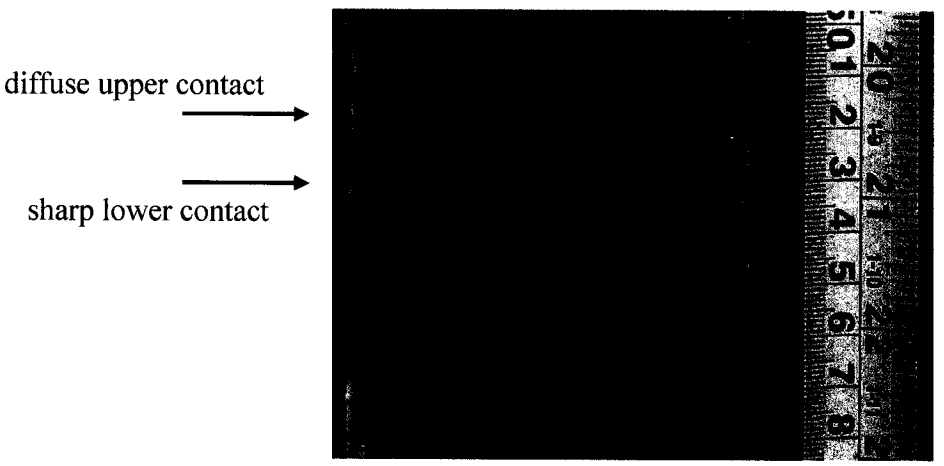

Figure 48: A photograph of sediments from PAD 15 showing dark beds having sharp lower contacts and diffuse upper contacts, which are indicative of flood events.

~600 Year Flood Frequency and Magnitude Reconstruction

Interpretations of Peace River flood frequency and magnitude reconstructed from oxbow lake sediments can be readily examined in the context of climate variability. During the last millennium, climate is generally characterized by three main intervals:

medieval times, the Little Ice Age (LIA), and the post-LIA. The medieval times, an interval of relatively warm temperatures, is largely understood to have occurred from AD ~1000 to ~1300 in the Northern Hemisphere extratropics, from 30° N to 90°N (Crowley 2000, Crowley and Lowery 2000). However, relatively warm temperatures have been detected occurring as far back as AD ~900 (Esper et al. 2002, Cook et al. 2004). The warmest interval in medieval times is classically understood to have occurred from ~1000 to ~1200 AD, and is termed the "High Medieval" (Bradley et al. 2003). More recently it has been termed the "Medieval Climate Anomaly" (MCA), and understood to have occurred from AD ~800 to ~1300 (MacDonald et al. 2008). The LIA, from AD ~1570 to ~1900) is characterized as a period when summer temperatures fell significantly below the AD 1961 to 1990 mean in the northern hemisphere (Matthews and Briffa 2005), and conditions were relatively dry (Kreutz et al. 1997). It is considered to be one of the coldest periods in the last 12,000 years (Bradley et al. 2003). The post-LIA (AD ~1900 to present) can be characterised as a period of recent climate warming.

Millennium-scale reconstructions of winter temperature (ΔT_{win}) and growth season relative humidity (ΔRHgrs; Edwards et al. 2008) in the Columbia Icefield help characterise the atmospheric climate in the eastern Rocky Mountains near the headwaters of the Athabasca and Smoky Rivers (Figure 49). During medieval times (AD ~1000 to ~1530), climate was characterised by relatively warm winters. The interval AD ~1100 to ~1250 was particularly mild and falls within the MCA, and corresponds to the "12th century megadrought" described by MacDonald et al. (2008). The interval AD ~1530s to ~1890s is marked by a strong coherence among the ΔRH_{grs}, ΔT_{win} reconstructions (Edwards et al. 2008). From AD ~1530 to the late 19th century cooler and drier

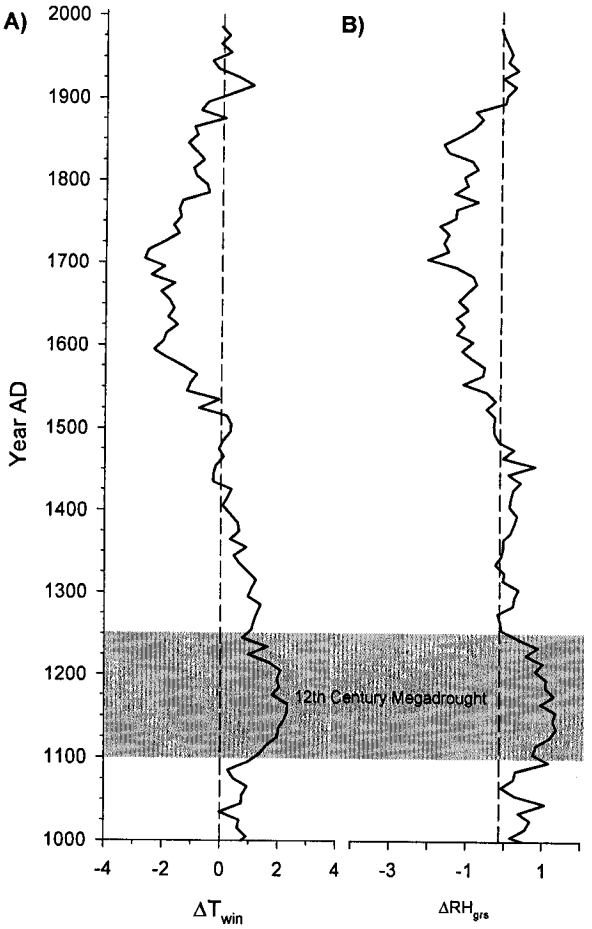

Figure 49: The winter temperature (A) and growth season relative humidity (B) reconstructions near the Columbia Icefield in the Rocky Mountains (from Edwards et al. 2008).

conditions persisted, and are associated with known advances of glaciers in decades around AD 1700 and the mid-1800s (Luckman 2000). The ΔTwin reconstruction indicated that by AD ~1800, 20th century winter temperatures in the Columbia Icefield had been attained. However, ΔRHgrs values remained relatively low until AD ~1900. During the 20th century, the climate reconstructions suggest that conditions are returning to those similar to the early millennium.

Magnetic Susceptibility and Stratigraphic Records

The detailed examination of magnetic susceptibility results for individual light and dark clay and silt laminations reveals that dark grey beds have relatively high magnetic susceptibility values, while the light grey beds have relatively low magnetic susceptibility values (Figure 50), consistent with results of Wolfe et al. (2006). During flood events, sediments that have higher magnetic susceptibility values from upstream along the Peace River flow into the oxbows and are deposited. Conversely, sediments that are deposited during periods of no flooding have low magnetic susceptibility values. Thus, the peaks in magnetic susceptibility are interpreted as flood deposits (high energy), while the troughs in magnetic susceptibility are interpreted as non-flood deposits (low energy) and are used as a key tool for interpreting Peace River ice-jam flood frequency over the last ~600 years.

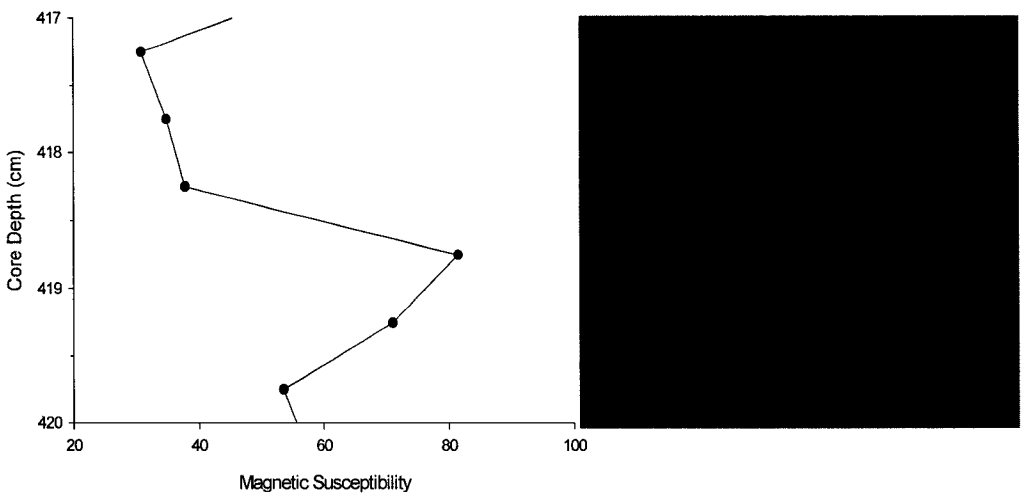

Figure 50: Dark grey deposits have a higher magnetic susceptibility than light grey deposits (photograph from PAD 15 VC3, the distal site).

Several trends are apparent when the magnetic susceptibility records are examined in conjunction with the stratigraphy of PAD 15 VC1 (proximal site) and PAD 15 VC3 (distal site) in Figure 51. As indicated previously, the z-scores of magnetic susceptibility values are significantly more variable during medieval times, prior to AD ~1595, when compared to any other interval in both cores. These high values are associated with overall relatively large grain sizes (fine- to coarse-grained sand and pebbles) in PAD 15 VC1 (proximal site) from the base of the core (757.5 cm) to 394 cm depth. Specifically, the large spikes in magnetic susceptibility (Figure 39, page 83) that occur at AD ~1364 (726.25 cm depth, z-score of 10.5559) and AD ~1457 (591.25 cm depth, z-score of 10.2269) are associated with coarse sand and pebbles, and medium to coarse sand deposits, respectively. The spikes at AD ~1391 (688.25 cm depth, z-score of 7.5375), AD ~1410 (659.25 cm depth, z-score of 6.6386), and AD ~1417 (649.25 cm depth, z-score of 10.9120) are associated with fine to medium sand deposits. The sediments containing these large spikes in magnetic susceptibility correspond to facies association A in Figure 47, and are interpreted as being deposited when the oxbow was a part of the main river channel (cut-off occurred in AD ~1460).

In PAD 15 VC3 (distal site), the highly variable and overall high magnetic susceptibility z-scores (zone 1) are associated with the unique, well-defined alternating light and dark grey clay and silt laminations not observed in any of the other cores (see Figure 27, page 66). The large spikes in magnetic susceptibility measurements found in the lower portion of zone 1 in PAD 15 VC1 (proximal site) are not found in zone 1 of PAD 15 VC3 (distal site). Importantly, previous core-to-core correlations based on sedimentological characteristics (Figures 44 and 45) and magnetic susceptibility

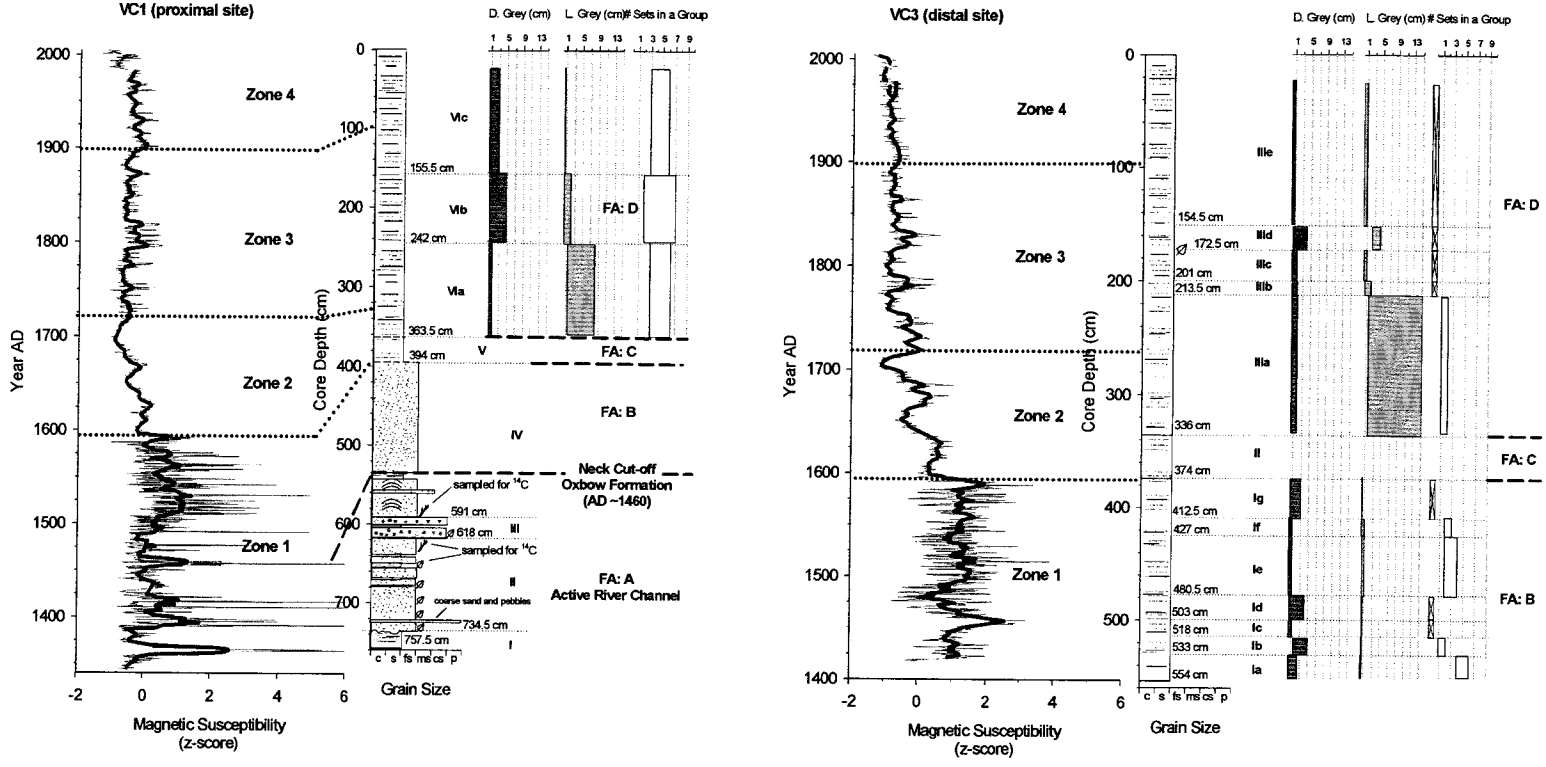

Figure 51: Magnetic susceptibility and stratigraphic profiles of PAD 15 VC1 (proximal) and VC3 (distal). The Roman Numerals and capital letters refer to facies and subfacies, and facies associations (FA) discussed previously, respectively. Note that the year AD and depth (cm) scales for the magnetic susceptibility and stratigraphic profiles are different.

measurements within PAD 15 (Figures 39) suggest that the entire oxbow flood frequency and magnitude record (~600 years) has been captured at PAD 15 VC3 (distal site). Thus, the period prior to AD ~1595 (zone 1) is interpreted as an interval of high Peace River flood frequency and magnitude. It is also important to note that this abrupt shift in flood frequency and magnitude likely occurs in PAD 54 during the same time period since all of the cores from both oxbows contain a similar abrupt stratigraphic shift from coarser-grain sizes (generally sand) to clay and silt (arrows in Figure 44).

However, an inconsistency between magnetic susceptibility and stratigraphic interpretations arises because the ^{14}C date from wood sampled from the lower sediments in VC1 (proximal site), contained within facies association A (river channel deposits, Figure 51), was used to help constrain the chronology of the lower sediments in VC3 (distal site), which is assumed to contain the entire oxbow flood frequency and magnitude record. Based on the chronology of VC1 (proximal site), the oxbow was cut-off from the main channel at AD ~1460 (Figure 51). However, the distal site, assumed to contain the entire oxbow record, spans the period AD ~1418 to 2005. Subsequent discussion included in the section titled "The Hydroecology of the Peace and Athabasca Sectors of the PAD" on page 125 and highlighted in Figure 60 on page 127, shows that the chronology of VC3 (distal site) remains a reasonable estimate of sediment age because of the strong agreement in shifts of hydroecological conditions among several basins in the PAD over similar time periods.

An abrupt shift from highly variable flood frequency and overall high flood magnitude to overall less variable flood frequency and relatively low flood magnitude is indicated by the three troughs in magnetic susceptibility, AD ~1595 to ~1720 (zone 2).

These three troughs are associated with massive clay and silt in both cores (facies V and II in VC1 and VC3, respectively), as well as relatively thick light grey clay and silt beds and relatively thin dark grey clay and silt beds in VC1 (proximal site, subfacies VIa) and VC3 (distal site, subfacies IIIa) cores.

Magnetic susceptibility has slightly higher frequency variability during AD ~1720 to ~1900 (zone 3) when compared to AD ~1595 to ~1720 (zone 2), suggesting that flood frequency slightly increased during this interval. These trends are reflected in the stratigraphy by a significant decrease in the light grey bed thickness range in VC1 (proximal site) and VC3 (distal site), and an increase in the dark grey bed thickness range in VC1 (proximal site) in Figure 51. In VC1 (proximal site), the light grey bed thickness range decreases from 1.5 cm to 8 cm (subfacies VIa) to 0.5 cm to 2 cm (subfacies VIb) and the dark grey bed thickness range increases from 0.5 cm to 1.5 cm (subfacies VIa) to 0.5 cm to 5 cm (subfacies VIb). Also, the number of sets of beds in a group increases slightly (from 3 to 6 sets to 2 to 7 sets) from subfacies VIa to VIb in PAD 15 VC1 (distal site). In VC3 (distal site), the light grey bed thickness range decreases from 1.5 cm to 15 cm (subfacies IIIa) to only 0.5 cm to 2 cm (subfacies IIIb). The dark grey bed thickness remains relatively constant (ranging from 0.5 cm to 1.5 cm) in VC3 (distal site) throughout the AD ~1720 to ~1900 interval (zone 3), with the exception of subfacies IIId. The magnetic susceptibility peaks from AD ~1820 to ~1835 may be associated with the relatively thick dark grey clay and silt beds in subfacies IId (ranging from 0.4 cm to 4 cm thick). The beds in the facies III of PAD 15 VC3 (distal) are not grouped, with the exception of IIIa, but this may be due to the increased proximity of PAD 15 VC1 (proximal site) to the inlet. The overall thickness of the dark grey beds is greater in PAD

15 VC1 (proximal) when compared to VC3 (distal), making the groupings easier to identify than in PAD 15 VC3 (distal).

The relatively low variability of the magnetic susceptibility values in zone 4 (AD ~1900 to 2005) suggests that flood frequency has been relatively stable during this period. This trend is also reflected in the uppermost subfacies in each core (Figure 51). Although the range of dark grey bed thickness is somewhat larger in PAD 15 VC1 (proximal site, from 0.5 cm to 3 cm thick) than in PAD 15 VC3 (distal site, from 0.2 cm to 1 cm thick), the range of light grey bed thickness is consistent for the two cores, ranging from 0.3 cm to 1 cm in VC1 (proximal) and 0.2 cm to 1 cm in VC3 (distal). In addition, the depths of the top subfacies (IVc) in VC1 (proximal site) and (IIIe) in VC3 (distal site) are similar (155.5 cm in VC1, and 154.5 cm in VC3).

Organic Carbon and Nitrogen Elemental and Stable Isotope Geochemistry

The interpretation of high magnetic susceptibility values and larger grain sizes as high energy events can be further tested by examining organic carbon and nitrogen elemental and stable isotope geochemistry (Figure 52). Overall, there is a negative correlation between C_{org} ($r^2 = 0.50$, $\alpha = 0.05$) and N ($r^2 = 0.59$, $\alpha = 0.05$), and magnetic susceptibility. This is likely due to the dilution of autochthonous organic material by relatively inorganic sediment (likely fluvial in origin, with high magnetic susceptibility values) and a reduction in lake productivity due to high turbidity, and is consistent with the interpretations by Brown et al. (2000) and Wolfe et al. (2006). For example, the large peak in magnetic susceptibility from AD ~1440 to ~1470 (highlighted by the lowermost shaded grey bar in Figure 52) coincides with decreases in both C_{org} and N. Furthermore,

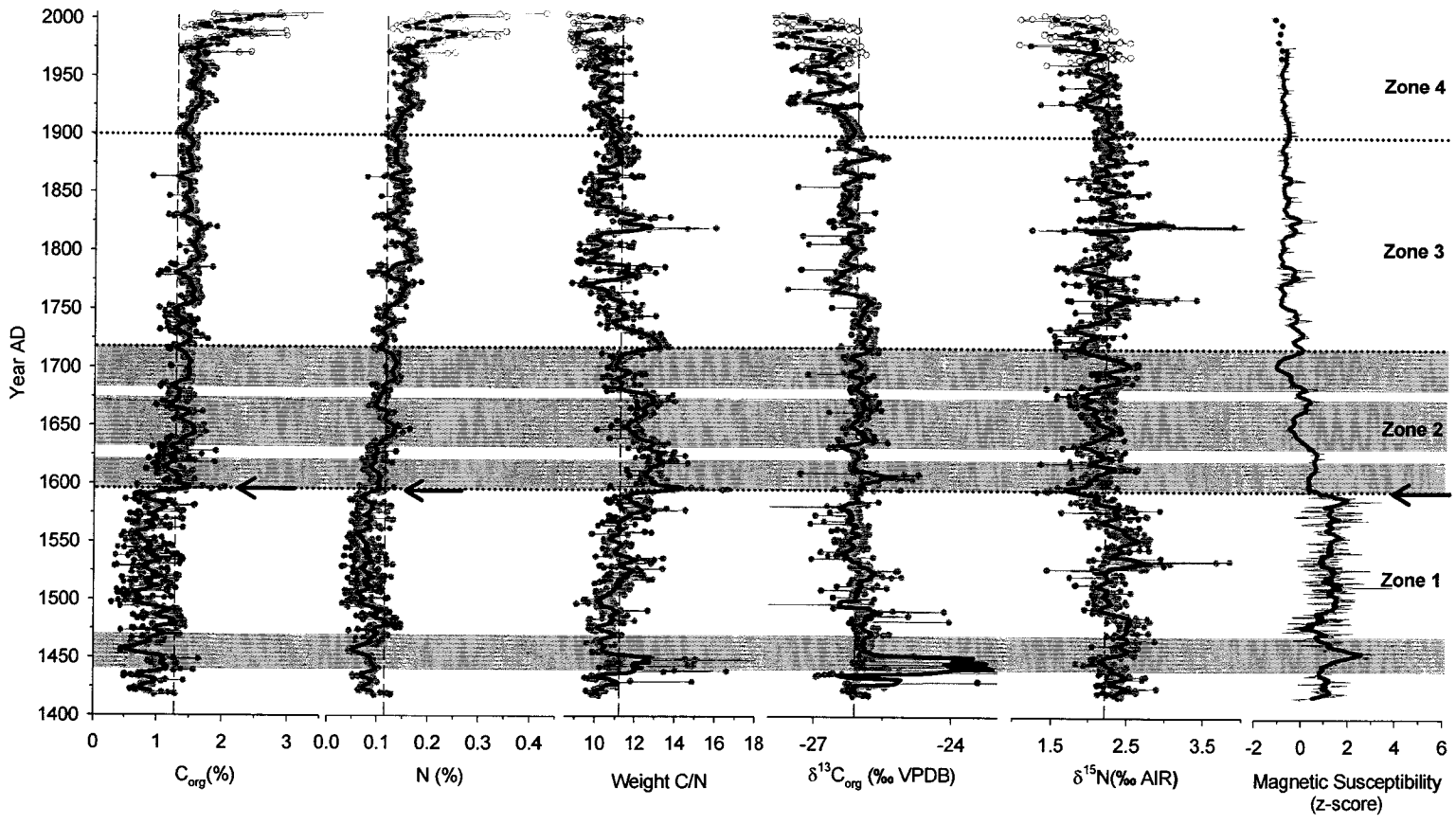

Figure 52: The geochemical stratigraphy and magnetic susceptibility profile of PAD 15 VC3 (distal). The solid black line indicates the 5-year running mean in each profile. The vertical dashed lines indicate the overall mean of each profile. The arrows and shaded grey bars refer to relationships discussed in the text.

the sharp decline in magnetic susceptibility at AD ~1595 coincides with an increase in C_{org} and a slight increase in N (arrows in Figure 52). The three distinct troughs in magnetic susceptibility during the interval AD ~1595 to ~1720 (zone 2) are also negatively correlated with C_{org} and N (shaded grey bars in Figure 52). During the interval AD ~1595 to ~1720 (zone 3), C_{org} and N gradually increase. The rise in C_{org} and N during the last ~100 years (zone 4) is likely due to both the overall better preservation of organic matter in the most recent sediments and a decrease in the flood frequency over the same time period (as shown most clearly by the C/N ratios and $\delta^{13}C_{org}$, discussed below).

There is a positive correlation between magnetic susceptibility and C/N ratios from AD ~1595 to 2005 ($r^2 = 0.42$, $\alpha = 0.05$). For example, the three distinct troughs in magnetic susceptibility during the interval AD ~1595 to ~1720 (zone 2) correspond to three distinct troughs in C/N ratios (shaded grey bars in Figure 52). This is likely because of the influx of relatively high amounts of terrestrial organic matter (with generally high C/N ratios) during flood events (Meyers and Teranes 2001). The relatively high C/N ratios of vegetation of terrestrial origin relative to that of aquatic origin arises from the presence of cellulose in terrestrial plants, while algae are generally rich in proteins (Meyers 1997). During AD ~1900 to 2005 (zone 4), the decline in C/N ratios is consistent with declining flood frequency and magnitude. Although the magnetic susceptibility records reflect overall stable conditions during AD ~1900 to 2005 (zone 4) in Figure 52, this may be because the significantly variable and overall higher magnetic susceptibility values prior to AD ~1595 are suppressing the z-scores in the most recent sediments. In addition, some of the uniformity of magnetic susceptibility record

during this period may be due to the relatively high water content in the upper sediments, which can dampen magnetic susceptibility measurements (Wolfe et al. 2006).

During AD ~1418 to ~1595, the relationship between the C/N ratios and magnetic susceptibility is less clear ($r^2 = 0.006$, $\alpha = 0.05$). Although the high frequency trends in C/N ratios appear to be positively correlated with magnetic susceptibility during this period (shaded grey bar near the base of the core in Figure 52), the C/N ratios are overall relatively low when compared to the entire ~600 year record of magnetic susceptibility. Unfortunately, the determination of bulk N by an elemental analyser does not allow the separation of organic and inorganic nitrogen. Inorganic N typically constitutes a small amount of the total N in lake sediments (Meyers 1997). In sediments with low organic matter content, inorganic N can represent a large proportion of the total N, artificially depressing the C/N ratio (Meyers 1997). Talbot (2001) suggests that inorganic N can be detected by plotting N versus C_{org}. If the regression line does not pass through the origin and intercepts the y-axis at a positive value, N is present in excess of C_{org}. Thus, the y-intercept value can be used as a constant to correct for inorganic N (Talbot 2001). Figure 53 shows the relationship between N and C_{org} for PAD 15 VC3 (distal) during each of the four time periods previously outlined.

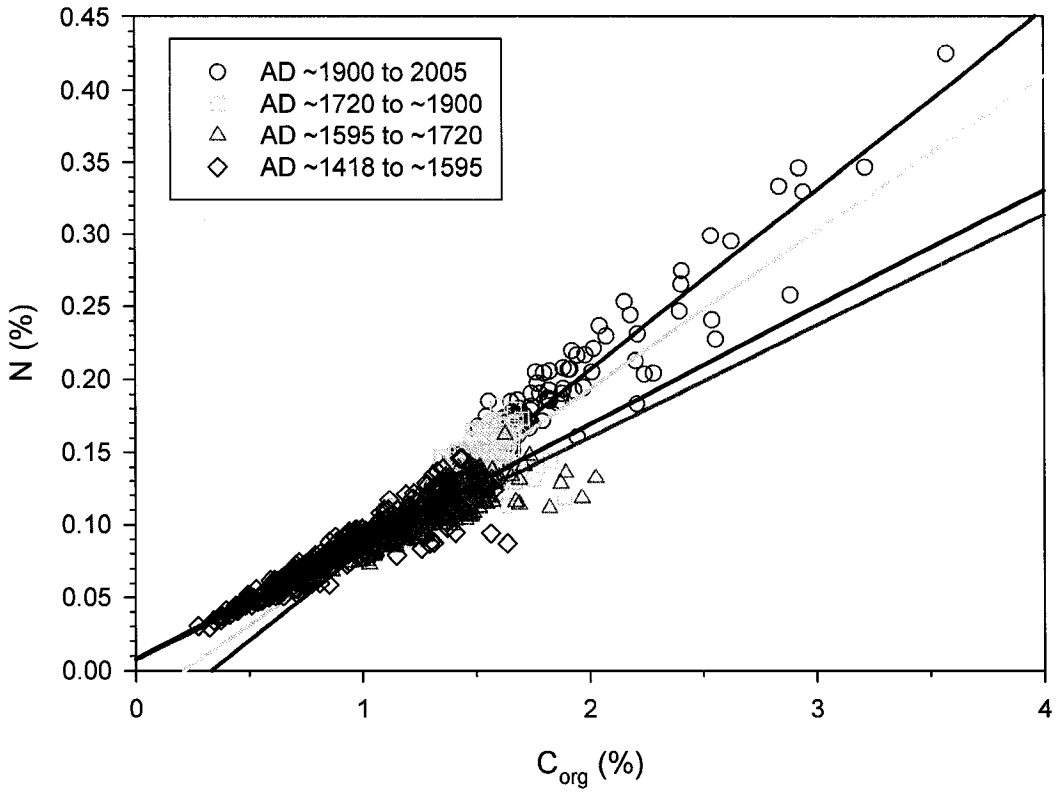

Figure 53: N (%) and C_{org} (%) cross-plot of PAD 15 VC3 (distal site). Note that for the intervals AD ~1418 to ~1595 (black) and AD ~1595 to ~1720 (dark grey), the linear regression lines intersect the y-axis. The value of the y-intercept indicates the average amount of inorganic nitrogen for those two periods (Talbot 2001).

During AD ~1720 to 2005, the linear regressions intercept the x-axis, indicating that C_{org} is present in excess of N. This may suggest an abundance of charcoal, possibly due to relatively high fire frequency and warrants further investigation. In contrast, during the intervals AD ~1418 to ~1595 and AD ~1595 to ~1720, the linear regressions intercept the y-axis at approximately 0.008 %. Although this value is relatively small, the C_{org} and the bulk N are also low, making this correction factor significant. Figure 54 shows the linear regressions and their 95 % confidence intervals. While the 95 % confidence interval for AD ~1418 to ~1595 is relatively narrow and closely follows the regression line, the 95 % confidence interval for AD ~1595 to ~1720 is relatively wide, and the

lower limit intersects on the x-axis. Therefore, a correction factor of 0.008 % was only applied to bulk N values in the interval AD ~1418 to ~1595. The correction factor results in an increase of the C/N ratios by a value of just over 1, causing the C/N ratios in zone 1 to shift to the right (Figure 55). However, $r^2 = 0.13$ ($\alpha = 0.05$), improving only slightly from the relationship prior to applying the correction. The entire corrected geochemical record is shown in Figure 56. The generally persistently high C/N ratios during medieval times (AD ~1418 to ~1595) are consistent with high flood frequency and magnitude inferred from the magnetic susceptibility and stratigraphic profiles.

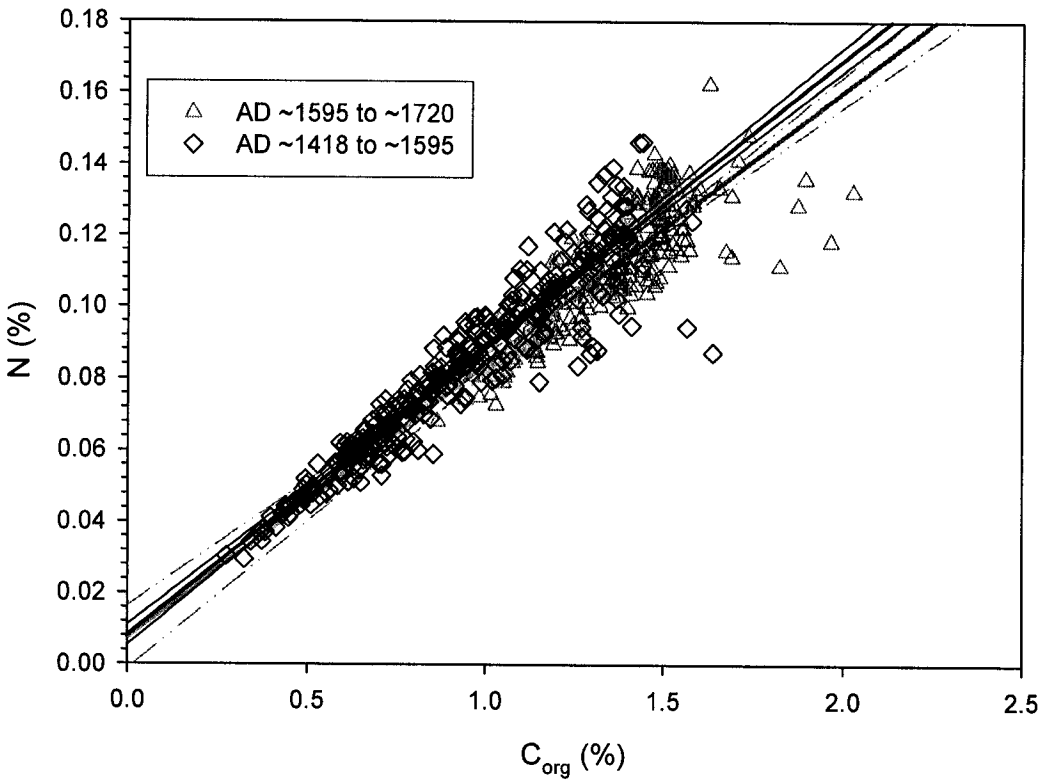

Figure 54: The 95% confidence intervals of AD ~1418 to ~1595 and AD ~1595 to ~1720 of PAD 15 VC3 (distal site). Note that the 95% confidence interval for zone 1 is relatively narrow while the confidence interval for zone 2 is relatively wide, with the lower limit passing through the origin.

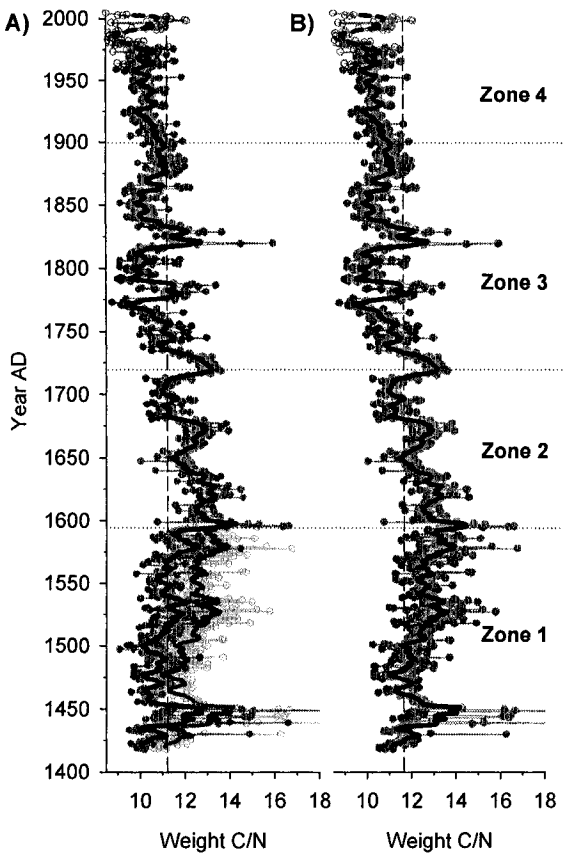

Figure 55: The corrected C/N record from PAD 15 VC3 (distal site). In A), the dark grey and black lines represent the original calculated C/N ratios and 5-year running mean, respectively. The light grey and thick dark grey lines represent the corrected (+0.008%) C/N ratios. In B), the entire C/N record with the corrected C/N ratios. The vertical dashed lines in both A and B indicate the overall mean of the entire record.

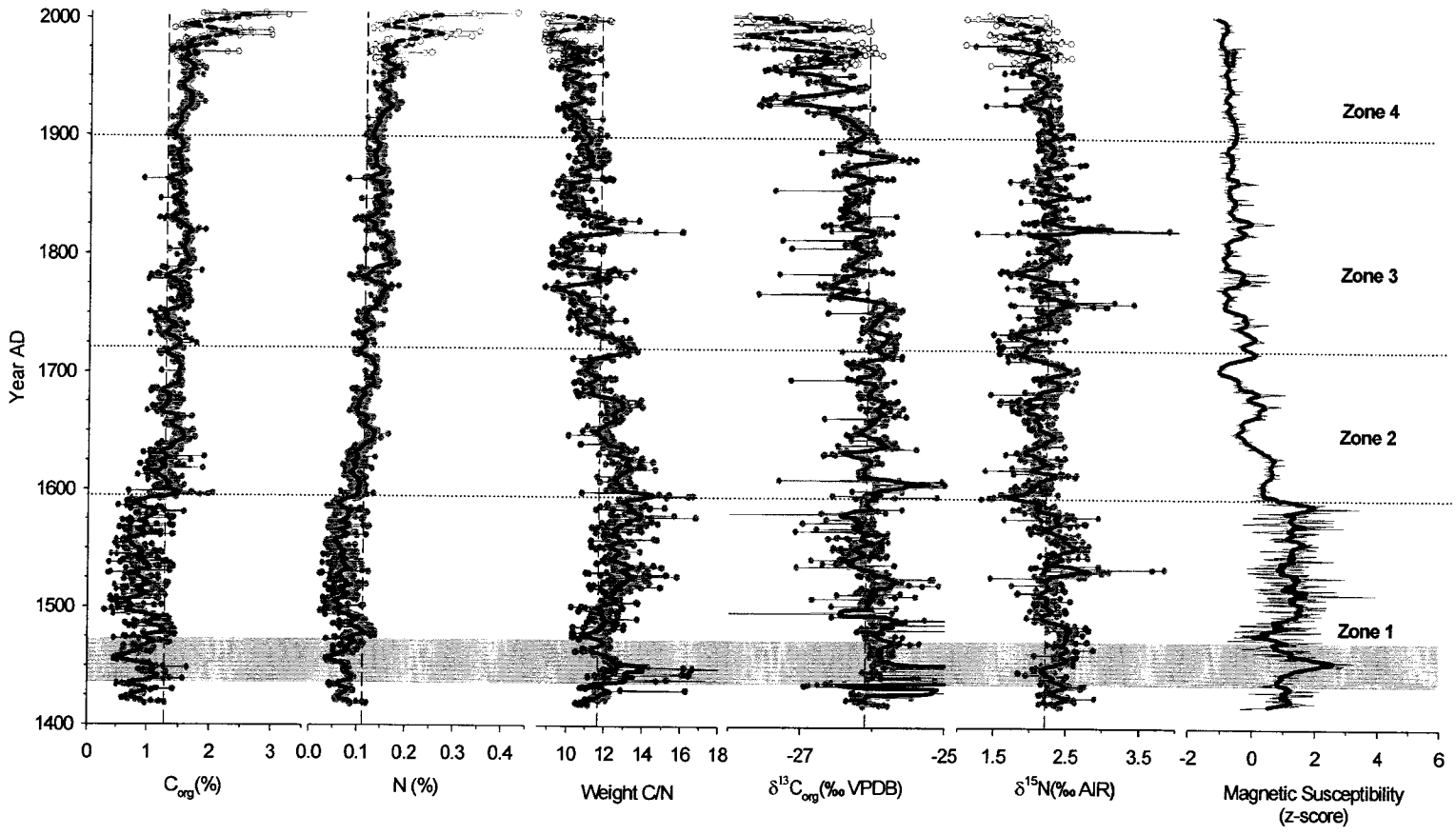

Figure 56: Geochemistry and magnetic susceptibility records with the corrected N and C/N ratios. The solid black line is the 5–year running mean in each profile. The dashed vertical lines represent the overall mean in each profile. Note that the $\delta^{13}C_{org}$ scale has been expanded resulting in some of the values in zone 1 being truncated.

Aquatic and terrestrial vegetation generally preferentially take up ^{12}C and discriminate against ^{13}C during photosynthesis. However, as lake productivity increases and ^{12}C becomes limiting, organisms begin to take up relatively more ^{13}C. Although there are a variety of factors that can influence $\delta^{13}C_{org}$ measured in lake sediments, increases in $\delta^{13}C_{org}$ often reflect increases in lake productivity, while decreases in $\delta^{13}C_{org}$ often reflect decreases in lake productivity (Meyers and Teranes 2001). However, in PAD 15, the relationship between $\delta^{13}C_{org}$ and the other proxies is less clear, with the exception of the large peak indicated by the grey bar in Figure 56, and the interval AD ~1900 to 2005. This large peak in $\delta^{13}C_{org}$ has a positive relationship with magnetic susceptibility and C/N ratios, and a negative relationship with C_{org}, N, and $\delta^{15}N$. Wolfe et al (2006) interpreted similar results as flood deposits, with increases in $\delta^{13}C_{org}$ indicating an increased influx of C-rich and N-poor hydrocarbons (bitumen) during flood events from the tar sands deposits that seep into the river, possibly from the banks of the Wabasca River upstream. Decreases in $\delta^{13}C_{org}$ during low energy events were attributed to the internal recycling of carbon in the water column, which contributes ^{13}C-depleted CO_2 to the dissolved inorganic carbon (DIC) pool. It is important to note that the strongest signal in the $\delta^{13}C_{org}$ record occurs during AD ~1900 to 2005. During this interval, $\delta^{13}C_{org}$ is weakly negatively correlated to magnetic susceptibility ($r^2 = 0.22$, $\alpha = 0.05$), positively correlated to C/N ratios ($r^2 = 0.41$, $\alpha = 0.05$) and $\delta^{15}N$ ($r^2 = 0.38$, $\alpha = 0.05$), and negatively correlated to C_{org} ($r^2 = 0.53$, $\alpha = 0.05$) and N ($r^2 = 0.61$, $\alpha = 0.05$). This is another indicator that this interval is characterised by the lowest flood frequency and magnitude of the entire ~600 year record. The relatively weak correlation between $\delta^{13}C_{org}$ and magnetic susceptibility

in the uppermost sediments may be due to the suppression of magnetic susceptibility measurements because of increasing water content in the upper sediments.

$\delta^{15}N$ has been used as an indicator of lake productivity but interpretation is often complicated because numerous processes can influence this parameter (Meyers 1997). In the case of PAD 15, the relationship between $\delta^{15}N$ and the other geochemical proxies and magnetic susceptibility is somewhat ambiguous. There is a substantial amount of variability that does not appear to be clearly associated with any of the other indicators, and is difficult to interpret.

In summary, the physical stratigraphy, magnetic susceptibility, and elemental and stable isotope geochemistry reflect a largely coherent history of flood frequency and magnitude for the past ~600 years at PAD 15. Of all of the proxies analysed, magnetic susceptibility measurements and C/N ratios are the clearest indicators. Flood frequency and magnitude were greatest from AD ~1418 to ~1595. Around AD ~1595, there was a sharp decline not only in the frequency of flooding but also in the magnitude of flooding, indicated most clearly in the magnetic susceptibility and the C/N records. The AD ~1595 to ~1720 interval was characterised by extended periods of low flood frequency and magnitude, as indicated by the three troughs in magnetic susceptibility and C/N ratios. Periods of low magnitude flooding were shorter in the interval AD ~1720 to ~1900, although the variability is slightly higher. During the last ~100 years there has been an overall decline in flood frequency.

Comparison of Peace River Flood Frequency and Magnitude Reconstruction to Hydrologic Records and Previous Research

Figure 57 shows the C/N ratios from VC3 (distal site) at PAD 15 and the daily water level data (1972-2005) from the water gauge at Rocky Point, a location of frequent ice-jam events on the Peace River and upstream of PAD 15 (see Figure 2, Rocky Point data from the Water Survey of Canada, station 07KC005). The C/N ratio is a more sensitive indicator of flood frequency in the upper sediments when compared to magnetic susceptibility because the magnetic susceptibility record was not corrected for the increased water content at shallower depths, which can suppress magnetic susceptibility measurements (Wolfe et al. 2006). The vertical dashed line represents the known sill elevation at PAD 54. Although the PAD 15 sill elevation is not known, it is thought to be slightly higher than that of PAD 54 because recent field observations indicate that during spring ice-jam events, flood waters have been observed entering PAD 54 but not PAD 15 (Wolfe et al. 2006). Tentative correlations have been drawn between these records based on known flood events and peaks in the C/N ratio. Years of high magnitude spring ice-jam flooding include 1972, 1974, 1990 (historic open water event measured at Peace Point), 1994 (spring ice-jam at Rocky Point, Peters 2003), 1996 (Prowse and Lalonde 1996), and 1997 and appear to be recorded in the C/N ratios of PAD 15. Other, somewhat lower magnitude events are 1973, 1976, 1977, 1981 and 1987 (reported in Wolfe et al. 2006), although only the events in 1973 and 1981 appear to be recorded in the C/N ratios at the distal site of PAD 15 (VC3). In addition, the absence of relatively high magnitude flooding during the latter half of the 1970s to the 1990s is recorded clearly in the C/N ratios.

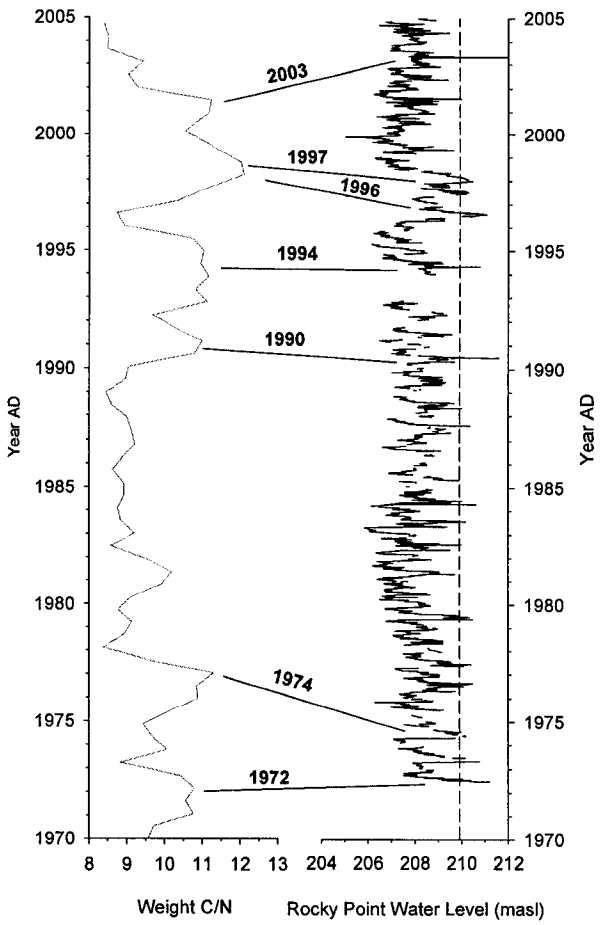

Figure 57: The C/N ratios from the distal site (VC3) at PAD 15 and the water level data from Rocky Point. The vertical dashed line on the Rocky Point water level plot is the sill elevation of PAD 54.

The magnetic susceptibility profiles of the two vibracores and the Russian peat core collected by Wolfe et al. (2006) are similar. Figure 58 shows tentative core-to-core correlations between the three magnetic susceptibility profiles using dashed lines. The Russian peat core is placed in the centre of the three magnetic susceptibility profiles in Figure 58 for convenience, as this core was collected at an intermediate site between the

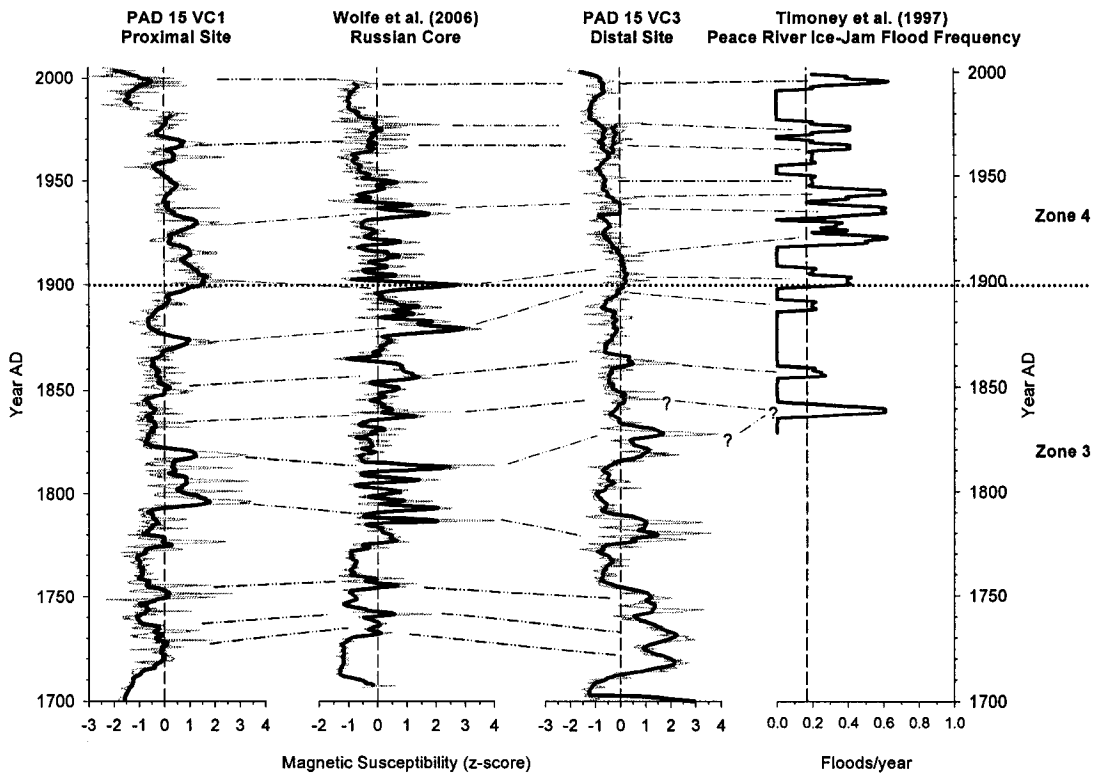

Figure 58: The magnetic susceptibility records of the two vibracores collected from PAD 15 (VC1 and VC3), the magnetic susceptibility record from the Russian core collected in PAD 15 during previous research by Wolfe et al. (2006), and the 5-year running mean of Peace River ice-jam flood frequency record reconstructed from Timoney et al. (1997). The vertical dashed lines represent the long-term average in each plot. Tentative lines of correlation are drawn between the sediment-based and historical-based flood frequency reconstructions.

proximal (VC1) and distal (VC3) vibracores. Also, the z-scores for VC1 and VC3 have been recalculated for Figure 58 from AD ~1700 to 2005 in order to show the variability in the magnetic susceptibility record of the upper sediments that would otherwise be suppressed because of the high variability in magnetic susceptibility in the lower sediments during AD ~1343 to ~1595. The sample measurement resolution of the Russian core was every 0.2 cm interval, while the sample resolution of the vibracores is every 0.5 cm interval. This may account for the relative smoothness of the two vibracore

profiles when compared to the Russian core profile. The slightly inclined correlation lines among the four profiles reflect chronological uncertainties. However, the temporal differences among the profiles do not appear to be greater than ±10 years.

The Timoney et al. (1997) Peace River flood frequency reconstruction in Figure 58 is based on a variety of written sources such as the Hudson Bay post records at Fort Chipewyan, Catholic church records from Fort Chipewyan, Wood Buffalo National Park warden and fur sales records, Fort Chipewyan oral history (Peterson 1994), as well as hydrometric records of Lake Athabasca and PAD water level records. Timoney et al. (1997) developed a binomial time series from 1826 to 1995, and assigned a value of 1 to years with flooding, and a value of 0 to years with minimal or no flooding. Although there is some offset because of the linear sedimentation rates used to calculate the chronologies (both the Russian peat core and vibracore records are loosely constrained by the 1964 ^{137}Cs peak and a single ^{14}C date), there is considerable agreement between the peaks in the magnetic susceptibility records and the Peace River spring ice-jam flood history developed by Timoney et al. (1997). Because the historical record only includes spring ice-jam flooding from the Peace River, it is likely that the majority of the floods reaching PAD 15 (and perhaps PAD 54), as measured by magnetic susceptibility and elemental and stable isotope geochemistry, are a result of ice-jams along the Peace River, and not flooding from large amounts of summer precipitation and/or high Lake Athabasca water levels.

The Hydroecology of the Peace and Athabasca Sectors of the PAD

Several additional datasets are available from other lakes in the Peace (PAD 5, 12, and 9) and Athabasca sectors (PAD 31) of the PAD for comparison with the flood frequency and magnitude reconstruction of the Peace River (Figure 59). PAD 5, also known as Spruce Island Lake, is a small isolated bedrock basin located between the Chenal des Quatre Fourches and the Revillon Coupé with a possible outlet to the north during high lake stages, or an inlet during high magnitude flood events (Wolfe et al. 2005). Because it is located relatively far from Peace River distributary channels to the east and west, it is only influenced by flooding during relatively extreme hydrologic events. Results of contemporary stable isotope analyses ($\delta^{18}O$ and $\delta^{2}H$) indicated that this basin has a strong sensitivity to seasonal hydrological variability including the effects of evaporative enrichment and dilution by precipitation (Wolfe et al. 2005). PAD 12 is a small, round, isolated basin located 750 m southwest of the Rivière des Rochers, near its confluence with the Peace River (Hall et al. 2004). Results of contemporary stable isotope analyses ($\delta^{18}O$ and $\delta^{2}H$) at this site indicated that this basin also has a strong sensitivity to seasonal hydrological variability including seasonal snowmelt input, precipitation events, Peace River input during flood events, and evaporation (Hall et al. 2004).

Analysis of $\delta^{18}O$ of lake sediment cellulose is frequently used as a proxy for hydrological variability and lake water balance reconstruction (Wolfe et al. 2001). The cellulose-inferred lake water $\delta^{18}O$ compositions for PAD 5 and PAD 12 are shown in D and E of Figure 60. The Peace River flood frequency and magnitude reconstruction

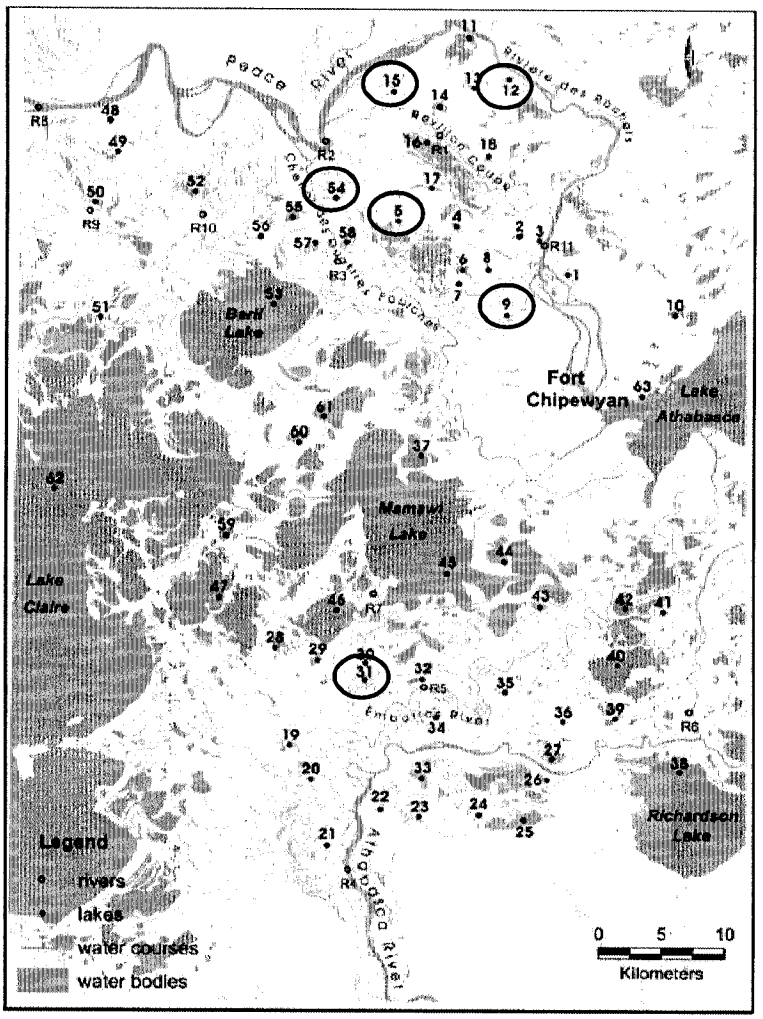

Figure 59: A map showing all of the lakes that are being studied in the PAD. Specific lakes discussed in the text are circled in black.

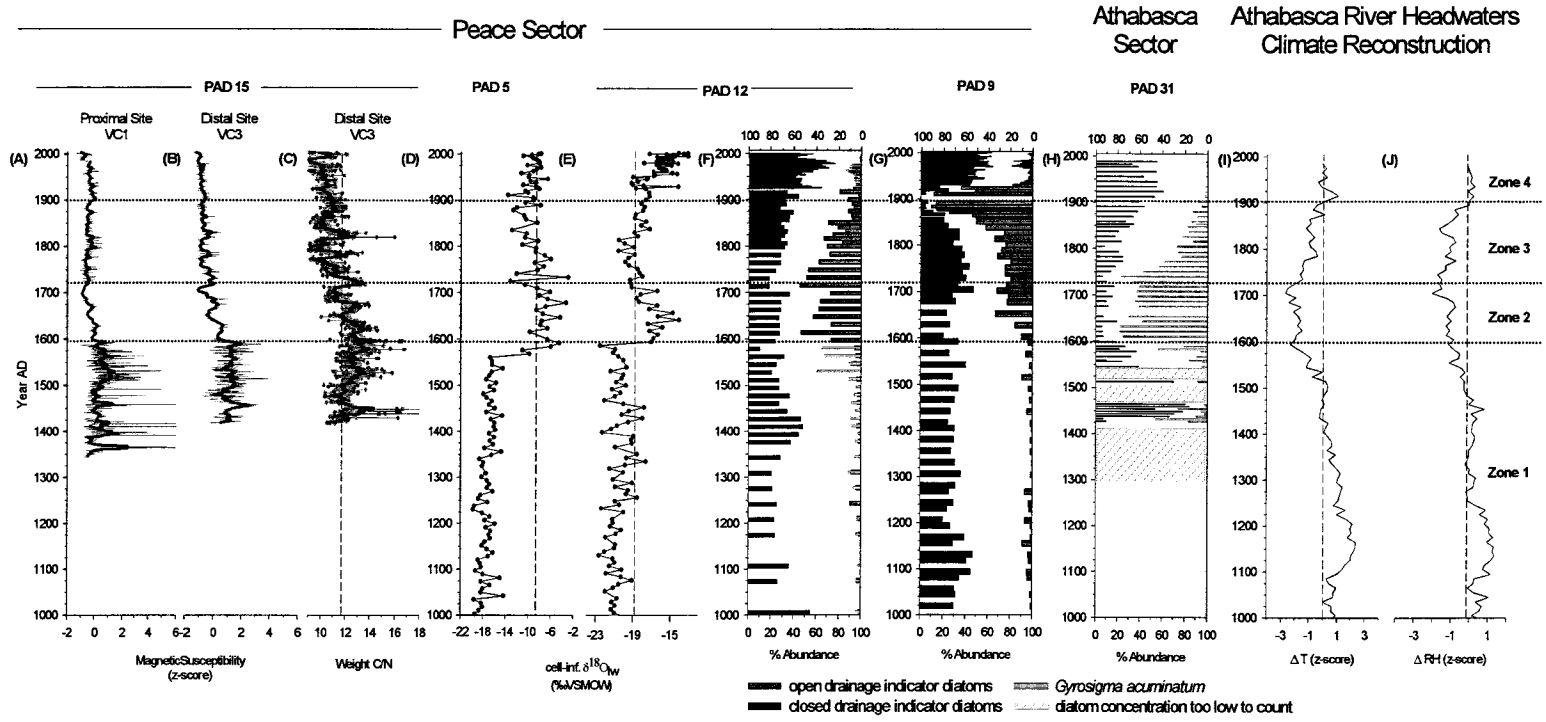

Figure 60: A) and B) PAD 15 magnetic susceptibility C) PAD 15 C/N ratios, D) and E) cellulose-inferred $\delta^{18}O$ of lake water from PAD 5 and PAD 12 (Yi, PhD in progress, Earth and Environmental Sciences Department, University of Waterloo), respectively, F) and G) diatom indicators from PAD 12 and PAD 9, respectively (Sinnatamby 2006), H) diatom indicators from PAD 31 (Wiklund, PhD in progress, Biology Department, University of Waterloo), and I) and J) Athabasca River headwater reconstruction of winter temperature (ΔT_{win}) and growth season relative humidity (ΔRH_{grs}) from Edwards et al. 2008.

based on magnetic susceptibility records and C/N ratios (plots A to C in Figure 60), and the $\delta^{18}O$ records of PAD 5 and PAD 12 show remarkable synchroneity in hydrological variability over the last ~600 years. Specifically, the abrupt shift from high flood frequency and magnitude during AD ~1418 to ~1595 to relatively low flood frequency and magnitude during AD ~1595 to ~1720 at PAD 15 coincides with a shift from ^{18}O-depleted lake water to significantly more enriched values in both PAD 5 and PAD 12. In fact, the consistently low ^{18}O values in PAD 5 and PAD 12 approach the isotopic signature of the contemporary Peace River (-20.1 ‰ to 19.0 ‰, Yi et al. 2008), suggesting that prior to AD ~1595, PAD 5 was also frequently flooded from the Peace River. Furthermore, the records from PAD 5 and PAD 12 are significantly longer than the PAD 15 flood frequency record, and show the consistently depleted $\delta^{18}O$ values extend to at least the base of the record (AD ~1000), suggesting that Peace River spring ice-jam flood frequency and magnitude may have been relatively high as far back as AD ~1000.

The PAD 5 record has a sharp shift (~12 ‰) to high $\delta^{18}O$ values around AD ~1595, suggesting PAD 5 became an evaporation-dominated closed basin at that time, and has remained so to the present. Overall, the lake water $\delta^{18}O$ composition during 1600s in PAD 5 is the most enriched of the entire record, suggesting that this was the driest period experienced at PAD 5. This is consistent with low flood frequency and magnitude in PAD 15. Hydrologic conditions were generally slightly more variable and less evaporatively enriched during AD ~1720 to ~1900 at PAD 5. However, since the beginning of the 20th century, the relatively low variability in the lake water $\delta^{18}O$ of PAD 5 and magnetic susceptibility records of PAD 15, and the decline in C/N ratios of PAD

15 reflect declining flood frequency. It is important to note that the PAD 5 chronology is well-constrained using ^{210}Pb and seven ^{14}C dates (r^2 = 0.99, Barkhouse 2007), providing strong support for the weakly constrained chronologies of PAD 15 VC1 (proximal site) and VC3 (distal site).

Important similarities are apparent between the lake water $\delta^{18}O$ and diatom records of PAD 12 (E and F in Figure 60, respectively). As previously discussed, the low lake water $\delta^{18}O$ values suggest that this basin had open-drainage conditions during medieval times (AD ~1000 to ~1550). The presence of closed-drainage diatom indicators initially suggests that this basin was generally hydrologically closed during this interval. However, the diatom taxon *Gryosigma acuminatum*, tolerant of river-borne sediment influxes, is also present (3 – 40 % abundance, shown on same side as the open-drainage indicator diatoms in G of Figure 60; Sinnatamby 2006), suggesting that PAD 12 was influenced by river flooding during medieval times. Similar to PAD 5, PAD 12 lake water $\delta^{18}O$ values rapidly increase around AD ~1600. At the same time, the diatom record shows a shift from closed-drainage to restricted-drainage conditions (indicated by increases in percent abundances of open-drainage indicator diatoms while maintaining moderate relative abundances of closed-drainage diatoms, Sinnatamby 2006). This shift in diatom communities indicates the influence of documented high water levels of Lake Athabasca (Vandermaelen 1827) on the limnology of PAD 12 (Sinnatamby 2006). By AD ~1900, PAD 12 had become a hydrologically closed lake basin, indicated by the increase in lake water $\delta^{18}O$ values and percent abundance of closed-drainage indicator diatoms.

The diatom record from PAD 9 in the Peace sector of the PAD (G in Figure 60) indicates somewhat different paleohydrological conditions compared to PAD 54, PAD 15, PAD 5, and PAD 12. PAD 9 is ~10 km northwest of Lake Athabasca and separated by a low-lying 70 km^2 sedge meadow (Sinnatamby 2006). This lake is low-lying, currently closed-drainage basins located in the northeast region of the PAD adjacent to the open-drainage network (Figure 59). During medieval times (AD ~1418 to ~1595), a period of high frequency and high magnitude flooding in PAD 15, PAD 5, and PAD 12, the PAD 9 diatom records suggests that this basin was hydrologically closed (until AD ~1600, Sinnatamby 2006). During AD ~1600 to ~1860, the diatom record suggests that PAD 9 was affected by outflow from the westward expansion of Lake Athabasca for at least 250 years due to relatively high water levels (Sinnatamby 2006, Vandermaelen 1827). As Lake Athabasca receded in the late 19^{th} century, PAD 9 briefly became an open-drainage basin with through-flow conditions while connected to Lake Athabasca by a river (Sinnatamby 2006). By ~1930, PAD 9 had returned to closed-drainage conditions similar to those that prevailed during medieval times. During the interval AD ~1600 to ~1930, PAD 9 likely maintained diatom communities indicative of open-drainage conditions longer than PAD 12 because of its proximity to Lake Athabasca, which had generally higher water levels during this period (Sinnatamby 2006).

PAD 31, known locally as Johnny Cabin Pond, is located in the Athabasca sector of the PAD (Figure 59). PAD 31 is a small, shallow basin located 150 m west of Mamawi Creek in an area of low relief dominated by marshes and willow swamps (Wolfe et al. 2008). During medieval times (H in Figure 60, AD ~1290 to ~1600), the diatom record from PAD 31 indicated that this basin was dominated by closed-drainage conditions.

However, in several portions of the sediment core diatoms numbers were too low to count. In these portions the sediment was observed as being relatively coarse when compared to upper sediments, where diatoms numbers were sufficiently high for counting (J. Wiklund, personal communication). This suggests that the diatom abundance was being diluted by a rapid sedimentation rate and may indicate that this basin was frequently flooded during this period (similar to PAD lakes 54, 15, 5, and 12). During AD ~1600 to ~1900, the diatom record reflects open-drainage conditions, as shown by the sharp increase in open-drainage diatom indicators. It is likely that PAD 31 was also influenced by high water levels in Lake Athabasca and perhaps relatively high annual flows along the Athabasca River (J. Wiklund, personal communication). The basin then returned to restricted-drainage conditions from AD ~1775 to ~1900, as shown by an increase in the relative abundance of closed-drainage diatoms while maintaining a moderate relative abundance of open-drainage diatoms. At the beginning of the 20th century, the closed-drainage diatom indicator abundance increases and the open-drainage diatom indicator abundance decreases.

Hydroclimatic Factors Affecting Flood Frequency and Magnitude during the Last Millennium – A Regional Perspective

The striking comparisons and contrasts in hydrological conditions among the basins discussed above reflect the complexity of this freshwater delta ecosystem. A variety of tree-ring reconstructions spanning the last millennium, which have the benefit of being absolutely dated, provide a regional framework in which the paleohydrological conditions of the PAD can be placed (Figure 61). The winter temperature (ΔT_{win}) and

growth season relative humidity (ΔRH_{grs}) reconstructions are based on tree-ring cellulose by Edwards et al. (2008, A and B in Figure 61), and the summer maximum temperature (ΔT_{max}) reconstruction based on maximum latewood density and ringwidth by Luckman and Wilson (2005, C in Figure 61). These reconstructions are based on live trees and snags collected in the Columbia Icefield (the headwater region of the Athabasca and Smoky rivers). Plots D and E in Figure 61 are the magnetic susceptibility and C/N ratio z-scores from the distal site at PAD 15 (only the distal site is shown here for convenience as it contains the complete oxbow record). Plot F in Figure 61 is a ring width-based reconstruction of annual discharge of the North Saskatchewan River (ΔQ_{NSR}), which also has its headwaters in the Columbia Icefield (Case and MacDonald 2003).

Climatic conditions during medieval times (AD ~1000 to ~1530) were relatively mild and humid in the headwater region of the Athabasca River. In addition, abundant snowfall at high elevations resulted in the expansion of alpine glaciers (shown by shaded grey bars in Figure 61). The divergence of ΔT_{max} from the trend in ΔT_{win} between the late 1100s and the late 1300s could be due to increased albedo feedback effects and cloudiness, suppressing ΔT_{max} (Luckman and Wilson 2005, Edwards et al. 2008). Another period of depression in the ΔT_{max} record also occurs in the mid to late 1400s, suggesting that this may also be a period of alpine glacier expansion (shown by the shaded bar in Figure 61, Edwards et al. 2008). Cooler and drier conditions persisted during the LIA (defined by Edwards et al. 2008 as AD ~1530s to ~1890s). Periods of

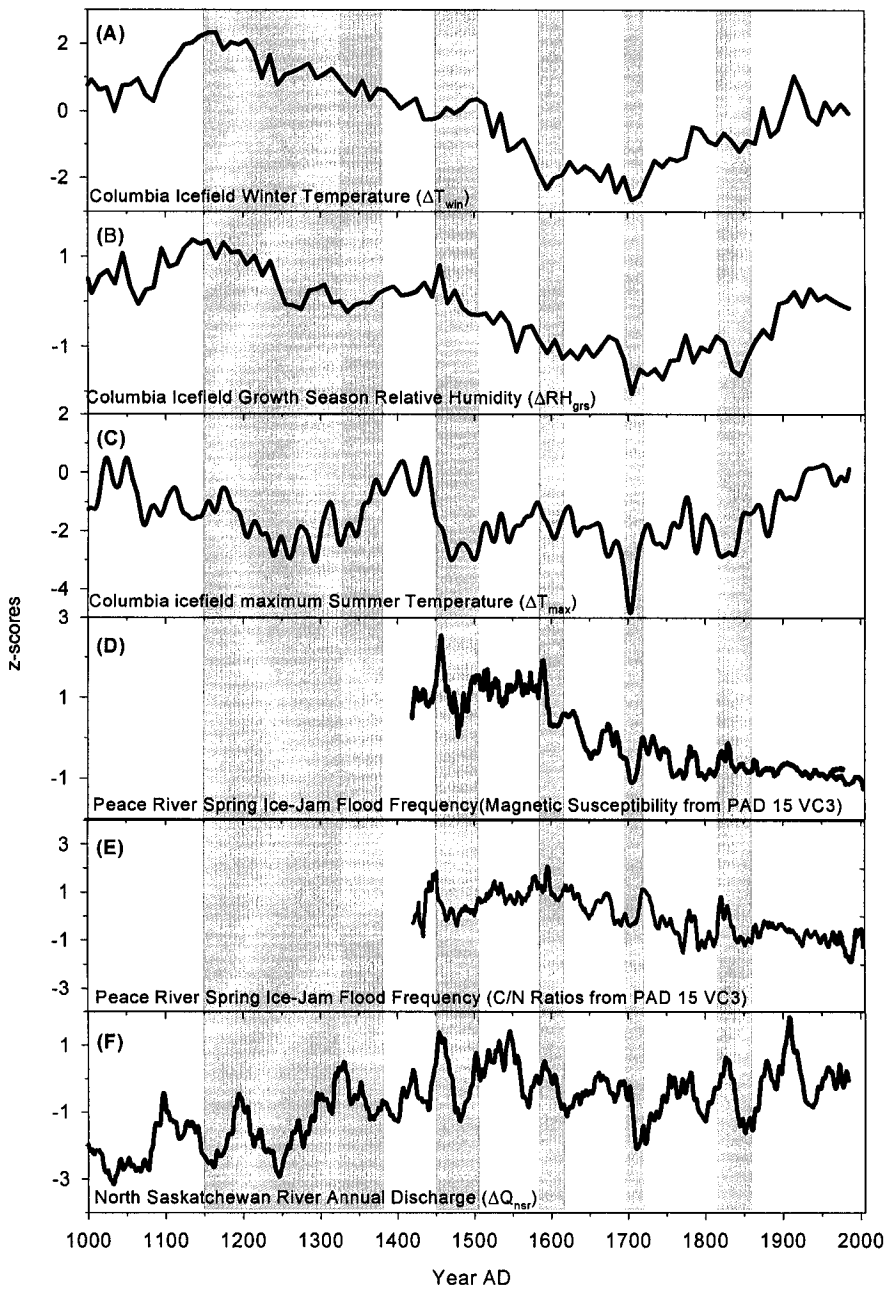

Figure 61: Columbia Icefield winter temperature (A) and growth season relative humidity (B) from Edwards et al. (2008), Columbia Icefield summer maximum temperature (C) from Luckman and Wilson (2005), Peace ice jam flood frequency interpreted from magnetic susceptibility (D) and C/N ratios (E) at PAD 15, and North Saskatchewan annual discharge record (F) from Case and MacDonald (2003). The shaded grey bars are periods of glacial advance (after Edwards et al. 2008).

glacial advance during this time are also reflected in the tree-ring records as intervals of relatively low ΔRH_{grs}, ΔT_{win}, and ΔT_{max} (Edwards et al. 2008). From the 1890s onward, conditions began to return to those similar to medieval times, relatively warm and moist (Edwards et al. 2008).

There are several trends to note between the Peace River flood frequency and magnitude and ΔQ_{NSR} reconstructions. The long-term, low frequency variations are negatively correlated. While Peace River flood frequency was relatively high during late medieval times (~1418 to ~1595), the ΔQ_{NSR} record shows relatively low annual discharge during AD ~1000 to ~1550. The relatively mild conditions during the early millennium, may have resulted in more rapid and/or earlier snowmelt (Edwards et al. 2008), climatic conditions that are conducive to ice-jam flooding (Figure 62). This would account for the high flood frequency and high magnitude ice-jam flooding along the Peace River during medieval times.

The relatively cool climate during the LIA would have likely caused a somewhat later and prolonged spring melt, and created conditions less conducive to spring ice-jam flooding (Figure 62). This accounts for the relatively low Peace River flood frequency and magnitude record at PAD 15. However, prolonged snowmelt during the summer months was likely adequate to sustain relatively high summer flows in many of the rivers draining the eastern Rocky Mountains during the LIA, as indicated by the ΔQ_{NSR} reconstruction. Thus, these hydrological records are measuring two distinct alpine run-off generation processes. The relatively high water levels of Lake Athabasca (as shown by the diatom records from PAD 9, PAD 31) during the same time period suggest that annual discharge of the Athabasca River was also relatively high. Many of the high

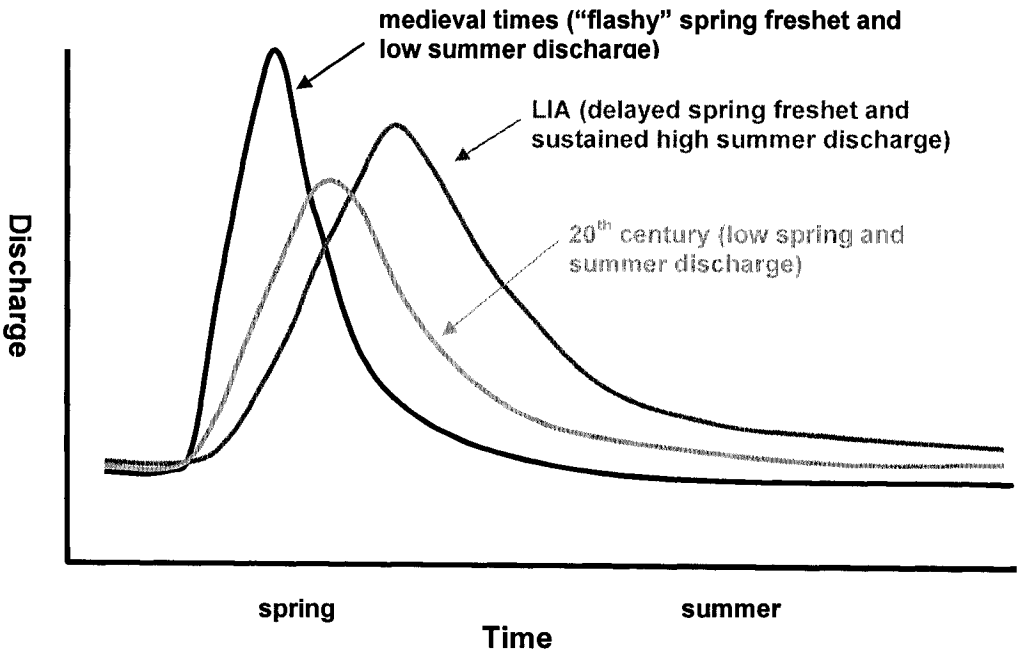

Figure 62: Schematic annual hydrograph of Peace River discharge during different climate intervals.

frequency trends in the hydrological records of Figure 61 are positively correlated, and coincide with intervals of glacial advance (shaded grey bars in Figure 61). Temporary reductions in Peace River flood frequency are correlated with temporary reductions in ΔQ_{NSR}, and consistent with the increased storage of water in advancing glaciers.

During the 20th century, climate conditions in the headwater region of the Athabasca River (Columbia Icefield ΔT_{win}, ΔRH_{grs}, and ΔT_{max} in Figure 61) appear to be returning to those similar to medieval times. However, Peace River flood frequency and magnitude are still declining. This is likely due to the decline of spring run-off generation in key tributaries of the Peace River (the Wabasca and Smoky rivers), particularly since the mid-1970s, and reduced winter snowpacks (Prowse and Conly 1998, Romolo et al. 2006a,

Figure 62). The relationship between climate variability and Peace River flood frequency and magnitude suggests that rather than the local climatic conditions of the PAD influencing its hydrology, the climate conditions in the headwater regions, upstream in the Rocky Mountains, have had a more significant impact on the hydrology of the PAD.

CONCLUSIONS

Summary

The vibracores collected from oxbow lakes PAD 54 and PAD 15 in the Peace-Athabasca Delta (PAD) provide a comprehensive history of Peace River flood frequency and magnitude over the past ~600 years. The sedimentological history interpreted from the stratigraphic record, magnetic susceptibility measurements, and elemental and stable isotope geochemistry are useful indicators of changing hydrological conditions in these oxbows. Overall, flood frequency and magnitude were greatest during AD ~1418 to ~1595. This is shown most clearly by overall large and variable sediment grain sizes, highly variable and overall high magnetic susceptibility values, and variable and relatively high C/N ratios. Extended periods of low flood frequency and magnitude occurred during AD ~1595 to ~1720. This is indicated by the massive or thick light grey clay and silt beds in the stratigraphic record, particularly from the distal site (VC3) at PAD 15, as well as overall lower magnetic susceptibility measurements, and relatively low C/N ratios. The interval AD ~1720 to ~1900 was a period of slightly more variability in flood frequency than AD ~1595 to ~1720, as reflected by thinner light grey clay and silt beds, and more variable magnetic susceptibility values and C/N ratios. During the past ~100 years, the stratigraphic record indicates that conditions have been oscillating on a relatively small scale, as indicated by alternating light and dark grey clay and silt beds in the upper sediments of all of the cores from both oxbows, while the C/N ratio and bulk organic $\delta^{13}C_{org}$ records indicate that flood frequency has been in overall decline.

When the ice-jam flood frequency and magnitude reconstruction is compared to other basins in the Peace (PAD 5, 12, and 9) and Athabasca sectors (PAD 31) of the PAD, several trends can be noted. The strong correlation between a sharp decrease in flood frequency and magnitude at PAD 54 and PAD 15, and the sharp shifts in cellulose-inferred lake water $\delta^{18}O$ ($\delta^{18}O_{lw}$) in PAD 5 and PAD 12, further suggests that high magnitude ice-jams along the Peace River frequently flooded lakes in the northern portions of the PAD during medieval times. In addition, the presence of diatom taxa *Gyrosigma acuminatum* in PAD 12 indicates the influence of river flooding during this period. Both PAD 5 and PAD 12 $\delta^{18}O_{lw}$ records indicate that these basins were consistently influenced by flood events, at least as far back as AD ~1000. Around AD ~1600, the PAD 5 record indicates that this basin shifted to hydrologically closed conditions, and has remained so to the present. Conversely, the PAD 12 $\delta^{18}O_{lw}$ and diatom records indicate that this basin was affected by Lake Athabasca outflow during the interval AD ~1600 to ~1900. Lakes PAD 9 and PAD 31 were also influenced by the high water levels in Lake Athabasca, with hydrological conditions ranging from open- to restricted-drainage. Lakes PAD 12, 9, and 31 became closed-drainage basins by the early 20^{th} century.

The interplay of several hydroclimatic factors has influenced Peace River ice-jam flood frequency and the ecohydrology of several other basins described in this thesis. The millennial-scale reconstructions of climate in the headwater region of the Athabasca River (Edwards et al. 2008) provide the framework in which these hydrological changes can be assessed. Relatively high ice-jam flood frequency and magnitude during medieval times is attributed to earlier and more rapid snowmelt, caused by warmer temperatures,

and relatively deep alpine snowpacks, caused by moister conditions, when compared to current conditions. Relatively cool and dry conditions in the headwater region, from AD ~1595 to ~1900, created conditions less-conducive to spring ice-jam flooding in the PAD. Superimposed on these long-term trends are the effects of intervals of glacial advance on the hydrology of the Peace River. During periods of glacial advance, ice-jam flood frequency is temporarily reduced due to the increased storage of water in glaciers. Although climate conditions appear to be returning to those similar in medieval times, ice-jam flood frequency and magnitude similar to that of medieval times have not returned to the PAD.

Management Implications

Because management strategies create frameworks for policy and practice, it is important to consider how information and knowledge gained from this kind of research can be utilized within such a plan (Sear and Arnell 2006). Because the Columbia Icefield is part of the hydrographic apex of North America, with headwaters of the Athabasca River draining northeastward into the Arctic Ocean, the North Saskatchewan River draining eastward into Hudson Bay, and the Fraser and Columbia rivers draining westward to the Pacific Ocean (Rood et al. 2005), the results of this research may have far-reaching implications for several drainage basins. Although climate conditions in the area of the Columbia Icefields may be returning to those similar to medieval times, with increasing winter temperatures and growth season relative humidity, the depth of alpine snowpacks, an important component of conditions conducive to spring ice-jam flooding, is in decline (Prowse et al. 2006, Romolo et al. 2006a). Therefore, it is unlikely that

Peace River spring ice-jam flood frequency and magnitude will return to that experienced during medieval times. Furthermore, as alpine glaciers continue to recede, this important water source in the headwater region that has contributed to annual flow in the past, will continue to decline (Figure 63).

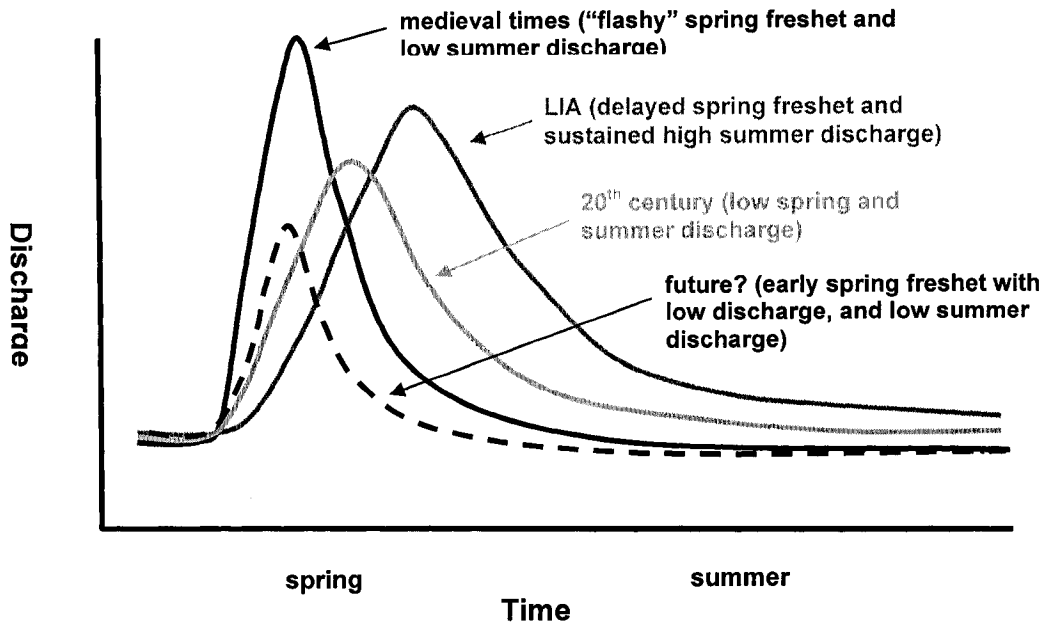

Figure 63: Schematic annual hydrograph of Peace River discharge during different climate intervals with a possible future scenario.

The recommendations for the mitigation of the apparent drying trends in the PAD from technical studies conducted from the mid-1970s to the mid-1990s, such as weirs and artificial ice-jams, only met with limited success. The improved understanding of the relationship between Peace River flood frequency and magnitude, and climate variability garnered from this research may be used as a predictive tool for managers and stakeholders, and can aid in adapting to future hydrological conditions along the Peace

River and in the PAD. Importantly, based on the results of this research, these conditions may include an ongoing reduction in Peace River flood frequency and magnitude.

The combination of declining streamflow and snowpacks, and warming temperatures could create many challenges for the natural environment and water supplies for hydroelectric facilities and consumptive use by humans (Rood et al. 2005). This is of particular concern in many areas because water allocation is based on historical records. If water consumption remains stable or rises with greater demands on water resources, it may lead to insufficiencies in the future (Rood et al. 2005). This will be of particular concern in the Athabasca sector of the PAD, as the Athabasca Tar Sands development continues to expand and remove surface and subsurface waters from the Athabasca River and its groundwater aquifer for use in oil extraction methods. This is also of significant concern for areas of the western United States, which has been subject to several droughts in the 20th century, as well as extreme droughts recorded in the Medieval Climate Anomaly, from AD ~900 to ~1300 (Cook et al. 2004). A natural response to long term warming similar to the Medieval Climate Anomaly, could lead to increasing aridity in western North America.

Future Recommendations

The ~600 year paleohydrological reconstruction of Peace River flood frequency and magnitude has brought to light several possible directions for future research. Since field work was completed, adjustments have been made to vibracore catchers (construction material and shape), leading to improved sediment core recovery (see Brock and Harms 2007). X-ray photography would be a useful tool to employ in the future for examining

stratigraphy in greater detail. While alternating dark and light grey laminated clay and silt beds were visually apparent, thin laminations not visually discernable may have been misinterpreted as massive, or noted as a relatively thick bed.

Several other sites could be investigated to further the understanding of the relationship between climate variability and hydrological conditions in the PAD. PAD 48 and PAD 49 (Figure 58), adjacent to the main channel of the Peace River, may improve the understanding of Peace River paleohydrology. Because they are located relatively far from outlets of Lake Athabasca, the possibility of northward flowing flood waters entering the oxbows from Lake Athabasca during high summer flows would be eliminated.

Considering the importance of tributaries such as the Smoky and Wabasca rivers for ice-jam events, collecting sediment cores from oxbows adjacent to these rivers would shed further light on the paleohydrology of this region. At present, little work has also been initiated and/or completed examining flood frequency and magnitude along the Athabasca River. This may be especially important considering how differently the Peace and Athabasca sectors may react to changes upstream of the delta (Wolfe et al. 2008). Information gathered from an examination of the Athabasca River system would provide valuable information for Wood Buffalo National Park (WBNP) managers and various stakeholders, particularly those concerned with and involved in Athabasca Tar Sands development and operations.

Vibracores have recently been extracted from several basins located in the Slave River delta (SRD), located at the mouth of the Slave River, Northwest Territories, in an attempt to answer similar research questions regarding the relationship between flood frequency

and climate variability (Brock and Harms 2007). Research questions that could be addressed to shed light on the relationship between the PAD and the SRD, two important nodes in the Mackenzie River drainage basin, and climate variability include 1) How does the paleohydrology of the Peace River affect that of the Slave River? 2) Were Slave River flood frequency and magnitude relatively high during medieval times and relatively low during the LIA, similar to the Peace River? 3) Were there high water levels in Great Slave Lake similar to that of Lake Athabasca during the LIA?

REFERENCES

Appleby PG. 2001. Chronostratigraphic techniques in recent sediments. In *Tracking Environmental Change Using Lake Sediments Volume 1: Basin Analysis, Coring, and Chronological Techniques, Developments in Paleoenvironmental Research.* Last WM, Smol JP (eds). Kluwer Academic Publishers, Dordrecht: 171-203.

Aziz OI and Burn DH. 2006. Trends and variability in the hydrological regime of the Mackenzie River Basin. *Journal of Hydrology* 319: 282-294.

Atmospheric Environment Service (AES), 1993. Canadian Climate Normals 1961– 1990. Minister of Supply and Services Canada.

Barkhouse T. 2007. *Late Holocene Paleohydrology of Spruce Island Lake, Peace-Athabasca Delta, AB, from Elemental and Stable Isotope Analysis of Lake Sediment Cores.* BA Undergraduate Thesis, Department of Geography and Environmental Studies. Wilfrid Laurier University, Waterloo, Ontario. 60 pp.

Beltaos S. 2003. Numerical modelling of ice-jam flooding on the Peace-Athabasca Delta. *Hydrological Processes* 17: 3685-3702.

Beltaos S and Burrell BC. 2003. Climate change and river ice break-up. *Canadian Journal of Civil Engineering* 30 (1): 145-155.

Beltaos S, Prowse TD and Carter T. 2006a. Ice regime of the lower Peace River and ice-jam flooding of the Peace-Athabasca Delta. *Hydrological Processes* 20: 4006-4029.

Beltaos S, Prowse TD, Bonsal B, MacKay R, Romolo L, Pietroniro A, and Toth B. 2006b. Climatic effects on ice-jam flooding of the Peace-Athabasca Delta. *Hydrological Processes* 20: 4031-4050.

Bierman PR, Lini A, Zehfuss P, Church A, Davis PT, Southon J, and Clark PU. 1997. Postglacial ponds and alluvial fans: recorders of Holocene landscape history. *Geological Society of America* 7: 1-8.

Björk S and Wohlfarth B. 2001. ^{14}C Chronostratigraphic techniques in paleolimnology. In *Tracking Environmental Change Using Lake Sediments. Volume 1: Basin Analysis, Coring, and Chronological Techniques, Developments in Paleoenvironmental Research.* Last WM, Smol JP (eds). Kluwer Academic Publishers, Dordrecht: 205-245.

Boggs Jr S. 2006. *Principles of Sedimentology and Stratigraphy* (4th Edition). Prentice Hall Inc: New Jersey. 662pp.

Bradley, RS, Hughes MK, and Diaz HF. 2003. Climate in Medieval Time. *Science* 302: 404-405.

Brock BE and Harms P. 2007. *Slave River Delta Winter Coring Field Report.* University of Waterloo, Waterloo, Ontario. Technical Report. 47pp.

Brown SL, Bierman PR, Lini A, and Southon J. 2000. 10 000 yr record of extreme hydrologic events. *Geology* 28: 335-338.

Burn DH. 1994. Hydrologic effects of climatic change in west-central Canada. *Journal of Hydrology* 160: 53-70.

Carbyn LN, Oosenbrug SM, and Anions DW. 1993. *Wolves, Bison, and the Dynamics Related to the Peace-Athabasca Delta in Canada's Wood Buffalo National Park.* Canadian Circumpolar Institute, Research Series Number 4 Edmonton, Alberta.

Case RA and MacDonald GM. 2003. Tree ring reconstructions of streamflow for three Canadian prairie rivers. *Journal of the American Water Resources Association* 39: 703-716.

Collinson JD. 1978. Alluvial Sediments. In *Sedimentary Environments and Facies.* Reading HG (ed.). Blackwell Scientific Publications, Oxford: 15-79.

Cook ER, Woodhouse CA, Eakin CM, Meko, DM, and Stahle DW. Long-term aridity changes in the western United States. *Science* 306: 1015-1018.

Craig BG. 1965. Glacial Lake McConnell, and the surficial geology of parts of the Slave River and Redstone River map areas, District of the Mackenzie. *Geological Survey of Canada Bulletin* 122: 12-33.

Crowley TJ. 2000. Causes of climate change over the past 1,000 years. *Science* 289: 270-277.

Crowley TJ and Lowery TS. 2000. How warm was the Medieval Warm Period? *Ambio* 29: 51-54.

Dearing J. 1999. *Environmental Magnetic Susceptibility: Using the Bartington MS2 System.* Chi Publishing, Kenilworth, England. 52pp.

De Boer A, Winhold T, and Garner L. 1994. *Embarras River Breakthrough to Mamawi Creek. Task D.2 - Embarras Breakthrough.* Peace-Athabasca Delta Technical Studies.

Demuth MN, Hicks FE, Prowse TD, and McKay K. 1996. A numerical modelling analysis of ice jam flooding on the Peace/Slave River, Peace-Athabasca delta. Peace-Athabasca Delta Technical Studies- P-ADJAM, Sub-component of Task F.2

Ice Studies. In *Peace-Athabasca Technical Studies Appendices: 1, Understanding the Ecosystem, Task Reports.* National Hydrology Research Institute Contribution Series CS-96016, Saskatoon, Canada.

Déry SJ and Wood EF. 2005. Decreasing river discharge in northern Canada. *Geophysical Research Letters* 32 LI0401 doi: 10.1029/2005GL022845.

Ecoregions Working Group. 1989. *Ecoclimatic regions of Canada, first approximation. Ecological Land Classification Series, No. 23.* Sustainable Development Branch, Conservation and Protection, Environment Canada, Ottawa, Ont. 199 pp. Report with map at 1:7.5 million scale.

Edwards TWD, Birks SJ, Luckman BH, and MacDonald GM. 2008. Climatic and hydrologic variability during the past millennium in the eastern Rocky Mountains and Northern Great Plains of western Canada. *Quaternary Research* doi: 10.1016/j.yqres.2008.04.013

Esper J, Cook ER, and Schweingruber, FH. 2002. Low-frequency signals in long tree-ring chronologies for reconstructing past temperature variability. *Science* 295: 2250-2253.

Fisher T. 2004. Vibracoring from lake ice using a lightweight monopod and piston coring apparatus. *Journal of Paleolimnology* 31: 377-382.

Fisher T and Souch C. 1998. Northwest outlet channels of Lake Agassiz, isostatic tilting and a migrating continental drainage divide, Saskatchewan, Canada. *Geomorphology* 25: 57-73.

Foster I, Mighall T., Proffitt H, Walling D, and Owens P. 2006. Post-depositional 137Cs mobility in the sediments of three shallow coastal lagoons, southwest England. *Journal of Paleolimnology* 35: 881-895.

Glew JR. 1989. A miniature gravity corer for recovering short sediment cores. *Journal of Paleolimnology* 5: 285-287.

Hall RI, Wolfe BB, Edwards TWD, Karst-Riddoch TL, Vardy S, McGowan S, Sjunneskog C, Paterson A, Last W, English MC, Sylvestre F, Leavitt PR, Warner BG, Boots B, Palmini R, Clogg-Wright K, Sokal M, Falcone M, van Driel P, and Asada T. 2004. *A Multi-Century Flood, Climatic, and Ecological History of the Peace-Athabasca Delta, Northern Alberta, Canada.* Final Report to B.C. Hydro, 163pp.

Hannah DH, Sadler JP, and Wood PJ. 2007. Hydroecology and ecohydrology: a potential route forward. *Hydrological Processes* 21: 3385-3390.

Jarvis SR, Brock BE, St. Amour N, Hall RI, and Wolfe BB. 2006. *Chronological techniques in paleolimnology: 210Pb measurement and data modeling.* WATER Laboratory, University of Waterloo, Ontario, Canada. 48pp.

Khazanie R. 1996. *Statistics in a world of applications* (4th ed). HarperCollins College Publishers. New York, New York. 887pp.

Kreutz KJ, Mayewski PA, Meeker LD, Twickler MS, Whitlow SI, and Pittalwala II. Bipolar changes in atmospheric circulation during the Little Ice Age. *Science* 277: 1294-1298.

Leconte R, Peters D, Pietroniro A, and Prowse TD. 2006. Modelling climate change impacts in the Peace and Athabasca Catchment and delta: II—variations in flow and water levels with varying winter severity. *Hydrological Processes* 20: 4215-4230.

Longmore ME. 1982. The cesium dating technique and associated applications in Australia. In *Archaeometry: An Australian Perspective.* (W. Ambrose and P. Duerden, eds.) ANU press, Canberra: 310-321.

Luckman BH. 2000. The Little Ice Age in the Canadian Rockies. *Geomorphology* 32: 357-384.

Luckman BH and Wilson RJS. 2005. Summer temperatures in the Canadian Rockies during the last millennium: a revised record. *Climate Dynamics* 24: 131-144.

MacDonald GM, Stahle DW, Diaz JV, Beer N, Busby SJ, Cerano-Peredes J, Cole JE, Cook ER, Endfield G, Gutierrez-Garcia G, Hall B, Magana V, Meko DM, Méndez-Pérez M, Sauchyn DJ, Watson E, and Woodhouse C. 2008. Climate warming and 21st-century drought in southwestern North America. *EOS* 89: 82.

Matthews JA and Briffa KA. 2005. The 'Little Ice Age': Re-evaluation of an evolving concept. *Geografiska Annaler Series A-Physical Geography* 87 A (1): 17-36.

Meyers PA. 1997. Organic geochemical proxies of paleoceanographic, paleolimnologic, and paleoclimatic processes. *Organic Geochemistry* 27: 213-250.

Meyers PA and Ishiwatari R. 1993. Lacustrine organic geochemistry - an overview of indicators of organic matter sources and diagenesis in lake sediments. *Organic Geochemistry* 20: 867-900.

Meyers PA and Teranes JL. 2001. Sediment organic matter. In *Tracking Environmental Change Using Lake Sediments. Volume 2: Physical and Chemical Techniques.* Last WM, Smol JP (eds.). Kluwer Academic Publishers, Dordrecht: 239-270.

Miall AD. 1992. Part II-Terrigenous clastic facies models: alluvial deposits. In *Facies Models: Response to Sea Level Change.* Walker RG, James NP (eds.). Geological Association of Canada: 119-142.

Mossop GD. 1980. Geology of the Athabasca Oil Sands. *Science* 207: 145-152.

Nielsen G. 1972. Groundwater investigation, Peace-Athabasca Delta, section J. In *Peace-Athabasca Delta Project, Technical Report and Appendices: Volume 1: Hydrological Investigations*, 1973. 36pp.

NRBS (Northern River Basins Study). 1997. *Northern River Basins Study: the legacy. The collective findings.* Alberta Environmental Protection, Edmonton, Alberta Canada.

PAD-IC (Peace-Athabasca Delta Implementation Committee). 1987. *Peace Athabasca Delta Water Management Works Evaluation. Final Report, Appendix A: Hydrological Assessment, Appendix B: Biological Assessment, Appendix C: Ancillary Studies.* Peace-Athabasca Delta Implementation Committee, Governments of Alberta, Saskatchewan and Canada. 63 pp.

PAD-PG (Peace-Athabasca Delta Project Group), 1973. *Peace-Athabasca Delta Project, Technical Report and Appendices. Volume 1: Hydrological Investigations, Volume 2: Ecological Investigations.*

PAD-TS (Peace-Athabasca Delta Technical Studies). 1996a. Macmillan S. (Editor). Final Report. PADTS Steering Committee, Fort Chipewyan, Alberta. Word Picture Communications. 106 pp.

Peters DL. 2003. *Controls on the persistence of water within perched basins of the Peace-Athabasca Delta, northern Canada.* Ph.D. Thesis, Watershed Ecosystems Graduate Program, Trent University, Peterborough, Ontario, Canada. 194pp.

Peters DL and Prowse TD. 2006. Generation of streamflow to seasonal high waters in a freshwater delta, northwestern Canada. *Hydrological Processes* 20: 4173-4196.

Peters DL, Prowse TD, Marsh P, Lafleur PM, and Buttle JM. 2006. Persistence of water within perched basins of the Peace-Athabasca Delta, Northern Canada. *Wetlands Ecology and Management* 14: 221-243.

Peterson M. 1994. *Peace-Athabasca Delta flood history study.* Task F. 1 of the Peace-Athabasca Delta Technical Studies. Wood Buffalo National Park, Fort Smith, Canada. [pagination unknown].

Pietroniro A, Prowse TD, and Peters DL. 1999. Hydrologic assessment of an inland freshwater delta using multi-temporal satellite remote sensing. *Hydrological Processes* 13: 2483-2498.

Pietroniro A, Leconte R, Toth B, Peters DL, Kouwen N, Conly FM, and Prowse TD. 2006. Modelling climate change impacts in the Peace and Athabasca catchment and delta: III—integrated model assessment. *Hydrological Processes* 20: 4231-4245.

Prowse TD and Beltaos S. 2002. Climatic control of river-ice hydrology: a review. *Hydrological Processes* 16: 805-822.

Prowse TD, Beltaos S, Gardner JT, Gibson JJ, Granger RJ, Leconte R, Peters DL, Pietroniro A, Romolo LA, and Toth B. 2006. Climate change, flow regulation and land-use effects on the hydrology of the Peace-Athabasca-Slave system, findings from the Northern Rivers Ecosystem Initiative. *Environmental Monitoring and Assessment* 113: 167-197.

Prowse TD and Conly FM. 1998. Effects of climate variability and flow regulation on ice-jam flooding of a northern delta. *Hydrological Processes* 12: 1589-1610.

Prowse TD and Conly FM. 2002. A review of hydroecological results of he Northern River Basins Study, Canada. Part 2. Peace-Athabasca Delta. *River Research and Applications* 18: 447-460.

Prowse TD, Conly FM, Church M., and English MC. 2002. A review of hydroecological results of the northern river basins study, Canada. Part 1. Peace and Slave Rivers. *River Research and Applications* 18: 429-446.

Prowse TD and Culp JM. 2003. Ice break-up: a neglected factor in river ecology. *Canadian Journal of Civil Engineering* 30: 128-144

Prowse TD and Lalonde V. 1996. Open-water and ice-jam flooding of a northern delta. *Nordic Hydrology* 27: 85-100.

Romolo L, Prowse TD, Blair D, Bonsal BR, and Martz WL. 2006a. The synoptic climate controls on hydrology in the upper reaches of the Peace River basin. Part I: snow accumulation. *Hydrological Processes* 20: 4097-4111.

Romolo L, Prowse TD, Blair D, Bonsal BR, Marsh P, and Martz LW. 2006b. The synoptic climate controls on hydrology in the upper reaches of the Peace River Basin. Part II: Snow ablation. *Hydrological Processes* 20: 4113-4129.

Rood SB, Samuelson GM, Weber JK, and Wyrwrot KA. 2005. Twentieth-century declines in streamflows from the hydrographic apex of North America. *Journal of Hydrology* 306: 215-233.

Rouse WR, Douglas MSV, Hecky RE, Hershey AE, Kling GW, Lesack L, Marsh P, Mcdonald M, Nicholson BJ, Roulet NT, and Smol JP. 1997. Effects of climate

change on the freshwaters of arctic and subarctic North America. *Hydrological Processes* 11: 873-902.

Schindler DW and Donahue WF. 2006. An impending water crisis in Canada's western prairie provinces. *Proceedings of the National Academy of Sciences* 103: 7210-7216.

Schindler DW and Smol JP. 2006. Cumulative effects of climate warming and other human activities on freshwaters of arctic and subarctic North America. *Ambio* 35: 160-168.

Sear DA and Arnell NW. 2006. The applications of paleohydrology in river management. *Catena* 66: 169-183.

Sinnatamby RN. 2006. *An assessment of hydro-ecological changes at two closed-drainage basins in the Peace Athabasca Delta, Alberta, Canada.* MSc Thesis. Department of Biology, University of Waterloo. Waterloo, Ontario. 116pp.

Smith DG. 1994. Glacial lake McConnell: Paleogeography, age, duration, and associated river deltas, Mackenzie River basin, western Canada. *Quaternary Science Reviews* 13: 829-843.

Smol JP. 1992. Paleolimnology: an important tool for effective ecosystem management. *Journal of Aquatic Ecosystem Health* 1:49-58.

Smol JP. 2008. *Pollution of Lakes and Rivers: A paleoenvironmental perspective* (2nd Edition). Blackwell Publishing, Oxford. 383pp.

Stanley Associates Engineering Ltd. 1982. *Final Synthesis of Environmental Studies for the Peace-Athabasca Delta Region, Task 4B.* Slave River Hydro Feasibility Study. Edmonton, Alberta, Canada. 117pp + figures and tables.

Stow DAV. 2005. Sedimentary rocks in the field: a color guide. Elsevier Academic Press. Burlington MA. 320pp.

Talbot MR. 2001. Nitrogen isotopes in paleolimnology. In *Tracking Environmental Change Using Lake Sediments. Volume 2: Physical and Chemical Techniques.* Last WM, Smol JP (eds.). Kluwer Academic Publishers, Dordrecht: 401-439.

Talma AS and Vogel JC. 1993. A simplified approach to calibrating 14C dates. *Radiocarbon* 35: 317-322.

Thompson R, Bloemendal J, Dearing JA, Oldfield F, Rummery TA, Stober JC, and Turner GM. 1980. Environmental applications of magnetic measurements. *Science* 207: 481-486.

Thompson R and Oldfield F. 1986. *Environmental Magnetism.* Allen and Unwin Ltd. London, England. 277pp.

Timoney KP. 2002. A dying delta? A case study of a wetland paradigm. *Wetlands* 22: 282-300.

Timoney KP and Marsh J. 2004. Lichen trimlines in northern Alberta: establishment, growth rates, and historic water levels. *The Bryologist* 107(4): 429-440.

Timoney KP, Peterson G, Fargey P, and Peterson M. 1997. Spring ice-jam flooding of the Peace-Athabasca Delta: evidence of a climatic oscillation. *Climatic Change* 35: 463-483.

Toth B, Pietroniro A, Conly FM, and Kouwen N. 2006. Modelling climate change impacts in the Peace and Athabasca catchment and delta: I—hydrological model application. *Hydrological Processes* 20: 4197-4214.

Townsend GH. 1975. Impact of the Bennett Dam on the Peace-Athabasca Delta. *Journal of the Fisheries Research Board of Canada* 32: 171–176.

Töyrä J, Pietroniro A, and Martz LW. 2001. Multisensor hydrologic assessment of a freshwater wetland. *Remote Sensing of Environment* 75: 162-173.

Vandermaelen P. 1827. Atlas universel de geographie physique, statistique et mineralogique.

Walker RG. 1992. General Introduction: Facies, Facies Sequences, and Facies Models. In *Facies Models: Response to Sea Level Change.* Walker RG, James NP (eds.) Geological Association of Canada: 1-10.

Wolfe BB, Edwards TWD, Elgood RJ, and Beuning KRM. 2001. Carbon and oxygen isotope analysis of lake sediment cellulose: methods and applications. In *Tracking Environmental Change Using Lake Sediments. Volume 2: Physical and Chemical Techniques.* Last WM, Smol JP (eds.). Kluwer Academic Publishers, Dordecht: 1-28.

Wolfe BB, Hall RI, Last WM, Edwards TWD, English MC, Karst-Riddoch TL, Paterson A, and Palmini R. 2006. Reconstruction of multi-century flood histories from oxbow lake sediments, Peace-Athabasca Delta, Canada. *Hydrological Processes* 20: 4131-4153.

Wolfe BB, Hall RI, Edwards TWD, Vardy SR, Falcone MD, Sjunneskog C, Sylvestre F, McGowan S, Leavitt PR, and van Driel P. 2008. Hydroecological response of the Athabasca Delta, Canada to changes in river flow and climate during the 20th century. *Ecohydrology* doi: 10.1002/eco.13.

Wolfe BB, Karst-Riddoch TL, Hall RI, Edwards TWD, English MC, Palmini R, McGowan S, Leavitt PR, and Vardy SR. 2007. Classification of hydrological regimes of a northern floodplain basin (Peace-Athabasca Delta, Canada) from analysis of stable isotopes (δ18O and δ2H) and water chemistry. *Hydrological Processes* 21: 151-168.

Wolfe BB, Karst-Riddoch TL, Vardy SR, Falcone MD Hall RI, and Edwards TWD. 2005. Impacts of climate and river flooding on the hydro-ecology of a floodplain basin, Peace-Athabasca Delta, Canada, since AD 1700. *Quaternary Research* 64: 147-162.

Yi Y, Brock BE, Falcone MD, Wolfe BB, and Edwards TWD. 2008. A coupled isotope tracer method to characterize input water to lakes. *Journal of Hydrology* 350: 1-13.

Appendix A: Sediment core photographs

Digital photographs of vibracores collected from PAD 54 and PAD 15 on accompanying compact disc

Vibracore Photograph Labels

The compact disc contains photographs of whole vibracore section halves and photographs of sediment at approximately 20 cm intervals, with allowance for some overlap between photographs. Each oxbow lake is contained within a separate folder. Within each folder the photographs are organized according to the coring site (proximal, intermediate, and distal). Within these folders there are two general types of file names, which are explained using the following examples:

Example 1

PAD15_VC1_S1_0-20.JPG,

In this case, PAD 15 refers to the oxbow lake basin, VC1 refers to the coring location within the basin, S1 refers to the core section, and 0-20 refers to the complete 20 cm interval visible below the core label in each the photograph. It is important to note that although more than 20 cm of the sediment core is visible in the photograph, this labelling was used to be consistent. When whole core section halves were photographed, the full core section length was used in the file name.

Example 2

PAD15_VC1_S3a_200-220 & 300-320.JPG,

This kind of label was used when the core section was cut perpendicular to its length in the laboratory prior to photographing because it was longer than the 1 m length of the

light table. The two resulting parts of each half are shown side-by-side in each picture, resulting in two different core lengths in the file name of those photographs. These core sections have two sets of photographs, one for each half. Therefore, in example 2, PAD 15 refers to the oxbow lake, VC1 refers to the coring location within the basin, S3a refers to the section number (3) and one half (a) of the core section, and 200-220 & 300-320 refers to the complete 20 cm intervals visible below the paper label within each photograph.

Important Note:

There is a labelling mistake in the photographs of section 6 of vibracore from PAD 15 VC1 (proximal site). The paper labels contained within the photographs indicate it is section 5, when it is actually section 6. The file name of each photograph uses the correct section number and core length (cm).

Appendix B: ^{210}Pb and ^{137}Cs results

PAD 15 VC3 Distal Site

	Calendar	Numeric
Coring Date:	March 15, 2005	38426

Total Activity - Corrected to coring date:

Depth Interval (cm)		*Mid-depth (cm)*	*^{210}Pb (dpm/g)*	*^{214}Bi (dpm/g)*	*^{137}Cs (dpm/g)*
0.0	0.5	0.25	2.476	2.215	0.352
1.0	1.5	1.25	3.183	2.318	0.179
2.0	2.5	2.25	3.337	2.423	0.042
3.0	3.5	3.25	3.051	2.221	0.103
4.0	4.5	4.25	3.131	2.170	0.160
5.0	5.5	5.25	2.187	2.165	0.023
6.0	6.5	6.25	2.405	2.576	0.143
7.0	7.5	7.25	2.329	1.823	0.038
7.5	8.5	8.00	2.825	2.050	0.242
9.0	9.5	9.25	3.348	2.055	0.377
10.0	10.5	10.25	3.325	1.944	0.311
11.0	11.5	11.25	2.928	2.255	0.650
12.5	13.0	12.75	1.815	1.676	0.929
13.0	13.5	13.25	3.426	2.131	1.157
13.5	14.0	13.75	2.426	2.000	1.454
14.0	14.5	14.25	3.013	2.196	1.263
14.5	15.0	14.75	2.550	2.198	0.794
15.0	15.5	15.25	2.256	1.986	0.793
15.5	16.0	15.75	2.103	2.060	1.114
16.0	16.5	16.25	1.464	1.737	1.055
16.5	17.0	16.75	2.902	2.302	0.935
17.0	17.5	17.25	3.428	2.494	0.848
18.0	18.5	18.25	2.705	2.194	0.932
18.5	19.0	18.75	3.294	2.142	0.792
19.0	19.5	19.25	2.465	2.416	0.691
19.5	20.0	19.75	2.382	1.977	0.715
30.0	30.5	30.25	3.239	1.793	-0.063
30.5	31.0	30.75	1.464	2.034	0.131
31.0	31.5	31.25	2.130	1.829	0.063
31.5	32.0	31.75	4.143	2.221	-0.107
32.0	32.5	32.25	2.100	1.807	-0.055
32.5	33.0	32.75	2.545	1.855	-0.113
33.0	33.5	33.25	2.895	1.935	0.034
33.5	34.0	33.75	2.897	1.863	-0.004
34.0	34.5	34.25	2.586	1.985	0.003
34.5	35.0	34.75	3.720	2.069	-0.055
35.0	35.5	35.25	3.479	2.235	0.033
35.5	36.0	35.75	3.588	2.117	-0.011
36.0	36.5	36.25	3.606	2.107	0.039

Depth Interval (cm)		Mid-depth (cm)	^{210}Pb (dpm/g)	^{214}Bi (dpm/g)	^{137}Cs (dpm/g)
36.5	37.0	36.75	1.824	2.253	-0.027
37.0	37.5	37.25	3.150	2.012	0.161
37.5	38.0	37.75	3.819	1.616	0.049
38.0	38.5	38.25	3.015	1.954	0.031
38.5	39.0	38.75	2.298	1.363	-0.011
39.0	40.0	39.50	3.316	2.001	0.123
40.0	40.5	40.25	3.196	1.846	-0.051
41.0	41.5	41.25	3.570	1.705	-0.135
42.0	42.5	42.25	2.250	2.362	0.107
43.0	43.5	43.25	2.432	2.006	0.048
44.0	44.5	44.25	2.192	2.334	-0.062
44.5	45.0	44.75	2.095	2.092	0.021
45.0	45.5	45.25	1.921	1.823	0.037
45.5	46.0	45.75	3.380	1.801	-0.041
46.0	46.5	46.25	2.441	2.076	0.010
47.0	47.5	47.25	2.761	1.797	0.089
47.5	48.0	47.75	3.379	2.026	0.037
48.0	48.5	48.25	3.391	1.732	-0.001
48.5	49.0	48.75	4.222	2.052	-0.130
49.0	49.5	49.25	3.485	2.442	0.049
49.5	50.0	49.75	2.673	2.206	-0.109

PAD 15 KB-05-03 Distal Site

	Calendar	Numeric
Coring Date:	March 15, 2005	38426

Total Activity - Corrected to coring date:

Depth Interval (cm)		*Mid-depth (cm)*	*^{210}Pb (dpm/g)*	*^{214}Bi (dpm/g)*	*^{137}Cs (dpm/g)*
0.0	0.5	0.25	6.440	1.901	0.049
5.0	5.5	5.25	3.532	1.468	0.163
10.0	10.5	10.25	3.026	2.077	0.104
15.0	15.5	15.25	3.167	1.135	0.039
20.0	20.5	20.25	4.119	1.792	0.217
25.0	25.5	25.25	2.667	2.206	0.120
30.0	30.5	30.25	2.066	2.163	0.141
30.5	31.0	30.75	2.883	2.110	0.049
31.0	31.5	31.25	1.754	2.090	0.122
31.5	32.0	31.75	3.781	2.045	0.682
32.0	32.5	32.25	3.267	1.986	0.830
32.5	33.0	32.75	3.321	2.330	0.608
33.0	33.5	33.25	3.322	2.164	0.402
33.5	34.0	33.75	3.241	2.267	0.592
34.0	34.5	34.25	2.615	2.093	0.447
34.5	35.0	34.75	3.488	2.306	0.788
35.0	35.5	35.25	3.076	2.284	1.052
35.5	36.0	35.75	2.483	2.131	0.331
36.0	36.5	36.25	2.708	1.839	0.404
36.5	37.0	36.75	2.337	1.987	0.564
37.0	37.5	37.25	2.416	1.724	1.306
37.5	38.0	37.75	4.202	2.127	2.678
38.0	38.5	38.25	2.501	2.566	2.527
38.5	39.0	38.75	3.160	2.518	0.989
39.0	39.5	39.25	3.277	1.895	0.874
39.5	40.0	39.75	2.839	2.242	1.088
40.0	40.5	40.25	4.016	2.440	1.261
40.5	41.0	40.75	3.517	2.251	0.982

Appendix C: ^{14}C results from Beta Analytic

BULK SEDIMENT SAMPLED FROM PAD 15 VC3 (DISTAL SITE)

LAB NUMBER: Beta - 225393
SAMPLE DESCRIPTION : light grey beds from 403-418 cm depth
MEASURED $^{13}C/^{12}C$: -25.3 ‰
CONVENTIONAL RADIOCARBON AGE: 22530 +/- 140 BP
RADIOCARBON AGE (*): 22530 +/- 140 BP
ANALYSIS : AMS-Standard delivery
MATERIAL/PRETREATMENT : (organic sediment): acid washes

LAB NUMBER: Beta - 225394 22040 +/- 130 BP
SAMPLE DESCRIPTION : light grey beds from 508-528 cm depth
MEASURED $^{13}C/^{12}C$: -25.2 ‰
CONVENTIONAL RADIOCARBON AGE: 22040 +/- 130 BP
RADIOCARBON AGE (*): 22040 +/- 130 BP
ANALYSIS : AMS-Standard delivery
MATERIAL/PRETREATMENT : (organic sediment): acid washes

WOOD SAMPLED FROM PAD 15 VC1 (PROXIMAL SITE)

LAB NUMBER: Beta - 229807
SAMPLE DESCRIPTION: branch from 588.5-590 cm depth
MEASURED $^{13}C/^{12}C$: -26.5 ‰
CONVENTIONAL RADIOCARBON AGE: 460 +/- 40 BP
RADIOCARBON AGE (*): 440 +/- 40 BP
ANALYSIS : AMS-Standard delivery
MATERIAL/PRETREATMENT : (wood): acid/alkali/acid
2 SIGMA CALIBRATION : Cal AD 1420 to 1490 (Cal BP 530 to 460)

LAB NUMBER: Beta - 229808
SAMPLE DESCRIPTION: branch from 629 to 633.5 cm depth
MEASURED $^{13}C/^{12}C$: -26.1 ‰
CONVENTIONAL RADIOCARBON AGE: 460 +/- 40 BP
RADIOCARBON AGE (*): 270 +/- 50 BP
ANALYSIS : Radiometric-Standard delivery
MATERIAL/PRETREATMENT : (wood): acid/alkali/acid
2 SIGMA CALIBRATION : Cal AD 1480 to 1680 (Cal BP 470 to 270) AND Cal AD 1770 to 1800 (Cal BP 180 to 150) AND Cal AD 1940 to 1950 (Cal BP 10 to 0)

LAB NUMBER: Beta - 229809
SAMPLE SESCRIPTION : wood fragments from 656.5 to 660.5 cm depth
MEASURED $^{13}C/^{12}C$: -26.8 ‰
CONVENTIONAL RADIOCARBON AGE: 1620 +/- 40 BP
RADIOCARBON AGE (*):1590 +/- 40 BP
ANALYSIS : AMS-Standard delivery
MATERIAL/PRETREATMENT : (wood): acid/alkali/acid
2 SIGMA CALIBRATION : Cal AD 390 to 560 (Cal BP 1560 to 1390)

CALIBRATION OF RADIOCARBON AGE TO CALENDAR YEARS

(Variables: C13/C12=-26.5;lab. mult=1)

Laboratory number: Beta-229807

Conventional radiocarbon age: 440±40 BP

2 Sigma calibrated result: (95% probability) Cal AD 1420 to 1490 (Cal BP 530 to 460)

Intercept data

Intercept of radiocarbon age with calibration curve: Cal AD 1440 (Cal BP 510)

1 Sigma calibrated result: (68% probability) Cal AD 1430 to 1460 (Cal BP 520 to 490)

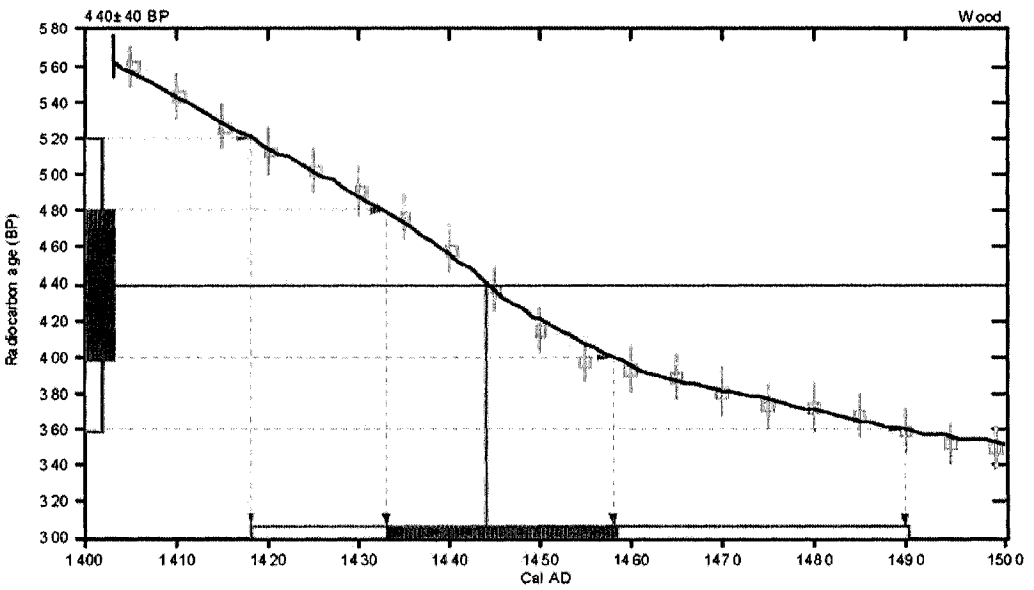

References:

Database used

INTCAL04

Calibration Database

INTCAL04 Radiocarbon Age Calibration

IntCal04: Calibration Issue of Radiocarbon (Volume 46, nr 3, 2004).

Mathematics

A Simplified Approach to Calibrating C14 Dates

Talma, A. S., Vogel, J. C., 1993, Radiocarbon 35(2), p317-322

Beta Analytic Radiocarbon Dating Laboratory

4985 S.W. 74th Court, Miami, Florida 33155 • Tel: (305)667-5167 • Fax: (305)663-0964 • E-Mail: beta@radiocarbon.com

CALIBRATION OF RADIOCARBON AGE TO CALENDAR YEARS

(Variables: C13/C12=-26.1;lab. mult=1)

Laboratory number: Beta-229808

Conventional radiocarbon age: 270±50 BP

2 Sigma calibrated results: Cal AD 1480 to 1680 (Cal BP 470 to 270) and
(95% probability) Cal AD 1770 to 1800 (Cal BP 180 to 150) and
Cal AD 1940 to 1950 (Cal BP 10 to 0)

Intercept data

Intercept of radiocarbon age with calibration curve: Cal AD 1650 (Cal BP 300)

1 Sigma calibrated results: Cal AD 1530 to 1560 (Cal BP 420 to 390) and
(68% probability) Cal AD 1630 to 1660 (Cal BP 320 to 290)

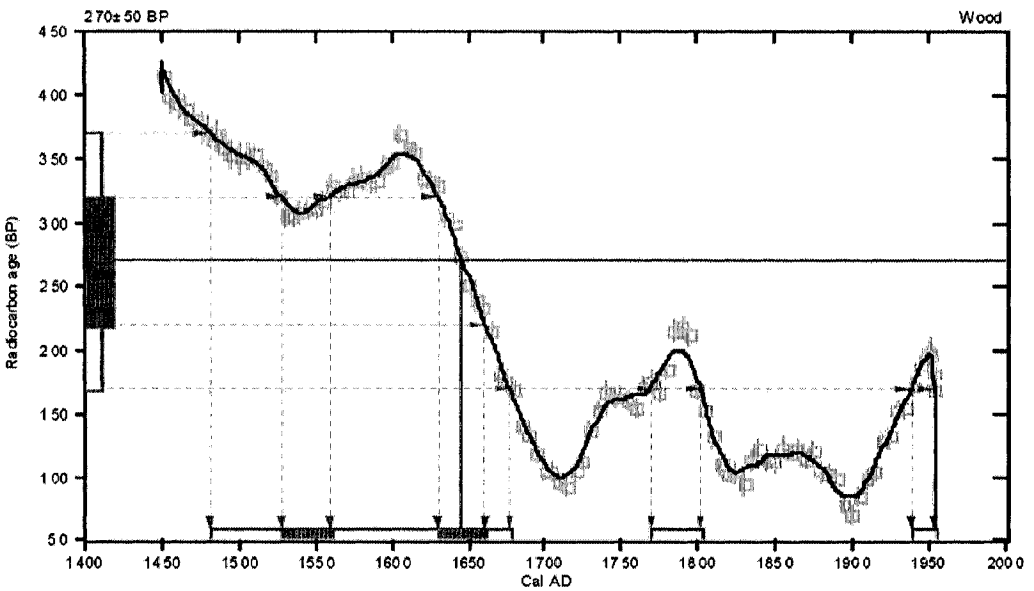

References:

Database used
INTCAL04
Calibration Database
INTCAL04 Radiocarbon Age Calibration
IntCal04: Calibration Issue of Radiocarbon (Volume 46, nr 3, 2004).
Mathematics
A Simplified Approach to Calibrating C14 Dates
Talma, A. S., Vogel, J. C., 1993, Radiocarbon 35(2), p317-322

Beta Analytic Radiocarbon Dating Laboratory
4985 S.W. 74th Court, Miami, Florida 33155 • Tel: (305)667-5167 • Fax: (305)663-0964 • E-Mail: beta@radiocarbon.com

CALIBRATION OF RADIOCARBON AGE TO CALENDAR YEARS

(Variables: C13/C12=-26.8:lab. mult=1)

Laboratory number: Beta-229809

Conventional radiocarbon age: 1590±40 BP

2 Sigma calibrated result: (95% probability) Cal AD 390 to 560 (Cal BP 1560 to 1390)

Intercept data

Intercept of radiocarbon age with calibration curve: Cal AD 430 (Cal BP 1520)

1 Sigma calibrated result: (68% probability) Cal AD 420 to 540 (Cal BP 1530 to 1410)

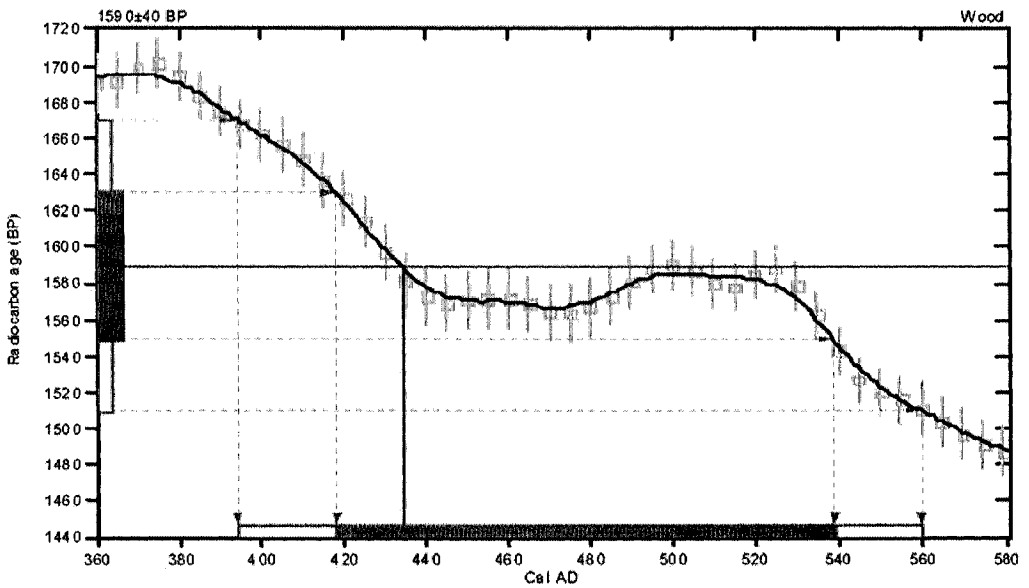

References:

Database used

INTCAL04

Calibration Database

INTCAL04 Radiocarbon Age Calibration

IntCal04: Calibration Issue of Radiocarbon (Volume 46, nr 3, 2004).

Mathematics

A Simplified Approach to Calibrating C14 Dates

Talma, A. S., Vogel, J. C., 1993, Radiocarbon 35(2), p317-322

Beta Analytic Radiocarbon Dating Laboratory

4985 S.W. 74th Court, Miami, Florida 33155 • Tel: (305)667-5167 • Fax: (305)663-0964 • E-Mail: beta@radiocarbon.com

Appendix D: Magnetic susceptibility and z-scores

KB-05-01 Proximal Site			
Sample Mid-depth	*Year AD*	*Magnetic Susceptibility*	*z-score*
0.25	2004.78	0.9	-1.1824
0.75	2004.34	5.1	-1.0399
1.25	2003.90	3.9	-1.0806
1.75	2003.47	12.4	-0.7923
2.25	2003.03	1.9	-1.1484
2.75	2002.59	6.7	-0.9856
3.25	2002.15	5.7	-1.0196
3.75	2001.71	2.5	-1.1281
4.25	2001.28	4.6	-1.0569
4.75	2000.84	-4.4	-1.3621
5.25	2000.40	19.4	-0.5549
5.75	1999.96	25.5	-0.3480
6.5	1999.30	13	-0.7720
7.25	1998.65	15	-0.7041
7.75	1998.21	28.4	-0.2497
8.25	1997.77	12.1	-0.8025
8.75	1997.33	27.9	-0.2666
9.25	1996.89	7.4	-0.9619
9.75	1996.46	8.9	-0.9110
10.25	1996.02	30.1	-0.1920
10.75	1995.58	11.8	-0.8127
11.25	1995.14	18.9	-0.5719
11.75	1994.70	10	-0.8737
12.25	1994.26	13.9	-0.7415
12.75	1993.83	9.5	-0.8907
13.25	1993.39	2.9	-1.1145
13.75	1992.95	20.6	-0.5142
14.25	1992.51	5.7	-1.0196
14.75	1992.07	10.6	-0.8534
15.25	1991.64	7.1	-0.9721
15.75	1991.20	14	-0.7381
16.25	1990.76	13.1	-0.7686
16.75	1990.32	11.6	-0.8195
17.25	1989.88	7	-0.9755
17.75	1989.44	5.3	-1.0331
18.25	1989.01	9	-0.9076
18.75	1988.57	11.3	-0.8296
19.25	1988.13	10	-0.8737
19.75	1987.69	15.2	-0.6974
20.25	1987.25	9.5	-0.8907
20.75	1986.82	0.9	-1.1824
21.25	1986.38	5.5	-1.0263
21.75	1985.94	9.8	-0.8805
22.25	1985.50	14	-0.7381
22.75	1985.06	14	-0.7381
23.25	1984.62	10.6	-0.8534
23.75	1984.19	20	-0.5346

VC1 Proximal Site									
Sample Mid-depth (cm)	*Adjusted Mid-depth (cm)*	*Year AD*	*Magnetic Susceptibility*	*z-score*	*Sample Mid-depth (cm)*	*Adjusted Mid-depth (cm)*	*Year AD*	*Magnetic Susceptibility*	*z-score*
0.25	24.25	1983.75	26.00	-0.3311	24.25	48.25	1962.72	19.00	-0.5685
0.75	24.75	1983.31	23.50	-0.4159	24.75	48.75	1962.28	25.00	-0.3650
1.25	25.25	1982.87	30.80	-0.1683	25.25	49.25	1961.84	36.00	0.0081
1.75	25.75	1982.43	26.70	-0.3073	25.75	49.75	1961.40	42.70	0.2353
2.25	26.25	1982.00	26.00	-0.3311	26.25	50.25	1960.96	35.20	-0.0191
2.75	26.75	1981.56	27.60	-0.2768	26.75	50.75	1960.53	22.50	-0.4498
3.25	27.25	1981.12	21.00	-0.5007	27.25	51.25	1960.09	26.60	-0.3107
3.75	27.75	1980.68	26.10	-0.3277	27.75	51.75	1959.65	27.60	-0.2768
4.25	28.25	1980.24	24.50	-0.3819	28.25	52.25	1959.21	21.70	-0.4769
4.75	28.75	1979.81	22.00	-0.4667	28.75	52.75	1958.77	19.10	-0.5651
5.25	29.25	1979.37	30.60	-0.1751	29.25	53.25	1958.33	16.00	-0.6702
5.75	29.75	1978.93	18.50	-0.5854	29.75	53.75	1957.90	19.00	-0.5685
6.25	30.25	1978.49	21.30	-0.4905	30.25	54.25	1957.46	24.00	-0.3989
6.75	30.75	1978.05	22.80	-0.4396	30.75	54.75	1957.02	19.50	-0.5515
7.25	31.25	1977.61	19.50	-0.5515	31.25	55.25	1956.58	10.10	-0.8703
7.75	31.75	1977.18	28.20	-0.2565	31.75	55.75	1956.14	20.60	-0.5142
8.25	32.25	1976.74	24.40	-0.3853	32.25	56.25	1955.71	23.20	-0.4260
8.75	32.75	1976.30	22.90	-0.4362	32.75	56.75	1955.27	18.40	-0.5888
9.25	33.25	1975.86	26.20	-0.3243	33.25	57.25	1954.83	23.60	-0.4125
9.75	33.75	1975.42	25.20	-0.3582	33.75	57.75	1954.39	20.10	-0.5312
10.25	34.25	1974.99	20.70	-0.5108	34.25	58.25	1953.95	23.30	-0.4226
10.75	34.75	1974.55	19.80	-0.5414	35.25	59.25	1953.08	21.60	-0.4803
11.25	35.25	1974.11	21.50	-0.4837	34.75	58.75	1953.51	21.90	-0.4701
11.75	35.75	1973.67	18.50	-0.5854	35.75	59.75	1952.64	22.50	-0.4498
12.25	36.25	1973.23	20.30	-0.5244	36.25	60.25	1952.20	25.00	-0.3650
12.75	36.75	1972.79	17.30	-0.6261	36.75	60.75	1951.76	24.30	-0.3887
13.25	37.25	1972.36	18.00	-0.6024	37.25	61.25	1951.32	19.50	-0.5515
13.75	37.75	1971.92	21.20	-0.4939	37.75	61.75	1950.89	24.60	-0.3786
14.25	38.25	1971.48	16.90	-0.6397	38.25	62.25	1950.45	24.00	-0.3989
14.75	38.75	1971.04	24.60	-0.3786	38.75	62.75	1950.01	25.50	-0.3480
15.25	39.25	1970.60	28.90	-0.2327	39.25	63.25	1949.57	28.50	-0.2463
15.75	39.75	1970.17	20.60	-0.5142	39.75	63.75	1949.13	24.00	-0.3989
16.25	40.25	1969.73	23.00	-0.4328	40.25	64.25	1948.69	28.70	-0.2395
16.75	40.75	1969.29	28.40	-0.2497	40.75	64.75	1948.26	26.00	-0.3311
17.25	41.25	1968.85	32.60	-0.1072	41.25	65.25	1947.82	31.50	-0.1445
17.75	41.75	1968.41	36.30	0.0183	41.75	65.75	1947.38	24.50	-0.3819
18.25	42.25	1967.97	35.30	-0.0157	42.25	66.25	1946.94	21.60	-0.4803
18.75	42.75	1967.54	33.00	-0.0937	42.75	66.75	1946.50	28.00	-0.2632
19.25	43.25	1967.10	34.90	-0.0292	43.25	67.25	1946.07	33.60	-0.0733
19.75	43.75	1966.66	26.50	-0.3141	43.75	67.75	1945.63	28.50	-0.2463
20.25	44.25	1966.22	31.10	-0.1581	44.25	68.25	1945.19	27.30	-0.2870
20.75	44.75	1965.78	20.30	-0.5244	44.75	68.75	1944.75	23.00	-0.4328
21.25	45.25	1965.35	21.00	-0.5007	45.25	69.25	1944.31	24.20	-0.3921
21.75	45.75	1964.91	23.80	-0.4057	45.75	69.75	1943.87	24.80	-0.3718
22.25	46.25	1964.47	26.30	-0.3209	46.25	70.25	1943.44	23.00	-0.4328
22.75	46.75	1964.03	17.30	-0.6261	46.75	70.75	1943.00	20.20	-0.5278
23.25	47.25	1963.59	21.00	-0.5007	47.25	71.25	1942.56	24.60	-0.3786
23.75	47.75	1963.15	19.90	-0.5380	47.75	71.75	1942.12	24.00	-0.3989

VC1 Proximal Site									
Sample Mid-depth (cm)	*Adjusted Mid-depth (cm)*	*Year AD*	*Magnetic Susceptibility*	*z-score*	*Sample Mid-depth (cm)*	*Adjusted Mid-depth (cm)*	*Year AD*	*Magnetic Susceptibility*	*z-score*
48.25	72.25	1941.68	23.00	-0.4328	72.25	96.25	1920.65	27.00	-0.2972
48.75	72.75	1941.25	24.10	-0.3955	72.75	96.75	1920.21	27.70	-0.2734
49.25	73.25	1940.81	22.80	-0.4396	73.25	97.25	1919.78	29.10	-0.2259
49.75	73.75	1940.37	24.00	-0.3989	73.75	97.75	1919.34	26.50	-0.3141
50.25	74.25	1939.93	26.60	-0.3107	74.25	98.25	1918.90	27.00	-0.2972
50.75	74.75	1939.49	24.00	-0.3989	74.75	98.75	1918.46	28.10	-0.2599
51.25	75.25	1939.05	19.70	-0.5447	75.25	99.25	1918.02	25.60	-0.3446
51.75	75.75	1938.62	23.50	-0.4159	75.75	99.75	1917.58	24.50	-0.3819
52.25	76.25	1938.18	20.00	-0.5346	76.25	100.25	1917.15	28.70	-0.2395
52.75	76.75	1937.74	21.00	-0.5007	76.75	100.75	1916.71	33.10	-0.0903
53.25	77.25	1937.30	21.40	-0.4871	77.25	101.25	1916.27	32.00	-0.1276
53.75	77.75	1936.86	41.10	0.1811	77.75	101.75	1915.83	40.00	0.1437
54.25	78.25	1936.43	26.00	-0.3311	78.25	102.25	1915.39	34.40	-0.0462
54.75	78.75	1935.99	20.00	-0.5346	78.75	102.75	1914.96	40.00	0.1437
55.25	79.25	1935.55	23.00	-0.4328	79.25	103.25	1914.52	27.60	-0.2768
55.75	79.75	1935.11	26.50	-0.3141	79.75	103.75	1914.08	32.10	-0.1242
56.25	80.25	1934.67	19.70	-0.5447	80.25	104.25	1913.64	28.90	-0.2327
56.75	80.75	1934.23	24.90	-0.3684	80.75	104.75	1913.20	29.00	-0.2293
57.25	81.25	1933.80	24.30	-0.3887	81.25	105.25	1912.76	25.50	-0.3480
57.75	81.75	1933.36	25.40	-0.3514	81.75	105.75	1912.33	26.00	-0.3311
58.25	82.25	1932.92	28.00	-0.2632	82.25	106.25	1911.89	31.00	-0.1615
58.75	82.75	1932.48	27.60	-0.2768	82.75	106.75	1911.45	22.80	-0.4396
59.25	83.25	1932.04	31.00	-0.1615	83.25	107.25	1911.01	27.60	-0.2768
59.75	83.75	1931.61	33.00	-0.0937	83.75	107.75	1910.57	34.00	-0.0597
60.25	84.25	1931.17	33.00	-0.0937	84.25	108.25	1910.14	30.50	-0.1785
60.75	84.75	1930.73	21.10	-0.4973	84.75	108.75	1909.70	28.70	-0.2395
61.25	85.25	1930.29	41.00	0.1777	85.25	109.25	1909.26	29.40	-0.2158
61.75	85.75	1929.85	37.30	0.0522	85.75	109.75	1908.82	33.10	-0.0903
62.25	86.25	1929.42	38.60	0.0963	86.25	110.25	1908.38	35.60	-0.0055
62.75	86.75	1928.98	46.10	0.3506	86.75	110.75	1907.94	32.00	-0.1276
63.25	87.25	1928.54	29.90	-0.1988	87.25	111.25	1907.51	35.90	0.0047
63.75	87.75	1928.10	32.50	-0.1106	87.75	111.75	1907.07	26.50	-0.3141
64.25	88.25	1927.66	31.90	-0.1310	88.25	112.25	1906.63	34.50	-0.0428
64.75	88.75	1927.22	28.50	-0.2463	88.75	112.75	1906.19	33.40	-0.0801
65.25	89.25	1926.79	32.00	-0.1276	89.25	113.25	1905.75	29.50	-0.2124
65.75	89.75	1926.35	25.50	-0.3480	89.75	113.75	1905.32	38.40	0.0895
66.25	90.25	1925.91	25.70	-0.3413	90.25	114.25	1904.88	34.00	-0.0597
66.75	90.75	1925.47	24.50	-0.3819	90.75	114.75	1904.44	38.10	0.0793
67.25	91.25	1925.03	24.00	-0.3989	91.25	115.25	1904.00	31.60	-0.1411
67.75	91.75	1924.60	32.80	-0.1004	91.75	115.75	1903.56	38.50	0.0929
68.25	92.25	1924.16	29.10	-0.2259	92.25	116.25	1903.12	37.80	0.0691
68.75	92.75	1923.72	26.50	-0.3141	92.75	116.75	1902.69	30.80	-0.1683
69.25	93.25	1923.28	30.60	-0.1751	93.25	117.25	1902.25	42.00	0.2116
69.75	93.75	1922.84	23.00	-0.4328	93.75	117.75	1901.81	46.20	0.3540
70.225	94.225	1922.43	22.50	-0.4498	94.25	118.25	1901.37	41.50	0.1946
70.75	94.75	1921.97	19.60	-0.5481	94.75	118.75	1900.93	26.50	-0.3141
71.25	95.25	1921.53	18.60	-0.5821	95.25	119.25	1900.50	25.50	-0.3480
71.75	95.75	1921.09	18.30	-0.5922	95.75	119.75	1900.06	35.50	-0.0089

VC1 Proximal Site									
Sample Mid-depth (cm)	*Adjusted Mid-depth (cm)*	*Year AD*	*Magnetic Susceptibility*	*z-score*	*Sample Mid-depth (cm)*	*Adjusted Mid-depth (cm)*	*Year AD*	*Magnetic Susceptibility*	*z-score*
96.25	120.25	1899.62	33.30	-0.0835	120.75	144.75	1878.15	19.50	-0.5515
96.75	120.75	1899.18	35.20	-0.0191	121.25	145.25	1877.71	22.00	-0.4667
97.25	121.25	1898.74	41.50	0.1946	121.75	145.75	1877.27	19.00	-0.5685
97.75	121.75	1898.30	35.10	-0.0224	122.25	146.25	1876.83	16.40	-0.6567
98.25	122.25	1897.87	33.10	-0.0903	122.75	146.75	1876.40	15.40	-0.6906
98.75	122.75	1897.43	30.50	-0.1785	123.25	147.25	1875.96	18.40	-0.5888
99.25	123.25	1896.99	30.50	-0.1785	123.75	147.75	1875.52	24.10	-0.3955
99.75	123.75	1896.55	26.00	-0.3311	124.25	148.25	1875.08	26.50	-0.3141
100.25	124.25	1896.11	19.10	-0.5651	124.75	148.75	1874.64	26.00	-0.3311
100.75	124.75	1895.68	23.50	-0.4159	125.25	149.25	1874.21	28.90	-0.2327
101.25	125.25	1895.24	26.50	-0.3141	125.75	149.75	1873.77	27.50	-0.2802
101.75	125.75	1894.80	24.00	-0.3989	126.25	150.25	1873.33	37.50	0.0590
102.25	126.25	1894.36	25.00	-0.3650	126.75	150.75	1872.89	37.30	0.0522
102.75	126.75	1893.92	24.90	-0.3684	127.25	151.25	1872.45	33.40	-0.0801
103.75	127.75	1893.05	23.10	-0.4294	127.75	151.75	1872.01	39.70	0.1336
104.25	128.25	1892.61	26.10	-0.3277	128.25	152.25	1871.58	37.00	0.0420
104.75	128.75	1892.17	19.00	-0.5685	128.75	152.75	1871.14	33.00	-0.0937
105.25	129.25	1891.73	21.00	-0.5007	129.25	153.25	1870.70	22.50	-0.4498
105.75	129.75	1891.29	26.00	-0.3311	129.75	153.75	1870.26	17.90	-0.6058
106.25	130.25	1890.86	29.70	-0.2056	130.25	154.25	1869.82	25.40	-0.3514
106.75	130.75	1890.42	21.00	-0.5007	130.75	154.75	1869.39	24.00	-0.3989
107.25	131.25	1889.98	30.50	-0.1785	131.25	155.25	1868.95	21.00	-0.5007
107.75	131.75	1889.54	20.00	-0.5346	131.75	155.75	1868.51	20.10	-0.5312
108.25	132.25	1889.10	24.50	-0.3819	132.25	156.25	1868.07	26.10	-0.3277
108.75	132.75	1888.66	23.40	-0.4193	132.75	156.75	1867.63	25.90	-0.3345
109.25	133.25	1888.23	24.00	-0.3989	133.25	157.25	1867.19	23.00	-0.4328
109.75	133.75	1887.79	20.50	-0.5176	134.25	158.25	1866.32	21.00	-0.5007
110.25	134.25	1887.35	15.40	-0.6906	134.75	158.75	1865.88	24.50	-0.3819
110.75	134.75	1886.91	16.50	-0.6533	135.25	159.25	1865.44	24.00	-0.3989
111.25	135.25	1886.47	20.50	-0.5176	135.75	159.75	1865.00	13.60	-0.7516
111.75	135.75	1886.04	17.00	-0.6363	136.25	160.25	1864.57	19.00	-0.5685
112.25	136.25	1885.60	19.40	-0.5549	136.75	160.75	1864.13	25.70	-0.3413
112.75	136.75	1885.16	20.00	-0.5346	137.25	161.25	1863.69	18.00	-0.6024
113.25	137.25	1884.72	21.90	-0.4701	137.75	161.75	1863.25	17.40	-0.6228
113.75	137.75	1884.28	19.50	-0.5515	138.25	162.25	1862.81	14.50	-0.7211
114.25	138.25	1883.84	18.50	-0.5854	138.75	162.75	1862.37	14.60	-0.7177
114.75	138.75	1883.41	21.00	-0.5007	139.25	163.25	1861.94	15.00	-0.7041
115.25	139.25	1882.97	19.00	-0.5685	139.75	163.75	1861.50	19.60	-0.5481
115.75	139.75	1882.53	21.00	-0.5007	140.25	164.25	1861.06	21.20	-0.4939
116.25	140.25	1882.09	14.00	-0.7381	140.75	164.75	1860.62	27.40	-0.2836
116.75	140.75	1881.65	11.00	-0.8398	141.25	165.25	1860.18	24.00	-0.3989
117.25	141.25	1881.22	13.40	-0.7584	141.75	165.75	1859.75	19.50	-0.5515
117.75	141.75	1880.78	13.00	-0.7720	142.25	166.25	1859.31	16.60	-0.6499
118.25	142.25	1880.34	20.50	-0.5176	142.75	166.75	1858.87	17.80	-0.6092
118.75	142.75	1879.90	22.50	-0.4498	143.25	167.25	1858.43	29.50	-0.2124
119.25	143.25	1879.46	17.60	-0.6160	144.25	168.25	1857.55	19.10	-0.5651
119.75	143.75	1879.03	19.30	-0.5583	144.75	168.75	1857.12	16.10	-0.6668
120.25	144.25	1878.59	22.40	-0.4532	145.25	169.25	1856.68	20.70	-0.5108

VC1 Proximal Site									
Sample Mid-depth (cm)	*Adjusted Mid-depth (cm)*	*Year AD*	*Magnetic Susceptibility*	*z-score*	*Sample Mid-depth (cm)*	*Adjusted Mid-depth (cm)*	*Year AD*	*Magnetic Susceptibility*	*z-score*
145.75	169.75	1856.24	23.50	-0.4159	169.75	193.75	1835.21	13.40	-0.7584
146.25	170.25	1855.80	19.50	-0.5515	170.25	194.25	1834.77	15.40	-0.6906
146.75	170.75	1855.36	17.00	-0.6363	170.75	194.75	1834.33	27.20	-0.2904
147.25	171.25	1854.93	20.50	-0.5176	171.25	195.25	1833.89	29.40	-0.2158
147.75	171.75	1854.49	25.50	-0.3480	171.75	195.75	1833.45	14.30	-0.7279
148.25	172.25	1854.05	16.50	-0.6533	172.25	196.25	1833.02	17.90	-0.6058
148.75	172.75	1853.61	24.00	-0.3989	172.75	196.75	1832.58	17.00	-0.6363
149.25	173.25	1853.17	28.50	-0.2463	173.25	197.25	1832.14	31.40	-0.1479
149.75	173.75	1852.73	25.80	-0.3379	173.75	197.75	1831.70	20.50	-0.5176
150.25	174.25	1852.30	19.00	-0.5685	174.25	198.25	1831.26	21.00	-0.5007
150.75	174.75	1851.86	19.50	-0.5515	174.75	198.75	1830.83	16.50	-0.6533
151.25	175.25	1851.42	15.50	-0.6872	175.25	199.25	1830.39	14.70	-0.7143
151.75	175.75	1850.98	20.60	-0.5142	175.75	199.75	1829.95	16.10	-0.6668
152.25	176.25	1850.54	21.50	-0.4837	176.25	200.25	1829.51	16.90	-0.6397
152.75	176.75	1850.11	28.50	-0.2463	176.75	200.75	1829.07	20.00	-0.5346
153.25	177.25	1849.67	32.50	-0.1106	177.25	201.25	1828.64	18.60	-0.5821
153.75	177.75	1849.23	27.50	-0.2802	177.75	201.75	1828.20	22.00	-0.4667
154.25	178.25	1848.79	30.80	-0.1683	178.25	202.25	1827.76	18.40	-0.5888
154.75	178.75	1848.35	28.00	-0.2632	178.75	202.75	1827.32	19.20	-0.5617
155.25	179.25	1847.91	17.40	-0.6228	179.25	203.25	1826.88	15.20	-0.6974
155.75	179.75	1847.48	14.50	-0.7211	179.75	203.75	1826.44	19.50	-0.5515
156.25	180.25	1847.04	17.40	-0.6228	180.25	204.25	1826.01	13.50	-0.7550
156.75	180.75	1846.60	19.50	-0.5515	180.75	204.75	1825.57	16.00	-0.6702
157.25	181.25	1846.16	18.40	-0.5888	181.25	205.25	1825.13	14.90	-0.7075
157.75	181.75	1845.72	19.40	-0.5549	181.75	205.75	1824.69	20.50	-0.5176
158.25	182.25	1845.29	18.00	-0.6024	182.25	206.25	1824.25	17.50	-0.6194
158.75	182.75	1844.85	15.00	-0.7041	182.75	206.75	1823.82	18.40	-0.5888
159.25	183.25	1844.41	17.60	-0.6160	183.25	207.25	1823.38	16.00	-0.6702
159.75	183.75	1843.97	15.40	-0.6906	183.75	207.75	1822.94	17.00	-0.6363
160.25	184.25	1843.53	11.90	-0.8093	184.25	208.25	1822.50	16.00	-0.6702
160.75	184.75	1843.09	21.10	-0.4973	184.75	208.75	1822.06	16.50	-0.6533
161.25	185.25	1842.66	13.40	-0.7584	185.25	209.25	1821.62	18.00	-0.6024
161.75	185.75	1842.22	18.00	-0.6024	185.75	209.75	1821.19	22.00	-0.4667
162.25	186.25	1841.78	19.40	-0.5549	186.25	210.25	1820.75	25.00	-0.3650
162.75	186.75	1841.34	25.40	-0.3514	186.75	210.75	1820.31	26.00	-0.3311
163.25	187.25	1840.90	23.00	-0.4328	187.25	211.25	1819.87	40.00	0.1437
163.75	187.75	1840.47	20.00	-0.5346	187.75	211.75	1819.43	40.50	0.1607
164.25	188.25	1840.03	21.50	-0.4837	188.75	212.75	1818.56	49.60	0.4693
164.75	188.75	1839.59	15.00	-0.7041	189.25	213.25	1818.12	47.00	0.3812
165.25	189.25	1839.15	16.70	-0.6465	189.75	213.75	1817.68	45.20	0.3201
165.75	189.75	1838.71	29.10	-0.2259	190.25	214.25	1817.24	37.50	0.0590
166.25	190.25	1838.27	20.20	-0.5278	190.75	214.75	1816.80	19.50	-0.5515
166.75	190.75	1837.84	15.50	-0.6872	191.25	215.25	1816.37	19.70	-0.5447
167.25	191.25	1837.40	14.00	-0.7381	191.75	215.75	1815.93	24.50	-0.3819
167.75	191.75	1836.96	13.90	-0.7415	192.25	216.25	1815.49	24.90	-0.3684
168.25	192.25	1836.52	18.40	-0.5888	192.75	216.75	1815.05	17.50	-0.6194
168.75	192.75	1836.08	14.90	-0.7075	193.25	217.25	1814.61	17.10	-0.6329
169.25	193.25	1835.65	16.60	-0.6499	193.75	217.75	1814.18	19.70	-0.5447

VC1 Proximal Site									
Sample Mid-depth (cm)	*Adjusted Mid-depth (cm)*	*Year AD*	*Magnetic Susceptibility*	*z-score*	*Sample Mid-depth (cm)*	*Adjusted Mid-depth (cm)*	*Year AD*	*Magnetic Susceptibility*	*z-score*
194.25	218.25	1813.74	16.00	-0.6702	218.25	242.25	1792.70	14.40	-0.7245
194.75	218.75	1813.30	30.00	-0.1954	218.75	242.75	1792.27	16.00	-0.6702
195.25	219.25	1812.86	38.00	0.0759	219.25	243.25	1791.83	14.50	-0.7211
195.75	219.75	1812.42	45.00	0.3133	219.75	243.75	1791.39	15.90	-0.6736
196.25	220.25	1811.98	36.00	0.0081	220.25	244.25	1790.95	19.60	-0.5481
196.75	220.75	1811.55	24.90	-0.3684	220.75	244.75	1790.51	16.10	-0.6668
197.25	221.25	1811.11	17.00	-0.6363	221.25	245.25	1790.08	15.20	-0.6974
197.75	221.75	1810.67	19.50	-0.5515	221.75	245.75	1789.64	16.80	-0.6431
198.25	222.25	1810.23	25.00	-0.3650	222.25	246.25	1789.20	15.20	-0.6974
198.75	222.75	1809.79	26.00	-0.3311	222.75	246.75	1788.76	17.30	-0.6261
199.25	223.25	1809.36	18.00	-0.6024	223.25	247.25	1788.32	25.10	-0.3616
199.75	223.75	1808.92	18.50	-0.5854	223.75	247.75	1787.88	30.50	-0.1785
200.25	224.25	1808.48	22.50	-0.4498	224.25	248.25	1787.45	27.00	-0.2972
200.75	224.75	1808.04	20.60	-0.5142	224.75	248.75	1787.01	17.60	-0.6160
201.25	225.25	1807.60	30.50	-0.1785	225.25	249.25	1786.57	15.00	-0.7041
201.75	225.75	1807.16	34.00	-0.0597	225.75	249.75	1786.13	17.90	-0.6058
202.25	226.25	1806.73	47.20	0.3879	226.25	250.25	1785.69	16.40	-0.6567
202.75	226.75	1806.29	50.60	0.5033	226.75	250.75	1785.26	20.50	-0.5176
203.25	227.25	1805.85	35.60	-0.0055	227.25	251.25	1784.82	22.90	-0.4362
203.75	227.75	1805.41	29.00	-0.2293	227.75	251.75	1784.38	20.50	-0.5176
204.25	228.25	1804.97	30.40	-0.1818	228.25	252.25	1783.94	14.90	-0.7075
204.75	228.75	1804.54	23.00	-0.4328	228.75	252.75	1783.50	20.10	-0.5312
205.25	229.25	1804.10	17.30	-0.6261	229.25	253.25	1783.07	30.50	-0.1785
205.75	229.75	1803.66	19.50	-0.5515	229.75	253.75	1782.63	18.50	-0.5854
206.25	230.25	1803.22	22.60	-0.4464	230.25	254.25	1782.19	14.60	-0.7177
206.75	230.75	1802.78	24.50	-0.3819	230.75	254.75	1781.75	14.00	-0.7381
207.25	231.25	1802.34	26.60	-0.3107	231.25	255.25	1781.31	18.40	-0.5888
207.75	231.75	1801.91	28.30	-0.2531	231.75	255.75	1780.87	15.50	-0.6872
208.25	232.25	1801.47	37.80	0.0691	232.25	256.25	1780.44	16.00	-0.6702
208.75	232.75	1801.03	48.10	0.4185	232.75	256.75	1780.00	11.10	-0.8364
209.25	233.25	1800.59	38.00	0.0759	233.25	257.25	1779.56	20.50	-0.5176
209.75	233.75	1800.15	20.50	-0.5176	233.75	257.75	1779.12	15.00	-0.7041
210.25	234.25	1799.72	20.80	-0.5074	234.25	258.25	1778.68	15.10	-0.7008
210.75	234.75	1799.28	19.70	-0.5447	234.75	258.75	1778.25	14.50	-0.7211
211.25	235.25	1798.84	20.90	-0.5040	235.25	259.25	1777.81	17.90	-0.6058
211.75	235.75	1798.40	28.50	-0.2463	236.25	260.25	1776.93	42.80	0.2387
212.25	236.25	1797.96	29.60	-0.2090	236.75	260.75	1776.49	42.70	0.2353
212.75	236.75	1797.52	35.00	-0.0258	237.25	261.25	1776.05	37.60	0.0623
213.25	237.25	1797.09	45.90	0.3438	237.75	261.75	1775.62	26.40	-0.3175
213.75	237.75	1796.65	50.90	0.5134	238.25	262.25	1775.18	17.20	-0.6295
214.25	238.25	1796.21	50.60	0.5033	238.75	262.75	1774.74	13.60	-0.7516
214.75	238.75	1795.77	47.10	0.3845	239.25	263.25	1774.30	13.00	-0.7720
215.25	239.25	1795.33	50.60	0.5033	239.75	263.75	1773.86	10.50	-0.8568
215.75	239.75	1794.90	37.10	0.0454	240.25	264.25	1773.43	23.60	-0.4125
216.25	240.25	1794.46	19.90	-0.5380	240.75	264.75	1772.99	27.90	-0.2666
216.75	240.75	1794.02	26.00	-0.3311	241.25	265.25	1772.55	29.00	-0.2293
217.25	241.25	1793.58	32.80	-0.1004	241.75	265.75	1772.11	19.20	-0.5617
217.75	241.75	1793.14	23.90	-0.4023	242.25	266.25	1771.67	12.90	-0.7754

VC1 Proximal Site									
Sample Mid-depth (cm)	*Adjusted Mid-depth (cm)*	*Year AD*	*Magnetic Susceptibility*	*z-score*	*Sample Mid-depth (cm)*	*Adjusted Mid-depth (cm)*	*Year AD*	*Magnetic Susceptibility*	*z-score*
242.75	266.75	1771.23	8.80	-0.9144	267.25	291.25	1749.76	39.50	0.1268
243.25	267.25	1770.80	17.90	-0.6058	267.75	291.75	1749.33	36.10	0.0115
243.75	267.75	1770.36	14.00	-0.7381	268.25	292.25	1748.89	23.20	-0.4260
244.25	268.25	1769.92	12.00	-0.8059	268.75	292.75	1748.45	3.90	-1.0806
244.75	268.75	1769.48	9.60	-0.8873	269.25	293.25	1748.01	13.70	-0.7482
245.25	269.25	1769.04	13.40	-0.7584	269.75	293.75	1747.57	14.40	-0.7245
245.75	269.75	1768.61	15.00	-0.7041	270.25	294.25	1747.13	20.50	-0.5176
246.25	270.25	1768.17	19.50	-0.5515	270.75	294.75	1746.70	15.80	-0.6770
246.75	270.75	1767.73	15.60	-0.6838	271.25	295.25	1746.26	13.20	-0.7652
247.25	271.25	1767.29	16.50	-0.6533	271.75	295.75	1745.82	15.80	-0.6770
247.75	271.75	1766.85	13.90	-0.7415	272.25	296.25	1745.38	12.80	-0.7788
248.25	272.25	1766.41	11.80	-0.8127	272.75	296.75	1744.94	15.60	-0.6838
248.75	272.75	1765.98	12.60	-0.7855	273.25	297.25	1744.51	20.30	-0.5244
249.25	273.25	1765.54	13.60	-0.7516	273.75	297.75	1744.07	18.70	-0.5787
249.75	273.75	1765.10	18.10	-0.5990	274.25	298.25	1743.63	14.80	-0.7109
250.25	274.25	1764.66	17.30	-0.6261	274.75	298.75	1743.19	31.60	-0.1411
250.75	274.75	1764.22	13.50	-0.7550	275.25	299.25	1742.75	13.40	-0.7584
251.25	275.25	1763.79	14.90	-0.7075	275.75	299.75	1742.31	14.10	-0.7347
251.75	275.75	1763.35	13.80	-0.7448	276.25	300.25	1741.88	18.70	-0.5787
252.25	276.25	1762.91	17.40	-0.6228	276.75	300.75	1741.44	20.70	-0.5108
252.75	276.75	1762.47	15.00	-0.7041	277.25	301.25	1741.00	16.60	-0.6499
253.25	277.25	1762.03	17.00	-0.6363	277.75	301.75	1740.56	9.40	-0.8941
253.75	277.75	1761.59	13.80	-0.7448	278.25	302.25	1740.12	9.50	-0.8907
254.25	278.25	1761.16	19.10	-0.5651	278.75	302.75	1739.69	12.10	-0.8025
254.75	278.75	1760.72	18.40	-0.5888	279.25	303.25	1739.25	9.40	-0.8941
255.25	279.25	1760.28	13.40	-0.7584	279.75	303.75	1738.81	12.50	-0.7889
255.75	279.75	1759.84	13.00	-0.7720	280.25	304.25	1738.37	14.50	-0.7211
256.25	280.25	1759.40	15.20	-0.6974	280.75	304.75	1737.93	14.50	-0.7211
256.75	280.75	1758.97	14.50	-0.7211	281.25	305.25	1737.49	17.50	-0.6194
257.25	281.25	1758.53	14.90	-0.7075	281.75	305.75	1737.06	13.30	-0.7618
257.75	281.75	1758.09	21.00	-0.5007	282.25	306.25	1736.62	21.10	-0.4973
258.25	282.25	1757.65	14.50	-0.7211	282.75	306.75	1736.18	23.30	-0.4226
258.75	282.75	1757.21	12.10	-0.8025	283.25	307.25	1735.74	19.90	-0.5380
259.25	283.25	1756.77	10.90	-0.8432	283.75	307.75	1735.30	12.40	-0.7923
259.75	283.75	1756.34	11.20	-0.8330	284.25	308.25	1734.87	12.60	-0.7855
260.25	284.25	1755.90	14.50	-0.7211	284.75	308.75	1734.43	20.50	-0.5176
260.75	284.75	1755.46	37.90	0.0725	285.25	309.25	1733.99	34.40	-0.0462
261.75	285.75	1754.58	26.20	-0.3243	285.75	309.75	1733.55	30.00	-0.1954
262.25	286.25	1754.15	21.00	-0.5007	286.25	310.25	1733.11	31.20	-0.1547
262.75	286.75	1753.71	18.30	-0.5922	286.75	310.75	1732.68	18.40	-0.5888
263.25	287.25	1753.27	14.40	-0.7245	287.25	311.25	1732.24	18.00	-0.6024
263.75	287.75	1752.83	11.50	-0.8229	288.25	312.25	1731.36	11.90	-0.8093
264.25	288.25	1752.39	12.50	-0.7889	288.75	312.75	1730.92	14.40	-0.7245
264.75	288.75	1751.95	23.50	-0.4159	289.25	313.25	1730.48	12.90	-0.7754
265.25	289.25	1751.52	45.00	0.3133	289.75	313.75	1730.05	18.10	-0.5990
265.75	289.75	1751.08	24.50	-0.3819	290.25	314.25	1729.61	19.00	-0.5685
266.25	290.25	1750.64	19.50	-0.5515	290.75	314.75	1729.17	38.90	0.1064
266.75	290.75	1750.20	28.30	-0.2531	291.25	315.25	1728.73	23.20	-0.4260

VC1 Proximal Site									
Sample Mid-depth (cm)	*Adjusted Mid-depth (cm)*	*Year AD*	*Magnetic Susceptibility*	*z-score*	*Sample Mid-depth (cm)*	*Adjusted Mid-depth (cm)*	*Year AD*	*Magnetic Susceptibility*	*z-score*
291.75	315.75	1728.29	23.40	-0.4193	315.75	339.75	1693.93	10.50	-0.8568
292.25	316.25	1727.86	19.30	-0.5583	316.25	340.25	1692.98	9.70	-0.8839
292.75	316.75	1727.42	23.50	-0.4159	316.75	340.75	1692.03	12.90	-0.7754
293.25	317.25	1726.98	23.00	-0.4328	317.25	341.25	1691.08	11.00	-0.8398
293.75	317.75	1726.54	24.80	-0.3718	317.75	341.75	1690.13	18.20	-0.5956
294.25	318.25	1726.10	29.10	-0.2259	318.25	342.25	1689.18	13.30	-0.7618
294.75	318.75	1725.66	26.70	-0.3073	318.75	342.75	1688.23	12.00	-0.8059
295.25	319.25	1725.23	20.10	-0.5312	319.25	343.25	1687.28	16.60	-0.6499
295.75	319.75	1724.79	11.70	-0.8161	319.75	343.75	1686.33	19.90	-0.5380
296.25	320.25	1724.35	23.20	-0.4260	320.25	344.25	1685.38	22.50	-0.4498
296.75	320.75	1723.91	23.70	-0.4091	320.75	344.75	1684.44	21.20	-0.4939
297.25	321.25	1723.47	19.90	-0.5380	321.25	345.25	1683.49	14.60	-0.7177
297.75	321.75	1723.04	18.90	-0.5719	321.75	345.75	1682.54	8.50	-0.9246
298.25	322.25	1722.60	20.90	-0.5040	322.25	346.25	1681.59	17.90	-0.6058
298.75	322.75	1722.16	22.50	-0.4498	322.75	346.75	1680.64	20.50	-0.5176
299.25	323.25	1721.72	25.00	-0.3650	323.25	347.25	1679.69	18.90	-0.5719
299.75	323.75	1721.28	23.70	-0.4091	323.75	347.75	1678.74	25.90	-0.3345
300.25	324.25	1720.84	25.00	-0.3650	324.25	348.25	1677.79	14.70	-0.7143
300.75	324.75	1720.41	26.20	-0.3243	324.75	348.75	1676.84	17.80	-0.6092
301.25	325.25	1719.97	26.00	-0.3311	325.25	349.25	1675.89	20.80	-0.5074
301.75	325.75	1719.53	25.30	-0.3548	325.75	349.75	1674.94	30.70	-0.1717
302.25	326.25	1719.09	25.40	-0.3514	326.25	350.25	1673.99	27.00	-0.2972
302.75	326.75	1718.62	13.40	-0.7584	326.75	350.75	1673.04	21.30	-0.4905
303.25	327.25	1717.67	18.50	-0.5854	327.25	351.25	1672.09	27.60	-0.2768
303.75	327.75	1716.72	20.50	-0.5176	327.75	351.75	1671.14	26.30	-0.3209
304.25	328.25	1715.77	16.10	-0.6668	328.25	352.25	1670.19	37.30	0.0522
304.75	328.75	1714.82	12.10	-0.8025	328.75	352.75	1669.24	38.70	0.0997
305.25	329.25	1713.87	13.00	-0.7720	329.25	353.25	1668.29	32.50	-0.1106
305.75	329.75	1712.92	12.30	-0.7957	329.75	353.75	1667.34	32.90	-0.0971
306.25	330.25	1711.97	14.40	-0.7245	330.25	354.25	1666.40	27.20	-0.2904
306.75	330.75	1711.02	12.50	-0.7889	330.75	354.75	1665.45	26.00	-0.3311
307.25	331.25	1710.07	12.10	-0.8025	331.25	355.25	1664.50	26.00	-0.3311
307.75	331.75	1709.12	13.20	-0.7652	331.75	355.75	1663.55	25.00	-0.3650
308.25	332.25	1708.17	11.30	-0.8296	332.25	356.25	1662.60	25.00	-0.3650
308.75	332.75	1707.22	12.20	-0.7991	332.75	356.75	1661.65	30.40	-0.1818
309.25	333.25	1706.27	10.80	-0.8466	333.25	357.25	1660.70	22.40	-0.4532
309.75	333.75	1705.32	8.90	-0.9110	333.75	357.75	1659.75	26.20	-0.3243
310.25	334.25	1704.37	11.90	-0.8093	334.25	358.25	1658.80	20.60	-0.5142
310.75	334.75	1703.43	11.00	-0.8398	334.75	358.75	1657.85	18.70	-0.5787
311.25	335.25	1702.48	9.50	-0.8907	335.25	359.25	1656.90	19.90	-0.5380
311.75	335.75	1701.53	10.70	-0.8500	335.75	359.75	1655.95	18.00	-0.6024
312.25	336.25	1700.58	8.50	-0.9246	336.25	360.25	1655.00	21.40	-0.4871
312.75	336.75	1699.63	8.10	-0.9382	336.75	360.75	1654.05	21.00	-0.5007
313.25	337.25	1698.68	5.50	-1.0263	337.25	361.25	1653.10	18.30	-0.5922
313.75	337.75	1697.73	10.50	-0.8568	337.75	361.75	1652.15	17.70	-0.6126
314.25	338.25	1696.78	10.40	-0.8602	338.25	362.25	1651.20	20.50	-0.5176
314.75	338.75	1695.83	9.70	-0.8839	338.75	362.75	1650.25	23.80	-0.4057
315.25	339.25	1694.88	10.30	-0.8636	339.25	363.25	1649.30	23.00	-0.4328

VC1 Proximal Site									
Sample Mid-depth (cm)	*Adjusted Mid-depth (cm)*	*Year AD*	*Magnetic Susceptibility*	*z-score*	*Sample Mid-depth (cm)*	*Adjusted Mid-depth (cm)*	*Year AD*	*Magnetic Susceptibility*	*z-score*
339.75	363.75	1648.35	24.60	-0.3786	363.75	387.75	1602.78	27.50	-0.2802
340.25	364.25	1647.41	22.40	-0.4532	364.25	388.25	1601.83	28.50	-0.2463
340.75	364.75	1646.46	25.50	-0.3480	364.75	388.75	1600.88	29.00	-0.2293
341.25	365.25	1645.51	24.30	-0.3887	365.25	389.25	1599.93	30.00	-0.1954
341.75	365.75	1644.56	31.20	-0.1547	365.75	389.75	1598.98	34.00	-0.0597
342.25	366.25	1643.61	32.90	-0.0971	366.25	390.25	1598.03	32.00	-0.1276
342.75	366.75	1642.66	31.10	-0.1581	366.75	390.75	1597.08	29.50	-0.2124
343.25	367.25	1641.71	32.80	-0.1004	367.25	391.25	1596.13	35.50	-0.0089
343.75	367.75	1640.76	29.40	-0.2158	367.75	391.75	1595.96	58.50	0.7712
344.25	368.25	1639.81	33.50	-0.0767	368.25	392.25	1595.60	52.00	0.5507
344.75	368.75	1638.86	31.60	-0.1411	368.75	392.75	1595.25	34.50	-0.0428
345.25	369.25	1637.91	32.70	-0.1038	369.25	393.25	1594.90	43.50	0.2624
345.75	369.75	1636.96	29.50	-0.2124	369.75	393.75	1594.55	38.70	0.0997
346.25	370.25	1636.01	29.10	-0.2259	370.25	394.25	1594.19	36.00	0.0081
346.75	370.75	1635.06	32.40	-0.1140	370.75	394.75	1593.84	50.50	0.4999
347.25	371.25	1634.11	32.20	-0.1208	371.25	395.25	1593.49	45.50	0.3303
347.75	371.75	1633.16	37.00	0.0420	371.75	395.75	1593.13	52.50	0.5677
348.25	372.25	1632.21	40.50	0.1607	372.25	396.25	1592.78	58.50	0.7712
348.75	372.75	1631.26	42.40	0.2251	372.75	396.75	1592.43	76.50	1.3817
349.25	373.25	1630.31	38.90	0.1064	373.25	397.25	1592.08	79.50	1.4834
349.75	373.75	1629.37	41.60	0.1980	373.75	397.75	1591.72	55.10	0.6559
350.25	374.25	1628.42	41.50	0.1946	374.25	398.25	1591.37	62.00	0.8899
350.75	374.75	1627.47	45.40	0.3269	374.75	398.75	1591.02	75.60	1.3511
351.25	375.25	1626.52	41.70	0.2014	375.25	399.25	1590.66	69.50	1.1443
351.75	375.75	1625.57	39.50	0.1268	375.75	399.75	1590.31	62.50	0.9068
352.25	376.25	1624.62	32.10	-0.1242	376.25	400.25	1589.96	55.00	0.6525
352.75	376.75	1623.67	38.00	0.0759	376.75	400.75	1589.61	69.00	1.1273
353.25	377.25	1622.72	38.60	0.0963	377.25	401.25	1589.25	56.00	0.6864
353.75	377.75	1621.77	36.70	0.0318	377.75	401.75	1588.90	42.50	0.2285
354.25	378.25	1620.82	36.00	0.0081	378.25	402.25	1588.55	53.00	0.5846
354.75	378.75	1619.87	32.10	-0.1242	378.75	402.75	1588.20	54.50	0.6355
355.25	379.25	1618.92	37.10	0.0454	379.25	403.25	1587.84	69.00	1.1273
355.75	379.75	1617.97	23.60	-0.4125	379.75	403.75	1587.49	48.50	0.4320
356.25	380.25	1617.02	33.50	-0.0767	380.25	404.25	1587.14	38.90	0.1064
356.75	380.75	1616.07	35.40	-0.0123	380.75	404.75	1586.78	6.80	-0.9823
357.25	381.25	1615.12	40.10	0.1471	381.25	405.25	1586.43	32.50	-0.1106
357.75	381.75	1614.17	40.00	0.1437	381.75	405.75	1586.08	67.00	1.0595
358.25	382.25	1613.22	36.30	0.0183	382.25	406.25	1585.73	48.00	0.4151
358.75	382.75	1612.27	39.50	0.1268	382.75	406.75	1585.37	34.00	-0.0597
359.25	383.25	1611.32	36.50	0.0250	383.25	407.25	1585.02	27.00	-0.2972
359.75	383.75	1610.38	35.60	-0.0055	383.75	407.75	1584.67	24.50	-0.3819
360.25	384.25	1609.43	34.60	-0.0394	384.25	408.25	1584.31	27.00	-0.2972
360.75	384.75	1608.48	32.00	-0.1276	384.75	408.75	1583.96	21.00	-0.5007
361.25	385.25	1607.53	32.40	-0.1140	385.25	409.25	1583.61	44.50	0.2964
361.75	385.75	1606.58	30.90	-0.1649	385.75	409.75	1583.26	24.50	-0.3819
362.25	386.25	1605.63	31.90	-0.1310	386.25	410.25	1582.90	41.00	0.1777
362.75	386.75	1604.68	33.50	-0.0767	386.75	410.75	1582.55	43.50	0.2624
363.25	387.25	1603.73	28.50	-0.2463	387.25	411.25	1582.20	52.60	0.5711

VC1 Proximal Site									
Sample Mid-depth (cm)	*Adjusted Mid-depth (cm)*	*Year AD*	*Magnetic Susceptibility*	*z-score*	*Sample Mid-depth (cm)*	*Adjusted Mid-depth (cm)*	*Year AD*	*Magnetic Susceptibility*	*z-score*
388.25	412.25	1581.85	56.00	0.6864	412.25	436.25	1564.91	35.50	-0.0089
388.75	412.75	1581.49	34.50	-0.0428	412.75	436.75	1564.56	40.50	0.1607
389.25	413.25	1581.14	38.00	0.0759	413.25	437.25	1564.21	90.30	1.8497
389.75	413.75	1580.79	42.50	0.2285	413.75	437.75	1563.85	76.00	1.3647
390.25	414.25	1580.43	28.50	-0.2463	414.25	438.25	1563.50	37.00	0.0420
390.75	414.75	1580.08	28.60	-0.2429	414.75	438.75	1563.15	143.90	3.6676
391.25	415.25	1579.73	29.50	-0.2124	415.25	439.25	1562.80	84.00	1.6360
391.75	415.75	1579.38	31.10	-0.1581	415.75	439.75	1562.44	57.00	0.7203
392.25	416.25	1579.02	28.60	-0.2429	416.25	440.25	1562.09	114.20	2.6603
392.75	416.75	1578.67	41.00	0.1777	416.75	440.75	1561.74	93.00	1.9413
393.25	417.25	1578.32	37.40	0.0556	417.25	441.25	1561.38	51.50	0.5338
393.75	417.75	1577.96	68.00	1.0934	417.75	441.75	1561.03	39.50	0.1268
394.25	418.25	1577.61	52.10	0.5541	418.25	442.25	1560.68	36.50	0.0250
394.75	418.75	1577.26	35.00	-0.0258	418.75	442.75	1560.33	78.40	1.4461
395.25	419.25	1576.91	29.60	-0.2090	419.25	443.25	1559.97	57.00	0.7203
395.75	419.75	1576.55	44.60	0.2998	419.75	443.75	1559.62	68.50	1.1103
396.25	420.25	1576.20	35.00	-0.0258	420.25	444.25	1559.27	52.40	0.5643
396.75	420.75	1575.85	40.50	0.1607	420.75	444.75	1558.91	34.40	-0.0462
397.25	421.25	1575.50	96.40	2.0566	421.25	445.25	1558.56	32.10	-0.1242
397.75	421.75	1575.14	82.50	1.5852	421.75	445.75	1558.21	122.50	2.9418
398.25	422.25	1574.79	39.00	0.1098	422.25	446.25	1557.86	49.50	0.4659
398.75	422.75	1574.44	36.30	0.0183	422.75	446.75	1557.50	50.70	0.5066
399.25	423.25	1574.08	37.00	0.0420	423.25	447.25	1557.15	72.40	1.2426
399.75	423.75	1573.73	71.60	1.2155	423.75	447.75	1556.80	93.00	1.9413
400.25	424.25	1573.38	102.00	2.2465	424.25	448.25	1556.44	48.90	0.4456
400.75	424.75	1573.03	90.00	1.8395	424.75	448.75	1556.09	49.00	0.4490
401.25	425.25	1572.67	71.10	1.1985	425.25	449.25	1555.74	72.00	1.2290
401.75	425.75	1572.32	119.50	2.8400	425.75	449.75	1555.39	68.40	1.1070
402.25	426.25	1571.97	46.80	0.3744	426.25	450.25	1555.03	37.50	0.0590
402.75	426.75	1571.61	30.00	-0.1954	426.75	450.75	1554.68	55.10	0.6559
403.25	427.25	1571.26	29.50	-0.2124	427.25	451.25	1554.33	39.60	0.1302
403.75	427.75	1570.91	68.50	1.1103	427.75	451.75	1553.98	33.70	-0.0699
404.25	428.25	1570.56	61.40	0.8695	428.25	452.25	1553.62	38.00	0.0759
404.75	428.75	1570.20	41.00	0.1777	428.75	452.75	1553.27	20.10	-0.5312
405.25	429.25	1569.85	42.50	0.2285	429.25	453.25	1552.92	31.50	-0.1445
405.75	429.75	1569.50	64.00	0.9577	429.75	453.75	1552.56	39.50	0.1268
406.25	430.25	1569.15	47.00	0.3812	430.25	454.25	1552.21	57.50	0.7373
406.75	430.75	1568.79	33.50	-0.0767	430.75	454.75	1551.86	78.90	1.4631
407.25	431.25	1568.44	48.00	0.4151	431.25	455.25	1551.51	57.40	0.7339
407.75	431.75	1568.09	74.50	1.3138	431.75	455.75	1551.15	37.00	0.0420
408.25	432.25	1567.73	35.50	-0.0089	432.25	456.25	1550.80	25.20	-0.3582
408.75	432.75	1567.38	56.40	0.7000	432.75	456.75	1550.45	49.60	0.4693
409.25	433.25	1567.03	33.90	-0.0631	433.25	457.25	1550.09	45.50	0.3303
409.75	433.75	1566.68	44.40	0.2930	433.75	457.75	1549.74	55.00	0.6525
410.25	434.25	1566.32	28.60	-0.2429	434.25	458.25	1549.39	34.50	-0.0428
410.75	434.75	1565.97	31.00	-0.1615	434.75	458.75	1549.04	36.00	0.0081
411.25	435.25	1565.62	27.00	-0.2972	435.25	459.25	1548.68	45.30	0.3235
411.75	435.75	1565.26	26.50	-0.3141	435.75	459.75	1548.33	40.00	0.1437

VC1 Proximal Site									
Sample Mid-depth (cm)	*Adjusted Mid-depth (cm)*	*Year AD*	*Magnetic Susceptibility*	*z-score*	*Sample Mid-depth (cm)*	*Adjusted Mid-depth (cm)*	*Year AD*	*Magnetic Susceptibility*	*z-score*
436.25	460.25	1547.98	116.20	2.7281	462.75	486.75	1531.04	92.00	1.9074
436.75	460.75	1547.63	46.60	0.3676	463.25	487.25	1530.69	181.20	4.9326
437.25	461.25	1547.27	29.60	-0.2090	463.75	487.75	1530.34	127.90	3.1249
437.75	461.75	1546.92	47.00	0.3812	464.23	488.23	1529.99	84.70	1.6598
438.25	462.25	1546.57	54.50	0.6355	464.75	488.75	1529.63	42.90	0.2421
438.75	462.75	1546.21	78.50	1.4495	465.25	489.25	1529.28	62.20	0.8967
439.25	463.25	1545.86	65.00	0.9916	465.75	489.75	1528.93	69.90	1.1578
439.75	463.75	1545.51	37.00	0.0420	466.25	490.25	1528.58	60.70	0.8458
440.25	464.25	1545.16	62.40	0.9035	466.75	490.75	1528.22	59.40	0.8017
440.75	464.75	1544.80	62.00	0.8899	467.25	491.25	1527.87	37.60	0.0623
441.635	465.635	1544.45	36.00	0.0081	467.75	491.75	1527.52	80.20	1.5072
442.905	466.905	1544.10	43.30	0.2557	468.25	492.25	1527.16	63.40	0.9374
444.175	468.175	1543.74	29.50	-0.2124	468.75	492.75	1526.81	51.50	0.5338
445.25	469.25	1543.39	82.50	1.5852	469.25	493.25	1526.46	67.50	1.0764
445.75	469.75	1543.04	34.50	-0.0428	469.75	493.75	1526.11	66.50	1.0425
446.25	470.25	1542.69	33.10	-0.0903	470.25	494.25	1525.75	84.00	1.6360
446.75	470.75	1542.33	104.80	2.3415	470.75	494.75	1525.40	64.60	0.9781
447.25	471.25	1541.98	151.80	3.9355	471.25	495.25	1525.05	73.40	1.2765
447.75	471.75	1541.63	26.80	-0.3039	471.75	495.75	1524.69	133.80	3.3250
448.25	472.25	1541.28	19.50	-0.5515	472.25	496.25	1524.34	62.00	0.8899
448.75	472.75	1540.92	35.00	-0.0258	472.75	496.75	1523.99	44.00	0.2794
449.25	473.25	1540.57	86.90	1.7344	473.25	497.25	1523.64	67.60	1.0798
449.75	473.75	1540.22	64.90	0.9882	473.75	497.75	1523.28	50.20	0.4897
450.25	474.25	1539.86	83.70	1.6259	474.25	498.25	1522.93	47.30	0.3913
450.75	474.75	1539.51	101.40	2.2262	474.75	498.75	1522.58	49.00	0.4490
451.25	475.25	1539.16	61.20	0.8628	475.25	499.25	1522.22	111.40	2.5653
451.75	475.75	1538.81	44.10	0.2828	475.75	499.75	1521.87	45.00	0.3133
452.25	476.25	1538.45	79.70	1.4902	476.25	500.25	1521.52	50.20	0.4897
452.75	476.75	1538.10	93.70	1.9650	476.75	500.75	1521.17	118.40	2.8027
453.25	477.25	1537.75	46.60	0.3676	477.25	501.25	1520.81	59.50	0.8051
453.75	477.75	1537.39	34.40	-0.0462	477.75	501.75	1520.46	73.00	1.2630
454.25	478.25	1537.04	38.40	0.0895	478.25	502.25	1520.11	64.50	0.9747
454.75	478.75	1536.69	35.50	-0.0089	478.75	502.75	1519.76	43.50	0.2624
455.25	479.25	1536.34	40.60	0.1641	479.25	503.25	1519.40	53.50	0.6016
455.75	479.75	1535.98	51.00	0.5168	479.75	503.75	1519.05	75.00	1.3308
456.25	480.25	1535.63	36.40	0.0216	480.25	504.25	1518.70	93.30	1.9515
456.75	480.75	1535.28	71.00	1.1951	480.75	504.75	1518.34	102.90	2.2770
457.25	481.25	1534.93	61.00	0.8560	481.25	505.25	1517.99	79.70	1.4902
457.75	481.75	1534.57	36.00	0.0081	481.75	505.75	1517.64	56.30	0.6966
458.25	482.25	1534.22	48.50	0.4320	482.25	506.25	1517.29	137.40	3.4471
458.75	482.75	1533.87	37.00	0.0420	482.75	506.75	1516.93	48.40	0.4286
459.25	483.25	1533.51	31.60	-0.1411	483.25	507.25	1516.58	38.50	0.0929
459.75	483.75	1533.16	63.50	0.9408	483.75	507.75	1516.23	81.40	1.5479
460.25	484.25	1532.81	58.00	0.7542	484.25	508.25	1515.87	45.50	0.3303
460.75	484.75	1532.46	59.50	0.8051	484.75	508.75	1515.52	87.10	1.7412
461.25	485.25	1532.10	54.00	0.6186	485.25	509.25	1515.17	32.20	-0.1208
461.75	485.75	1531.75	56.60	0.7067	485.75	509.75	1514.82	52.00	0.5507
462.25	486.25	1531.40	69.50	1.1443	486.25	510.25	1514.46	43.40	0.2591

VC1 Proximal Site									
Sample Mid-depth (cm)	*Adjusted Mid-depth (cm)*	*Year AD*	*Magnetic Susceptibility*	*z-score*	*Sample Mid-depth (cm)*	*Adjusted Mid-depth (cm)*	*Year AD*	*Magnetic Susceptibility*	*z-score*
486.75	510.75	1514.11	124.50	3.0096	510.75	534.75	1497.18	33.00	-0.0937
487.25	511.25	1513.76	71.10	1.1985	511.25	535.25	1496.82	30.60	-0.1751
487.75	511.75	1513.41	51.90	0.5473	511.75	535.75	1496.47	24.00	-0.3989
488.25	512.25	1513.05	45.40	0.3269	512.25	536.25	1496.12	66.70	1.0493
488.75	512.75	1512.70	62.20	0.8967	512.75	536.75	1495.77	77.10	1.4020
489.25	513.25	1512.35	73.10	1.2664	513.25	537.25	1495.41	47.50	0.3981
489.75	513.75	1511.99	49.40	0.4626	513.75	537.75	1495.06	40.00	0.1437
490.25	514.25	1511.64	71.70	1.2189	514.25	538.25	1494.71	52.00	0.5507
490.75	514.75	1511.29	135.00	3.3657	514.75	538.75	1494.36	43.30	0.2557
491.25	515.25	1510.94	42.50	0.2285	515.25	539.25	1494.00	36.20	0.0149
491.75	515.75	1510.58	106.40	2.3957	515.75	539.75	1493.65	30.90	-0.1649
492.25	516.25	1510.23	47.10	0.3845	516.25	540.25	1493.30	39.50	0.1268
492.75	516.75	1509.88	128.50	3.1453	516.75	540.75	1492.94	25.50	-0.3480
493.25	517.25	1509.52	54.00	0.6186	517.25	541.25	1492.59	55.30	0.6627
493.75	517.75	1509.17	63.30	0.9340	517.75	541.75	1492.24	39.50	0.1268
494.25	518.25	1508.82	69.60	1.1477	518.25	542.25	1491.89	43.30	0.2557
494.75	518.75	1508.47	67.10	1.0629	518.75	542.75	1491.53	181.00	4.9259
495.25	519.25	1508.11	33.10	-0.0903	519.25	543.25	1491.18	113.00	2.6196
495.75	519.75	1507.76	24.40	-0.3853	519.75	543.75	1490.83	45.90	0.3438
496.25	520.25	1507.41	30.10	-0.1920	520.25	544.25	1490.47	53.00	0.5846
496.75	520.75	1507.06	53.90	0.6152	520.75	544.75	1490.12	37.00	0.0420
497.25	521.25	1506.70	30.10	-0.1920	521.25	545.25	1489.77	23.50	-0.4159
497.75	521.75	1506.35	30.50	-0.1785	521.75	545.75	1489.42	26.50	-0.3141
498.25	522.25	1506.00	70.60	1.1816	522.25	546.25	1489.06	26.00	-0.3311
498.75	522.75	1505.64	54.30	0.6287	522.75	546.75	1488.71	25.40	-0.3514
499.25	523.25	1505.29	74.00	1.2969	523.25	547.25	1488.36	25.90	-0.3345
499.75	523.75	1504.94	40.00	0.1437	523.75	547.75	1488.00	33.60	-0.0733
500.25	524.25	1504.59	32.10	-0.1242	524.25	548.25	1487.65	37.90	0.0725
500.75	524.75	1504.23	82.30	1.5784	524.75	548.75	1487.30	35.70	-0.0021
501.25	525.25	1503.88	58.50	0.7712	525.25	549.25	1486.95	32.20	-0.1208
501.75	525.75	1503.53	30.50	-0.1785	525.75	549.75	1486.59	42.50	0.2285
502.25	526.25	1503.17	52.30	0.5609	526.25	550.25	1486.24	37.30	0.0522
502.75	526.75	1502.82	56.50	0.7034	526.75	550.75	1485.89	29.50	-0.2124
503.25	527.25	1502.47	28.00	-0.2632	527.25	551.25	1485.54	30.00	-0.1954
503.75	527.75	1502.12	37.90	0.0725	527.75	551.75	1485.18	28.10	-0.2599
504.25	528.25	1501.76	69.00	1.1273	528.25	552.25	1484.83	26.20	-0.3243
504.75	528.75	1501.41	66.00	1.0256	528.75	552.75	1484.48	30.00	-0.1954
505.25	529.25	1501.06	38.50	0.0929	529.25	553.25	1484.12	30.80	-0.1683
505.75	529.75	1500.71	30.00	-0.1954	529.75	553.75	1483.77	37.20	0.0488
506.25	530.25	1500.35	43.50	0.2624	530.25	554.25	1483.42	32.00	-0.1276
506.75	530.75	1500.00	42.80	0.2387	530.75	554.75	1483.07	28.50	-0.2463
507.25	531.25	1499.65	48.50	0.4320	531.25	555.25	1482.71	23.50	-0.4159
507.75	531.75	1499.29	51.50	0.5338	531.75	555.75	1482.36	27.00	-0.2972
508.25	532.25	1498.94	58.60	0.7746	532.25	556.25	1482.01	30.00	-0.1954
508.75	532.75	1498.59	26.70	-0.3073	532.75	556.75	1481.65	37.00	0.0420
509.25	533.25	1498.24	51.40	0.5304	533.25	557.25	1481.30	30.00	-0.1954
509.75	533.75	1497.88	38.60	0.0963	533.75	557.75	1480.95	29.50	-0.2124
510.25	534.25	1497.53	58.60	0.7746	534.25	558.25	1480.60	31.60	-0.1411

VC1 Proximal Site									
Sample Mid-depth (cm)	*Adjusted Mid-depth (cm)*	*Year AD*	*Magnetic Susceptibility*	*z-score*	*Sample Mid-depth (cm)*	*Adjusted Mid-depth (cm)*	*Year AD*	*Magnetic Susceptibility*	*z-score*
534.75	558.75	1480.24	31.40	-0.1479	558.75	582.75	1463.31	28.40	-0.2497
535.25	559.25	1479.89	32.00	-0.1276	559.25	583.25	1462.96	28.00	-0.2632
535.75	559.75	1479.54	29.50	-0.2124	559.75	583.75	1462.60	35.90	0.0047
536.25	560.25	1479.19	33.50	-0.0767	560.25	584.25	1462.25	40.00	0.1437
536.75	560.75	1478.83	19.40	-0.5549	560.75	584.75	1461.90	33.90	-0.0631
537.25	561.25	1478.48	27.50	-0.2802	561.25	585.25	1461.55	28.00	-0.2632
537.75	561.75	1478.13	24.00	-0.3989	561.75	585.75	1461.19	29.50	-0.2124
538.25	562.25	1477.77	24.50	-0.3819	562.25	586.25	1460.84	36.90	0.0386
538.75	562.75	1477.42	45.50	0.3303	562.75	586.75	1460.49	33.00	-0.0937
539.25	563.25	1477.07	106.40	2.3957	563.25	587.25	1460.14	38.10	0.0793
539.75	563.75	1476.72	149.00	3.8406	563.75	587.75	1459.78	31.50	-0.1445
540.25	564.25	1476.36	41.50	0.1946	564.25	588.25	1459.43	105.10	2.3517
540.75	564.75	1476.01	34.10	-0.0564	564.75	588.75	1459.08	90.10	1.8429
541.25	565.25	1475.66	27.50	-0.2802	565.25	589.25	1458.72	37.30	0.0522
541.75	565.75	1475.30	21.00	-0.5007	565.75	589.75	1458.37	43.90	0.2760
542.25	566.25	1474.95	25.50	-0.3480	566.75	590.75	1458.02	17.00	-0.6363
542.75	566.75	1474.60	28.00	-0.2632	567.25	591.25	1457.67	337.30	10.2269
543.25	567.25	1474.25	22.50	-0.4498	567.75	591.75	1457.31	131.40	3.2436
543.75	567.75	1473.89	26.50	-0.3141	568.25	592.25	1456.96	83.00	1.6021
544.25	568.25	1473.54	30.20	-0.1886	568.75	592.75	1456.61	77.70	1.4224
544.75	568.75	1473.19	32.20	-0.1208	569.25	593.25	1456.25	78.00	1.4325
545.25	569.25	1472.84	41.50	0.1946	569.75	593.75	1455.90	89.00	1.8056
545.75	569.75	1472.48	37.50	0.0590	570.25	594.25	1455.55	104.50	2.3313
546.25	570.25	1472.13	42.00	0.2116	570.75	594.75	1455.20	69.30	1.1375
546.75	570.75	1471.78	62.50	0.9068	571.25	595.25	1454.84	56.00	0.6864
547.25	571.25	1471.42	86.60	1.7242	571.75	595.75	1454.49	39.50	0.1268
547.75	571.75	1471.07	41.60	0.1980	572.25	596.25	1454.14	46.60	0.3676
548.25	572.25	1470.72	41.00	0.1777	572.75	596.75	1453.78	30.90	-0.1649
548.75	572.75	1470.37	43.20	0.2523	573.25	597.25	1453.43	20.50	-0.5176
549.25	573.25	1470.01	40.00	0.1437	573.75	597.75	1453.08	22.10	-0.4633
549.75	573.75	1469.66	36.90	0.0386	574.25	598.25	1452.73	24.10	-0.3955
550.25	574.25	1469.31	32.50	-0.1106	574.75	598.75	1452.37	51.90	0.5473
550.75	574.75	1468.95	28.50	-0.2463	575.25	599.25	1452.02	45.30	0.3235
551.25	575.25	1468.60	32.30	-0.1174	575.75	599.75	1451.67	22.50	-0.4498
551.75	575.75	1468.25	29.40	-0.2158	576.25	600.25	1451.32	27.70	-0.2734
552.25	576.25	1467.90	24.40	-0.3853	576.75	600.75	1450.96	46.00	0.3472
552.75	576.75	1467.54	20.50	-0.5176	577.25	601.25	1450.61	73.00	1.2630
553.25	577.25	1467.19	24.40	-0.3853	577.75	601.75	1450.26	68.10	1.0968
553.75	577.75	1466.84	22.00	-0.4667	578.25	602.25	1449.90	37.50	0.0590
554.25	578.25	1466.49	22.00	-0.4667	578.75	602.75	1449.55	36.50	0.0250
554.75	578.75	1466.13	22.90	-0.4362	579.25	603.25	1449.20	34.60	-0.0394
555.25	579.25	1465.78	28.60	-0.2429	579.75	603.75	1448.85	34.40	-0.0462
555.75	579.75	1465.43	52.00	0.5507	580.25	604.25	1448.49	29.70	-0.2056
556.25	580.25	1465.07	47.80	0.4083	580.75	604.75	1448.14	47.40	0.3947
556.75	580.75	1464.72	43.00	0.2455	581.25	605.25	1447.79	44.40	0.2930
557.25	581.25	1464.37	34.50	-0.0428	581.75	605.75	1447.43	27.00	-0.2972
557.75	581.75	1464.02	33.50	-0.0767	582.25	606.25	1447.08	25.20	-0.3582
558.25	582.25	1463.66	32.80	-0.1004	582.75	606.75	1446.73	41.40	0.1912

VC1 Proximal Site									
Sample Mid-depth (cm)	*Adjusted Mid-depth (cm)*	*Year AD*	*Magnetic Susceptibility*	*z-score*	*Sample Mid-depth (cm)*	*Adjusted Mid-depth (cm)*	*Year AD*	*Magnetic Susceptibility*	*z-score*
583.25	607.25	1446.38	20.50	-0.5176	607.25	631.25	1429.44	wood	wood
583.75	607.75	1446.02	25.10	-0.3616	607.75	631.75	1429.09	wood	wood
584.25	608.25	1445.67	33.10	-0.0903	608.25	632.25	1428.74	wood	wood
584.75	608.75	1445.32	32.10	-0.1242	608.75	632.75	1428.38	wood	wood
585.25	609.25	1444.97	38.20	0.0827	609.25	633.25	1428.03	wood	wood
585.75	609.75	1444.61	34.00	-0.0597	609.75	633.75	1427.68	wood	wood
586.25	610.25	1444.26	50.60	0.5033	610.25	634.25	1427.33	17.00	-0.6363
586.75	610.75	1443.91	28.50	-0.2463	610.75	634.75	1426.97	19.00	-0.5685
587.25	611.25	1443.55	32.90	-0.0971	611.25	635.25	1426.62	15.00	-0.7041
587.75	611.75	1443.20	30.70	-0.1717	611.75	635.75	1426.27	16.10	-0.6668
588.25	612.25	1442.85	44.20	0.2862	612.25	636.25	1425.92	25.50	-0.3480
588.75	612.75	1442.50	35.80	0.0013	612.75	636.75	1425.56	35.60	-0.0055
589.25	613.25	1442.14	29.50	-0.2124	613.25	637.25	1425.21	42.60	0.2319
589.75	613.75	1441.79	26.70	-0.3073	613.75	637.75	1424.86	63.40	0.9374
590.25	614.25	1441.44	24.20	-0.3921	614.25	638.25	1424.50	43.30	0.2557
590.75	614.75	1441.08	13.00	-0.7720	614.75	638.75	1424.15	45.10	0.3167
591.25	615.25	1440.73	27.60	-0.2768	615.25	639.25	1423.80	32.50	-0.1106
591.75	615.75	1440.38	24.60	-0.3786	615.75	639.75	1423.45	23.00	-0.4328
592.25	616.25	1440.03	21.10	-0.4973	616.25	640.25	1423.09	21.80	-0.4735
592.75	616.75	1439.67	49.30	0.4592	616.75	640.75	1422.74	18.80	-0.5753
593.25	617.25	1439.32	37.90	0.0725	617.25	641.25	1422.39	19.70	-0.5447
593.75	617.75	1438.97	31.60	-0.1411	617.75	641.75	1422.03	29.50	-0.2124
594.25	618.25	1438.62	37.50	0.0590	618.25	642.25	1421.68	38.00	0.0759
594.75	618.75	1438.26	32.60	-0.1072	618.75	642.75	1421.33	99.60	2.1651
595.25	619.25	1437.91	42.50	0.2285	619.25	643.25	1420.98	108.40	2.4636
595.75	619.75	1437.56	51.00	0.5168	619.75	643.75	1420.62	86.00	1.7039
596.25	620.25	1437.20	39.00	0.1098	620.25	644.25	1420.27	31.00	-0.1615
596.75	620.75	1436.85	41.90	0.2082	620.75	644.75	1419.92	58.50	0.7712
597.25	621.25	1436.50	52.00	0.5507	621.25	645.25	1419.56	63.50	0.9408
597.75	621.75	1436.15	45.10	0.3167	621.75	645.75	1419.21	35.50	-0.0089
598.25	622.25	1435.79	43.00	0.2455	622.25	646.25	1418.86	38.50	0.0929
598.75	622.75	1435.44	50.60	0.5033	622.75	646.75	1418.51	60.20	0.8288
599.25	623.25	1435.09	43.20	0.2523	623.25	647.25	1418.15	38.90	0.1064
599.75	623.75	1434.73	55.00	0.6525	623.75	647.75	1417.80	58.60	0.7746
600.25	624.25	1434.38	42.50	0.2285	624.25	648.25	1417.45	52.50	0.5677
600.75	624.75	1434.03	43.40	0.2591	624.75	648.75	1417.10	49.80	0.4761
601.25	625.25	1433.68	56.00	0.6864	625.25	649.25	1416.74	357.50	10.9120
601.75	625.75	1433.32	48.40	0.4286	625.75	649.75	1416.39	103.00	2.2804
602.25	626.25	1432.97	42.00	0.2116	626.25	650.25	1416.04	33.00	-0.0937
602.75	626.75	1432.62	59.00	0.7881	626.75	650.75	1415.68	28.00	-0.2632
603.25	627.25	1432.27	47.60	0.4015	627.25	651.25	1415.33	27.00	-0.2972
603.75	627.75	1431.91	45.10	0.3167	627.75	651.75	1414.98	28.50	-0.2463
604.25	628.25	1431.56	54.50	0.6355	628.25	652.25	1414.63	31.50	-0.1445
604.75	628.75	1431.21	wood	wood	628.75	652.75	1414.27	27.00	-0.2972
605.25	629.25	1430.85	wood	wood	629.25	653.25	1413.92	27.00	-0.2972
605.75	629.75	1430.50	wood	wood	629.75	653.75	1413.57	25.00	-0.3650
606.25	630.25	1430.15	wood	wood	630.25	654.25	1413.21	28.50	-0.2463
606.75	630.75	1429.80	wood	wood	630.75	654.75	1412.86	31.00	-0.1615

VC1 Proximal Site									
Sample Mid-depth (cm)	*Adjusted Mid-depth (cm)*	*Year AD*	*Magnetic Susceptibility*	*z-score*	*Sample Mid-depth (cm)*	*Adjusted Mid-depth (cm)*	*Year AD*	*Magnetic Susceptibility*	*z-score*
631.25	655.25	1412.51	32.00	-0.1276	657.75	681.75	1395.58	86.50	1.7208
631.75	655.75	1412.16	30.50	-0.1785	658.25	682.25	1395.22	130.40	3.2097
632.25	656.25	1411.80	36.50	0.0250	658.75	682.75	1394.87	154.00	4.0101
632.75	656.75	1411.45	18.50	-0.5854	659.25	683.25	1394.52	49.50	0.4659
633.25	657.25	1411.10	20.50	-0.5176	659.75	683.75	1394.16	31.40	-0.1479
633.75	657.75	1410.75	13.10	-0.7686	660.25	684.25	1393.81	42.50	0.2285
635.25	659.25	1410.39	231.50	6.6386	660.75	684.75	1393.46	27.30	-0.2870
636.25	660.25	1410.04	120.30	2.8672	661.25	685.25	1393.11	50.50	0.4999
636.75	660.75	1409.69	93.60	1.9616	661.75	685.75	1392.75	33.00	-0.0937
637.25	661.25	1409.33	68.10	1.0968	662.25	686.25	1392.40	40.10	0.1471
637.75	661.75	1408.98	41.30	0.1878	662.75	686.75	1392.05	41.50	0.1946
638.25	662.25	1408.63	29.00	-0.2293	663.25	687.25	1391.70	67.50	1.0764
638.75	662.75	1408.28	25.50	-0.3480	663.75	687.75	1391.34	118.60	2.8095
639.25	663.25	1407.92	31.90	-0.1310	664.25	688.25	1390.99	258.00	7.5374
639.75	663.75	1407.57	39.20	0.1166	664.75	688.75	1390.64	207.50	5.8246
640.25	664.25	1407.22	30.00	-0.1954	665.25	689.25	1390.28	22.50	-0.4498
640.75	664.75	1406.86	31.00	-0.1615	665.75	689.75	1389.93	15.00	-0.7041
641.25	665.25	1406.51	52.60	0.5711	666.25	690.25	1389.58	17.40	-0.6228
641.75	665.75	1406.16	43.60	0.2658	666.75	690.75	1389.23	15.00	-0.7041
642.25	666.25	1405.81	28.50	-0.2463	667.25	691.25	1388.87	14.00	-0.7381
642.75	666.75	1405.45	43.50	0.2624	667.75	691.75	1388.52	18.30	-0.5922
643.25	667.25	1405.10	78.90	1.4631	668.25	692.25	1388.17	22.50	-0.4498
643.75	667.75	1404.75	23.50	-0.4159	668.75	692.75	1387.81	36.10	0.0115
644.25	668.25	1404.40	17.40	-0.6228	669.25	693.25	1387.46	27.50	-0.2802
644.75	668.75	1404.04	23.00	-0.4328	669.75	693.75	1387.11	20.50	-0.5176
645.25	669.25	1403.69	27.00	-0.2972	670.25	694.25	1386.76	15.10	-0.7008
645.75	669.75	1403.34	30.00	-0.1954	670.75	694.75	1386.40	18.00	-0.6024
646.25	670.25	1402.98	31.40	-0.1479	671.25	695.25	1386.05	22.50	-0.4498
646.75	670.75	1402.63	50.30	0.4931	671.75	695.75	1385.70	19.10	-0.5651
647.25	671.25	1402.28	63.80	0.9509	672.25	696.25	1385.34	32.00	-0.1276
647.75	671.75	1401.93	52.50	0.5677	672.75	696.75	1384.99	16.00	-0.6702
648.25	672.25	1401.57	68.60	1.1137	673.25	697.25	1384.64	18.30	-0.5922
648.75	672.75	1401.22	43.00	0.2455	673.75	697.75	1384.29	23.90	-0.4023
649.25	673.25	1400.87	54.20	0.6253	674.25	698.25	1383.93	22.70	-0.4430
649.75	673.75	1400.51	55.50	0.6694	674.75	698.75	1383.58	32.40	-0.1140
650.25	674.25	1400.16	42.00	0.2116	675.25	699.25	1383.23	26.10	-0.3277
650.75	674.75	1399.81	62.40	0.9035	675.75	699.75	1382.88	30.10	-0.1920
651.25	675.25	1399.46	29.60	-0.2090	676.25	700.25	1382.52	33.00	-0.0937
651.75	675.75	1399.10	49.30	0.4592	676.75	700.75	1382.17	47.50	0.3981
652.25	676.25	1398.75	72.50	1.2460	677.25	701.25	1381.82	27.50	-0.2802
652.75	676.75	1398.40	83.30	1.6123	677.75	701.75	1381.46	27.60	-0.2768
653.25	677.25	1398.05	98.10	2.1142	678.25	702.25	1381.11	29.40	-0.2158
653.75	677.75	1397.69	85.60	1.6903	678.75	702.75	1380.76	28.60	-0.2429
654.25	678.25	1397.34	152.00	3.9423	679.25	703.25	1380.41	28.00	-0.2632
655.75	679.75	1396.99	31.00	-0.1615	679.75	703.75	1380.05	32.00	-0.1276
656.25	680.25	1396.63	42.10	0.2150	680.25	704.25	1379.70	43.50	0.2624
656.75	680.75	1396.28	73.50	1.2799	680.75	704.75	1379.35	33.50	-0.0767
657.25	681.25	1395.93	82.40	1.5818	681.25	705.25	1378.99	38.00	0.0759

VC1 Proximal Site									
Sample Mid-depth (cm)	*Adjusted Mid-depth (cm)*	*Year AD*	*Magnetic Susceptibility*	*z-score*	*Sample Mid-depth (cm)*	*Adjusted Mid-depth (cm)*	*Year AD*	*Magnetic Susceptibility*	*z-score*
681.75	705.75	1378.64	37.00	0.0420	706.25	730.25	1361.71	65.50	1.0086
682.25	706.25	1378.29	25.00	-0.3650	706.75	730.75	1361.36	57.50	0.7373
682.75	706.75	1377.94	35.40	-0.0123	707.25	731.25	1361.00	53.90	0.6152
683.25	707.25	1377.58	22.50	-0.4498	707.75	731.75	1360.65	44.80	0.3065
683.75	707.75	1377.23	24.00	-0.3989	708.25	732.25	1360.30	44.50	0.2964
684.25	708.25	1376.88	20.00	-0.5346	708.75	732.75	1359.94	46.70	0.3710
684.75	708.75	1376.53	18.50	-0.5854	709.25	733.25	1359.59	46.00	0.3472
685.25	709.25	1376.17	18.00	-0.6024	709.75	733.75	1359.24	37.70	0.0657
685.75	709.75	1375.82	20.50	-0.5176	710.25	734.25	1358.89	31.80	-0.1344
686.25	710.25	1375.47	21.00	-0.5007	710.75	734.75	1358.53	26.60	-0.3107
686.75	710.75	1375.11	19.50	-0.5515	711.25	735.25	1358.18	26.20	-0.3243
687.25	711.25	1374.76	15.00	-0.7041	711.75	735.75	1357.83	18.20	-0.5956
687.75	711.75	1374.41	19.60	-0.5481	712.25	736.25	1357.48	20.10	-0.5312
688.25	712.25	1374.06	19.00	-0.5685	712.75	736.75	1357.12	20.40	-0.5210
688.75	712.75	1373.70	25.50	-0.3480	713.25	737.25	1356.77	28.80	-0.2361
689.25	713.25	1373.35	31.60	-0.1411	713.75	737.75	1356.42	24.10	-0.3955
689.75	713.75	1373.00	16.50	-0.6533	714.25	738.25	1356.06	24.90	-0.3684
690.25	714.25	1372.64	23.00	-0.4328	714.75	738.75	1355.71	30.00	-0.1954
690.75	714.75	1372.29	23.50	-0.4159	715.25	739.25	1355.36	38.00	0.0759
691.25	715.25	1371.94	27.00	-0.2972	715.75	739.75	1355.01	53.40	0.5982
691.75	715.75	1371.59	28.00	-0.2632	716.25	740.25	1354.65	40.00	0.1437
692.25	716.25	1371.23	53.00	0.5846	716.75	740.75	1354.30	33.10	-0.0903
692.75	716.75	1370.88	39.40	0.1234	717.25	741.25	1353.95	21.90	-0.4701
693.25	717.25	1370.53	39.20	0.1166	717.75	741.75	1353.59	27.50	-0.2802
693.75	717.75	1370.18	39.40	0.1234	718.25	742.25	1353.24	43.40	0.2591
694.25	718.25	1369.82	36.00	0.0081	718.75	742.75	1352.89	24.90	-0.3684
694.75	718.75	1369.47	48.00	0.4151	719.25	743.25	1352.54	26.60	-0.3107
695.25	719.25	1369.12	53.60	0.6050	719.75	743.75	1352.18	36.50	0.0250
695.75	719.75	1368.76	50.60	0.5033	720.25	744.25	1351.83	19.40	-0.5549
696.25	720.25	1368.41	52.00	0.5507	720.75	744.75	1351.48	25.50	-0.3480
696.75	720.75	1368.06	64.60	0.9781	721.25	745.25	1351.12	20.00	-0.5346
697.25	721.25	1367.71	53.20	0.5914	721.75	745.75	1350.77	33.50	-0.0767
697.75	721.75	1367.35	55.40	0.6660	722.25	746.25	1350.42	35.40	-0.0123
698.75	722.75	1367.00	73.90	1.2935	722.75	746.75	1350.07	25.90	-0.3345
699.25	723.25	1366.65	45.40	0.3269	723.25	747.25	1349.71	26.70	-0.3073
699.75	723.75	1366.29	62.00	0.8899	723.75	747.75	1349.36	24.90	-0.3684
700.25	724.25	1365.94	93.40	1.9548	724.25	748.25	1349.01	22.10	-0.4633
700.75	724.75	1365.59	194.00	5.3668	724.75	748.75	1348.66	24.50	-0.3819
701.25	725.25	1365.24	167.40	4.4646	725.25	749.25	1348.30	23.50	-0.4159
701.75	725.75	1364.88	100.00	2.1787	725.75	749.75	1347.95	24.90	-0.3684
702.25	726.25	1364.53	237.50	6.8421	726.25	750.25	1347.60	21.50	-0.4837
702.75	726.75	1364.18	347.00	10.5559	726.75	750.75	1347.24	17.00	-0.6363
703.25	727.25	1363.83	269.00	7.9104	727.25	751.25	1346.89	20.00	-0.5346
703.75	727.75	1363.47	87.00	1.7378	727.75	751.75	1346.54	19.50	-0.5515
704.25	728.25	1363.12	74.30	1.3071	728.25	752.25	1346.19	20.50	-0.5176
704.75	728.75	1362.77	96.50	2.0600	728.75	752.75	1345.83	22.90	-0.4362
705.25	729.25	1362.41	85.50	1.6869	729.25	753.25	1345.48	23.50	-0.4159
705.75	729.75	1362.06	58.50	0.7712	729.75	753.75	1345.13	28.50	-0.2463

VC1 Proximal Site				
Sample Mid-depth (cm)	*Adjusted Mid-depth (cm)*	*Year AD*	*Magnetic Susceptibility*	*z-score*
730.25	754.25	1344.77	19.20	-0.5617
730.75	754.75	1344.42	13.90	-0.7415
731.25	755.25	1344.07	15.00	-0.7041
731.75	755.75	1343.72	22.40	-0.4532
732.25	756.25	1343.36	21.50	-0.4837
732.75	756.75	1343.01	22.50	-0.4498

KB-05-03 Distal site							
Sample Mid-Depth (cm)	*Year AD*	*Magnetic Susceptibility*	*z-score*	*Sample Mid-Depth (cm)*	*Year AD*	*Magnetic Susceptibility*	*z-score*
0.25	2004.73	3.5	-1.4518	26.25	1976.49	17.5	-0.2699
0.75	2004.19	3.5	-1.4518	26.75	1975.95	12.5	-0.6920
1.25	2003.64	3	-1.4940	27.25	1975.40	12.5	-0.6920
1.75	2003.10	5.5	-1.2829	27.75	1974.86	8.5	-1.0297
2.25	2002.56	5.3	-1.2998	28.25	1974.32	11	-0.8186
2.75	2002.01	7	-1.1563	28.75	1973.77	12	-0.7342
3.25	2001.47	9.9	-0.9115	29.25	1973.23	7	-1.1563
3.75	2000.93	8.5	-1.0297	29.75	1972.69	13.5	-0.6076
4.5	2000.11	8.5	-1.0297	30.25	1972.14	14	-0.5654
5.25	1999.30	12.5	-0.6920	30.75	1971.60	14	-0.5654
5.75	1998.75	14.5	-0.5232	31.25	1971.06	13.1	-0.6414
6.25	1998.21	13	-0.6498	31.75	1970.52	8.5	-1.0297
6.75	1997.67	12	-0.7342	32.25	1969.97	9.5	-0.9453
7.25	1997.13	11.5	-0.7764	32.75	1969.43	10.5	-0.8609
7.75	1996.58	7.5	-1.1141	33.25	1968.89	12	-0.7342
8.25	1996.04	7.4	-1.1226	33.75	1968.34	11.6	-0.7680
8.75	1995.50	12	-0.7342	34.25	1967.80	11	-0.8186
9.25	1994.95	13.5	-0.6076	34.75	1967.26	11	-0.8186
9.75	1994.41	13.5	-0.6076	35.25	1966.71	9	-0.9875
10.25	1993.87	11.6	-0.7680	35.75	1966.17	10.5	-0.8609
10.75	1993.32	11.5	-0.7764	36.25	1965.63	14	-0.5654
11.25	1992.78	15.6	-0.4303	36.75	1965.08	14	-0.5654
11.75	1992.24	7.5	-1.1141	37.25	1964.54	11.5	-0.7764
12.25	1991.69	9.4	-0.9537	37.75	1964.00	8	-1.0719
12.75	1991.15	11	-0.8186	38.25	1963.46	10.5	-0.8609
13.25	1990.61	11.5	-0.7764	38.75	1962.91	15	-0.4810
13.75	1990.07	12	-0.7342	39.25	1962.37	12	-0.7342
14.25	1989.52	8	-1.0719	39.75	1961.83	13.5	-0.6076
14.75	1988.98	8	-1.0719	40.25	1961.28	15	-0.4810
15.25	1988.44	8.5	-1.0297	40.75	1960.74	12.5	-0.6920
15.75	1987.89	8	-1.0719				
16.25	1987.35	10	-0.9031				
16.75	1986.81	10	-0.9031				
17.25	1986.26	8.5	-1.0297				
17.75	1985.72	8	-1.0719				
18.25	1985.18	10	-0.9031				
18.75	1984.64	8	-1.0719				
19.25	1984.09	5.9	-1.2492				
19.75	1983.55	8	-1.0719				
20.25	1983.01	10	-0.9031				
20.75	1982.46	6.5	-1.1985				
21.25	1981.92	7.4	-1.1226				
21.75	1981.38	10	-0.9031				
22.25	1980.83	12	-0.7342				
22.75	1980.29	7.9	-1.0803				
23.25	1979.75	8	-1.0719				
23.75	1979.20	8	-1.0719				
24.25	1978.66	6.5	-1.1985				
24.75	1978.12	6	-1.2407				
25.25	1977.58	7.5	-1.1141				
25.75	1977.03	14	-0.5654				

VC3 Distal Site									
Sample mid-depth	*Adjusted mid-depth*	*Year AD*	*Mag. Sus*	*z-scores*	*Sample mid-depth*	*Adjusted mid-depth*	*Year AD*	*Mag. Sus.*	*z-scores*
0.25	24.25	1978.66	21.6	-0.3932	26.25	50.25	1950.42	10.0	-1.0385
0.75	24.75	1978.12	12.0	-0.9272	26.75	50.75	1949.88	13.2	-0.8605
1.25	25.25	1977.58	14.4	-0.7937	27.25	51.25	1949.34	12.4	-0.9050
1.75	25.75	1977.03	14.6	-0.7826	27.75	51.75	1948.79	12.4	-0.9050
2.25	26.25	1976.49	12.6	-0.8939	28.25	52.25	1948.25	11.4	-0.9606
2.75	26.75	1975.95	12.5	-0.8994	28.75	52.75	1947.71	12.0	-0.9272
3.25	27.25	1975.40	17.5	-0.6213	29.25	53.25	1947.16	13.5	-0.8438
3.75	27.75	1974.86	17.3	-0.6324	29.75	53.75	1946.62	14.5	-0.7882
4.25	28.25	1974.32	16.0	-0.7047	30.25	54.25	1946.08	13.0	-0.8716
4.75	28.75	1973.77	14.5	-0.7882	30.75	54.75	1945.53	13.5	-0.8438
5.25	29.25	1973.23	12.4	-0.9050	31.25	55.25	1944.99	12.0	-0.9272
5.75	29.75	1972.69	16.0	-0.7047	31.75	55.75	1944.45	7.5	-1.1775
6.25	30.25	1972.14	14.5	-0.7882	32.25	56.25	1943.91	12.7	-0.8883
6.75	30.75	1971.60	13.5	-0.8438	32.75	56.75	1943.36	10.8	-0.9940
7.25	31.25	1971.06	19.5	-0.5100	33.25	57.25	1942.82	13.5	-0.8438
8.00	32.00	1970.24	13.6	-0.8382	33.75	57.75	1942.28	20.1	-0.4767
8.75	32.75	1969.43	15.5	-0.7325	34.25	58.25	1941.73	14.9	-0.7659
9.25	33.25	1968.89	16.7	-0.6658	34.75	58.75	1941.19	15.1	-0.7548
9.75	33.75	1968.34	13.5	-0.8438	35.25	59.25	1940.65	14.9	-0.7659
10.25	34.25	1967.80	11.9	-0.9328	35.75	59.75	1940.10	9.8	-1.0496
10.75	34.75	1967.26	14.5	-0.7882	36.25	60.25	1939.56	19.0	-0.5379
11.25	35.25	1966.71	13.1	-0.8660	36.75	60.75	1939.02	15.5	-0.7325
11.75	35.75	1966.17	16.5	-0.6769	37.25	61.25	1938.47	12.1	-0.9217
12.25	36.25	1965.63	17.0	-0.6491	37.75	61.75	1937.93	11.4	-0.9606
12.75	36.75	1965.08	14.0	-0.8160	38.25	62.25	1937.39	14.6	-0.7826
13.25	37.25	1964.54	13.4	-0.8494	38.75	62.75	1936.85	10.5	-1.0107
13.75	37.75	1964.00	14.0	-0.8160	39.25	63.25	1936.30	x	x
14.25	38.25	1963.46	15.0	-0.7604	39.75	63.75	1935.76	13.4	-0.8494
14.75	38.75	1962.91	16.6	-0.6714	40.25	64.25	1935.22	11.0	-0.9829
15.25	39.25	1962.37	15.0	-0.7604	40.75	64.75	1934.67	11.5	-0.9550
15.75	39.75	1961.83	14.0	-0.8160	41.25	65.25	1934.13	11.0	-0.9829
16.25	40.25	1961.28	12.9	-0.8772	41.75	65.75	1933.59	10.9	-0.9884
16.75	40.75	1960.74	10.5	-1.0107	42.25	66.25	1933.04	10.5	-1.0107
17.25	41.25	1960.20	11.6	-0.9495	42.75	66.75	1932.50	10.8	-0.9940
17.75	41.75	1959.65	12.4	-0.9050	43.25	67.25	1931.96	11.1	-0.9773
18.25	42.25	1959.11	12.0	-0.9272	43.75	67.75	1931.41	9.0	-1.0941
18.75	42.75	1958.57	16.5	-0.6769	44.25	68.25	1930.87	12.4	-0.9050
19.25	43.25	1958.02	11.6	-0.9495	44.75	68.75	1930.33	13.6	-0.8382
19.75	43.75	1957.48	11.0	-0.9829	45.25	69.25	1929.79	15.5	-0.7325
20.25	44.25	1956.94	12.0	-0.9272	45.75	69.75	1929.24	16.7	-0.6658
20.75	44.75	1956.40	12.6	-0.8939	46.25	70.25	1928.70	16.0	-0.7047
21.25	45.25	1955.85	11.0	-0.9829	46.75	70.75	1928.16	14.0	-0.8160
21.75	45.75	1955.31	6.5	-1.2332	47.25	71.25	1927.61	13.0	-0.8716
22.25	46.25	1954.77	11.0	-0.9829	47.75	71.75	1927.07	12.8	-0.8827
22.75	46.75	1954.22	12.0	-0.9272	48.25	72.25	1926.53	12.0	-0.9272
23.25	47.25	1953.68	8.4	-1.1275	48.75	72.75	1925.98	10.2	-1.0274
23.75	47.75	1953.14	10.0	-1.0385	49.25	73.25	1925.44	15.3	-0.7437
24.25	48.25	1952.59	15.6	-0.7270	49.75	73.75	1924.90	8.3	-1.1330
24.75	48.75	1952.05	17.6	-0.6157	50.25	74.25	1924.35	14.0	-0.8160
25.25	49.25	1951.51	12.6	-0.8939	50.75	74.75	1923.81	10.4	-1.0162
25.75	49.75	1950.97	11.9	-0.9328	51.25	75.25	1923.27	17.0	-0.6491

VC3 Distal Site									
Sample mid-depth	*Adjusted mid-depth*	*Year AD*	*Mag. Sus.*	*z-scores*	*Sample mid-depth*	*Adjusted mid-depth*	*Year AD*	*Mag. Sus.*	*z-scores*
51.75	75.75	1922.73	10.4	-1.0162	77.25	101.25	1895.03	11.7	-0.9439
52.25	76.25	1922.18	11.0	-0.9829	77.75	101.75	1894.49	14.3	-0.7993
52.75	76.75	1921.64	13.0	-0.8716	78.25	102.25	1893.94	16.5	-0.6769
53.25	77.25	1921.10	15.5	-0.7325	78.75	102.75	1893.40	18.5	-0.5657
53.75	77.75	1920.55	17.0	-0.6491	79.25	103.25	1892.86	11.9	-0.9328
54.25	78.25	1920.01	9.2	-1.0830	79.75	103.75	1892.31	14.5	-0.7882
54.75	78.75	1919.47	13.9	-0.8215	80.25	104.25	1891.77	13.7	-0.8327
55.25	79.25	1918.92	18.8	-0.5490	80.75	104.75	1891.23	11.8	-0.9384
55.75	79.75	1918.38	12.5	-0.8994	81.25	105.25	1890.68	10.5	-1.0107
56.25	80.25	1917.84	16.6	-0.6714	81.75	105.75	1890.14	8.6	-1.1164
56.75	80.75	1917.29	15.4	-0.7381	82.25	106.25	1889.60	8.0	-1.1497
57.25	81.25	1916.75	12.0	-0.9272	82.75	106.75	1889.06	14.0	-0.8160
57.75	81.75	1916.21	15.2	-0.7492	83.25	107.25	1888.51	17.0	-0.6491
58.25	82.25	1915.67	13.5	-0.8438	83.75	107.75	1887.97	16.1	-0.6992
58.75	82.75	1915.12	16.4	-0.6825	84.25	108.25	1887.43	12.3	-0.9105
59.25	83.25	1914.58	21.9	-0.3766	84.75	108.75	1886.88	13.0	-0.8716
59.75	83.75	1914.04	15.3	-0.7437	85.25	109.25	1886.34	7.6	-1.1720
60.25	84.25	1913.49	14.7	-0.7770	85.75	109.75	1885.80	12.5	-0.8994
60.75	84.75	1912.95	12.7	-0.8883	86.25	110.25	1885.25	19.1	-0.5323
61.25	85.25	1912.41	21.6	-0.3932	86.75	110.75	1884.71	18.4	-0.5712
61.75	85.75	1911.86	16.3	-0.6880	87.25	111.25	1884.17	19.0	-0.5379
62.25	86.25	1911.32	16.0	-0.7047	87.75	111.75	1883.62	16.1	-0.6992
62.75	86.75	1910.78	17.2	-0.6380	88.25	112.25	1883.08	12.0	-0.9272
63.25	87.25	1910.24	15.5	-0.7325	88.75	112.75	1882.54	14.0	-0.8160
63.75	87.75	1909.69	16.6	-0.6714	89.25	113.25	1882.00	15.6	-0.7270
64.25	88.25	1909.15	16.0	-0.7047	89.75	113.75	1881.45	8.5	-1.1219
64.75	88.75	1908.61	17.0	-0.6491	90.25	114.25	1880.91	15.5	-0.7325
65.25	89.25	1908.06	17.5	-0.6213	90.75	114.75	1880.37	16.0	-0.7047
65.75	89.75	1907.52	17.9	-0.5990	91.25	115.25	1879.82	17.2	-0.6380
66.25	90.25	1906.98	14.7	-0.7770	91.75	115.75	1879.28	14.5	-0.7882
66.75	90.75	1906.43	18.0	-0.5935	92.25	116.25	1878.74	14.8	-0.7715
67.25	91.25	1905.89	22.0	-0.3710	92.75	116.75	1878.19	16.9	-0.6547
67.75	91.75	1905.35	17.6	-0.6157	93.25	117.25	1877.65	16.0	-0.7047
68.25	92.25	1904.80	13.1	-0.8660	93.75	117.75	1877.11	13.4	-0.8494
68.75	92.75	1904.26	15.7	-0.7214	94.25	118.25	1876.57	12.4	-0.9050
69.25	93.25	1903.72	17.1	-0.6435	94.75	118.75	1876.02	18.2	-0.5824
69.75	93.75	1903.18	19.6	-0.5045	95.25	119.25	1875.48	15.0	-0.7604
70.25	94.25	1902.63	23.5	-0.2876	95.75	119.75	1874.94	15.1	-0.7548
70.75	94.75	1902.09	15.4	-0.7381	96.25	120.25	1874.39	13.5	-0.8438
71.25	95.25	1901.55	12.1	-0.9217	96.75	120.75	1873.85	12.5	-0.8994
71.75	95.75	1901.00	17.3	-0.6324	97.25	121.25	1873.31	15.5	-0.7325
72.25	96.25	1900.46	18.6	-0.5601	97.75	121.75	1872.76	10.6	-1.0051
72.75	96.75	1899.92	19.3	-0.5212	98.25	122.25	1872.22	16.5	-0.6769
73.25	97.25	1899.37	17.6	-0.6157	98.75	122.75	1871.68	13.5	-0.8438
73.75	97.75	1898.83	15.0	-0.7604	99.25	123.25	1871.13	12.9	-0.8772
74.25	98.25	1898.29	17.0	-0.6491	99.75	123.75	1870.59	12.0	-0.9272
74.75	98.75	1897.74	14.1	-0.8104	100.25	124.25	1870.05	13.0	-0.8716
75.25	99.25	1897.20	18.1	-0.5879	100.75	124.75	1869.51	11.4	-0.9606
75.75	99.75	1896.66	17.0	-0.6491	101.25	125.25	1868.96	8.6	-1.1164
76.25	100.25	1896.12	15.6	-0.7270	101.75	125.75	1868.42	13.0	-0.8716
76.75	100.75	1895.57	15.0	-0.7604	102.25	126.25	1867.88	13.6	-0.8382

VC3 Distal Site									
Sample mid-depth	*Adjusted mid-depth*	*Year AD*	*Mag. Sus.*	*z-scores*	*Sample mid-depth*	*Adjusted mid-depth*	*Year AD*	*Mag. Sus.*	*z-scores*
102.75	126.75	1867.33	15.0	-0.7604	128.25	152.25	1839.64	14.5	-0.7882
103.25	127.25	1866.79	13.5	-0.8438	128.75	152.75	1839.09	12.0	-0.9272
103.75	127.75	1866.25	13.0	-0.8716	129.25	153.25	1838.55	13.0	-0.8716
104.25	128.25	1865.70	11.5	-0.9550	129.75	153.75	1838.01	14.5	-0.7882
104.75	128.75	1865.16	14.0	-0.8160	130.25	154.25	1837.46	13.4	-0.8494
105.25	129.25	1864.62	24.0	-0.2597	130.75	154.75	1836.92	14.0	-0.8160
105.75	129.75	1864.07	21.0	-0.4266	131.25	155.25	1836.38	14.2	-0.8049
106.25	130.25	1863.53	28.0	-0.0372	131.75	155.75	1835.84	15.0	-0.7604
106.75	130.75	1862.99	30.0	0.0740	132.25	156.25	1835.29	17.0	-0.6491
107.25	131.25	1862.45	13.1	-0.8660	132.75	156.75	1834.75	21.0	-0.4266
107.75	131.75	1861.90	14.0	-0.8160	133.25	157.25	1834.21	16.5	-0.6769
108.25	132.25	1861.36	11.5	-0.9550	133.75	157.75	1833.66	19.6	-0.5045
108.75	132.75	1860.82	15.0	-0.7604	134.25	158.25	1833.12	15.6	-0.7270
109.25	133.25	1860.27	19.5	-0.5100	134.75	158.75	1832.58	13.9	-0.8215
109.75	133.75	1859.73	16.0	-0.7047	135.25	159.25	1832.03	11.5	-0.9550
110.25	134.25	1859.19	12.5	-0.8994	135.75	159.75	1831.49	16.0	-0.7047
110.75	134.75	1858.64	11.0	-0.9829	136.25	160.25	1830.95	19.0	-0.5379
111.25	135.25	1858.10	14.0	-0.8160	136.75	160.75	1830.40	32.5	0.2131
111.75	135.75	1857.56	14.0	-0.8160	137.25	161.25	1829.86	33.0	0.2409
112.25	136.25	1857.01	14.0	-0.8160	137.75	161.75	1829.32	39.2	0.5858
112.75	136.75	1856.47	11.0	-0.9829	138.25	162.25	1828.78	36.5	0.4356
113.25	137.25	1855.93	16.0	-0.7047	138.75	162.75	1828.23	28.0	-0.0372
113.75	137.75	1855.39	12.0	-0.9272	139.25	163.25	1827.69	20.5	-0.4544
114.25	138.25	1854.84	14.5	-0.7882	139.75	163.75	1827.15	18.9	-0.5434
114.75	138.75	1854.30	14.5	-0.7882	140.25	164.25	1826.60	20.5	-0.4544
115.25	139.25	1853.76	14.5	-0.7882	140.75	164.75	1826.06	14.0	-0.8160
115.75	139.75	1853.21	12.4	-0.9050	141.25	165.25	1825.52	16.0	-0.7047
116.25	140.25	1852.67	12.0	-0.9272	141.75	165.75	1824.97	16.0	-0.7047
116.75	140.75	1852.13	15.0	-0.7604	142.25	166.25	1824.43	18.5	-0.5657
117.25	141.25	1851.58	12.5	-0.8994	142.75	166.75	1823.89	18.6	-0.5601
117.75	141.75	1851.04	12.5	-0.8994	143.25	167.25	1823.34	18.8	-0.5490
118.25	142.25	1850.50	13.5	-0.8438	143.75	167.75	1822.80	22.5	-0.3432
118.75	142.75	1849.95	24.2	-0.2486	144.25	168.25	1822.26	23.0	-0.3154
119.25	143.25	1849.41	13.0	-0.8716	144.75	168.75	1821.72	24.0	-0.2597
119.75	143.75	1848.87	12.5	-0.8994	145.25	169.25	1821.17	20.5	-0.4544
120.25	144.25	1848.33	15.5	-0.7325	145.75	169.75	1820.63	16.0	-0.7047
120.75	144.75	1847.78	15.5	-0.7325	146.25	170.25	1820.09	27.5	-0.0651
121.25	145.25	1847.24	20.5	-0.4544	146.75	170.75	1819.54	23.0	-0.3154
121.75	145.75	1846.70	15.5	-0.7325	147.25	171.25	1819.00	30.0	0.0740
122.25	146.25	1846.15	27.0	-0.0929	147.75	171.75	1818.46	23.5	-0.2876
122.75	146.75	1845.61	14.5	-0.7882	148.25	172.25	1817.91	19.0	-0.5379
123.25	147.25	1845.07	15.5	-0.7325	148.75	172.75	1817.37	21.0	-0.4266
123.75	147.75	1844.52	14.0	-0.8160	149.25	173.25	1816.83	14.0	-0.8160
124.25	148.25	1843.98	16.1	-0.6992	149.75	173.75	1816.28	21.5	-0.3988
124.75	148.75	1843.44	15.5	-0.7325	150.25	174.25	1815.74	15.5	-0.7325
125.25	149.25	1842.90	16.0	-0.7047	150.75	174.75	1815.20	16.5	-0.6769
125.75	149.75	1842.35	17.5	-0.6213	151.25	175.25	1814.66	15.0	-0.7604
126.25	150.25	1841.81	18.5	-0.5657	151.75	175.75	1814.11	15.5	-0.7325
126.75	150.75	1841.27	17.0	-0.6491	152.25	176.25	1813.57	8.6	-1.1164
127.25	151.25	1840.72	12.0	-0.9272	152.75	176.75	1813.03	11.0	-0.9829
127.75	151.75	1840.18	14.5	-0.7882	153.25	177.25	1812.48	12.0	-0.9272

VC3 Distal Site									
Sample mid-depth	*Adjusted mid-depth*	*Year AD*	*Mag. Sus.*	*z-scores*	*Sample mid-depth*	*Adjusted mid-depth*	*Year AD*	*Mag. Sus.*	*z-scores*
153.75	177.75	1811.94	14.5	-0.7882	179.25	203.25	1784.24	11.1	-0.9773
154.25	178.25	1811.40	13.3	-0.8549	179.75	203.75	1783.70	15.0	-0.7604
154.75	178.75	1810.85	12.4	-0.9050	180.25	204.25	1783.16	16.5	-0.6769
155.25	179.25	1810.31	12.5	-0.8994	180.75	204.75	1782.61	19.6	-0.5045
155.75	179.75	1809.77	12.0	-0.9272	181.25	205.25	1782.07	26.7	-0.1096
156.25	180.25	1809.23	11.5	-0.9550	181.75	205.75	1781.53	37.5	0.4912
156.75	180.75	1808.68	11.5	-0.9550	182.25	206.25	1780.99	32.6	0.2186
157.25	181.25	1808.14	11.0	-0.9829	182.75	206.75	1780.44	18.0	-0.5935
157.75	181.75	1807.60	15.5	-0.7325	183.25	207.25	1779.90	11.0	-0.9829
158.25	182.25	1807.05	18.0	-0.5935	183.75	207.75	1779.36	15.5	-0.7325
158.75	182.75	1806.51	18.5	-0.5657	184.25	208.25	1778.81	30.0	0.0740
159.25	183.25	1805.97	10.5	-1.0107	184.75	208.75	1778.27	31.7	0.1686
159.75	183.75	1805.42	12.0	-0.9272	185.25	209.25	1777.73	25.2	-0.1930
160.25	184.25	1804.88	10.9	-0.9884	185.75	209.75	1777.18	21.9	-0.3766
160.75	184.75	1804.34	12.0	-0.9272	186.25	210.25	1776.64	16.7	-0.6658
161.25	185.25	1803.79	16.0	-0.7047	186.75	210.75	1776.10	8.6	-1.1164
161.75	185.75	1803.25	21.0	-0.4266	187.25	211.25	1775.56	11.0	-0.9829
162.25	186.25	1802.71	14.0	-0.8160	187.75	211.75	1775.01	17.5	-0.6213
162.75	186.75	1802.17	9.0	-1.0941	188.25	212.25	1774.47	21.0	-0.4266
163.25	187.25	1801.62	13.0	-0.8716	188.75	212.75	1773.93	11.0	-0.9829
163.75	187.75	1801.08	9.5	-1.0663	189.25	213.25	1773.38	6.5	-1.2332
164.25	188.25	1800.54	11.5	-0.9550	189.75	213.75	1772.84	9.0	-1.0941
164.75	188.75	1799.99	10.5	-1.0107	190.25	214.25	1772.30	10.5	-1.0107
165.25	189.25	1799.45	9.5	-1.0663	190.75	214.75	1771.75	11.5	-0.9550
165.75	189.75	1798.91	10.0	-1.0385	191.25	215.25	1771.21	12.0	-0.9272
166.25	190.25	1798.36	9.9	-1.0440	191.75	215.75	1770.67	11.1	-0.9773
166.75	190.75	1797.82	10.1	-1.0329	192.25	216.25	1770.12	12.5	-0.8994
167.25	191.25	1797.28	11.5	-0.9550	192.75	216.75	1769.58	12.0	-0.9272
167.75	191.75	1796.73	13.5	-0.8438	193.25	217.25	1769.04	11.3	-0.9662
168.25	192.25	1796.19	12.4	-0.9050	193.75	217.75	1768.50	18.3	-0.5768
168.75	192.75	1795.65	13.6	-0.8382	194.25	218.25	1767.95	12.9	-0.8772
169.25	193.25	1795.11	15.2	-0.7492	194.75	218.75	1767.41	16.7	-0.6658
169.75	193.75	1794.56	12.0	-0.9272	195.25	219.25	1766.87	16.2	-0.6936
170.25	194.25	1794.02	11.0	-0.9829	195.75	219.75	1766.32	13.5	-0.8438
170.75	194.75	1793.48	14.6	-0.7826	196.25	220.25	1765.78	12.0	-0.9272
171.25	195.25	1792.93	11.0	-0.9829	196.75	220.75	1765.24	18.0	-0.5935
171.75	195.75	1792.39	15.5	-0.7325	197.25	221.25	1764.69	11.5	-0.9550
172.25	196.25	1791.85	11.7	-0.9439	197.75	221.75	1764.15	12.0	-0.9272
172.75	196.75	1791.30	12.0	-0.9272	198.25	222.25	1763.61	13.0	-0.8716
173.25	197.25	1790.76	12.0	-0.9272	198.75	222.75	1763.06	9.6	-1.0607
173.75	197.75	1790.22	12.3	-0.9105	199.25	223.25	1762.52	10.9	-0.9884
174.25	198.25	1789.67	8.0	-1.1497	199.75	223.75	1761.98	12.8	-0.8827
174.75	198.75	1789.13	10.0	-1.0385	200.25	224.25	1761.44	15.0	-0.7604
175.25	199.25	1788.59	15.4	-0.7381	200.75	224.75	1760.89	11.5	-0.9550
175.75	199.75	1788.05	24.0	-0.2597	201.25	225.25	1760.35	15.3	-0.7437
176.25	200.25	1787.50	27.5	-0.0651	201.75	225.75	1759.81	10.0	-1.0385
176.75	200.75	1786.96	35.5	0.3799	202.25	226.25	1759.26	10.5	-1.0107
177.25	201.25	1786.42	34.0	0.2965	202.75	226.75	1758.72	13.4	-0.8494
177.75	201.75	1785.87	19.5	-0.5100	203.25	227.25	1758.18	10.6	-1.0051
178.25	202.25	1785.33	22.5	-0.3432	203.75	227.75	1757.63	10.5	-1.0107
178.75	202.75	1784.79	18.5	-0.5657	204.25	228.25	1757.09	11.4	-0.9606

VC3 Distal Site									
Sample mid-depth	*Adjusted mid-depth*	*Year AD*	*Mag. Sus.*	*z-scores*	*Sample mid-depth*	*Adjusted mid-depth*	*Year AD*	*Mag. Sus.*	*z-scores*
204.75	228.75	1756.55	11.0	-0.9829	230.25	254.25	1728.85	28.0	-0.0372
205.25	229.25	1756.00	11.5	-0.9550	230.75	254.75	1728.31	24.8	-0.2152
205.75	229.75	1755.46	12.7	-0.8883	231.25	255.25	1727.77	22.5	-0.3432
206.25	230.25	1754.92	13.9	-0.8215	231.75	255.75	1727.22	19.9	-0.4878
206.75	230.75	1754.38	15.0	-0.7604	232.25	256.25	1726.68	19.4	-0.5156
207.25	231.25	1753.83	20.0	-0.4822	232.75	256.75	1726.14	20.8	-0.4377
207.75	231.75	1753.29	20.5	-0.4544	233.25	257.25	1725.59	24.5	-0.2319
208.25	232.25	1752.75	20.4	-0.4600	233.75	257.75	1725.05	21.0	-0.4266
208.75	232.75	1752.20	16.3	-0.6880	234.25	258.25	1724.51	20.9	-0.4322
209.25	233.25	1751.66	24.3	-0.2431	234.75	258.75	1723.96	23.0	-0.3154
209.75	233.75	1751.12	23.7	-0.2764	235.25	259.25	1723.42	22.0	-0.3710
210.25	234.25	1750.57	24.6	-0.2264	235.75	259.75	1722.88	21.5	-0.3988
210.75	234.75	1750.03	28.3	-0.0206	236.25	260.25	1722.33	24.0	-0.2597
211.25	235.25	1749.49	26.4	-0.1262	236.75	260.75	1721.79	25.0	-0.2041
211.75	235.75	1748.94	22.8	-0.3265	237.25	261.25	1721.25	26.5	-0.1207
212.25	236.25	1748.40	20.6	-0.4489	237.75	261.75	1720.71	26.5	-0.1207
212.75	236.75	1747.86	25.4	-0.1819	238.25	262.25	1720.16	31.1	0.1352
213.25	237.25	1747.32	20.0	-0.4822	238.75	262.75	1719.62	26.5	-0.1207
213.75	237.75	1746.77	19.5	-0.5100	239.25	263.25	1719.08	32.5	0.2131
214.25	238.25	1746.23	15.8	-0.7159	239.75	263.75	1718.53	31.5	0.1574
214.75	238.75	1745.69	19.6	-0.5045	240.25	264.25	1717.99	28.5	-0.0094
215.25	239.25	1745.14	24.3	-0.2431	240.75	264.75	1717.45	28.5	-0.0094
215.75	239.75	1744.60	35.9	0.4022	241.25	265.25	1716.90	29.1	0.0239
216.25	240.25	1744.06	31.4	0.1519	241.75	265.75	1716.36	29.6	0.0518
216.75	240.75	1743.51	30.9	0.1241	242.25	266.25	1715.82	25.8	-0.1596
217.25	241.25	1742.97	21.0	-0.4266	242.75	266.75	1715.27	25.6	-0.1707
217.75	241.75	1742.43	22.9	-0.3209	243.25	267.25	1714.73	27.5	-0.0651
218.25	242.25	1741.88	20.4	-0.4600	243.75	267.75	1714.19	15.2	-0.7492
218.75	242.75	1741.34	14.6	-0.7826	244.25	268.25	1713.65	20.5	-0.4544
219.25	243.25	1740.80	16.4	-0.6825	244.75	268.75	1713.10	15.0	-0.7604
219.75	243.75	1740.26	19.6	-0.5045	245.25	269.25	1712.56	17.5	-0.6213
220.25	244.25	1739.71	16.5	-0.6769	245.75	269.75	1712.02	16.8	-0.6602
220.75	244.75	1739.17	20.0	-0.4822	246.25	270.25	1711.47	18.9	-0.5434
221.25	245.25	1738.63	21.8	-0.3821	246.75	270.75	1710.93	9.0	-1.0941
221.75	245.75	1738.08	20.6	-0.4489	247.25	271.25	1710.39	12.4	-0.9050
222.25	246.25	1737.54	24.5	-0.2319	247.75	271.75	1709.84	11.7	-0.9439
222.75	246.75	1737.00	24.1	-0.2542	248.25	272.25	1709.30	8.4	-1.1275
223.25	247.25	1736.45	26.4	-0.1262	248.75	272.75	1708.76	10.5	-1.0107
223.75	247.75	1735.91	22.5	-0.3432	249.25	273.25	1708.21	9.5	-1.0663
224.25	248.25	1735.37	26.0	-0.1485	249.75	273.75	1707.67	11.5	-0.9550
224.75	248.75	1734.83	23.5	-0.2876	250.25	274.25	1707.13	12.5	-0.8994
225.25	249.25	1734.28	27.0	-0.0929	250.75	274.75	1706.59	8.5	-1.1219
225.75	249.75	1733.74	28.4	-0.0150	251.25	275.25	1706.04	7.0	-1.2054
226.25	250.25	1733.20	27.0	-0.0929	251.75	275.75	1705.50	8.4	-1.1275
226.75	250.75	1732.65	28.0	-0.0372	252.25	276.25	1704.96	9.4	-1.0719
227.25	251.25	1732.11	25.0	-0.2041	252.75	276.75	1704.41	9.0	-1.0941
227.75	251.75	1731.57	32.5	0.2131	253.25	277.25	1703.87	7.7	-1.1664
228.25	252.25	1731.02	31.5	0.1574	253.75	277.75	1703.33	8.8	-1.1052
228.75	252.75	1730.48	32.0	0.1853	254.25	278.25	1702.78	7.5	-1.1775
229.25	253.25	1729.94	34.0	0.2965	254.75	278.75	1702.24	9.5	-1.0663
229.75	253.75	1729.39	28.0	-0.0372	255.25	279.25	1701.70	11.4	-0.9606

VC3 Distal Site									
Sample mid-depth	*Adjusted mid-depth*	*Year AD*	*Mag. Sus.*	*z-scores*	*Sample mid-depth*	*Adjusted mid-depth*	*Year AD*	*Mag. Sus.*	*z-scores*
255.75	279.75	1701.16	9.0	-1.0941	281.25	305.25	1673.46	35.0	0.3521
256.25	280.25	1700.61	9.0	-1.0941	281.75	305.75	1672.92	33.3	0.2576
256.75	280.75	1700.07	14.6	-0.7826	282.25	306.25	1672.37	30.0	0.0740
257.25	281.25	1699.53	14.0	-0.8160	282.75	306.75	1671.83	34.9	0.3466
257.75	281.75	1698.98	19.9	-0.4878	283.25	307.25	1671.29	29.4	0.0406
258.25	282.25	1698.44	19.8	-0.4934	283.75	307.75	1670.74	33.2	0.2520
258.75	282.75	1697.90	19.1	-0.5323	284.25	308.25	1670.20	33.3	0.2576
259.25	283.25	1697.35	22.0	-0.3710	284.75	308.75	1669.66	27.9	-0.0428
259.75	283.75	1696.81	15.5	-0.7325	285.25	309.25	1669.11	32.0	0.1853
260.25	284.25	1696.27	21.0	-0.4266	285.75	309.75	1668.57	29.5	0.0462
260.75	284.75	1695.72	22.0	-0.3710	286.25	310.25	1668.03	36.2	0.4189
261.25	285.25	1695.18	20.8	-0.4377	286.75	310.75	1667.49	31.8	0.1741
261.75	285.75	1694.64	19.0	-0.5379	287.25	311.25	1666.94	30.7	0.1129
262.25	286.25	1694.10	18.1	-0.5879	287.75	311.75	1666.40	33.2	0.2520
262.75	286.75	1693.55	16.5	-0.6769	288.25	312.25	1665.86	30.0	0.0740
263.25	287.25	1693.01	20.0	-0.4822	288.75	312.75	1665.31	32.7	0.2242
263.75	287.75	1692.47	24.3	-0.2431	289.25	313.25	1664.77	35.0	0.3521
264.25	288.25	1691.92	17.4	-0.6269	289.75	313.75	1664.23	25.5	-0.1763
264.75	288.75	1691.38	22.0	-0.3710	290.25	314.25	1663.68	27.0	-0.0929
265.25	289.25	1690.84	19.7	-0.4989	290.75	314.75	1663.14	23.5	-0.2876
265.75	289.75	1690.29	19.1	-0.5323	291.25	315.25	1662.60	23.7	-0.2764
266.25	290.25	1689.75	25.5	-0.1763	291.75	315.75	1662.05	24.4	-0.2375
266.75	290.75	1689.21	23.1	-0.3098	292.25	316.25	1661.51	23.4	-0.2931
267.25	291.25	1688.66	18.1	-0.5879	292.75	316.75	1660.97	20.4	-0.4600
267.75	291.75	1688.12	20.7	-0.4433	293.25	317.25	1660.43	22.3	-0.3543
268.25	292.25	1687.58	16.5	-0.6769	293.75	317.75	1659.88	18.7	-0.5545
268.75	292.75	1687.04	23.1	-0.3098	294.25	318.25	1659.34	22.2	-0.3599
269.25	293.25	1686.49	30.3	0.0907	294.75	318.75	1658.80	23.6	-0.2820
269.75	293.75	1685.95	39.6	0.6080	295.25	319.25	1658.25	22.5	-0.3432
270.25	294.25	1685.41	46.6	0.9974	295.75	319.75	1657.71	20.5	-0.4544
270.75	294.75	1684.86	34.4	0.3188	296.25	320.25	1657.17	20.3	-0.4656
271.25	295.25	1684.32	24.5	-0.2319	296.75	320.75	1656.62	22.3	-0.3543
271.75	295.75	1683.78	33.9	0.2909	297.25	321.25	1656.08	23.8	-0.2709
272.25	296.25	1683.23	31.3	0.1463	297.75	321.75	1655.54	26.0	-0.1485
272.75	296.75	1682.69	23.8	-0.2709	298.25	322.25	1654.99	24.7	-0.2208
273.25	297.25	1682.15	24.5	-0.2319	298.75	322.75	1654.45	22.7	-0.3321
273.75	297.75	1681.60	23.5	-0.2876	299.25	323.25	1653.91	22.6	-0.3376
274.25	298.25	1681.06	26.0	-0.1485	299.75	323.75	1653.37	22.5	-0.3432
274.75	298.75	1680.52	25.1	-0.1986	300.25	324.25	1652.82	20.2	-0.4711
275.25	299.25	1679.98	26.4	-0.1262	300.75	324.75	1652.28	17.5	-0.6213
275.75	299.75	1679.43	25.4	-0.1819	301.25	325.25	1651.74	21.0	-0.4266
276.25	300.25	1678.89	21.8	-0.3821	301.75	325.75	1651.19	15.6	-0.7270
276.75	300.75	1678.35	26.5	-0.1207	302.25	326.25	1650.65	19.2	-0.5267
277.25	301.25	1677.80	27.5	-0.0651	302.75	326.75	1650.11	19.3	-0.5212
277.75	301.75	1677.26	32.0	0.1853	303.25	327.25	1649.56	18.0	-0.5935
278.25	302.25	1676.72	31.0	0.1296	303.75	327.75	1649.02	18.4	-0.5712
278.75	302.75	1676.17	28.0	-0.0372	304.25	328.25	1648.48	23.9	-0.2653
279.25	303.25	1675.63	40.9	0.6803	304.75	328.75	1647.93	24.9	-0.2097
279.75	303.75	1675.09	44.0	0.8527	305.25	329.25	1647.39	23.4	-0.2931
280.25	304.25	1674.54	34.4	0.3188	305.75	329.75	1646.85	23.8	-0.2709
280.75	304.75	1674.00	35.5	0.3799	306.25	330.25	1646.31	24.6	-0.2264

VC3 Distal Site									
Sample mid-depth	*Adjusted mid-depth*	*Year AD*	*Mag. Sus.*	*z-scores*	*Sample mid-depth*	*Adjusted mid-depth*	*Year AD*	*Mag. Sus.*	*z-scores*
306.75	330.75	1645.76	27.9	-0.0428	332.25	356.25	1618.07	34.5	0.3243
307.25	331.25	1645.22	20.6	-0.4489	332.75	356.75	1617.52	43.4	0.8194
307.75	331.75	1644.68	20.5	-0.4544	333.25	357.25	1616.98	35.3	0.3688
308.25	332.25	1644.13	20.3	-0.4656	333.75	357.75	1616.44	39.7	0.6136
308.75	332.75	1643.59	24.3	-0.2431	334.25	358.25	1615.89	40.9	0.6803
309.25	333.25	1643.05	23.1	-0.3098	334.75	358.75	1615.35	39.1	0.5802
309.75	333.75	1642.50	23.5	-0.2876	335.25	359.25	1614.81	43.6	0.8305
310.25	334.25	1641.96	29.5	0.0462	335.75	359.75	1614.26	38.2	0.5301
310.75	334.75	1641.42	29.0	0.0184	336.25	360.25	1613.72	37.4	0.4856
311.25	335.25	1640.87	27.5	-0.0651	336.75	360.75	1613.18	37.0	0.4634
311.75	335.75	1640.33	29.0	0.0184	337.25	361.25	1612.64	39.3	0.5913
312.25	336.25	1639.79	31.5	0.1574	337.75	361.75	1612.09	37.0	0.4634
312.75	336.75	1639.25	29.0	0.0184	338.25	362.25	1611.55	35.4	0.3744
313.25	337.25	1638.70	24.4	-0.2375	338.75	362.75	1611.01	36.6	0.4411
313.75	337.75	1638.16	29.5	0.0462	339.25	363.25	1610.46	32.0	0.1853
314.25	338.25	1637.62	33.5	0.2687	339.75	363.75	1609.92	34.5	0.3243
314.75	338.75	1637.07	31.5	0.1574	340.25	364.25	1609.38	33.0	0.2409
315.25	339.25	1636.53	31.0	0.1296	340.75	364.75	1608.83	36.6	0.4411
315.75	339.75	1635.99	32.0	0.1853	341.25	365.25	1608.29	35.5	0.3799
316.25	340.25	1635.44	39.0	0.5746	341.75	365.75	1607.75	33.7	0.2798
316.75	340.75	1634.90	32.9	0.2353	342.25	366.25	1607.20	34.8	0.3410
317.25	341.25	1634.36	35.5	0.3799	342.75	366.75	1606.66	30.5	0.1018
317.75	341.75	1633.82	37.0	0.4634	343.25	367.25	1606.12	33.4	0.2631
318.25	342.25	1633.27	32.3	0.2019	343.75	367.75	1605.58	35.9	0.4022
318.75	342.75	1632.73	32.6	0.2186	344.25	368.25	1605.03	32.9	0.2353
319.25	343.25	1632.19	34.4	0.3188	344.75	368.75	1604.49	31.9	0.1797
319.75	343.75	1631.64	42.0	0.7415	345.25	369.25	1603.95	36.8	0.4523
320.25	344.25	1631.10	37.1	0.4689	345.75	369.75	1603.40	37.7	0.5023
320.75	344.75	1630.56	46.0	0.9640	346.25	370.25	1602.86	37.7	0.5023
321.25	345.25	1630.01	42.1	0.7471	346.75	370.75	1602.32	34.6	0.3299
321.75	345.75	1629.47	40.6	0.6636	347.25	371.25	1601.77	31.4	0.1519
322.25	346.25	1628.93	35.0	0.3521	347.75	371.75	1601.23	34.4	0.3188
322.75	346.75	1628.38	39.5	0.6024	348.25	372.25	1600.69	34.9	0.3466
323.25	347.25	1627.84	40.5	0.6581	348.75	372.75	1600.14	28.5	-0.0094
323.75	347.75	1627.30	38.5	0.5468	349.25	373.25	1599.60	30.7	0.1129
324.25	348.25	1626.76	40.0	0.6303	349.75	373.75	1599.06	32.0	0.1853
324.75	348.75	1626.21	40.0	0.6303	350.25	374.25	1598.52	38.5	0.5468
325.25	349.25	1625.67	46.4	0.9862	350.75	374.75	1597.97	41.0	0.6859
325.75	349.75	1625.13	36.0	0.4078	351.25	375.25	1597.43	38.2	0.5301
326.25	350.25	1624.58	41.7	0.7248	351.75	375.75	1596.89	40.0	0.6303
326.75	350.75	1624.04	37.5	0.4912	352.25	376.25	1596.34	31.7	0.1686
327.25	351.25	1623.50	37.3	0.4801	352.75	376.75	1595.80	27.2	-0.0817
327.75	351.75	1622.95	34.4	0.3188	353.25	377.25	1595.26	47.0	1.0196
328.25	352.25	1622.41	39.0	0.5746	353.75	377.75	1594.75	59.0	1.6871
328.75	352.75	1621.87	39.4	0.5969	354.25	378.25	1594.24	53.4	1.3756
329.25	353.25	1621.32	39.0	0.5746	354.75	378.75	1593.74	41.1	0.6914
329.75	353.75	1620.78	36.0	0.4078	355.25	379.25	1593.23	43.5	0.8249
330.25	354.25	1620.24	40.4	0.6525	355.75	379.75	1592.73	45.0	0.9084
330.75	354.75	1619.70	40.0	0.6303	356.25	380.25	1592.23	33.9	0.2909
331.25	355.25	1619.15	39.1	0.5802	356.75	380.75	1591.72	69.4	2.2656
331.75	355.75	1618.61	40.8	0.6747	357.25	381.25	1591.22	66.0	2.0765

VC3 Distal Site									
Sample mid-depth	*Adjusted mid-depth*	*Year AD*	*Mag. Sus.*	*z-scores*	*Sample mid-depth*	*Adjusted mid-depth*	*Year AD*	*Mag. Sus.*	*z-scores*
357.75	381.75	1590.71	52.5	1.3256	383.25	407.25	1564.99	53.5	1.3812
358.25	382.25	1590.21	66.0	2.0765	383.75	407.75	1564.48	52.2	1.3089
358.75	382.75	1589.70	59.5	1.7149	384.25	408.25	1563.98	45.5	0.9362
359.25	383.25	1589.20	60.6	1.7761	384.75	408.75	1563.48	41.0	0.6859
359.75	383.75	1588.70	64.3	1.9819	385.25	409.25	1562.97	38.1	0.5246
360.25	384.25	1588.19	89.9	3.4059	385.75	409.75	1562.47	54.0	1.4090
360.75	384.75	1587.69	57.9	1.6259	386.25	410.25	1561.96	59.0	1.6871
361.25	385.25	1587.18	58.0	1.6315	386.75	410.75	1561.46	40.7	0.6692
361.75	385.75	1586.68	52.3	1.3144	387.25	411.25	1560.95	41.3	0.7026
362.25	386.25	1586.17	56.5	1.5481	387.75	411.75	1560.45	46.6	0.9974
362.75	386.75	1585.67	72.5	2.4380	388.25	412.25	1559.95	52.1	1.3033
363.25	387.25	1585.16	58.6	1.6649	388.75	412.75	1559.44	58.0	1.6315
363.75	387.75	1584.66	46.5	0.9918	389.25	413.25	1558.94	61.5	1.8262
364.25	388.25	1584.16	31.0	0.1296	389.75	413.75	1558.43	62.4	1.8762
364.75	388.75	1583.65	56.6	1.5536	390.25	414.25	1557.93	57.5	1.6037
365.25	389.25	1583.15	60.5	1.7706	390.75	414.75	1557.42	61.2	1.8095
365.75	389.75	1582.64	57.6	1.6092	391.25	415.25	1556.92	58.1	1.6371
366.25	390.25	1582.14	49.5	1.1587	391.75	415.75	1556.41	66.0	2.0765
366.75	390.75	1581.63	41.0	0.6859	392.25	416.25	1555.91	51.0	1.2421
367.25	391.25	1581.13	28.5	-0.0094	392.75	416.75	1555.41	55.7	1.5036
367.75	391.75	1580.62	28.6	-0.0039	393.25	417.25	1554.90	45.5	0.9362
368.25	392.25	1580.12	52.6	1.3311	393.75	417.75	1554.40	60.1	1.7483
368.75	392.75	1579.62	74.5	2.5493	394.25	418.25	1553.89	63.1	1.9152
369.25	393.25	1579.11	75.0	2.5771	394.75	418.75	1553.39	64.6	1.9986
369.75	393.75	1578.61	50.0	1.1865	395.25	419.25	1552.88	33.0	0.2409
370.25	394.25	1578.10	44.4	0.8750	395.75	419.75	1552.38	35.1	0.3577
370.75	394.75	1577.60	74.0	2.5215	396.25	420.25	1551.87	57.6	1.6092
371.25	395.25	1577.09	52.6	1.3311	396.75	420.75	1551.37	50.8	1.2310
371.75	395.75	1576.59	41.5	0.7137	397.25	421.25	1550.87	48.1	1.0808
372.25	396.25	1576.09	31.5	0.1574	397.75	421.75	1550.36	53.0	1.3534
372.75	396.75	1575.58	23.0	-0.3154	398.25	422.25	1549.86	56.0	1.5202
373.25	397.25	1575.08	24.0	-0.2597	398.75	422.75	1549.35	45.2	0.9195
373.75	397.75	1574.57	64.0	1.9652	399.25	423.25	1548.85	46.7	1.0029
374.25	398.25	1574.07	74.5	2.5493	399.75	423.75	1548.34	64.9	2.0153
374.75	398.75	1573.56	65.5	2.0487	400.25	424.25	1547.84	64.0	1.9652
375.25	399.25	1573.06	63.0	1.9096	400.75	424.75	1547.34	41.1	0.6914
375.75	399.75	1572.55	46.6	0.9974	401.25	425.25	1546.83	42.0	0.7415
376.25	400.25	1572.05	80.4	2.8775	401.75	425.75	1546.33	51.5	1.2699
376.75	400.75	1571.55	62.1	1.8595	402.25	426.25	1545.82	35.0	0.3521
377.25	401.25	1571.04	58.0	1.6315	402.75	426.75	1545.32	42.5	0.7693
377.75	401.75	1570.54	43.8	0.8416	403.25	427.25	1544.81	66.8	2.1210
378.25	402.25	1570.03	46.0	0.9640	403.75	427.75	1544.31	48.1	1.0808
378.75	402.75	1569.53	34.6	0.3299	404.25	428.25	1543.80	75.0	2.5771
379.25	403.25	1569.02	28.5	-0.0094	404.75	428.75	1543.30	45.5	0.9362
379.75	403.75	1568.52	32.0	0.1853	405.25	429.25	1542.80	50.0	1.1865
380.25	404.25	1568.02	59.9	1.7372	405.75	429.75	1542.29	41.5	0.7137
380.75	404.75	1567.51	66.1	2.0820	406.25	430.25	1541.79	57.0	1.5759
381.25	405.25	1567.01	58.5	1.6593	406.75	430.75	1541.28	51.5	1.2699
381.75	405.75	1566.50	54.0	1.4090	407.25	431.25	1540.78	33.0	0.2409
382.25	406.25	1566.00	51.6	1.2755	407.75	431.75	1540.27	47.3	1.0363
382.75	406.75	1565.49	59.0	1.6871	408.25	432.25	1539.77	60.3	1.7594

VC3 Distal Site									
Sample mid-depth	*Adjusted mid-depth*	*Year AD*	*Mag. Sus.*	*z-scores*	*Sample mid-depth*	*Adjusted mid-depth*	*Year AD*	*Mag. Sus.*	*z-scores*
408.75	1539.27	1556.90	45.9	0.9584	434.25	458.25	1513.54	50.5	1.2143
409.25	1538.76	1556.55	32.0	0.1853	434.75	458.75	1513.04	37.1	0.4689
409.75	1538.26	1556.21	25.4	-0.1819	435.25	459.25	1512.53	37.1	0.4689
410.25	1537.75	1555.86	56.0	1.5202	435.75	459.75	1512.03	64.6	1.9986
410.75	1537.25	1555.52	57.7	1.6148	436.25	460.25	1511.52	60.8	1.7872
411.25	1536.74	1555.17	50.5	1.2143	436.75	460.75	1511.02	38.3	0.5357
411.75	1536.24	1554.83	44.1	0.8583	437.25	461.25	1510.51	70.5	2.3268
412.25	1535.73	1554.48	30.8	0.1185	437.75	461.75	1510.01	61.6	1.8317
412.75	1535.23	1554.14	45.5	0.9362	438.25	462.25	1509.51	30.8	0.1185
413.25	1534.73	1553.79	57.3	1.5926	438.75	462.75	1509.00	48.6	1.1086
413.75	1534.22	1553.45	46.3	0.9807	439.25	463.25	1508.50	48.3	1.0919
414.25	1533.72	1553.10	26.0	-0.1485	439.75	463.75	1507.99	58.1	1.6371
414.75	1533.21	1552.76	31.3	0.1463	440.25	464.25	1507.49	58.6	1.6649
415.25	1532.71	1552.41	60.7	1.7817	440.75	464.75	1506.98	40.4	0.6525
415.75	1532.20	1552.07	45.6	0.9417	441.25	465.25	1506.48	34.5	0.3243
416.25	1531.70	1551.72	59.7	1.7261	441.75	465.75	1505.98	60.0	1.7427
416.75	1531.19	1551.38	60.0	1.7427	442.25	466.25	1505.47	57.5	1.6037
417.25	1530.69	1551.03	30.8	0.1185	442.75	466.75	1504.97	53.4	1.3756
417.75	1530.19	1550.69	34.8	0.3410	443.25	467.25	1504.46	70.9	2.3490
418.25	1529.68	1550.34	37.8	0.5079	443.75	467.75	1503.96	53.0	1.3534
418.75	1529.18	1550.00	81.5	2.9387	444.25	468.25	1503.45	60.3	1.7594
419.25	1528.67	1549.66	71.0	2.3546	444.75	468.75	1502.95	70.1	2.3045
419.75	1528.17	1549.31	53.5	1.3812	445.25	469.25	1502.44	62.4	1.8762
420.25	1527.66	1548.97	57.7	1.6148	445.75	469.75	1501.94	54.6	1.4424
420.75	1527.16	1548.62	59.1	1.6927	446.25	470.25	1501.44	33.0	0.2409
421.25	1526.66	1548.28	44.6	0.8861	446.75	470.75	1500.93	38.4	0.5413
421.75	1526.15	1547.93	35.1	0.3577	447.25	471.25	1500.43	54.7	1.4479
422.25	1525.65	1547.59	57.0	1.5759	447.75	471.75	1499.92	66.9	2.1265
422.75	1525.14	1547.24	58.3	1.6482	448.25	472.25	1499.42	57.4	1.5981
423.25	1524.64	1546.90	49.6	1.1642	448.75	472.75	1498.91	52.4	1.3200
423.75	1524.13	1546.55	38.8	0.5635	449.25	473.25	1498.41	62.0	1.8540
424.25	1523.63	1546.21	52.1	1.3033	449.75	473.75	1497.91	59.3	1.7038
424.75	1523.12	1545.86	70.5	2.3268	450.25	474.25	1497.40	45.0	0.9084
425.25	1522.62	1545.52	61.9	1.8484	450.75	474.75	1496.90	67.8	2.1766
425.75	1522.12	1545.17	56.1	1.5258	451.25	475.25	1496.39	56.7	1.5592
426.25	1521.61	1544.83	59.4	1.7094	451.75	475.75	1495.89	39.5	0.6024
426.75	1521.11	1544.48	41.4	0.7081	452.25	476.25	1495.38	53.1	1.3589
427.25	1520.60	1544.14	41.4	0.7081	452.75	476.75	1494.88	53.1	1.3589
427.75	1520.10	1543.79	30.1	0.0796	453.25	477.25	1494.37	46.0	0.9640
428.25	1519.59	1543.45	36.9	0.4578	453.75	477.75	1493.87	64.3	1.9819
428.75	1519.09	1543.10	33.9	0.2909	454.25	478.25	1493.37	51.9	1.2922
429.25	1518.59	1542.76	71.9	2.4047	454.75	478.75	1492.86	53.8	1.3979
429.75	1518.08	1542.41	76.8	2.6772	455.25	479.25	1492.36	56.6	1.5536
430.25	1517.58	1542.07	42.9	0.7916	455.75	479.75	1491.85	34.0	0.2965
430.75	1517.07	1541.72	32.1	0.1908	456.25	480.25	1491.35	31.0	0.1296
431.25	1516.57	1541.38	36.1	0.4133	456.75	480.75	1490.84	50.0	1.1865
431.75	1516.06	1541.03	58.5	1.6593	457.25	481.25	1490.34	44.5	0.8806
432.25	1515.56	1540.69	58.4	1.6537	457.75	481.75	1489.84	46.9	1.0141
432.75	1515.05	1540.34	71.0	2.3546	458.25	482.25	1489.33	26.0	-0.1485
433.25	1514.55	1540.00	98.6	3.8898	458.75	482.75	1488.83	21.0	-0.4266
433.75	1514.05	1539.66	57.3	1.5926	459.25	483.25	1488.32	28.2	-0.0261

VC3 Distal Site									
Sample mid-depth	*Adjusted mid-depth*	*Year AD*	*Mag. Sus.*	*z-scores*	*Sample mid-depth*	*Adjusted mid-depth*	*Year AD*	*Mag. Sus.*	*z-scores*
459.75	483.75	1487.82	65.5	2.0487	485.25	509.25	1462.09	58.5	1.6593
460.25	484.25	1487.31	52.5	1.3256	485.75	509.75	1461.59	54.5	1.4368
460.75	484.75	1486.81	43.0	0.7971	486.25	510.25	1461.08	47.0	1.0196
461.25	485.25	1486.30	60.8	1.7872	486.75	510.75	1460.58	57.0	1.5759
461.75	485.75	1485.80	53.5	1.3812	487.25	511.25	1460.08	44.5	0.8806
462.25	486.25	1485.30	59.0	1.6871	487.75	511.75	1459.57	53.4	1.3756
462.75	486.75	1484.79	30.0	0.0740	488.25	512.25	1459.07	62.5	1.8818
463.25	487.25	1484.29	20.0	-0.4822	488.75	512.75	1458.56	62.0	1.8540
463.75	487.75	1483.78	18.7	-0.5545	489.25	513.25	1458.06	62.5	1.8818
464.25	488.25	1483.28	62.6	1.8874	489.75	513.75	1457.55	81.6	2.9442
464.75	488.75	1482.77	67.9	2.1822	490.25	514.25	1457.05	86.5	3.2168
465.25	489.25	1482.27	40.5	0.6581	490.75	514.75	1456.55	71.0	2.3546
465.75	489.75	1481.76	35.0	0.3521	491.25	515.25	1456.04	69.0	2.2434
466.25	490.25	1481.26	33.0	0.2409	491.75	515.75	1455.54	68.0	2.1877
466.75	490.75	1480.76	23.2	-0.3042	492.25	516.25	1455.03	81.0	2.9109
467.25	491.25	1480.25	26.0	-0.1485	492.75	516.75	1454.53	80.0	2.8552
467.75	491.75	1479.75	30.0	0.0740	493.25	517.25	1454.02	76.5	2.6605
468.25	492.25	1479.24	18.5	-0.5657	493.75	517.75	1453.52	79.6	2.8330
468.75	492.75	1478.74	28.2	-0.0261	494.25	518.25	1453.01	65.0	2.0209
469.25	493.25	1478.23	51.8	1.2866	494.75	518.75	1452.51	58.5	1.6593
469.75	493.75	1477.73	57.6	1.6092	495.25	519.25	1452.01	54.0	1.4090
470.25	494.25	1477.23	25.0	-0.2041	495.75	519.75	1451.50	56.5	1.5481
470.75	494.75	1476.72	27.0	-0.0929	496.25	520.25	1451.00	50.0	1.1865
471.25	495.25	1476.22	14.9	-0.7659	496.75	520.75	1450.49	60.0	1.7427
471.75	495.75	1475.71	17.8	-0.6046	497.25	521.25	1449.99	53.5	1.3812
472.25	496.25	1475.21	68.3	2.2044	497.75	521.75	1449.48	58.0	1.6315
472.75	496.75	1474.70	55.0	1.4646	498.25	522.25	1448.98	54.0	1.4090
473.25	497.25	1474.20	60.1	1.7483	498.75	522.75	1448.48	57.0	1.5759
473.75	497.75	1473.69	40.7	0.6692	499.25	523.25	1447.97	56.0	1.5202
474.25	498.25	1473.19	53.7	1.3923	499.75	523.75	1447.47	48.0	1.0752
474.75	498.75	1472.69	52.4	1.3200	500.25	524.25	1446.96	41.0	0.6859
475.25	499.25	1472.18	54.1	1.4146	500.75	524.75	1446.46	43.0	0.7971
475.75	499.75	1471.68	51.1	1.2477	501.25	525.25	1445.95	44.2	0.8639
476.25	500.25	1471.17	33.5	0.2687	501.75	525.75	1445.45	55.5	1.4924
476.75	500.75	1470.67	33.7	0.2798	502.25	526.25	1444.94	44.0	0.8527
477.25	501.25	1470.16	33.0	0.2409	502.75	526.75	1444.44	46.5	0.9918
477.75	501.75	1469.66	26.0	-0.1485	503.25	527.25	1443.94	42.5	0.7693
478.25	502.25	1469.16	23.0	-0.3154	503.75	527.75	1443.43	47.0	1.0196
478.78	502.78	1468.65	36.5	0.4356	504.25	528.25	1442.93	41.5	0.7137
479.25	503.25	1468.15	61.6	1.8317	504.75	528.75	1442.42	41.0	0.6859
479.75	503.75	1467.64	40.5	0.6581	505.25	529.25	1441.92	43.5	0.8249
480.25	504.25	1467.14	57.5	1.6037	505.75	529.75	1441.41	45.5	0.9362
480.75	504.75	1466.63	62.5	1.8818	506.25	530.25	1440.91	47.0	1.0196
481.25	505.25	1466.13	55.0	1.4646	506.75	530.75	1440.41	52.5	1.3256
481.75	505.75	1465.62	51.1	1.2477	507.25	531.25	1439.90	44.5	0.8806
482.25	506.25	1465.12	29.5	0.0462	507.75	531.75	1439.40	39.6	0.6080
482.75	506.75	1464.62	44.5	0.8806	508.25	532.25	1438.89	49.0	1.1309
483.25	507.25	1464.11	48.3	1.0919	508.75	532.75	1438.39	35.6	0.3855
483.75	507.75	1463.61	36.6	0.4411	509.25	533.25	1437.88	40.0	0.6303
484.25	508.25	1463.10	65.0	2.0209	509.75	533.75	1437.38	32.0	0.1853
484.75	508.75	1462.60	59.0	1.6871	510.25	534.25	1436.87	42.0	0.7415

VC3 Distal Site				
Sample mid-depth	*Adjusted mid-depth*	*Year AD*	*Mag. Sus.*	*z-scores*
510.75	534.75	1436.37	42.0	0.7415
511.25	535.25	1435.87	51.5	1.2699
511.75	535.75	1435.36	46.0	0.9640
512.25	536.25	1434.86	52.5	1.3256
512.75	536.75	1434.35	49.5	1.1587
513.25	537.25	1433.85	51.5	1.2699
513.75	537.75	1433.34	67.0	2.1321
514.25	538.25	1432.84	53.5	1.3812
514.75	538.75	1432.33	47.0	1.0196
515.25	539.25	1431.83	44.0	0.8527
515.75	539.75	1431.33	27.0	-0.0929
516.25	540.25	1430.82	35.0	0.3521
516.75	540.75	1430.32	64.0	1.9652
517.25	541.25	1429.81	63.5	1.9374
517.75	541.75	1429.31	43.5	0.8249
518.25	542.25	1428.80	42.4	0.7637
518.75	542.75	1428.30	45.0	0.9084
519.25	543.25	1427.80	38.5	0.5468
519.75	543.75	1427.29	51.5	1.2699
520.25	544.25	1426.79	50.0	1.1865
520.75	544.75	1426.28	46.2	0.9751
521.25	545.25	1425.78	52.1	1.3033
521.75	545.75	1425.27	37.0	0.4634
522.25	546.25	1424.77	49.7	1.1698
522.75	546.75	1424.26	41.0	0.6859
523.25	547.25	1423.76	45.1	0.9139
523.75	547.75	1423.26	52.5	1.3256
524.25	548.25	1422.75	58.0	1.6315
524.75	548.75	1422.25	64.2	1.9764
525.25	549.25	1421.74	51.0	1.2421
525.75	549.75	1421.24	54.0	1.4090
526.25	550.25	1420.73	55.6	1.4980
526.75	550.75	1420.23	46.2	0.9751
527.25	551.25	1419.73	44.6	0.8861
527.75	551.75	1419.22	38.0	0.5190
528.25	552.25	1418.72	27.0	-0.0929
528.75	552.75	1418.21	22.4	-0.3487
529.25	553.25	1417.71	29.0	0.0184

Appendix E: Organic Carbon and Nitrogen Elemental and Stable Isotope Geochemistry

PAD 15 KB-05-03 Distal Site														
Sample mid-depth	*Year AD*	*C_{org} (%)*	*Rpt*	*Avg*	*N (%)*	*Rpt*	*Avg*	*$\delta 13C_{org}$*	*Rpt*	*Avg*	*$\delta 15N$*	*Rpt*	*Avg*	*C/N*
0.25	2004.73	3.57		3.57	0.43		0.43	-28.78		-28.78	1.36		1.36	8.40
0.75	2004.19	2.84		2.84	0.33		0.33	-28.38		-28.38	1.53		1.53	8.50
1.25	2003.64	2.15		2.15	0.25		0.25	-27.77		-27.77	2.14		2.14	8.49
1.75	2003.10	1.82		1.82	0.19		0.19	-27.27		-27.27	1.93		1.93	9.44
2.25	2002.56	1.88		1.88	0.21		0.21	-27.37		-27.37	1.46		1.46	9.04
2.75	2002.01	3.21		3.21	0.35		0.35	-28.63		-28.63	1.20		1.20	9.27
3.25	2001.47	2.55		2.55	0.23		0.23	-27.23		-27.23	1.05		1.05	11.23
3.75	2000.93	2.88		2.88	0.26		0.26	-27.73		-27.73	0.88		0.88	11.18
4.50	2000.11	2.54		2.54	0.24		0.24	-27.26		-27.26	1.52		1.52	10.55
5.25	1999.30	2.24	2.16	2.20	0.20	0.18	0.19	-26.81	-26.63	-26.72	1.72	1.61	1.67	11.41
5.75	1998.75	2.21		2.21	0.18		0.18	-26.49		-26.49	1.75		1.75	12.02
6.25	1998.21	1.94		1.94	0.16		0.16	-26.74		-26.74	1.76		1.76	12.10
6.75	1997.67	2.28		2.28	0.20		0.20	-27.22		-27.22	1.72		1.72	11.16
7.25	1997.13	2.20		2.20	0.21		0.21	-27.90		-27.90	2.15		2.15	10.34
7.75	1996.58	1.92		1.92	0.22		0.22	-28.60		-28.60	1.45		1.45	8.74
8.25	1996.04	1.77		1.77	0.20		0.20	-27.55		-27.55	1.98		1.98	8.95
8.75	1995.50	1.65		1.65	0.15		0.15	-26.59		-26.59	2.14		2.14	10.75
9.25	1994.95	1.59		1.59	0.14		0.14	-26.51		-26.51	1.79		1.79	11.04
9.75	1994.41	1.66		1.66	0.15		0.15	-26.36		-26.36	2.17		2.17	10.96
10.25	1993.87	1.47		1.47	0.13		0.13	-26.23		-26.23	2.22		2.22	11.17
10.75	1993.32	1.55		1.55	0.14		0.14	-26.29		-26.29	2.05		2.05	10.82
11.25	1992.78	1.53		1.53	0.14		0.14	-26.27		-26.27	2.19		2.19	11.13
11.75	1992.24	1.81		1.81	0.19		0.19	-27.68		-27.68	1.97		1.97	9.68
12.25	1991.69	1.57		1.57	0.15		0.15	-26.32		-26.32	2.29		2.29	10.31
12.75	1991.15	1.37		1.37	0.12		0.12	-26.10		-26.10	2.08		2.08	11.00
13.25	1990.61	1.53		1.53	0.14		0.14	-26.14		-26.14	2.18		2.18	10.78
13.75	1990.07	2.40		2.40	0.27		0.27	-27.42		-27.42	1.81		1.81	9.06
14.25	1989.52	1.94		1.94	0.22		0.22	-27.35		-27.35	1.79		1.79	8.97
14.75	1988.98	2.92		2.92	0.35		0.35	-28.05		-28.05	1.37		1.37	8.45
15.25	1988.44	2.53	2.63	2.58	0.30	0.30	0.30	-28.52	-28.42	-28.47	1.29	1.43	1.36	8.60
15.75	1987.89	2.07		2.07	0.23		0.23	-28.12		-28.12	1.74		1.74	9.01
16.25	1987.35	1.98		1.98	0.22		0.22	-27.85		-27.85	1.50		1.50	9.12
16.75	1986.81	1.91		1.91	0.21		0.21	-27.58		-27.58	1.65		1.65	9.22

PAD 15 KB-05-03 Distal Site														
Sample mid-depth	*Year AD*	*C_{org} (%)*	*Rpt*	*Avg*	*N (%)*	*Rpt*	*Avg*	*$\delta 13C_{org}$*	*Rpt*	*Avg*	*$\delta 15N$*	*Rpt*	*Avg*	*C/N*
17.25	1986.26	2.62		2.62	0.30		0.30	-27.68		-27.68	1.66		1.66	8.89
17.75	1985.72	2.04		2.04	0.24		0.24	-27.39		-27.39	2.05		2.05	8.63
18.25	1985.18	2.18		2.18	0.24		0.24	-27.45		-27.45	1.84		1.84	8.92
18.75	1984.64	2.94		2.94	0.33		0.33	-28.35		-28.35	1.44		1.44	8.93
19.25	1984.09	2.41		2.41	0.27		0.27	-27.38		-27.38	1.89		1.89	8.76
19.75	1983.55	1.82		1.82	0.21		0.21	-26.76		-26.76	2.06		2.06	8.85
20.25	1983.01	1.91		1.91	0.21		0.21	-27.32		-27.32	2.36		2.36	9.20
20.75	1982.46	1.76		1.76	0.21		0.21	-27.47		-27.47	2.10		2.10	8.58
21.25	1981.92	1.53		1.53	0.16		0.16	-26.41		-26.41	2.35		2.35	9.53
21.75	1981.38	1.56		1.56	0.15		0.15	-26.23		-26.23	2.49		2.49	10.20
22.25	1980.83	1.62		1.62	0.16		0.16	-26.56		-26.56	1.82		1.82	9.94
22.75	1980.29	2.02		2.02	0.22		0.22	-27.30		-27.30	2.19		2.19	9.11
23.25	1979.75	1.80		1.80	0.20		0.20	-27.33		-27.33	1.04		1.04	8.78
23.75	1979.20	1.74		1.74	0.19		0.19	-27.24		-27.24	2.17		2.17	9.14
24.25	1978.66	1.65		1.65	0.19		0.19	-27.26		-27.26	2.02		2.02	8.93
24.75	1978.12	1.55		1.55	0.19		0.19	-27.00		-27.00	1.95		1.95	8.39
25.25	1977.58	1.39	1.45	1.42	0.15	0.15	0.15	-26.33	-26.36	-26.35	2.21	2.03	2.12	9.57
25.75	1977.03	1.45		1.45	0.13		0.13	-26.06		-26.06	2.26		2.26	11.30
26.25	1976.49	1.59		1.59	0.15		0.15	-26.16		-26.16	2.22		2.22	10.86
26.75	1975.95	1.55		1.55	0.14		0.14	-26.24		-26.24	2.24		2.24	10.89
27.25	1975.40	1.53		1.53	0.15		0.15	-26.46		-26.46	2.06		2.06	10.09
27.75	1974.86	1.39		1.39	0.15		0.15	-26.42		-26.42	1.98		1.98	9.44
28.25	1974.32	1.33		1.33	0.14		0.14	-26.21		-26.21	1.80		1.80	9.68
28.75	1973.77	1.53		1.53	0.15		0.15	-26.61		-26.61	1.79		1.79	10.07
29.25	1973.23	1.54		1.54	0.17		0.17	-26.65		-26.65	2.06		2.06	8.83
29.75	1972.69	1.33		1.33	0.13		0.13	-26.04		-26.04	1.68		1.68	10.43
30.25	1972.14	1.32		1.32	0.12		0.12	-26.03		-26.03	1.97		1.97	10.79
30.75	1971.60	1.37		1.37	0.13		0.13	-26.15		-26.15	2.20		2.20	10.56
31.25	1971.06	1.66		1.66	0.15		0.15	-26.25		-26.25	2.21		2.21	10.77
31.75	1970.52	2.40		2.40	0.25		0.25	-26.19		-26.19	2.09		2.09	9.71
32.25	1969.97	2.21		2.21	0.23		0.23	-25.94		-25.94	2.35		2.35	9.55
32.75	1969.43	1.63		1.63	0.16		0.16	-26.48		-26.48	2.25		2.25	10.20
33.25	1968.89	1.66		1.66	0.17		0.17	-26.71		-26.71	2.50		2.50	9.75
33.75	1968.34	1.63		1.63	0.17		0.17	-26.87		-26.87	2.26		2.26	9.56
34.25	1967.80	1.51		1.51	0.16		0.16	-26.85		-26.85	2.39		2.39	9.62
34.75	1967.26	1.63		1.63	0.17		0.17	-27.01		-27.01	1.94		1.94	9.79
35.25	1966.71	1.64	1.59	1.62	0.17	0.16	0.17	-26.86	-26.87	-26.86	1.98	1.97	1.97	9.63

PAD 15 KB-05-03 Distal Site														
Sample mid-depth	*Year AD*	*C_{org} (%)*	*Rpt*	*Avg*	*N (%)*	*Rpt*	*Avg*	*$\delta 13C_{org}$*	*Rpt*	*Avg*	*$\delta 15N$*	*Rpt*	*Avg*	*C/N*
35.75	1966.17	1.40		1.40	0.13		0.13	-26.35		-26.35	1.83		1.83	10.57
36.25	1965.63	1.49		1.49	0.13		0.13	-26.30		-26.30	2.14		2.14	11.52
36.75	1965.08	1.48		1.48	0.14		0.14	-26.34		-26.34	1.71		1.71	10.82
37.25	1964.54	1.51		1.51	0.15		0.15	-26.86		-26.86	2.11		2.11	10.34
37.75	1964.00	1.68		1.68	0.19		0.19	-27.25		-27.25	1.93		1.93	9.02
38.25	1963.46	1.65		1.65	0.18		0.18	-26.91		-26.91	2.11		2.11	9.32
38.75	1962.91	1.48		1.48	0.14		0.14	-26.27		-26.27	2.15		2.15	10.67
39.25	1962.37	1.45		1.45	0.14		0.14	-26.32		-26.32	2.10		2.10	10.35
39.75	1961.83	1.45		1.45	0.14		0.14	-26.45		-26.45	1.39		1.39	10.55
40.25	1961.28	1.66		1.66	0.16		0.16	-26.89		-26.89	2.01		2.01	10.35
40.75	1960.74	1.78		1.78	0.19		0.19	-27.35		-27.35	2.03		2.03	9.33

PAD 15 VC3 Distal Site																	
Sample mid-depth	*Adjusted mid-depth (+24cm)*	*Year AD*	*C_{org} (%)*	*Rpt*	*Avg*	*N (%)*	*Rpt*	*Avg*	*Corrected N (%) (-0.008%)*	*$\delta^{13}C_{org}$ (‰)*	*Rpt*	*Avg*	*$\delta^{15}N$ (‰)*	*Rpt*	*Avg*	*C/N*	*Corrected C/N*
0.25	24.25	1978.66	1.97		1.97	0.195		0.19	0.195	-27.79		-27.79	1.18		1.18	10.12	10.12
0.75	24.75	1978.12	1.93		1.93	0.193		0.19	0.193	-28.13		-28.13	1.57		1.57	10.02	10.02
1.25	25.25	1977.58	2.01		2.01	0.205		0.21	0.205	-27.88		-27.88	1.51		1.51	9.80	9.80
1.75	25.75	1977.03	1.88		1.88	0.194		0.19	0.194	-27.79		-27.79	1.50		1.50	9.71	9.71
2.25	26.25	1976.49	1.88		1.88	0.190		0.19	0.190	-27.68		-27.68	1.64		1.64	9.86	9.86
2.75	26.75	1975.95	1.71		1.71	0.169		0.17	0.169	-27.45		-27.45	1.50		1.50	10.11	10.11
3.25	27.25	1975.40	1.56		1.56	0.135		0.14	0.135	-26.65		-26.65	1.58		1.58	11.52	11.52
3.75	27.75	1974.86	1.52		1.52	0.140		0.14	0.140	-26.78		-26.78	1.55		1.55	10.82	10.82
4.25	28.25	1974.32	1.66		1.66	0.157		0.16	0.157	-26.87		-26.87	1.81		1.81	10.53	10.53
4.75	28.75	1973.77	1.59		1.59	0.146		0.15	0.146	-26.69		-26.69	1.57		1.57	10.86	10.86
5.25	29.25	1973.23	1.61	1.62	1.62	0.159	0.16	0.16	0.158	-26.80	-26.77	-26.79	1.74	1.83	1.78	10.23	10.23
5.75	29.75	1972.69	1.47		1.47	0.140		0.14	0.140	-26.78		-26.78	1.99		1.99	10.45	10.45
6.25	30.25	1972.14	1.51		1.51	0.143		0.14	0.143	-26.78		-26.78	2.32		2.32	10.55	10.55
6.75	30.75	1971.60	1.56		1.56	0.154		0.15	0.154	-26.73		-26.73	2.35		2.35	10.11	10.11
7.25	31.25	1971.06	1.31		1.31	0.117		0.12	0.117	-26.30		-26.30	2.19		2.19	11.22	11.22
8.00	32.00	1970.24	1.72		1.72	0.169		0.17	0.169	-26.37		-26.37	1.95		1.95	10.19	10.19
8.75	32.75	1969.43	1.66		1.66	0.160		0.16	0.160	-26.36		-26.36	2.20		2.20	10.42	10.42
9.25	33.25	1968.89	1.61		1.61	0.165		0.16	0.165	-27.11		-27.11	2.14		2.14	9.75	9.75
9.75	33.75	1968.34	1.69		1.69	0.167		0.17	0.167	-26.94		-26.94	2.15		2.15	10.11	10.11
10.25	34.25	1967.80	1.58	1.52	1.55	0.159	0.16	0.16	0.157	-26.86	-26.91	-26.89	1.99	1.80	1.89	9.85	9.85
10.75	34.75	1967.26	1.67		1.67	0.165		0.17	0.165	-27.14		-27.14	2.27		2.27	10.12	10.12
11.25	35.25	1966.71	1.62		1.62	0.156		0.16	0.156	-26.97		-26.97	1.98		1.98	10.35	10.35
11.75	35.75	1966.17	1.52		1.52	0.141		0.14	0.141	-26.57		-26.57	2.11		2.11	10.82	10.82
12.25	36.25	1965.63	1.48		1.48	0.128		0.13	0.128	-26.33		-26.33	2.08		2.08	11.59	11.59
12.75	36.75	1965.08	1.57		1.57	0.149		0.15	0.149	-26.91		-26.91	1.98		1.98	10.52	10.52
13.25	37.25	1964.54	1.56		1.56	0.160		0.16	0.160	-27.09		-27.09	1.85		1.85	9.77	9.77
13.75	37.75	1964.00	1.53		1.53	0.148		0.15	0.148	-26.57		-26.57	1.92		1.92	10.32	10.32
14.25	38.25	1963.46	1.55		1.55	0.148		0.15	0.148	-26.30		-26.30	1.91		1.91	10.51	10.51
14.75	38.75	1962.91	1.52		1.52	0.137		0.14	0.137	-26.38		-26.38	1.87		1.87	11.12	11.12
15.25	39.25	1962.37	1.54	1.57	1.55	0.142	0.14	0.14	0.142	-26.51	-26.66	-26.58	2.06	1.91	1.98	10.90	10.90
15.75	39.75	1961.83	1.61		1.61	0.152		0.15	0.152	-26.59		-26.59	1.89		1.89	10.62	10.62
16.25	40.25	1961.28	1.57		1.57	0.156		0.16	0.156	-27.10		-27.10	1.91		1.91	10.10	10.10
16.75	40.75	1960.74	1.66		1.66	0.163		0.16	0.163	-26.92		-26.92	1.90		1.90	10.16	10.16
17.25	41.25	1960.20	1.74		1.74	0.182		0.18	0.182	-27.00		-27.00	1.89		1.89	9.57	9.57
17.75	41.75	1959.65	1.74		1.74	0.179		0.18	0.179	-27.42		-27.42	2.05		2.05	9.71	9.71

PAD 15 VC3 Distal Site																	
Sample mid-depth	Adjusted mid-depth (+24cm)	Year AD	C_{org} (%)	Rpt	Avg	N (%)	Rpt	Avg	Corrected N (%) (-0.008%)	$\delta^{13}C_{org}$ (‰)	Rpt	Avg	$\delta^{15}N$ (‰)	Rpt	Avg	C/N	Corrected C/N
18.25	42.25	1959.11	1.51		1.51	0.168		0.17	0.168	-27.11		-27.11	1.97		1.97	8.98	8.98
18.75	42.75	1958.57	1.53		1.53	0.147		0.15	0.147	-26.47		-26.47	2.13		2.13	10.39	10.39
19.25	43.25	1958.02	1.81		1.81	0.186		0.19	0.186	-27.52		-27.52	1.88		1.88	9.73	9.73
19.75	43.75	1957.48	1.69		1.69	0.180		0.18	0.180	-27.41		-27.41	1.81		1.81	9.36	9.36
20.25	44.25	1956.94	1.71		1.71	0.176		0.18	0.176	-27.56		-27.56	1.95		1.95	9.72	9.72
20.75	44.75	1956.40	1.67		1.67	0.172		0.17	0.172	-27.20		-27.20	1.70		1.70	9.73	9.73
21.25	45.25	1955.85	1.87		1.87	0.185		0.19	0.185	-27.35		-27.35	1.97		1.97	10.10	10.10
21.75	45.75	1955.31	1.58		1.58	0.155		0.15	0.155	-27.07		-27.07	1.58		1.58	10.22	10.22
22.25	46.25	1954.77	1.62		1.62	0.161		0.16	0.161	-27.09		-27.09	2.23		2.23	10.10	10.10
22.75	46.75	1954.22	1.66		1.66	0.160		0.16	0.160	-26.80		-26.80	2.15		2.15	10.39	10.39
23.25	47.25	1953.68	1.73		1.73	0.171		0.17	0.171	-27.19		-27.19	1.81		1.81	10.13	10.13
23.75	47.75	1953.14	1.65		1.65	0.163		0.16	0.163	-27.01		-27.01	2.07		2.07	10.10	10.10
24.25	48.25	1952.59	1.49		1.49	0.126		0.13	0.126	-26.33		-26.33	2.31		2.31	11.87	11.87
24.75	48.75	1952.05	1.58		1.58	0.145		0.14	0.145	-26.39		-26.39	2.13		2.13	10.90	10.90
25.25	49.25	1951.51	1.66	1.68	1.67	0.157	0.16	0.16	0.157	-26.62	-26.67	-26.65	2.14	2.11	2.13	10.63	10.63
25.75	49.75	1950.97	1.56		1.56	0.154		0.15	0.154	-26.73		-26.73	2.09		2.09	10.14	10.14
26.25	50.25	1950.42	1.82		1.82	0.186		0.19	0.186	-26.71		-26.71	2.19		2.19	9.82	9.82
26.75	50.75	1949.88	1.55		1.55	0.160		0.16	0.160	-26.65		-26.65	2.17		2.17	9.70	9.70
27.25	51.25	1949.34	1.57		1.57	0.154		0.15	0.154	-26.61		-26.61	2.04		2.04	10.16	10.16
27.75	51.75	1948.79	1.66		1.66	0.164		0.16	0.164	-26.95		-26.95	2.27		2.27	10.09	10.09
28.25	52.25	1948.25	1.65		1.65	0.166		0.17	0.166	-26.79		-26.79	2.27		2.27	9.90	9.90
28.75	52.75	1947.71	1.65		1.65	0.168		0.17	0.168	-26.85		-26.85	1.97		1.97	9.83	9.83
29.25	53.25	1947.16	1.65		1.65	0.166		0.17	0.166	-26.77		-26.77	2.26		2.26	9.94	9.94
29.75	53.75	1946.62	1.63		1.63	0.162		0.16	0.162	-26.97		-26.97	2.29		2.29	10.07	10.07
30.25	54.25	1946.08	1.52		1.52	0.152		0.15	0.152	-26.54		-26.54	2.17		2.17	9.98	9.98
30.75	54.75	1945.53	1.55		1.55	0.147		0.15	0.147	-26.60		-26.60	2.24		2.24	10.51	10.51
31.25	55.25	1944.99	1.53		1.53	0.151		0.15	0.151	-26.77		-26.77	2.35		2.35	10.10	10.10
31.75	55.75	1944.45	1.49		1.49	0.154		0.15	0.154	-26.51		-26.51	1.99		1.99	9.65	9.65
32.25	56.25	1943.91	1.53		1.53	0.148		0.15	0.148	-26.18		-26.18	1.99		1.99	10.33	10.33
32.75	56.75	1943.36	1.45		1.45	0.129		0.13	0.129	-26.23		-26.23	2.16		2.16	11.18	11.18
33.25	57.25	1942.82	1.59		1.59	0.145		0.14	0.145	-26.27		-26.27	2.32		2.32	11.00	11.00
33.75	57.75	1942.28	1.47		1.47	0.138		0.14	0.138	-26.16		-26.16	1.60		1.60	10.66	10.66
34.25	58.25	1941.73	1.50		1.50	0.138		0.14	0.138	-26.26		-26.26	2.21		2.21	10.85	10.85
34.75	58.75	1941.19	1.54		1.54	0.158		0.16	0.158	-26.72		-26.72	2.07		2.07	9.79	9.79
35.25	59.25	1940.65	1.56	1.61	1.58	0.147	0.15	0.15	0.150	-26.25	-26.59	-26.42	2.16	2.19	2.18	10.58	10.58
35.75	59.75	1940.10	1.43		1.43	0.135		0.13	0.135	-26.22		-26.22	2.10		2.10	10.62	10.62
36.25	60.25	1939.56	1.50		1.50	0.134		0.13	0.134	-26.27		-26.27	2.16		2.16	11.14	11.14

PAD 15 VC3 Distal Site																	
Sample mid-depth	Adjusted mid-depth (+24cm)	Year AD	C_{org} (%)	Rpt	Avg	N (%)	Rpt	Avg	Corrected N (%) (-0.008%)	$\delta^{13}C_{org}$ (‰)	Rpt	Avg	$\delta^{15}N$ (‰)	Rpt	Avg	C/N	Corrected C/N
36.75	60.75	1939.02	1.46		1.46	0.141		0.14	0.141	-26.50		-26.50	2.19		2.19	10.37	10.37
37.25	61.25	1938.47	1.52		1.52	0.144		0.14	0.144	-26.47		-26.47	2.02		2.02	10.57	10.57
37.75	61.75	1937.93	1.59		1.59	0.155		0.16	0.155	-26.50		-26.50	2.11		2.11	10.25	10.25
38.25	62.25	1937.39	1.62		1.62	0.159		0.16	0.159	-27.17		-27.17	2.18		2.18	10.21	10.21
38.75	62.75	1936.85	1.55		1.55	0.148		0.15	0.148	-26.54		-26.54	2.26		2.26	10.47	10.47
39.25	63.25	1936.30	1.55		1.55	0.147		0.15	0.147	-26.75		-26.75	2.21		2.21	10.53	10.53
39.75	63.75	1935.76	1.63		1.63	0.160		0.16	0.160	-27.42		-27.42	1.94		1.94	10.21	10.21
40.25	64.25	1935.22	1.64		1.64	0.158		0.16	0.158	-26.86		-26.86	2.11		2.11	10.34	10.34
40.75	64.75	1934.67	1.67		1.67	0.164		0.16	0.164	-26.89		-26.89	2.33		2.33	10.13	10.13
41.25	65.25	1934.13	1.74		1.74	0.171		0.17	0.171	-26.90		-26.90	2.03		2.03	10.18	10.18
41.75	65.75	1933.59	1.59		1.59	0.150		0.15	0.150	-27.07		-27.07	2.00		2.00	10.57	10.57
42.25	66.25	1933.04	1.64		1.64	0.162		0.16	0.162	-27.47		-27.47	1.86		1.86	10.09	10.09
42.75	66.75	1932.50	1.68		1.68	0.162		0.16	0.162	-27.59		-27.59	1.98		1.98	10.41	10.41
43.25	67.25	1931.96	1.79		1.79	0.172		0.17	0.172	-27.54		-27.54	2.05		2.05	10.43	10.43
43.75	67.75	1931.41	1.56		1.56	0.146		0.15	0.146	-27.25		-27.25	2.08		2.08	10.73	10.73
44.25	68.25	1930.87	1.56		1.56	0.140		0.14	0.140	-27.03		-27.03	2.02		2.02	11.10	11.10
44.75	68.75	1930.33	1.60		1.60	0.145		0.14	0.145	-27.17		-27.17	1.86		1.86	11.08	11.08
45.25	69.25	1929.79	1.57		1.57	0.144		0.14	0.144	-27.00		-27.00	2.04		2.04	10.90	10.90
45.75	69.75	1929.24	1.61		1.61	0.145		0.14	0.145	-26.96		-26.96	2.00		2.00	11.15	11.15
46.25	70.25	1928.70	1.61		1.61	0.146		0.15	0.146	-27.28		-27.28	1.59		1.59	11.04	11.04
46.75	70.75	1928.16	1.65		1.65	0.160		0.16	0.160	-27.64		-27.64	1.81		1.81	10.30	10.30
47.25	71.25	1927.61	1.86		1.86	0.184		0.18	0.184	-27.49		-27.49	1.32		1.32	10.13	10.13
47.75	71.75	1927.07	1.69		1.69	0.176		0.18	0.176	-27.60		-27.60	2.21		2.21	9.62	9.62
48.25	72.25	1926.53	1.49		1.49	0.150		0.15	0.150	-26.19		-26.19	2.35		2.35	9.95	9.95
48.75	72.75	1925.98	1.60		1.60	0.164		0.16	0.164	-26.47		-26.47	2.06		2.06	9.74	9.74
49.25	73.25	1925.44	1.65		1.65	0.158		0.16	0.158	-26.25		-26.25	1.99		1.99	10.44	10.44
49.75	73.75	1924.90	1.73		1.73	0.167		0.17	0.167	-26.06		-26.06	1.84		1.84	10.38	10.38
50.25	74.25	1924.35	1.49		1.49	0.156		0.16	0.156	-26.36		-26.36	2.28		2.28	9.56	9.56
50.75	74.75	1923.81	1.62		1.62	0.174		0.17	0.174	-26.52		-26.52	2.35		2.35	9.33	9.33
51.25	75.25	1923.27	1.53		1.53	0.155		0.16	0.155	-26.49		-26.49	2.00		2.00	9.88	9.88
51.75	75.75	1922.73	1.66		1.66	0.178		0.18	0.178	-26.81		-26.81	2.10		2.10	9.33	9.33
52.25	76.25	1922.18	1.69		1.69	0.175		0.17	0.175	-26.97		-26.97	2.25		2.25	9.66	9.66
52.75	76.75	1921.64	1.64		1.64	0.156		0.16	0.156	-26.68		-26.68	2.07		2.07	10.51	10.51
53.25	77.25	1921.10	1.52		1.52	0.142		0.14	0.142	-26.60		-26.60	2.36		2.36	10.71	10.71
53.75	77.75	1920.55	1.44		1.44	0.135		0.13	0.135	-26.56		-26.56	2.18		2.18	10.67	10.67
54.25	78.25	1920.01	1.52		1.52	0.156		0.16	0.156	-26.88		-26.88	2.19		2.19	9.74	9.74
54.75	78.75	1919.47	1.49		1.49	0.142		0.14	0.142	-26.56		-26.56	2.18		2.18	10.51	10.51

PAD 15 VC3 Distal Site																	
Sample mid-depth	Adjusted mid-depth (+24cm)	Year AD	C_{org} (%)	Rpt	Avg	N (%)	Rpt	Avg	Corrected N (%) (-0.008%)	$\delta^{13}C_{org}$ (‰)	Rpt	Avg	$\delta^{15}N$ (‰)	Rpt	Avg	C/N	Corrected C/N
55.25	79.25	1918.92	1.50	1.49	1.49	0.147	0.14	0.14	0.143	-26.59	-26.46	-26.52	2.30	2.29	2.29	10.40	10.40
55.75	79.75	1918.38	1.46		1.46	0.138		0.14	0.138	-26.40		-26.40	2.19		2.19	10.59	10.59
56.25	80.25	1917.84	1.51		1.51	0.144		0.14	0.144	-26.46		-26.46	2.27		2.27	10.46	10.46
56.75	80.75	1917.29	1.49		1.49	0.153		0.15	0.153	-26.62		-26.62	2.31		2.31	9.71	9.71
57.25	81.25	1916.75	1.48		1.48	0.148		0.15	0.148	-26.38		-26.38	2.19		2.19	10.04	10.04
57.75	81.75	1916.21	1.57		1.57	0.160		0.16	0.160	-26.40		-26.40	2.06		2.06	9.85	9.85
58.25	82.25	1915.67	1.42		1.42	0.137		0.14	0.137	-26.51		-26.51	2.12		2.12	10.39	10.39
58.75	82.75	1915.12	1.52		1.52	0.139		0.14	0.139	-26.32		-26.32	2.29		2.29	10.92	10.92
59.25	83.25	1914.58	1.34		1.34	0.115		0.11	0.115	-26.27		-26.27	2.12		2.12	11.68	11.68
59.75	83.75	1914.04	1.51		1.51	0.138		0.14	0.138	-26.35		-26.35	2.22		2.22	10.93	10.93
60.25	84.25	1913.49	1.42		1.42	0.137		0.14	0.137	-26.49		-26.49	2.29		2.29	10.42	10.42
60.75	84.75	1912.95	1.55		1.55	0.148		0.15	0.148	-26.46		-26.46	2.27		2.27	10.48	10.48
61.25	85.25	1912.41	1.49		1.49	0.144		0.14	0.144	-26.29		-26.29	2.14		2.14	10.38	10.38
61.75	85.75	1911.86	1.47		1.47	0.136		0.14	0.136	-26.21		-26.21	2.37		2.37	10.87	10.87
62.25	86.25	1911.32	1.50		1.50	0.148		0.15	0.148	-26.44		-26.44	2.16		2.16	10.16	10.16
62.75	86.75	1910.78	1.45		1.45	0.140		0.14	0.140	-26.23		-26.23	2.21		2.21	10.40	10.40
63.25	87.25	1910.24	1.53		1.53	0.139		0.14	0.139	-26.22		-26.22	2.15		2.15	10.98	10.98
63.75	87.75	1909.69	1.43		1.43	0.130		0.13	0.130	-26.29		-26.29	2.23		2.23	11.06	11.06
64.25	88.25	1909.15	1.48		1.48	0.142		0.14	0.142	-26.46		-26.46	2.35		2.35	10.39	10.39
64.75	88.75	1908.61	1.42		1.42	0.131		0.13	0.131	-26.15		-26.15	2.37		2.37	10.89	10.89
65.25	89.25	1908.06	1.42	1.42	1.42	0.137	0.13	0.13	0.134	-26.63	-26.09	-26.36	2.25	2.09	2.17	10.58	10.58
65.75	89.75	1907.52	1.46		1.46	0.146		0.15	0.146	-26.33		-26.33	2.21		2.21	10.00	10.00
66.25	90.25	1906.98	1.44		1.44	0.132		0.13	0.132	-26.15		-26.15	2.32		2.32	10.90	10.90
66.75	90.75	1906.43	1.37		1.37	0.124		0.12	0.124	-26.20		-26.20	2.09		2.09	11.03	11.03
67.25	91.25	1905.89	1.35		1.35	0.117		0.12	0.117	-26.08		-26.08	2.16		2.16	11.56	11.56
67.75	91.75	1905.35	1.41		1.41	0.131		0.13	0.131	-26.30		-26.30	2.11		2.11	10.82	10.82
68.25	92.25	1904.80	1.43		1.43	0.148		0.15	0.148	-26.38		-26.38	2.11		2.11	9.61	9.61
68.75	92.75	1904.26	1.34		1.34	0.125		0.12	0.125	-26.18		-26.18	2.04		2.04	10.71	10.71
69.25	93.25	1903.72	1.31		1.31	0.126		0.13	0.126	-26.08		-26.08	2.06		2.06	10.38	10.38
69.75	93.75	1903.18	1.48		1.48	0.141		0.14	0.141	-26.23		-26.23	2.47		2.47	10.49	10.49
70.25	94.25	1902.63	1.39		1.39	0.126		0.13	0.126	-26.12		-26.12	2.53		2.53	10.99	10.99
70.75	94.75	1902.09	1.44		1.44	0.130		0.13	0.130	-26.19		-26.19	2.53		2.53	11.10	11.10
71.25	95.25	1901.55	1.35		1.35	0.130		0.13	0.130	-26.17		-26.17	2.29		2.29	10.38	10.38
71.75	95.75	1901.00	1.38		1.38	0.124		0.12	0.124	-26.03		-26.03	2.41		2.41	11.16	11.16
72.25	96.25	1900.46	1.33		1.33	0.112		0.11	0.112	-26.20		-26.20	2.20		2.20	11.93	11.93
72.75	96.75	1899.92	1.27		1.27	0.111		0.11	0.111	-26.35		-26.35	2.15		2.15	11.43	11.43
73.25	97.25	1899.37	1.34		1.34	0.126		0.13	0.126	-26.36		-26.36	2.34		2.34	10.60	10.60

PAD 15 VC3 Distal Site																	
Sample mid-depth	Adjusted mid-depth (+24cm)	Year AD	C_{org} (%)	Rpt	Avg	N (%)	Rpt	Avg	Corrected N (%) (-0.008%)	$\delta^{13}C_{org}$ (‰)	Rpt	Avg	$\delta^{15}N$ (‰)	Rpt	Avg	C/N	Corrected C/N
73.75	97.75	1898.83	1.46		1.46	0.131		0.13	0.131	-26.27		-26.27	2.04		2.04	11.10	11.10
74.25	98.25	1898.29	1.47		1.47	0.137		0.14	0.137	-26.27		-26.27	2.15		2.15	10.72	10.72
74.75	98.75	1897.74	1.49		1.49	0.146		0.15	0.146	-26.27		-26.27	2.24		2.24	10.20	10.20
75.25	99.25	1897.20	1.34	1.39	1.37	0.117	0.12	0.12	0.118	-26.26	-25.76	-26.01	2.20	2.19	2.19	11.55	11.55
75.75	99.75	1896.66	1.38		1.38	0.123		0.12	0.123	-26.26		-26.26	2.23		2.23	11.24	11.24
76.25	100.25	1896.12	1.52		1.52	0.135		0.13	0.135	-26.43		-26.43	2.24		2.24	11.30	11.30
76.75	100.75	1895.57	1.58		1.58	0.140		0.14	0.140	-26.47		-26.47	2.06		2.06	11.30	11.30
77.25	101.25	1895.03	1.47		1.47	0.137		0.14	0.137	-26.36		-26.36	2.10		2.10	10.67	10.67
77.75	101.75	1894.49	1.50		1.50	0.131		0.13	0.131	-26.25		-26.25	2.09		2.09	11.48	11.48
78.25	102.25	1893.94	1.52		1.52	0.135		0.14	0.135	-26.53		-26.53	2.27		2.27	11.26	11.26
78.75	102.75	1893.40	1.47		1.47	0.135		0.14	0.135	-26.27		-26.27	2.26		2.26	10.83	10.83
79.25	103.25	1892.86	1.47		1.47	0.139		0.14	0.139	-26.44		-26.44	2.35		2.35	10.61	10.61
79.75	103.75	1892.31	1.49		1.49	0.139		0.14	0.139	-26.50		-26.50	2.50		2.50	10.72	10.72
80.25	104.25	1891.77	1.51		1.51	0.138		0.14	0.138	-26.47		-26.47	2.36		2.36	10.94	10.94
80.75	104.75	1891.23	1.55		1.55	0.146		0.15	0.146	-26.33		-26.33	2.18		2.18	10.57	10.57
81.25	105.25	1890.68	1.52		1.52	0.142		0.14	0.142	-26.35		-26.35	2.11		2.11	10.71	10.71
81.75	105.75	1890.14	1.57		1.57	0.151		0.15	0.151	-26.38		-26.38	2.05		2.05	10.44	10.44
82.25	106.25	1889.60	1.57		1.57	0.143		0.14	0.143	-26.52		-26.52	2.32		2.32	11.04	11.04
82.75	106.75	1889.06	1.56		1.56	0.143		0.14	0.143	-25.97		-25.97	2.32		2.32	10.90	10.90
83.25	107.25	1888.51	1.34		1.34	0.114		0.11	0.114	-25.93		-25.93	2.30		2.30	11.77	11.77
83.75	107.75	1887.97	1.34		1.34	0.118		0.12	0.118	-26.37		-26.37	2.29		2.29	11.40	11.40
84.25	108.25	1887.43	1.52		1.52	0.143		0.14	0.143	-26.77		-26.77	2.40		2.40	10.59	10.59
84.75	108.75	1886.88	1.57		1.57	0.148		0.15	0.148	-26.37		-26.37	2.22		2.22	10.63	10.63
85.25	109.25	1886.34	1.53	1.50	1.52	0.145	0.14	0.14	0.144	-26.02	-25.94	-25.98	2.25	2.42	2.33	10.52	10.52
85.75	109.75	1885.80	1.48		1.48	0.138		0.14	0.138	-25.86		-25.86	2.16		2.16	10.75	10.75
86.25	110.25	1885.25	1.41		1.41	0.117		0.12	0.117	-25.80		-25.80	2.19		2.19	12.03	12.03
86.75	110.75	1884.71	1.36		1.36	0.121		0.12	0.121	-25.85		-25.85	2.23		2.23	11.21	11.21
87.25	111.25	1884.17	1.43		1.43	0.122		0.12	0.122	-25.75		-25.75	2.17		2.17	11.73	11.73
87.75	111.75	1883.62	1.33		1.33	0.123		0.12	0.123	-26.04		-26.04	2.22		2.22	10.82	10.82
88.25	112.25	1883.08	1.48		1.48	0.150		0.15	0.150	-26.07		-26.07	2.28		2.28	9.91	9.91
88.75	112.75	1882.54	1.48		1.48	0.135		0.13	0.135	-25.97		-25.97	2.12		2.12	10.98	10.98
89.25	113.25	1882.00	1.39		1.39	0.121		0.12	0.121	-25.55		-25.55	2.24		2.24	11.44	11.44
89.75	113.75	1881.45	1.48		1.48	0.138		0.14	0.138	-25.66		-25.66	2.39		2.39	10.78	10.78
90.25	114.25	1880.91	1.48		1.48	0.133		0.13	0.133	-25.46		-25.46	2.14		2.14	11.17	11.17
90.75	114.75	1880.37	1.50		1.50	0.125		0.12	0.125	-25.56		-25.56	2.13		2.13	12.01	12.01
91.25	115.25	1879.82	1.40		1.40	0.126		0.13	0.126	-25.57		-25.57	2.14		2.14	11.10	11.10
91.75	115.75	1879.28	1.48		1.48	0.144		0.14	0.144	-26.03		-26.03	2.43		2.43	10.28	10.28

PAD 15 VC3 Distal Site																	
Sample mid-depth	*Adjusted mid-depth (+24cm)*	*Year AD*	*C_{org} (%)*	*Rpt*	*Avg*	*N (%)*	*Rpt*	*Avg*	*Corrected N (%) (-0.008%)*	*$\delta^{13}C_{org}$ (‰)*	*Rpt*	*Avg*	*$\delta^{15}N$ (‰)*	*Rpt*	*Avg*	*C/N*	*Corrected C/N*
92.25	116.25	1878.74	1.47		1.47	0.143		0.14	0.143	-26.41		-26.41	2.41		2.41	10.28	10.28
92.75	116.75	1878.19	1.51		1.51	0.129		0.13	0.129	-26.11		-26.11	2.71		2.71	11.68	11.68
93.25	117.25	1877.65	1.35		1.35	0.116		0.12	0.116	-26.15		-26.15	2.64		2.64	11.61	11.61
93.75	117.75	1877.11	1.58		1.58	0.134		0.13	0.134	-26.24		-26.24	2.01		2.01	11.80	11.80
94.25	118.25	1876.57	1.54		1.54	0.145		0.14	0.145	-26.42		-26.42	2.24		2.24	10.60	10.60
94.75	118.75	1876.02	1.50		1.50	0.134		0.13	0.134	-26.47		-26.47	2.36		2.36	11.19	11.19
95.25	119.25	1875.48	1.47	1.50	1.48	0.137	0.14	0.14	0.138	-26.34	-26.23	-26.29	2.36	2.30	2.33	10.80	10.80
95.75	119.75	1874.94	1.48		1.48	0.132		0.13	0.132	-26.27		-26.27	2.26		2.26	11.22	11.22
96.25	120.25	1874.39	1.51		1.51	0.130		0.13	0.130	-26.33		-26.33	2.03		2.03	11.63	11.63
96.75	120.75	1873.85	1.46		1.46	0.134		0.13	0.134	-26.33		-26.33	2.20		2.20	10.88	10.88
97.25	121.25	1873.31	1.40		1.40	0.123		0.12	0.123	-26.30		-26.30	2.20		2.20	11.40	11.40
97.75	121.75	1872.76	1.36		1.36	0.125		0.13	0.125	-26.29		-26.29	2.06		2.06	10.91	10.91
98.25	122.25	1872.22	1.52		1.52	0.151		0.15	0.151	-26.58		-26.58	2.13		2.13	10.06	10.06
98.75	122.75	1871.68	1.58		1.58	0.153		0.15	0.153	-26.59		-26.59	2.05		2.05	10.32	10.32
99.25	123.25	1871.13	1.54		1.54	0.148		0.15	0.148	-26.56		-26.56	2.20		2.20	10.40	10.40
99.75	123.75	1870.59	1.55		1.55	0.150		0.15	0.150	-26.48		-26.48	2.20		2.20	10.31	10.31
100.25	124.25	1870.05	1.62		1.62	0.157		0.16	0.157	-26.48		-26.48	2.21		2.21	10.27	10.27
100.75	124.75	1869.51	1.53		1.53	0.151		0.15	0.151	-26.25		-26.25	2.09		2.09	10.13	10.13
101.25	125.25	1868.96	1.45		1.45	0.144		0.14	0.144	-26.37		-26.37	2.52		2.52	10.10	10.10
101.75	125.75	1868.42	1.51		1.51	0.146		0.15	0.146	-26.50		-26.50	2.43		2.43	10.38	10.38
102.25	126.25	1867.88	1.56		1.56	0.153		0.15	0.153	-26.60		-26.60	2.03		2.03	10.22	10.22
102.75	126.75	1867.33	1.46		1.46	0.133		0.13	0.133	-26.24		-26.24	2.11		2.11	10.95	10.95
103.25	127.25	1866.79	1.47		1.47	0.141		0.14	0.141	-26.20		-26.20	2.45		2.45	10.43	10.43
103.75	127.75	1866.25	1.50		1.50	0.143		0.14	0.143	-26.01		-26.01	2.07		2.07	10.49	10.49
104.25	128.25	1865.70	1.46		1.46	0.152		0.15	0.152	-25.95		-25.95	2.25		2.25	9.62	9.62
104.75	128.75	1865.16	1.43		1.43	0.134		0.13	0.134	-25.79		-25.79	2.17		2.17	10.66	10.66
105.25	129.25	1864.62	1.32	1.35	1.33	0.113	0.12	0.11	0.114	-25.73	-26.00	-25.87	2.25	2.08	2.16	11.70	11.70
105.75	129.75	1864.07	1.36		1.36	0.113		0.11	0.113	-26.24		-26.24	1.90		1.90	12.09	12.09
106.25	130.25	1863.53	1.33		1.33	0.108		0.11	0.108	-26.15		-26.15	1.67		1.67	12.26	12.26
106.75	130.75	1862.99	0.90		0.90	0.076		0.08	0.076	-26.05		-26.05	1.85		1.85	11.87	11.87
107.25	131.25	1862.45	1.29		1.29	0.121		0.12	0.121	-26.10		-26.10	2.19		2.19	10.70	10.70
107.75	131.75	1861.90	1.35		1.35	0.144		0.14	0.144	-26.22		-26.22	2.31		2.31	9.39	9.39
108.25	132.25	1861.36	1.40		1.40	0.143		0.14	0.143	-26.07		-26.07	2.21		2.21	9.78	9.78
108.75	132.75	1860.82	1.47		1.47	0.145		0.15	0.145	-26.20		-26.20	2.10		2.10	10.08	10.08
109.25	133.25	1860.27	1.37		1.37	0.125		0.13	0.125	-26.21		-26.21	1.84		1.84	10.92	10.92
109.75	133.75	1859.73	1.33		1.33	0.130		0.13	0.130	-26.29		-26.29	2.16		2.16	10.23	10.23
110.25	134.25	1859.19	1.48		1.48	0.159		0.16	0.159	-26.34		-26.34	2.35		2.35	9.34	9.34

PAD 15 VC3 Distal Site																	
Sample mid-depth	Adjusted mid-depth (+24cm)	Year AD	C_{org} (%)	Rpt	Avg	N (%)	Rpt	Avg	Corrected N (%) (-0.008%)	$\delta^{13}C_{org}$ (‰)	Rpt	Avg	$\delta^{15}N$ (‰)	Rpt	Avg	C/N	Corrected C/N
110.75	134.75	1858.64	1.52		1.52	0.154		0.15	0.154	-26.32		-26.32	2.14		2.14	9.90	9.90
111.25	135.25	1858.10	1.46		1.46	0.144		0.14	0.144	-26.35		-26.35	2.43		2.43	10.12	10.12
111.75	135.75	1857.56	1.54		1.54	0.154		0.15	0.154	-26.44		-26.44	2.35		2.35	10.01	10.01
112.25	136.25	1857.01	1.49		1.49	0.148		0.15	0.148	-26.34		-26.34	1.97		1.97	10.06	10.06
112.75	136.75	1856.47	1.49		1.49	0.152		0.15	0.152	-26.40		-26.40	2.18		2.18	9.80	9.80
113.25	137.25	1855.93	1.47		1.47	0.137		0.14	0.137	-26.18		-26.18	2.11		2.11	10.74	10.74
113.75	137.75	1855.39	1.41		1.41	0.135		0.14	0.135	-27.40		-27.40	1.96		1.96	10.44	10.44
114.25	138.25	1854.84	1.38		1.38	0.140		0.14	0.140	-26.07		-26.07	2.23		2.23	9.83	9.83
114.75	138.75	1854.30	1.47		1.47	0.132		0.13	0.132	-26.27		-26.27	2.05		2.05	11.14	11.14
115.25	139.25	1853.76	1.47	1.52	1.50	0.144	0.15	0.15	0.148	-26.37	-26.38	-26.38	2.05	2.41	2.23	10.13	10.13
115.75	139.75	1853.21	1.49		1.49	0.146		0.15	0.146	-26.36		-26.36	2.11		2.11	10.20	10.20
116.25	140.25	1852.67	1.48		1.48	0.154		0.15	0.154	-26.27		-26.27	2.48		2.48	9.62	9.62
116.75	140.75	1852.13	1.49		1.49	0.152		0.15	0.152	-26.26		-26.26	2.22		2.22	9.83	9.83
117.25	141.25	1851.58	1.50		1.50	0.164		0.16	0.164	-26.32		-26.32	2.39		2.39	9.13	9.13
117.75	141.75	1851.04	1.50		1.50	0.152		0.15	0.152	-26.25		-26.25	2.75		2.75	9.85	9.85
118.25	142.25	1850.50	1.51		1.51	0.152		0.15	0.152	-26.12		-26.12	2.38		2.38	9.96	9.96
118.75	142.75	1849.95	1.55		1.55	0.156		0.16	0.156	-26.19		-26.19	2.44		2.44	9.94	9.94
119.25	143.25	1849.41	1.50		1.50	0.150		0.15	0.150	-26.31		-26.31	2.66		2.66	9.97	9.97
119.75	143.75	1848.87	1.44		1.44	0.151		0.15	0.151	-26.43		-26.43	2.62		2.62	9.55	9.55
120.25	144.25	1848.33	1.49		1.49	0.144		0.14	0.144	-26.31		-26.31	2.21		2.21	10.37	10.37
120.75	144.75	1847.78	1.45		1.45	0.138		0.14	0.138	-26.26		-26.26	2.01		2.01	10.49	10.49
121.25	145.25	1847.24	1.40		1.40	0.133		0.13	0.133	-26.26		-26.26	2.09		2.09	10.56	10.56
121.75	145.75	1846.70	1.37		1.37	0.132		0.13	0.132	-26.21		-26.21	2.09		2.09	10.35	10.35
122.25	146.25	1846.15	1.16		1.16	0.103		0.10	0.103	-26.13		-26.13	1.81		1.81	11.32	11.32
122.75	146.75	1845.61	1.42		1.42	0.139		0.14	0.139	-26.38		-26.38	2.23		2.23	10.22	10.22
123.25	147.25	1845.07	1.40		1.40	0.143		0.14	0.143	-26.42		-26.42	2.31		2.31	9.76	9.76
123.75	147.75	1844.52	1.50		1.50	0.152		0.15	0.152	-26.28		-26.28	2.21		2.21	9.87	9.87
124.25	148.25	1843.98	1.45		1.45	0.139		0.14	0.139	-26.27		-26.27	2.23		2.23	10.48	10.48
124.75	148.75	1843.44	1.48		1.48	0.149		0.15	0.149	-26.44		-26.44	2.12		2.12	9.98	9.98
125.25	149.25	1842.90	1.53	1.43	1.48	0.149	0.14	0.14	0.143	-26.45	-26.41	-26.43	2.17	2.13	2.15	10.33	10.33
125.75	149.75	1842.35	1.39		1.39	0.130		0.13	0.130	-26.30		-26.30	2.24		2.24	10.68	10.68
126.25	150.25	1841.81	1.40		1.40	0.141		0.14	0.141	-26.43		-26.43	2.31		2.31	9.97	9.97
126.75	150.75	1841.27	1.46		1.46	0.147		0.15	0.147	-26.38		-26.38	2.44		2.44	9.94	9.94
127.25	151.25	1840.72	1.44		1.44	0.152		0.15	0.152	-26.38		-26.38	2.44		2.44	9.45	9.45
127.75	151.75	1840.18	1.47		1.47	0.153		0.15	0.153	-26.35		-26.35	2.36		2.36	9.61	9.61
128.25	152.25	1839.64	1.56		1.56	0.160		0.16	0.160	-26.50		-26.50	2.35		2.35	9.71	9.71
128.75	152.75	1839.09	1.48		1.48	0.149		0.15	0.149	-26.36		-26.36	2.25		2.25	9.95	9.95

PAD 15 VC3 Distal Site																	
Sample mid-depth	*Adjusted mid-depth (+24cm)*	*Year AD*	*C_{org} (%)*	*Rpt*	*Avg*	*N (%)*	*Rpt*	*Avg*	*Corrected N (%) (-0.008%)*	*$\delta^{13}C_{org}$ (‰)*	*Rpt*	*Avg*	*$\delta^{15}N$ (‰)*	*Rpt*	*Avg*	*C/N*	*Corrected C/N*
129.25	153.25	1838.55	1.48		1.48	0.141		0.14	0.141	-26.31		-26.31	2.27		2.27	10.48	10.48
129.75	153.75	1838.01	1.49		1.49	0.138		0.14	0.138	-26.46		-26.46	2.26		2.26	10.75	10.75
130.25	154.25	1837.46	1.47		1.47	0.142		0.14	0.142	-26.40		-26.40	2.23		2.23	10.37	10.37
130.75	154.75	1836.92	1.46		1.46	0.133		0.13	0.133	-26.28		-26.28	2.22		2.22	10.96	10.96
131.25	155.25	1836.38	1.49		1.49	0.147		0.15	0.147	-26.40		-26.40	2.24		2.24	10.14	10.14
131.75	155.75	1835.84	1.45		1.45	0.134		0.13	0.134	-26.37		-26.37	2.23		2.23	10.80	10.80
132.25	156.25	1835.29	1.53		1.53	0.133		0.13	0.133	-26.28		-26.28	2.15		2.15	11.46	11.46
132.75	156.75	1834.75	1.52		1.52	0.133		0.13	0.133	-26.17		-26.17	2.27		2.27	11.42	11.42
133.25	157.25	1834.21	1.47		1.47	0.130		0.13	0.130	-26.19		-26.19	2.34		2.34	11.34	11.34
133.75	157.75	1833.66	1.41		1.41	0.119		0.12	0.119	-25.73		-25.73	2.49		2.49	11.84	11.84
134.25	158.25	1833.12	1.58		1.58	0.147		0.15	0.147	-26.46		-26.46	2.32		2.32	10.75	10.75
134.75	158.75	1832.58	1.55		1.55	0.156		0.16	0.156	-26.51		-26.51	2.54		2.54	9.94	9.94
135.25	159.25	1832.03	1.47	1.49	1.48	0.139	0.14	0.14	0.141	-26.28	-26.30	-26.29	2.02	2.24	2.13	10.54	10.54
135.75	159.75	1831.49	1.44		1.44	0.131		0.13	0.131	-26.11		-26.11	2.32		2.32	10.95	10.95
136.25	160.25	1830.95	1.36		1.36	0.119		0.12	0.119	-26.11		-26.11	2.25		2.25	11.47	11.47
136.75	160.75	1830.40	1.27		1.27	0.104		0.10	0.104	-26.23		-26.23	2.39		2.39	12.20	12.20
137.25	161.25	1829.86	1.15		1.15	0.095		0.09	0.095	-26.14		-26.14	2.04		2.04	12.18	12.18
137.75	161.75	1829.32	1.48		1.48	0.115		0.12	0.115	-26.41		-26.41	1.99		1.99	12.87	12.87
138.25	162.25	1828.78	1.23		1.23	0.090		0.09	0.090	-26.35		-26.35	1.85		1.85	13.66	13.66
138.75	162.75	1828.23	1.35		1.35	0.104		0.10	0.104	-26.13		-26.13	1.93		1.93	12.90	12.90
139.25	163.25	1827.69	1.36		1.36	0.108		0.11	0.108	-26.21		-26.21	2.01		2.01	12.66	12.66
139.75	163.75	1827.15	1.42		1.42	0.125		0.12	0.125	-26.31		-26.31	2.14		2.14	11.38	11.38
140.25	164.25	1826.60	1.53		1.53	0.136		0.14	0.136	-26.64		-26.64	2.95		2.95	11.24	11.24
140.75	164.75	1826.06	1.57		1.57	0.141		0.14	0.141	-26.71		-26.71	2.89		2.89	11.14	11.14
141.25	165.25	1825.52	1.56		1.56	0.146		0.15	0.146	-26.73		-26.73	2.75		2.75	10.74	10.74
141.75	165.75	1824.97	1.57		1.57	0.141		0.14	0.141	-26.47		-26.47	2.64		2.64	11.12	11.12
142.25	166.25	1824.43	1.47		1.47	0.129		0.13	0.129	-26.46		-26.46	2.38		2.38	11.35	11.35
142.75	166.75	1823.89	1.49		1.49	0.131		0.13	0.131	-26.32		-26.32	2.22		2.22	11.42	11.42
143.25	167.25	1823.34	1.56		1.56	0.138		0.14	0.138	-25.98		-25.98	2.40		2.40	11.34	11.34
143.75	167.75	1822.80	1.44		1.44	0.121		0.12	0.121	-25.93		-25.93	3.87		3.87	11.95	11.95
144.25	168.25	1822.26	1.63		1.63	0.133		0.13	0.133	-26.16		-26.16	3.03		3.03	12.24	12.24
144.75	168.75	1821.72	1.48		1.48	0.129		0.13	0.129	-26.05		-26.05	5.62		5.62	11.46	11.46
145.25	169.25	1821.17	1.58	1.58	1.58	0.139	0.13	0.14	0.135	-26.10	-27.15	-26.62	1.58	2.01	1.80	11.66	11.66
145.75	169.75	1820.63	1.77		1.77	0.139		0.14	0.139	-26.04		-26.04	2.07		2.07	12.70	12.70
146.25	170.25	1820.09	1.59		1.59	0.127		0.13	0.127	-25.99		-25.99	1.93		1.93	12.54	12.54
146.75	170.75	1819.54	1.89		1.89	0.118		0.12	0.118	-25.78		-25.78	1.22		1.22	15.95	15.95
147.25	171.25	1819.00	1.64		1.64	0.113		0.11	0.113	-25.87		-25.87	1.64		1.64	14.50	14.50

PAD 15 VC3 Distal Site																	
Sample mid-depth	Adjusted mid-depth (+24cm)	Year AD	C_{org} (%)	Rpt	Avg	N (%)	Rpt	Avg	Corrected N (%) (-0.008%)	$\delta^{13}C_{org}$ (‰)	Rpt	Avg	$\delta^{15}N$ (‰)	Rpt	Avg	C/N	Corrected C/N
147.75	171.75	1818.46	1.72		1.72	0.136		0.14	0.136	-25.98		-25.98	2.05		2.05	12.58	12.58
148.25	172.25	1817.91	1.63		1.63	0.141		0.14	0.141	-25.89		-25.89	2.00		2.00	11.56	11.56
148.75	172.75	1817.37	1.63		1.63	0.155		0.15	0.155	-26.19		-26.19	2.13		2.13	10.57	10.57
149.25	173.25	1816.83	1.67		1.67	0.167		0.17	0.167	-26.20		-26.20	2.26		2.26	10.00	10.00
149.75	173.75	1816.28	1.56		1.56	0.140		0.14	0.140	-26.20		-26.20	2.19		2.19	11.08	11.08
150.25	174.25	1815.74	1.57		1.57	0.153		0.15	0.153	-26.28		-26.28	2.36		2.36	10.29	10.29
150.75	174.75	1815.20	1.55		1.55	0.148		0.15	0.148	-26.15		-26.15	2.20		2.20	10.43	10.43
151.25	175.25	1814.66	1.59		1.59	0.158		0.16	0.158	-26.21		-26.21	2.24		2.24	10.06	10.06
151.75	175.75	1814.11	1.58		1.58	0.146		0.15	0.146	-26.19		-26.19	2.11		2.11	10.82	10.82
152.25	176.25	1813.57	1.63		1.63	0.161		0.16	0.161	-27.29		-27.29	2.47		2.47	10.13	10.13
152.75	176.75	1813.03	1.58		1.58	0.162		0.16	0.162	-26.03		-26.03	2.43		2.43	9.75	9.75
153.25	177.25	1812.48	1.57		1.57	0.159		0.16	0.159	-26.04		-26.04	2.41		2.41	9.86	9.86
153.75	177.75	1811.94	1.66		1.66	0.169		0.17	0.169	-26.26		-26.26	2.43		2.43	9.79	9.79
154.25	178.25	1811.40	1.55		1.55	0.161		0.16	0.161	-26.23		-26.23	2.18		2.18	9.62	9.62
154.75	178.75	1810.85	1.59		1.59	0.162		0.16	0.162	-26.13		-26.13	2.39		2.39	9.84	9.84
155.25	179.25	1810.31	1.60	1.60	1.60	0.164	0.16	0.16	0.165	-26.36	-26.36	-26.36	2.31	2.43	2.37	9.72	9.72
155.75	179.75	1809.77	1.61		1.61	0.168		0.17	0.168	-26.43		-26.43	2.37		2.37	9.56	9.56
156.25	180.25	1809.23	1.64		1.64	0.162		0.16	0.162	-26.27		-26.27	2.14		2.14	10.08	10.08
156.75	180.75	1808.68	1.61		1.61	0.168		0.17	0.168	-26.32		-26.32	2.24		2.24	9.59	9.59
157.25	181.25	1808.14	1.60		1.60	0.154		0.15	0.154	-26.18		-26.18	2.16		2.16	10.37	10.37
157.75	181.75	1807.60	1.60		1.60	0.150		0.15	0.150	-26.03		-26.03	2.11		2.11	10.66	10.66
158.25	182.25	1807.05	1.47		1.47	0.125		0.12	0.125	-26.02		-26.02	2.05		2.05	11.81	11.81
158.75	182.75	1806.51	1.52		1.52	0.137		0.14	0.137	-27.17		-27.17	2.35		2.35	11.15	11.15
159.25	183.25	1805.97	1.52		1.52	0.167		0.17	0.167	-26.24		-26.24	2.38		2.38	9.12	9.12
159.75	183.75	1805.42	1.55		1.55	0.157		0.16	0.157	-26.24		-26.24	2.08		2.08	9.83	9.83
160.25	184.25	1804.88	1.59		1.59	0.154		0.15	0.154	-26.04		-26.04	2.08		2.08	10.36	10.36
160.75	184.75	1804.34	1.54		1.54	0.155		0.16	0.155	-26.18		-26.18	2.26		2.26	9.95	9.95
161.25	185.25	1803.79	1.53		1.53	0.132		0.13	0.132	-26.03		-26.03	2.15		2.15	11.59	11.59
161.75	185.75	1803.25	1.32		1.32	0.112		0.11	0.112	-26.02		-26.02	1.93		1.93	11.76	11.76
162.25	186.25	1802.71	1.54		1.54	0.146		0.15	0.146	-25.96		-25.96	2.25		2.25	10.57	10.57
162.75	186.75	1802.17	1.63		1.63	0.162		0.16	0.162	-26.11		-26.11	2.31		2.31	10.02	10.02
163.25	187.25	1801.62	1.68		1.68	0.171		0.17	0.171	-26.15		-26.15	2.30		2.30	9.79	9.79
163.75	187.75	1801.08	1.57		1.57	0.172		0.17	0.172	-26.23		-26.23	2.50		2.50	9.12	9.12
164.25	188.25	1800.54	1.60		1.60	0.170		0.17	0.170	-26.05		-26.05	2.39		2.39	9.42	9.42
164.75	188.75	1799.99	1.57		1.57	0.165		0.17	0.165	-26.18		-26.18	2.29		2.29	9.48	9.48
165.25	189.25	1799.45	1.56	1.62	1.59	0.164	0.17	0.16	0.165	-26.30	-26.23	-26.27	2.36	2.26	2.31	9.66	9.66
165.75	189.75	1798.91	1.60		1.60	0.162		0.16	0.162	-26.12		-26.12	2.29		2.29	9.90	9.90

PAD 15 VC3 Distal Site																	
Sample mid-depth	*Adjusted mid-depth (+24cm)*	*Year AD*	*C_{org} (%)*	*Rpt*	*Avg*	*N (%)*	*Rpt*	*Avg*	*Corrected N (%) (-0.008%)*	*$\delta^{13}C_{org}$ (‰)*	*Rpt*	*Avg*	*$\delta^{15}N$ (‰)*	*Rpt*	*Avg*	*C/N*	*Corrected C/N*
166.25	190.25	1798.36	1.42		1.42	0.150		0.15	0.150	-26.23		-26.23	2.11		2.11	9.43	9.43
166.75	190.75	1797.82	1.58		1.58	0.164		0.16	0.164	-26.28		-26.28	2.27		2.27	9.64	9.64
167.25	191.25	1797.28	1.59		1.59	0.153		0.15	0.153	-26.19		-26.19	2.30		2.30	10.39	10.39
167.75	191.75	1796.73	1.64		1.64	0.162		0.16	0.162	-26.38		-26.38	2.46		2.46	10.15	10.15
168.25	192.25	1796.19	1.66		1.66	0.164		0.16	0.164	-26.36		-26.36	2.37		2.37	10.12	10.12
168.75	192.75	1795.65	1.66		1.66	0.161		0.16	0.161	-26.30		-26.30	2.01		2.01	10.34	10.34
169.25	193.25	1795.11	1.64		1.64	0.153		0.15	0.153	-26.18		-26.18	1.93		1.93	10.71	10.71
169.75	193.75	1794.56	1.70		1.70	0.173		0.17	0.173	-26.27		-26.27	2.21		2.21	9.84	9.84
170.25	194.25	1794.02	1.58		1.58	0.156		0.16	0.156	-26.28		-26.28	2.14		2.14	10.08	10.08
170.75	194.75	1793.48	1.65		1.65	0.157		0.16	0.157	-26.26		-26.26	2.21		2.21	10.48	10.48
171.25	195.25	1792.93	1.57		1.57	0.171		0.17	0.171	-26.32		-26.32	1.87		1.87	9.17	9.17
171.75	195.75	1792.39	1.50		1.50	0.163		0.16	0.163	-26.40		-26.40	2.21		2.21	9.18	9.18
172.25	196.25	1791.85	1.67		1.67	0.180		0.18	0.180	-26.44		-26.44	2.22		2.22	9.28	9.28
172.75	196.75	1791.30	1.49		1.49	0.165		0.16	0.165	-26.42		-26.42	2.14		2.14	9.00	9.00
173.25	197.25	1790.76	1.63		1.63	0.164		0.16	0.164	-26.34		-26.34	2.04		2.04	9.94	9.94
173.75	197.75	1790.22	1.56		1.56	0.163		0.16	0.163	-26.31		-26.31	2.22		2.22	9.55	9.55
174.25	198.25	1789.67	1.56		1.56	0.170		0.17	0.170	-26.45		-26.45	2.04		2.04	9.17	9.17
174.75	198.75	1789.13	1.57		1.57	0.164		0.16	0.164	-26.41		-26.41	1.81		1.81	9.61	9.61
175.25	199.25	1788.59	1.47	1.64	1.55	0.141	0.15	0.15	0.147	-25.99	-25.84	-25.91	2.06	2.13	2.09	10.56	10.56
175.75	199.75	1788.05	1.19		1.19	0.103		0.10	0.103	-26.30		-26.30	1.57		1.57	11.53	11.53
176.25	200.25	1787.50	1.22		1.22	0.098		0.10	0.098	-26.11		-26.11	1.64		1.64	12.38	12.38
176.75	200.75	1786.96	1.26		1.26	0.103		0.10	0.103	-26.02		-26.02	1.77		1.77	12.28	12.28
177.25	201.25	1786.42	1.52		1.52	0.113		0.11	0.113	-25.86		-25.86	1.54		1.54	13.39	13.39
177.75	201.75	1785.87	1.55		1.55	0.128		0.13	0.128	-25.78		-25.78	2.15		2.15	12.09	12.09
178.25	202.25	1785.33	1.82		1.82	0.145		0.14	0.145	-26.07		-26.07	1.84		1.84	12.62	12.62
178.75	202.75	1784.79	1.50		1.50	0.141		0.14	0.141	-27.33		-27.33	2.05		2.05	10.65	10.65
179.25	203.25	1784.24	1.61		1.61	0.159		0.16	0.159	-26.26		-26.26	1.69		1.69	10.09	10.09
179.75	203.75	1783.70	1.46		1.46	0.147		0.15	0.147	-26.18		-26.18	1.82		1.82	9.97	9.97
180.25	204.25	1783.16	1.40		1.40	0.132		0.13	0.132	-26.57		-26.57	1.82		1.82	10.67	10.67
180.75	204.75	1782.61	1.12		1.12	0.100		0.10	0.100	-26.36		-26.36	2.10		2.10	11.18	11.18
181.25	205.25	1782.07	1.15		1.15	0.096		0.10	0.096	-26.42		-26.42	2.01		2.01	11.97	11.97
181.75	205.75	1781.53	1.03		1.03	0.079		0.08	0.079	-26.32		-26.32	2.08		2.08	12.95	12.95
182.25	206.25	1780.99	1.04		1.04	0.086		0.09	0.086	-26.44		-26.44	2.06		2.06	12.11	12.11
182.75	206.75	1780.44	1.28		1.28	0.110		0.11	0.110	-26.35		-26.35	2.57		2.57	11.63	11.63
183.25	207.25	1779.90	1.60		1.60	0.144		0.14	0.144	-26.50		-26.50	2.60		2.60	11.09	11.09
183.75	207.75	1779.36	1.62		1.62	0.138		0.14	0.138	-26.57		-26.57	2.07		2.07	11.78	11.78
184.25	208.25	1778.81	1.30		1.30	0.107		0.11	0.107	-26.39		-26.39	2.30		2.30	12.12	12.12

PAD 15 VC3 Distal Site																	
Sample mid-depth	Adjusted mid-depth (+24cm)	Year AD	C_{org} (%)	Rpt	Avg	N (%)	Rpt	Avg	Corrected N (%) (-0.008%)	$\delta^{13}C_{org}$ (‰)	Rpt	Avg	$\delta^{15}N$ (‰)	Rpt	Avg	C/N	Corrected C/N
184.75	208.75	1778.27	0.99		0.99	0.087		0.09	0.087	-26.34		-26.34	2.32		2.32	11.45	11.45
185.25	209.25	1777.73	1.43	1.41	1.42	0.116	0.12	0.12	0.119	-26.25	-26.32	-26.28	1.84	2.10	1.97	11.97	11.97
185.75	209.75	1777.18	1.37		1.37	0.114		0.11	0.114	-26.56		-26.56	2.27		2.27	11.98	11.98
186.25	210.25	1776.64	1.51		1.51	0.135		0.13	0.135	-26.71		-26.71	2.42		2.42	11.23	11.23
186.75	210.75	1776.10	1.41		1.41	0.150		0.15	0.150	-26.79		-26.79	2.38		2.38	9.39	9.39
187.25	211.25	1775.56	1.49		1.49	0.133		0.13	0.133	-26.66		-26.66	2.23		2.23	11.24	11.24
187.75	211.75	1775.01	1.34		1.34	0.115		0.12	0.115	-26.55		-26.55	2.28		2.28	11.59	11.59
188.25	212.25	1774.47	1.54		1.54	0.133		0.13	0.133	-26.71		-26.71	2.02		2.02	11.57	11.57
188.75	212.75	1773.93	1.44		1.44	0.144		0.14	0.144	-26.72		-26.72	1.64		1.64	9.99	9.99
189.25	213.25	1773.38	1.54		1.54	0.166		0.17	0.166	-26.64		-26.64	1.81		1.81	9.27	9.27
189.75	213.75	1772.84	1.59		1.59	0.182		0.18	0.182	-26.61		-26.61	1.85		1.85	8.76	8.76
190.25	214.25	1772.30	1.58		1.58	0.168		0.17	0.168	-26.36		-26.36	2.00		2.00	9.38	9.38
190.75	214.75	1771.75	1.39		1.39	0.145		0.15	0.145	-26.30		-26.30	2.43		2.43	9.53	9.53
191.25	215.25	1771.21	1.35		1.35	0.147		0.15	0.147	-26.36		-26.36	2.07		2.07	9.16	9.16
191.75	215.75	1770.67	1.53		1.53	0.166		0.17	0.166	-26.25		-26.25	2.12		2.12	9.23	9.23
192.25	216.25	1770.12	1.50		1.50	0.160		0.16	0.160	-26.12		-26.12	2.48		2.48	9.41	9.41
192.75	216.75	1769.58	1.47		1.47	0.155		0.16	0.155	-26.31		-26.31	2.02		2.02	9.49	9.49
193.25	217.25	1769.04	1.47		1.47	0.151		0.15	0.151	-26.30		-26.30	2.05		2.05	9.71	9.71
193.75	217.75	1768.50	1.52		1.52	0.149		0.15	0.149	-26.42		-26.42	2.58		2.58	10.20	10.20
194.25	218.25	1767.95	1.63		1.63	0.152		0.15	0.152	-27.62		-27.62	2.22		2.22	10.76	10.76
194.75	218.75	1767.41	1.48		1.48	0.145		0.15	0.145	-26.61		-26.61	1.99		1.99	10.21	10.21
195.25	219.25	1766.87	1.46	1.48	1.47	0.143	0.14	0.14	0.143	-26.40	-26.44	-26.42	2.19	2.35	2.27	10.25	10.25
195.75	219.75	1766.32	1.58		1.58	0.153		0.15	0.153	-26.60		-26.60	2.15		2.15	10.33	10.33
196.25	220.25	1765.78	1.56		1.56	0.154		0.15	0.154	-26.50		-26.50	2.09		2.09	10.07	10.07
196.75	220.75	1765.24	1.61		1.61	0.150		0.15	0.150	-26.46		-26.46	2.19		2.19	10.74	10.74
197.25	221.25	1764.69	1.47		1.47	0.123		0.12	0.123	-26.49		-26.49	2.47		2.47	11.95	11.95
197.75	221.75	1764.15	1.52		1.52	0.157		0.16	0.157	-26.65		-26.65	2.11		2.11	9.69	9.69
198.25	222.25	1763.61	1.61		1.61	0.155		0.15	0.155	-26.12		-26.12	2.10		2.10	10.44	10.44
198.75	222.75	1763.06	1.64		1.64	0.149		0.15	0.149	-25.91		-25.91	2.39		2.39	11.00	11.00
199.25	223.25	1762.52	1.45		1.45	0.142		0.14	0.142	-25.95		-25.95	2.54		2.54	10.22	10.22
199.75	223.75	1761.98	1.50		1.50	0.140		0.14	0.140	-25.89		-25.89	3.12		3.12	10.70	10.70
200.25	224.25	1761.44	1.54		1.54	0.141		0.14	0.141	-25.95		-25.95	2.36		2.36	10.88	10.88
200.75	224.75	1760.89	1.48		1.48	0.143		0.14	0.143	-25.93		-25.93	2.38		2.38	10.33	10.33
201.25	225.25	1760.35	1.34		1.34	0.133		0.13	0.133	-26.02		-26.02	3.39		3.39	10.11	10.11
201.75	225.75	1759.81	1.53		1.53	0.141		0.14	0.141	-25.83		-25.83	1.69		1.69	10.88	10.88
202.25	226.25	1759.26	1.66		1.66	0.151		0.15	0.151	-25.75		-25.75	1.75		1.75	11.00	11.00
202.75	226.75	1758.72	1.54		1.54	0.143		0.14	0.143	-25.78		-25.78	2.83		2.83	10.78	10.78

PAD 15 VC3 Distal Site																	
Sample mid-depth	Adjusted mid-depth (+24cm)	Year AD	C_{org} (%)	Rpt	Avg	N (%)	Rpt	Avg	Corrected N (%) (-0.008%)	$\delta^{13}C_{org}$ (‰)	Rpt	Avg	$\delta^{15}N$ (‰)	Rpt	Avg	C/N	Corrected C/N
203.25	227.25	1758.18	1.40		1.40	0.136		0.14	0.136	-25.88		-25.88	3.02		3.02	10.28	10.28
203.75	227.75	1757.63	1.62		1.62	0.143		0.14	0.143	-25.74		-25.74	2.61		2.61	11.26	11.26
204.25	228.25	1757.09	1.63		1.63	0.144		0.14	0.144	-26.02		-26.02	2.34		2.34	11.30	11.30
204.75	228.75	1756.55	1.57		1.57	0.142		0.14	0.142	-25.83		-25.83	2.42		2.42	11.06	11.06
205.25	229.25	1756.00	1.53	1.56	1.54	0.136	0.14	0.14	0.137	-25.81	-25.79	-25.80	1.99	2.10	2.04	11.29	11.29
205.75	229.75	1755.46	1.59		1.59	0.135		0.14	0.135	-25.78		-25.78	2.13		2.13	11.77	11.77
206.25	230.25	1754.92	1.50		1.50	0.136		0.14	0.136	-25.63		-25.63	2.46		2.46	11.06	11.06
206.75	230.75	1754.38	1.61		1.61	0.131		0.13	0.131	-25.63		-25.63	2.06		2.06	12.30	12.30
207.25	231.25	1753.83	1.42		1.42	0.121		0.12	0.121	-25.71		-25.71	2.17		2.17	11.77	11.77
207.75	231.75	1753.29	1.43		1.43	0.121		0.12	0.121	-25.66		-25.66	2.42		2.42	11.86	11.86
208.25	232.25	1752.75	1.17		1.17	0.111		0.11	0.111	-26.05		-26.05	2.29		2.29	10.54	10.54
208.75	232.75	1752.20	1.54		1.54	0.153		0.15	0.153	-26.66		-26.66	2.13		2.13	10.10	10.10
209.25	233.25	1751.66	1.22		1.22	0.117		0.12	0.117	-25.97		-25.97	2.49		2.49	10.45	10.45
209.75	233.75	1751.12	1.34		1.34	0.121		0.12	0.121	-25.86		-25.86	2.33		2.33	11.09	11.09
210.25	234.25	1750.57	1.01		1.01	0.098		0.10	0.098	-26.02		-26.02	2.27		2.27	10.33	10.33
210.75	234.75	1750.03	1.29		1.29	0.115		0.11	0.115	-25.91		-25.91	2.14		2.14	11.27	11.27
211.25	235.25	1749.49	1.36		1.36	0.112		0.11	0.112	-25.77		-25.77	1.80		1.80	12.16	12.16
211.75	235.75	1748.94	1.30		1.30	0.109		0.11	0.109	-25.75		-25.75	2.29		2.29	11.97	11.97
212.25	236.25	1748.40	1.26		1.26	0.114		0.11	0.114	-25.97		-25.97	2.07		2.07	11.05	11.05
212.75	236.75	1747.86	1.36		1.36	0.121		0.12	0.121	-25.72		-25.72	2.43		2.43	11.32	11.32
213.25	237.25	1747.32	1.10		1.10	0.110		0.11	0.110	-26.18		-26.18	2.06		2.06	9.99	9.99
213.75	237.75	1746.77	1.35		1.35	0.118		0.12	0.118	-26.08		-26.08	2.40		2.40	11.48	11.48
214.25	238.25	1746.23	1.21		1.21	0.116		0.12	0.116	-26.06		-26.06	2.44		2.44	10.48	10.48
214.75	238.75	1745.69	1.37		1.37	0.124		0.12	0.124	-26.05		-26.05	2.49		2.49	11.03	11.03
215.25	239.25	1745.14	1.53	1.24	1.38	0.128	0.11	0.12	0.121	-25.84	-25.96	-25.90	2.23	2.09	2.16	11.43	11.43
215.75	239.75	1744.60	1.28		1.28	0.099		0.10	0.099	-26.03		-26.03	2.09		2.09	12.98	12.98
216.25	240.25	1744.06	1.17		1.17	0.095		0.10	0.095	-25.95		-25.95	2.08		2.08	12.21	12.21
216.75	240.75	1743.51	1.18		1.18	0.100		0.10	0.100	-26.06		-26.06	2.27		2.27	11.87	11.87
217.25	241.25	1742.97	1.48		1.48	0.128		0.13	0.128	-25.85		-25.85	2.20		2.20	11.52	11.52
217.75	241.75	1742.43	1.10		1.10	0.103		0.10	0.103	-26.12		-26.12	2.34		2.34	10.71	10.71
218.25	242.25	1741.88	1.25		1.25	0.106		0.11	0.106	-26.04		-26.04	1.88		1.88	11.84	11.84
218.75	242.75	1741.34	1.39		1.39	0.129		0.13	0.129	-26.03		-26.03	2.36		2.36	10.81	10.81
219.25	243.25	1740.80	1.32		1.32	0.125		0.12	0.125	-26.01		-26.01	2.26		2.26	10.54	10.54
219.75	243.75	1740.26	1.60		1.60	0.148		0.15	0.148	-26.18		-26.18	2.01		2.01	10.79	10.79
220.25	244.25	1739.71	1.52		1.52	0.140		0.14	0.140	-26.06		-26.06	1.88		1.88	10.90	10.90
220.75	244.75	1739.17	1.48		1.48	0.135		0.14	0.135	-26.16		-26.16	2.33		2.33	10.95	10.95
221.25	245.25	1738.63	1.49		1.49	0.136		0.14	0.136	-25.97		-25.97	1.83		1.83	10.95	10.95

PAD 15 VC3 Distal Site																	
Sample mid-depth	Adjusted mid-depth (+24cm)	Year AD	C_{org} (%)	Rpt	Avg	N (%)	Rpt	Avg	Corrected N (%) (-0.008%)	$\delta^{13}C_{org}$ (‰)	Rpt	Avg	$\delta^{15}N$ (‰)	Rpt	Avg	C/N	Corrected C/N
221.75	245.75	1738.08	1.36		1.36	0.129		0.13	0.129	-26.13		-26.13	1.88		1.88	10.54	10.54
222.25	246.25	1737.54	1.14		1.14	0.113		0.11	0.113	-26.03		-26.03	1.72		1.72	10.13	10.13
222.75	246.75	1737.00	1.44		1.44	0.128		0.13	0.128	-25.99		-25.99	2.08		2.08	11.21	11.21
223.25	247.25	1736.45	1.43		1.43	0.128		0.13	0.128	-26.18		-26.18	1.85		1.85	11.24	11.24
223.75	247.75	1735.91	1.35		1.35	0.123		0.12	0.123	-26.19		-26.19	1.89		1.89	11.02	11.02
224.25	248.25	1735.37	1.54		1.54	0.131		0.13	0.131	-25.96		-25.96	1.74		1.74	11.79	11.79
224.75	248.75	1734.83	1.30		1.30	0.118		0.12	0.118	-25.80		-25.80	1.46		1.46	11.02	11.02
225.25	249.25	1734.28	1.09	1.23	1.16	0.108	0.11	0.11	0.111	-26.06	-26.04	-26.05	1.86	1.72	1.79	10.52	10.52
225.75	249.75	1733.74	1.15		1.15	0.100		0.10	0.100	-25.68		-25.68	1.96		1.96	11.55	11.55
226.25	250.25	1733.20	1.28		1.28	0.110		0.11	0.110	-25.79		-25.79	1.68		1.68	11.62	11.62
226.75	250.75	1732.65	1.39		1.39	0.114		0.11	0.114	-25.72		-25.72	1.71		1.71	12.21	12.21
227.25	251.25	1732.11	1.02		1.02	0.089		0.09	0.089	-25.73		-25.73	1.79		1.79	11.46	11.46
227.75	251.75	1731.57	1.47		1.47	0.120		0.12	0.120	-25.82		-25.82	2.03		2.03	12.25	12.25
228.25	252.25	1731.02	1.24		1.24	0.104		0.10	0.104	-25.72		-25.72	1.96		1.96	11.97	11.97
228.75	252.75	1730.48	1.19		1.19	0.101		0.10	0.101	-25.82		-25.82	2.03		2.03	11.77	11.77
229.25	253.25	1729.94	1.42		1.42	0.111		0.11	0.111	-25.76		-25.76	2.45		2.45	12.81	12.81
229.75	253.75	1729.39	1.58		1.58	0.120		0.12	0.120	-26.22		-26.22	1.53		1.53	13.20	13.20
230.25	254.25	1728.85	1.25		1.25	0.100		0.10	0.100	-26.03		-26.03	2.13		2.13	12.59	12.59
230.75	254.75	1728.31	1.39		1.39	0.110		0.11	0.110	-25.83		-25.83	2.29		2.29	12.62	12.62
231.25	255.25	1727.77	1.35		1.35	0.110		0.11	0.110	-25.82		-25.82	2.16		2.16	12.32	12.32
231.75	255.75	1727.22	1.37		1.37	0.112		0.11	0.112	-25.74		-25.74	2.20		2.20	12.23	12.23
232.25	256.25	1726.68	1.67		1.67	0.129		0.13	0.129	-25.72		-25.72	2.16		2.16	12.91	12.91
232.75	256.75	1726.14	1.47		1.47	0.117		0.12	0.117	-25.74		-25.74	1.89		1.89	12.61	12.61
233.25	257.25	1725.59	1.46		1.46	0.111		0.11	0.111	-25.97		-25.97	2.09		2.09	13.21	13.21
233.75	257.75	1725.05	1.46		1.46	0.112		0.11	0.112	-26.03		-26.03	2.07		2.07	13.08	13.08
234.25	258.25	1724.51	1.44		1.44	0.110		0.11	0.110	-26.06		-26.06	1.59		1.59	13.14	13.14
234.75	258.75	1723.96	1.75		1.75	0.131		0.13	0.131	-26.12		-26.12	1.54		1.54	13.36	13.36
235.25	259.25	1723.42	1.46	1.42	1.44	0.115	0.11	0.11	0.113	-25.97	-25.90	-25.94	1.82	1.92	1.87	12.79	12.79
235.75	259.75	1722.88	1.45		1.45	0.115		0.12	0.115	-25.72		-25.72	1.92		1.92	12.62	12.62
236.25	260.25	1722.33	1.45		1.45	0.113		0.11	0.113	-25.99		-25.99	2.00		2.00	12.89	12.89
236.75	260.75	1721.79	1.40		1.40	0.108		0.11	0.108	-25.94		-25.94	2.24		2.24	12.89	12.89
237.25	261.25	1721.25	1.41		1.41	0.108		0.11	0.108	-25.89		-25.89	2.07		2.07	13.11	13.11
237.75	261.75	1720.71	1.46		1.46	0.111		0.11	0.111	-25.96		-25.96	2.08		2.08	13.15	13.15
238.25	262.25	1720.16	1.52		1.52	0.112		0.11	0.112	-26.07		-26.07	1.77		1.77	13.50	13.50
238.75	262.75	1719.62	1.41		1.41	0.106		0.11	0.106	-26.46		-26.46	1.97		1.97	13.26	13.26
239.25	263.25	1719.08	1.55		1.55	0.114		0.11	0.114	-25.74		-25.74	1.54		1.54	13.51	13.51
239.75	263.75	1718.53	1.24		1.24	0.091		0.09	0.091	-25.79		-25.79	1.54		1.54	13.63	13.63

PAD 15 VC3 Distal Site																	
Sample mid-depth	*Adjusted mid-depth (+24cm)*	*Year AD*	*C_{org} (%)*	*Rpt*	*Avg*	*N (%)*	*Rpt*	*Avg*	*Corrected N (%) (-0.008%)*	*$\delta^{13}C_{org}$ (‰)*	*Rpt*	*Avg*	*$\delta^{15}N$ (‰)*	*Rpt*	*Avg*	*C/N*	*Corrected C/N*
240.25	264.25	1717.99	1.29		1.29	0.099		0.10	0.099	-25.92		-25.92	1.93		1.93	12.94	12.94
240.75	264.75	1717.45	1.37		1.37	0.108		0.11	0.108	-25.93		-25.93	2.03		2.03	12.67	12.67
241.25	265.25	1716.90	1.22		1.22	0.093		0.09	0.093	-25.89		-25.89	1.75		1.75	13.04	13.04
241.75	265.75	1716.36	1.16		1.16	0.091		0.09	0.091	-25.85		-25.85	1.65		1.65	12.73	12.73
242.25	266.25	1715.82	1.38		1.38	0.105		0.10	0.105	-25.63		-25.63	2.13		2.13	13.15	13.15
242.75	266.75	1715.27	1.19		1.19	0.098		0.10	0.098	-25.84		-25.84	1.85		1.85	12.16	12.16
243.25	267.25	1714.73	1.18		1.18	0.097		0.10	0.097	-25.80		-25.80	2.14		2.14	12.08	12.08
243.75	267.75	1714.19	1.39		1.39	0.116		0.12	0.116	-25.76		-25.76	1.90		1.90	12.01	12.01
244.25	268.25	1713.65	1.34		1.34	0.113		0.11	0.113	-25.64		-25.64	2.17		2.17	11.82	11.82
244.75	268.75	1713.10	1.45		1.45	0.130		0.13	0.130	-25.91		-25.91	2.17		2.17	11.13	11.13
245.25	269.25	1712.56	1.40	1.45	1.42	0.140	0.14	0.14	0.139	-26.04	-26.31	-26.17	2.09	1.80	1.94	10.25	10.25
245.75	269.75	1712.02	1.39		1.39	0.121		0.12	0.121	-26.07		-26.07	1.67		1.67	11.44	11.44
246.25	270.25	1711.47	1.46		1.46	0.119		0.12	0.119	-26.05		-26.05	2.16		2.16	12.31	12.31
246.75	270.75	1710.93	1.52		1.52	0.136		0.14	0.136	-26.30		-26.30	2.25		2.25	11.17	11.17
247.25	271.25	1710.39	1.40		1.40	0.131		0.13	0.131	-26.40		-26.40	2.33		2.33	10.69	10.69
247.75	271.75	1709.84	1.41		1.41	0.121		0.12	0.121	-26.23		-26.23	2.36		2.36	11.66	11.66
248.25	272.25	1709.30	1.50		1.50	0.138		0.14	0.138	-26.37		-26.37	2.42		2.42	10.81	10.81
248.75	272.75	1708.76	1.38		1.38	0.122		0.12	0.122	-26.04		-26.04	2.39		2.39	11.29	11.29
249.25	273.25	1708.21	1.42		1.42	0.131		0.13	0.131	-26.29		-26.29	2.35		2.35	10.84	10.84
249.75	273.75	1707.67	1.40		1.40	0.126		0.13	0.126	-26.06		-26.06	2.36		2.36	11.04	11.04
250.25	274.25	1707.13	1.48		1.48	0.132		0.13	0.132	-25.97		-25.97	2.41		2.41	11.22	11.22
250.75	274.75	1706.59	1.49		1.49	0.131		0.13	0.131	-26.23		-26.23	2.33		2.33	11.40	11.40
251.25	275.25	1706.04	1.52		1.52	0.137		0.14	0.137	-26.32		-26.32	2.45		2.45	11.13	11.13
251.75	275.75	1705.50	1.51		1.51	0.136		0.14	0.136	-25.95		-25.95	2.62		2.62	11.07	11.07
252.25	276.25	1704.96	1.50		1.50	0.134		0.13	0.134	-25.94		-25.94	2.40		2.40	11.19	11.19
252.75	276.75	1704.41	1.51		1.51	0.139		0.14	0.139	-26.13		-26.13	2.52		2.52	10.90	10.90
253.25	277.25	1703.87	1.51		1.51	0.136		0.14	0.136	-25.96		-25.96	2.63		2.63	11.05	11.05
253.75	277.75	1703.33	1.51		1.51	0.136		0.14	0.136	-25.92		-25.92	2.63		2.63	11.06	11.06
254.25	278.25	1702.78	1.50		1.50	0.138		0.14	0.138	-25.96		-25.96	2.58		2.58	10.91	10.91
254.75	278.75	1702.24	1.49		1.49	0.139		0.14	0.139	-26.03		-26.03	2.43		2.43	10.77	10.77
255.25	279.25	1701.70	1.52	1.51	1.51	0.137	0.14	0.14	0.137	-25.97	-25.98	-25.98	2.48	2.59	2.53	11.05	11.05
255.75	279.75	1701.16	1.53		1.53	0.137		0.14	0.137	-25.90		-25.90	2.41		2.41	11.10	11.10
256.25	280.25	1700.61	1.20		1.20	0.113		0.11	0.113	-26.09		-26.09	2.44		2.44	10.57	10.57
256.75	280.75	1700.07	1.51		1.51	0.135		0.13	0.135	-26.04		-26.04	2.40		2.40	11.25	11.25
257.25	281.25	1699.53	1.52		1.52	0.133		0.13	0.133	-26.14		-26.14	2.21		2.21	11.43	11.43
257.75	281.75	1698.98	1.49		1.49	0.138		0.14	0.138	-26.04		-26.04	2.37		2.37	10.86	10.86
258.25	282.25	1698.44	1.48		1.48	0.130		0.13	0.130	-25.98		-25.98	2.32		2.32	11.40	11.40

PAD 15 VC3 Distal Site																	
Sample mid-depth	Adjusted mid-depth (+24cm)	Year AD	C_{org} (%)	Rpt	Avg	N (%)	Rpt	Avg	Corrected N (%) (-0.008%)	$\delta^{13}C_{org}$ (‰)	Rpt	Avg	$\delta^{15}N$ (‰)	Rpt	Avg	C/N	Corrected C/N
258.75	282.75	1697.90	1.45		1.45	0.129		0.13	0.129	-26.12		-26.12	2.13		2.13	11.21	11.21
259.25	283.25	1697.35	1.48		1.48	0.129		0.13	0.129	-25.95		-25.95	2.07		2.07	11.46	11.46
259.75	283.75	1696.81	1.50		1.50	0.129		0.13	0.129	-26.39		-26.39	2.02		2.02	11.59	11.59
260.25	284.25	1696.27	1.51		1.51	0.130		0.13	0.130	-26.20		-26.20	2.25		2.25	11.59	11.59
260.75	284.75	1695.72	1.42		1.42	0.117		0.12	0.117	-26.32		-26.32	2.16		2.16	12.21	12.21
261.25	285.25	1695.18	1.49		1.49	0.120		0.12	0.120	-27.17		-27.17	2.23		2.23	12.44	12.44
261.75	285.75	1694.64	1.49		1.49	0.121		0.12	0.121	-26.09		-26.09	2.36		2.36	12.30	12.30
262.25	286.25	1694.10	1.49		1.49	0.125		0.12	0.125	-25.74		-25.74	2.61		2.61	11.91	11.91
262.75	286.75	1693.55	1.46		1.46	0.138		0.14	0.138	-26.11		-26.11	2.49		2.49	10.55	10.55
263.25	287.25	1693.01	1.47		1.47	0.138		0.14	0.138	-26.25		-26.25	2.34		2.34	10.60	10.60
263.75	287.75	1692.47	1.48		1.48	0.138		0.14	0.138	-26.14		-26.14	2.10		2.10	10.67	10.67
264.25	288.25	1691.92	1.47		1.47	0.143		0.14	0.143	-26.14		-26.14	2.45		2.45	10.30	10.30
264.75	288.75	1691.38	1.52		1.52	0.129		0.13	0.129	-25.84		-25.84	2.41		2.41	11.84	11.84
265.25	289.25	1690.84	1.48	1.47	1.48	0.131	0.13	0.13	0.131	-25.91	-25.96	-25.93	2.55	2.29	2.42	11.23	11.23
265.75	289.75	1690.29	1.48		1.48	0.129		0.13	0.129	-25.88		-25.88	2.37		2.37	11.43	11.43
266.25	290.25	1689.75	1.37		1.37	0.120		0.12	0.120	-25.95		-25.95	2.29		2.29	11.37	11.37
266.75	290.75	1689.21	1.42		1.42	0.131		0.13	0.131	-26.03		-26.03	2.35		2.35	10.88	10.88
267.25	291.25	1688.66	1.42		1.42	0.129		0.13	0.129	-25.95		-25.95	2.34		2.34	11.03	11.03
267.75	291.75	1688.12	1.47		1.47	0.135		0.13	0.135	-26.00		-26.00	2.56		2.56	10.91	10.91
268.25	292.25	1687.58	1.52		1.52	0.140		0.14	0.140	-26.13		-26.13	2.41		2.41	10.84	10.84
268.75	292.75	1687.04	1.41		1.41	0.124		0.12	0.124	-26.10		-26.10	2.24		2.24	11.42	11.42
269.25	293.25	1686.49	1.33		1.33	0.118		0.12	0.118	-25.94		-25.94	2.37		2.37	11.31	11.31
269.75	293.75	1685.95	1.13		1.13	0.095		0.09	0.095	-26.01		-26.01	1.90		1.90	11.92	11.92
270.25	294.25	1685.41	1.06		1.06	0.087		0.09	0.087	-25.96		-25.96	1.91		1.91	12.22	12.22
270.75	294.75	1684.86	1.14		1.14	0.101		0.10	0.101	-26.04		-26.04	2.09		2.09	11.34	11.34
271.25	295.25	1684.32	1.24		1.24	0.119		0.12	0.119	-26.22		-26.22	2.18		2.18	10.41	10.41
271.75	295.75	1683.78	1.28		1.28	0.111		0.11	0.111	-26.21		-26.21	1.42		1.42	11.54	11.54
272.25	296.25	1683.23	1.04		1.04	0.096		0.10	0.096	-26.02		-26.02	2.34		2.34	10.80	10.80
272.75	296.75	1682.69	1.30		1.30	0.122		0.12	0.122	-26.23		-26.23	2.27		2.27	10.65	10.65
273.25	297.25	1682.15	1.30		1.30	0.114		0.11	0.114	-25.94		-25.94	2.22		2.22	11.32	11.32
273.75	297.75	1681.60	1.28		1.28	0.118		0.12	0.118	-25.95		-25.95	2.06		2.06	10.80	10.80
274.25	298.25	1681.06	1.38		1.38	0.124		0.12	0.124	-26.11		-26.11	2.33		2.33	11.15	11.15
274.75	298.75	1680.52	1.19		1.19	0.113		0.11	0.113	-26.15		-26.15	2.24		2.24	10.53	10.53
275.25	299.25	1679.98	1.52	1.46	1.49	0.123	0.12	0.12	0.119	-26.11	-26.29	-26.20	1.95	1.70	1.83	12.48	12.48
275.75	299.75	1679.43	1.37		1.37	0.106		0.11	0.106	-25.89		-25.89	2.26		2.26	12.86	12.86
276.25	300.25	1678.89	1.23		1.23	0.104		0.10	0.104	-26.00		-26.00	1.81		1.81	11.80	11.80
276.75	300.75	1678.35	1.26		1.26	0.107		0.11	0.107	-26.05		-26.05	1.57		1.57	11.75	11.75

PAD 15 VC3 Distal Site																	
Sample mid-depth	Adjusted mid-depth (+24cm)	Year AD	C_{org} (%)	Rpt	Avg	N (%)	Rpt	Avg	Corrected N (%) (-0.008%)	$\delta^{13}C_{org}$ (‰)	Rpt	Avg	$\delta^{15}N$ (‰)	Rpt	Avg	C/N	Corrected C/N
277.25	301.25	1677.80	1.46		1.46	0.115		0.11	0.115	-25.88		-25.88	1.72		1.72	12.69	12.69
277.75	301.75	1677.26	1.48		1.48	0.107		0.11	0.107	-25.69		-25.69	1.56		1.56	13.83	13.83
278.25	302.25	1676.72	1.16		1.16	0.091		0.09	0.091	-26.03		-26.03	2.28		2.28	12.75	12.75
278.75	302.75	1676.17	1.18		1.18	0.095		0.10	0.095	-25.80		-25.80	2.18		2.18	12.38	12.38
279.25	303.25	1675.63	1.55		1.55	0.119		0.12	0.119	-25.73		-25.73	1.55		1.55	13.04	13.04
279.75	303.75	1675.09	1.19		1.19	0.099		0.10	0.099	-25.80		-25.80	2.34		2.34	11.98	11.98
280.25	304.25	1674.54	1.28		1.28	0.103		0.10	0.103	-25.79		-25.79	2.17		2.17	12.48	12.48
280.75	304.75	1674.00	1.41		1.41	0.103		0.10	0.103	-25.92		-25.92	1.73		1.73	13.61	13.61
281.25	305.25	1673.46	1.28		1.28	0.101		0.10	0.101	-25.79		-25.79	2.32		2.32	12.62	12.62
281.75	305.75	1672.92	1.27		1.27	0.097		0.10	0.097	-26.20		-26.20	1.83		1.83	13.04	13.04
282.25	306.25	1672.37	1.49		1.49	0.115		0.12	0.115	-25.81		-25.81	2.16		2.16	12.91	12.91
282.75	306.75	1671.83	1.18		1.18	0.091		0.09	0.091	-26.21		-26.21	2.01		2.01	12.92	12.92
283.25	307.25	1671.29	1.47		1.47	0.106		0.11	0.106	-25.61		-25.61	2.01		2.01	13.94	13.94
283.75	307.75	1670.74	1.07		1.07	0.089		0.09	0.089	-26.10		-26.10	1.84		1.84	12.05	12.05
284.25	308.25	1670.20	1.12		1.12	0.091		0.09	0.091	-26.12		-26.12	1.74		1.74	12.40	12.40
284.75	308.75	1669.66	1.32		1.32	0.100		0.10	0.100	-25.79		-25.79	1.87		1.87	13.21	13.21
285.25	309.25	1669.11	1.55	1.34	1.45	0.122	0.11	0.11	0.114	-26.00	-25.99	-25.99	1.89	1.99	1.94	12.67	12.67
285.75	309.75	1668.57	1.24		1.24	0.097		0.10	0.097	-26.13		-26.13	1.81		1.81	12.79	12.79
286.25	310.25	1668.03	1.16		1.16	0.091		0.09	0.091	-25.95		-25.95	1.83		1.83	12.71	12.71
286.75	310.75	1667.49	1.27		1.27	0.097		0.10	0.097	-25.67		-25.67	2.20		2.20	13.09	13.09
287.25	311.25	1666.94	0.97		0.97	0.081		0.08	0.081	-26.01		-26.01	2.03		2.03	12.08	12.08
287.75	311.75	1666.40	1.18		1.18	0.093		0.09	0.093	-25.86		-25.86	1.97		1.97	12.73	12.73
288.25	312.25	1665.86	1.14		1.14	0.094		0.09	0.094	-26.02		-26.02	2.12		2.12	12.10	12.10
288.75	312.75	1665.31	1.13		1.13	0.097		0.10	0.097	-25.90		-25.90	2.23		2.23	11.73	11.73
289.25	313.25	1664.77	1.38		1.38	0.110		0.11	0.110	-25.73		-25.73	2.33		2.33	12.46	12.46
289.75	313.75	1664.23	1.37		1.37	0.109		0.11	0.109	-25.56		-25.56	2.15		2.15	12.58	12.58
290.25	314.25	1663.68	1.31		1.31	0.106		0.11	0.106	-25.84		-25.84	1.96		1.96	12.42	12.42
290.75	314.75	1663.14	1.21		1.21	0.101		0.10	0.101	-26.02		-26.02	2.04		2.04	12.05	12.05
291.25	315.25	1662.60	1.46		1.46	0.116		0.12	0.116	-26.70		-26.70	2.07		2.07	12.65	12.65
291.75	315.75	1662.05	1.55		1.55	0.122		0.12	0.122	-25.83		-25.83	1.89		1.89	12.72	12.72
292.25	316.25	1661.51	1.69		1.69	0.131		0.13	0.131	-25.99		-25.99	2.05		2.05	12.88	12.88
292.75	316.75	1660.97	1.55		1.55	0.122		0.12	0.122	-25.89		-25.89	2.06		2.06	12.76	12.76
293.25	317.25	1660.43	1.52		1.52	0.127		0.13	0.127	-26.11		-26.11	1.90		1.90	11.97	11.97
293.75	317.75	1659.88	1.52		1.52	0.122		0.12	0.122	-26.12		-26.12	1.94		1.94	12.49	12.49
294.25	318.25	1659.34	1.41		1.41	0.111		0.11	0.111	-26.04		-26.04	2.29		2.29	12.70	12.70
294.75	318.75	1658.80	1.41		1.41	0.117		0.12	0.117	-26.10		-26.10	2.22		2.22	12.07	12.07
295.25	319.25	1658.25	1.30	1.29	1.30	0.107	0.11	0.11	0.107	-26.13	-26.04	-26.08	2.30	2.20	2.25	12.13	12.13

PAD 15 VC3 Distal Site																	
Sample mid-depth	*Adjusted mid-depth (+24cm)*	*Year AD*	*C_{org} (%)*	*Rpt*	*Avg*	*N (%)*	*Rpt*	*Avg*	*Corrected N (%) (-0.008%)*	*$\delta^{13}C_{org}$ (‰)*	*Rpt*	*Avg*	*$\delta^{15}N$ (‰)*	*Rpt*	*Avg*	*C/N*	*Corrected C/N*
295.75	319.75	1657.71	1.49		1.49	0.120		0.12	0.120	-25.85		-25.85	2.23		2.23	12.44	12.44
296.25	320.25	1657.17	1.35		1.35	0.110		0.11	0.110	-25.91		-25.91	2.12		2.12	12.33	12.33
296.75	320.75	1656.62	1.28		1.28	0.105		0.10	0.105	-26.04		-26.04	2.04		2.04	12.25	12.25
297.25	321.25	1656.08	1.41		1.41	0.116		0.12	0.116	-26.07		-26.07	2.09		2.09	12.14	12.14
297.75	321.75	1655.54	1.49		1.49	0.123		0.12	0.123	-26.02		-26.02	2.02		2.02	12.17	12.17
298.25	322.25	1654.99	1.25		1.25	0.113		0.11	0.113	-26.27		-26.27	1.96		1.96	11.04	11.04
298.75	322.75	1654.45	1.30		1.30	0.110		0.11	0.110	-26.27		-26.27	2.08		2.08	11.75	11.75
299.25	323.25	1653.91	1.33		1.33	0.111		0.11	0.111	-26.12		-26.12	1.99		1.99	11.92	11.92
299.75	323.75	1653.37	1.46		1.46	0.123		0.12	0.123	-26.17		-26.17	2.31		2.31	11.88	11.88
300.25	324.25	1652.82	1.40		1.40	0.116		0.12	0.116	-26.01		-26.01	2.16		2.16	12.03	12.03
300.75	324.75	1652.28	1.40		1.40	0.119		0.12	0.119	-26.18		-26.18	2.27		2.27	11.72	11.72
301.25	325.25	1651.74	1.46		1.46	0.125		0.13	0.125	-26.20		-26.20	2.11		2.11	11.66	11.66
301.75	325.75	1651.19	1.48		1.48	0.131		0.13	0.131	-26.07		-26.07	2.11		2.11	11.32	11.32
302.25	326.25	1650.65	1.49		1.49	0.138		0.14	0.138	-26.25		-26.25	2.38		2.38	10.76	10.76
302.75	326.75	1650.11	1.71		1.71	0.141		0.14	0.141	-26.24		-26.24	2.06		2.06	12.10	12.10
303.25	327.25	1649.56	1.48		1.48	0.128		0.13	0.128	-26.25		-26.25	2.38		2.38	11.58	11.58
303.75	327.75	1649.02	1.57		1.57	0.138		0.14	0.138	-26.39		-26.39	2.20		2.20	11.41	11.41
304.25	328.25	1648.48	1.54		1.54	0.133		0.13	0.133	-26.37		-26.37	2.38		2.38	11.60	11.60
304.75	328.75	1647.93	1.50		1.50	0.126		0.13	0.126	-26.30		-26.30	2.40		2.40	11.94	11.94
305.25	329.25	1647.39	1.63	1.64	1.63	0.161	0.16	0.16	0.162	-25.92	-25.85	-25.88	2.31	2.27	2.29	10.02	10.02
305.75	329.75	1646.85	1.42		1.42	0.120		0.12	0.120	-25.85		-25.85	2.41		2.41	11.84	11.84
306.25	330.25	1646.31	1.58		1.58	0.129		0.13	0.129	-25.84		-25.84	2.39		2.39	12.30	12.30
306.75	330.75	1645.76	1.51		1.51	0.129		0.13	0.129	-25.91		-25.91	2.23		2.23	11.76	11.76
307.25	331.25	1645.22	1.58		1.58	0.130		0.13	0.130	-25.97		-25.97	2.12		2.12	12.20	12.20
307.75	331.75	1644.68	1.49		1.49	0.124		0.12	0.124	-26.01		-26.01	2.31		2.31	11.96	11.96
308.25	332.25	1644.13	1.73		1.73	0.148		0.15	0.148	-26.32		-26.32	2.25		2.25	11.73	11.73
308.75	332.75	1643.59	1.57		1.57	0.132		0.13	0.132	-25.83		-25.83	2.23		2.23	11.85	11.85
309.25	333.25	1643.05	1.50		1.50	0.126		0.13	0.126	-25.95		-25.95	2.23		2.23	11.86	11.86
309.75	333.75	1642.50	1.59		1.59	0.131		0.13	0.131	-25.81		-25.81	2.06		2.06	12.11	12.11
310.25	334.25	1641.96	1.65		1.65	0.133		0.13	0.133	-25.72		-25.72	2.14		2.14	12.41	12.41
310.75	334.75	1641.42	1.39		1.39	0.117		0.12	0.117	-25.93		-25.93	2.03		2.03	11.87	11.87
311.25	335.25	1640.87	1.55		1.55	0.125		0.12	0.125	-25.74		-25.74	2.18		2.18	12.41	12.41
311.75	335.75	1640.33	1.60		1.60	0.133		0.13	0.133	-25.73		-25.73	2.23		2.23	12.02	12.02
312.25	336.25	1639.79	1.21		1.21	0.114		0.11	0.114	-26.50		-26.50	2.46		2.46	10.67	10.67
312.75	336.75	1639.25	1.50		1.50	0.118		0.12	0.118	-25.87		-25.87	2.17		2.17	12.75	12.75
313.25	337.25	1638.70	1.40		1.40	0.109		0.11	0.109	-25.79		-25.79	1.92		1.92	12.91	12.91
313.75	337.75	1638.16	1.30		1.30	0.108		0.11	0.108	-25.69		-25.69	1.94		1.94	12.01	12.01

PAD 15 VC3 Distal Site																	
Sample mid-depth	Adjusted mid-depth (+24cm)	Year AD	C_{org} (%)	Rpt	Avg	N (%)	Rpt	Avg	Corrected N (%) (-0.008%)	$\delta^{13}C_{org}$ (‰)	Rpt	Avg	$\delta^{15}N$ (‰)	Rpt	Avg	C/N	Corrected C/N
314.25	338.25	1637.62	1.15		1.15	0.095		0.09	0.095	-25.85		-25.85	2.00		2.00	12.15	12.15
314.75	338.75	1637.07	1.52		1.52	0.118		0.12	0.118	-25.76		-25.76	1.93		1.93	12.97	12.97
315.25	339.25	1636.53	1.48	1.92	1.48	0.111	0.14	0.12	0.125	-25.56	-25.28	-25.42	1.78	2.04	1.91	11.86	11.86
315.75	339.75	1635.99	1.38		1.38	0.105		0.11	0.105	-26.39		-26.39	1.94		1.94	13.09	13.09
316.25	340.25	1635.44	1.46		1.46	0.108		0.11	0.108	-26.05		-26.05	1.91		1.91	13.58	13.58
316.75	340.75	1634.90	1.18		1.18	0.091		0.09	0.091	-26.47		-26.47	2.00		2.00	12.97	12.97
317.25	341.25	1634.36	1.39		1.39	0.105		0.10	0.105	-26.35		-26.35	1.80		1.80	13.24	13.24
317.75	341.75	1633.82	1.47		1.47	0.109		0.11	0.109	-26.22		-26.22	2.09		2.09	13.43	13.43
318.25	342.25	1633.27	1.52		1.52	0.115		0.12	0.115	-26.42		-26.42	1.85		1.85	13.14	13.14
318.75	342.75	1632.73	1.03		1.03	0.084		0.08	0.084	-26.58		-26.58	1.64		1.64	12.30	12.30
319.25	343.25	1632.19	1.10		1.10	0.088		0.09	0.088	-26.69		-26.69	2.02		2.02	12.52	12.52
319.75	343.75	1631.64	1.34		1.34	0.106		0.11	0.106	-26.54		-26.54	1.88		1.88	12.71	12.71
320.25	344.25	1631.10	0.92		0.92	0.079		0.08	0.079	-26.70		-26.70	2.07		2.07	11.64	11.64
320.75	344.75	1630.56	1.12		1.12	0.091		0.09	0.091	-26.14		-26.14	2.17		2.17	12.26	12.26
321.25	345.25	1630.01	1.20		1.20	0.093		0.09	0.093	-25.97		-25.97	2.35		2.35	12.94	12.94
321.75	345.75	1629.47	1.04		1.04	0.085		0.09	0.085	-26.10		-26.10	2.46		2.46	12.20	12.20
322.25	346.25	1628.93	1.44		1.44	0.110		0.11	0.110	-26.12		-26.12	1.84		1.84	13.06	13.06
322.75	346.75	1628.38	1.37		1.37	0.107		0.11	0.107	-26.00		-26.00	2.12		2.12	12.86	12.86
323.25	347.25	1627.84	1.89		1.89	0.136		0.14	0.136	-26.09		-26.09	2.12		2.12	13.94	13.94
323.75	347.75	1627.30	1.14		1.14	0.088		0.09	0.088	-26.16		-26.16	1.90		1.90	13.04	13.04
324.25	348.25	1626.76	1.42		1.42	0.106		0.11	0.106	-26.16		-26.16	2.16		2.16	13.44	13.44
324.75	348.75	1626.21	1.14		1.14	0.086		0.09	0.086	-26.02		-26.02	2.41		2.41	13.30	13.30
325.25	349.25	1625.67	1.12	0.98	1.05	0.084	0.07	0.08	0.079	-26.03	-26.24	-26.13	2.12	2.13	2.12	13.27	13.27
325.75	349.75	1625.13	1.28		1.28	0.092		0.09	0.092	-25.95		-25.95	2.24		2.24	13.85	13.85
326.25	350.25	1624.58	1.67		1.67	0.116		0.12	0.116	-25.90		-25.90	2.02		2.02	14.47	14.47
326.75	350.75	1624.04	1.11		1.11	0.090		0.09	0.090	-26.01		-26.01	2.18		2.18	12.37	12.37
327.25	351.25	1623.50	1.16		1.16	0.091		0.09	0.091	-26.02		-26.02	2.40		2.40	12.66	12.66
327.75	351.75	1622.95	1.00		1.00	0.083		0.08	0.083	-26.10		-26.10	2.29		2.29	12.00	12.00
328.25	352.25	1622.41	1.36		1.36	0.103		0.10	0.103	-26.11		-26.11	2.12		2.12	13.22	13.22
328.75	352.75	1621.87	1.05		1.05	0.080		0.08	0.080	-26.14		-26.14	2.25		2.25	13.10	13.10
329.25	353.25	1621.32	0.87		0.87	0.068		0.07	0.068	-26.12		-26.12	1.74		1.74	12.68	12.68
329.75	353.75	1620.78	1.49		1.49	0.108		0.11	0.108	-26.09		-26.09	2.23		2.23	13.74	13.74
330.25	354.25	1620.24	1.45		1.45	0.104		0.10	0.104	-26.10		-26.10	2.09		2.09	14.01	14.01
330.75	354.75	1619.70	1.56		1.56	0.119		0.12	0.119	-26.13		-26.13	2.06		2.06	13.18	13.18
331.25	355.25	1619.15	1.02		1.02	0.076		0.08	0.076	-26.16		-26.16	1.36		1.36	13.43	13.43
331.75	355.75	1618.61	1.08		1.08	0.085		0.09	0.085	-26.10		-26.10	2.07		2.07	12.65	12.65
332.25	356.25	1618.07	1.87		1.87	0.128		0.13	0.128	-26.14		-26.14	2.20		2.20	14.59	14.59

PAD 15 VC3 Distal Site																	
Sample mid-depth	Adjusted mid-depth (+24cm)	Year AD	C_{org} (%)	Rpt	Avg	N (%)	Rpt	Avg	Corrected N (%) (-0.008%)	$\delta^{13}C_{org}$ (‰)	Rpt	Avg	$\delta^{15}N$ (‰)	Rpt	Avg	C/N	Corrected C/N
332.75	356.75	1617.52	1.14		1.14	0.087		0.09	0.087	-26.21		-26.21	2.01		2.01	13.04	13.04
333.25	357.25	1616.98	1.19		1.19	0.089		0.09	0.089	-26.08		-26.08	2.40		2.40	13.31	13.31
333.75	357.75	1616.44	0.94		0.94	0.074		0.07	0.074	-26.14		-26.14	1.76		1.76	12.69	12.69
334.25	358.25	1615.89	1.14		1.14	0.088		0.09	0.088	-26.16		-26.16	2.44		2.44	13.06	13.06
334.75	358.75	1615.35	1.08		1.08	0.085		0.08	0.085	-26.11		-26.11	2.63		2.63	12.72	12.72
335.25	359.25	1614.81	1.02	1.10	1.06	0.079	0.08	0.08	0.082	-26.14	-26.12	-26.13	2.46	2.56	2.51	12.94	12.94
335.75	359.75	1614.26	1.34		1.34	0.104		0.10	0.104	-26.13		-26.13	2.33		2.33	12.98	12.98
336.25	360.25	1613.72	1.02		1.02	0.081		0.08	0.081	-26.21		-26.21	2.41		2.41	12.58	12.58
336.75	360.75	1613.18	0.98		0.98	0.075		0.07	0.075	-26.11		-26.11	2.61		2.61	13.13	13.13
337.25	361.25	1612.64	1.25		1.25	0.095		0.10	0.095	-26.03		-26.03	2.08		2.08	13.10	13.10
337.75	361.75	1612.09	0.83		0.83	0.072		0.07	0.072	-26.14		-26.14	2.11		2.11	11.57	11.57
338.25	362.25	1611.55	1.40		1.40	0.111		0.11	0.111	-25.97		-25.97	2.09		2.09	12.64	12.64
338.75	362.75	1611.01	1.12		1.12	0.088		0.09	0.088	-26.15		-26.15	1.96		1.96	12.77	12.77
339.25	363.25	1610.46	1.54		1.54	0.116		0.12	0.116	-25.66		-25.66	2.07		2.07	13.22	13.22
339.75	363.75	1609.92	1.00		1.00	0.080		0.08	0.080	-27.32		-27.32	2.15		2.15	12.39	12.39
340.25	364.25	1609.38	1.26		1.26	0.101		0.10	0.101	-25.06		-25.06	2.20		2.20	12.45	12.45
340.75	364.75	1608.83	1.33		1.33	0.108		0.11	0.108	-24.74		-24.74	2.28		2.28	12.30	12.30
341.25	365.25	1608.29	1.38		1.38	0.111		0.11	0.111	-24.73		-24.73	2.18		2.18	12.42	12.42
341.75	365.75	1607.75	1.00		1.00	0.085		0.09	0.085	-25.99		-25.99	2.10		2.10	11.71	11.71
342.25	366.25	1607.20	1.47		1.47	0.111		0.11	0.111	-25.45		-25.45	1.90		1.90	13.29	13.29
342.75	366.75	1606.66	1.37		1.37	0.110		0.11	0.110	-25.96		-25.96	2.01		2.01	12.38	12.38
343.25	367.25	1606.12	1.38		1.38	0.108		0.11	0.108	-25.02		-25.02	2.05		2.05	12.83	12.83
343.75	367.75	1605.58	1.21		1.21	0.095		0.09	0.095	-25.20		-25.20	1.79		1.79	12.74	12.74
344.25	368.25	1605.03	1.32		1.32	0.104		0.10	0.104	-25.43		-25.43	2.17		2.17	12.67	12.67
344.75	368.75	1604.49	1.31		1.31	0.107		0.11	0.107	-24.88		-24.88	2.28		2.28	12.27	12.27
345.25	369.25	1603.95	1.32	1.54	1.43	0.107	0.12	0.11	0.113	-25.81	-25.79	-25.80	2.25	2.21	2.23	12.68	12.68
345.75	369.75	1603.40	1.57		1.57	0.116		0.12	0.116	-25.82		-25.82	1.81		1.81	13.56	13.56
346.25	370.25	1602.86	1.15		1.15	0.085		0.08	0.085	-25.99		-25.99	1.72		1.72	13.56	13.56
346.75	370.75	1602.32	1.35		1.35	0.108		0.11	0.108	-25.84		-25.84	2.12		2.12	12.56	12.56
347.25	371.25	1601.77	1.11		1.11	0.089		0.09	0.089	-25.92		-25.92	1.81		1.81	12.41	12.41
347.75	371.75	1601.23	1.19		1.19	0.093		0.09	0.093	-25.93		-25.93	1.76		1.76	12.91	12.91
348.25	372.25	1600.69	1.46		1.46	0.115		0.11	0.115	-26.30		-26.30	2.25		2.25	12.78	12.78
348.75	372.75	1600.14	1.33		1.33	0.111		0.11	0.111	-25.62		-25.62	2.17		2.17	12.05	12.05
349.25	373.25	1599.60	1.51		1.51	0.111		0.11	0.111	-25.91		-25.91	1.99		1.99	13.58	13.58
349.75	373.75	1599.06	1.40		1.40	0.100		0.10	0.100	-26.00		-26.00	1.58		1.58	14.03	14.03
350.25	374.25	1598.52	0.69		0.69	0.064		0.06	0.064	-26.10		-26.10	2.37		2.37	10.75	10.75
350.75	374.75	1597.97	1.45		1.45	0.107		0.11	0.107	-25.98		-25.98	1.90		1.90	13.51	13.51

PAD 15 VC3 Distal Site																	
Sample mid-depth	Adjusted mid-depth (+24cm)	Year AD	C_{org} (%)	Rpt	Avg	N (%)	Rpt	Avg	Corrected N (%) (-0.008%)	$\delta^{13}C_{org}$ (‰)	Rpt	Avg	$\delta^{15}N$ (‰)	Rpt	Avg	C/N	Corrected C/N
351.25	375.25	1597.43	1.69		1.69	0.114		0.11	0.114	-25.94		-25.94	1.63		1.63	14.81	14.81
351.75	375.75	1596.89	2.03		2.03	0.132		0.13	0.132	-26.57		-26.57	1.67		1.67	15.31	15.31
352.25	376.25	1596.34	1.03		1.03	0.073		0.07	0.073	-26.14		-26.14	1.48		1.48	14.14	14.14
352.75	376.75	1595.80	1.96		1.96	0.118		0.12	0.118	-25.13		-25.13	1.41		1.41	16.61	16.61
353.25	377.25	1595.26	1.82		1.82	0.111		0.11	0.111	-25.72		-25.72	1.45		1.45	16.37	16.37
353.75	377.75	1594.75	1.27		1.27	0.092		0.09	0.084	-26.25		-26.25	1.30		1.30	13.87	15.20
354.25	378.25	1594.24	1.11		1.11	0.089		0.09	0.081	-26.09		-26.09	2.04		2.04	12.44	13.67
354.75	378.75	1593.74	1.16		1.16	0.096		0.10	0.088	-26.15		-26.15	2.09		2.09	12.12	13.22
355.25	379.25	1593.23	1.46	1.42	1.44	0.114	0.11	0.11	0.104	-25.98	-25.98	-25.98	1.97	2.05	2.01	12.87	13.86
355.75	379.75	1592.73	1.26		1.26	0.107		0.11	0.099	-26.12		-26.12	2.16		2.16	11.81	12.76
356.25	380.25	1592.23	1.19		1.19	0.101		0.10	0.093	-26.03		-26.03	2.18		2.18	11.71	12.71
356.75	380.75	1591.72	0.73		0.73	0.063		0.06	0.055	-26.17		-26.17	2.13		2.13	11.54	13.21
357.25	381.25	1591.22	0.89		0.89	0.075		0.08	0.067	-26.04		-26.04	2.14		2.14	11.84	13.25
357.75	381.75	1590.71	0.81		0.81	0.070		0.07	0.062	-26.15		-26.15	2.11		2.11	11.49	12.97
358.25	382.25	1590.21	0.70		0.70	0.062		0.06	0.054	-26.09		-26.09	1.90		1.90	11.30	12.97
358.75	382.75	1589.70	0.66		0.66	0.057		0.06	0.049	-26.05		-26.05	2.04		2.04	11.46	13.32
359.25	383.25	1589.20	0.88		0.88	0.080		0.08	0.072	-26.11		-26.11	2.32		2.32	10.95	12.16
359.75	383.75	1588.70	0.75		0.75	0.064		0.06	0.056	-26.11		-26.11	2.30		2.30	11.79	13.48
360.25	384.25	1588.19	0.94		0.94	0.075		0.07	0.067	-26.07		-26.07	1.99		1.99	12.61	14.13
360.75	384.75	1587.69	0.91		0.91	0.078		0.08	0.070	-26.12		-26.12	2.05		2.05	11.73	13.07
361.25	385.25	1587.18	0.84		0.84	0.077		0.08	0.069	-26.17		-26.17	2.21		2.21	10.84	12.09
361.75	385.75	1586.68	0.84		0.84	0.079		0.08	0.071	-26.16		-26.16	2.24		2.24	10.56	11.75
362.25	386.25	1586.17	0.51		0.51	0.045		0.04	0.037	-26.05		-26.05	1.83		1.83	11.42	13.92
362.75	386.75	1585.67	0.65		0.65	0.051		0.05	0.043	-26.12		-26.12	1.76		1.76	12.74	15.10
363.25	387.25	1585.16	0.93		0.93	0.073		0.07	0.065	-25.62		-25.62	2.12		2.12	12.75	14.32
363.75	387.75	1584.66	1.17		1.17	0.093		0.09	0.085	-26.03		-26.03	2.06		2.06	12.51	13.69
364.25	388.25	1584.16	1.21		1.21	0.113		0.11	0.105	-25.95		-25.95	2.38		2.38	10.71	11.52
364.75	388.75	1583.65	0.87		0.87	0.078		0.08	0.070	-26.07		-26.07	2.39		2.39	11.14	12.42
365.25	389.25	1583.15	0.74	0.71	0.72	0.062	0.06	0.06	0.053	-26.12	-25.93	-26.03	1.93	1.88	1.91	11.88	13.67
365.75	389.75	1582.64	0.99		0.99	0.079		0.08	0.071	-25.84		-25.84	2.02		2.02	12.47	13.88
366.25	390.25	1582.14	1.03		1.03	0.084		0.08	0.076	-26.73		-26.73	2.51		2.51	12.24	13.53
366.75	390.75	1581.63	1.26		1.26	0.102		0.10	0.094	-26.45		-26.45	2.36		2.36	12.37	13.42
367.25	391.25	1581.13	1.58		1.58	0.124		0.12	0.116	-28.10		-28.10	2.57		2.57	12.71	13.59
367.75	391.75	1580.62	1.56		1.56	0.128		0.13	0.120	-26.18		-26.18	2.09		2.09	12.23	13.05
368.25	392.25	1580.12	1.07		1.07	0.095		0.09	0.087	-26.32		-26.32	2.33		2.33	11.30	12.34
368.75	392.75	1579.62	0.85		0.85	0.069		0.07	0.061	-26.15		-26.15	2.58		2.58	12.27	13.88
369.25	393.25	1579.11	0.81		0.81	0.060		0.06	0.052	-26.26		-26.26	2.93		2.93	13.54	15.62

PAD 15 VC3 Distal Site																		
Sample mid-depth	Adjusted mid-depth (+24cm)	Year AD	C_{org} (%)	Rpt	Avg	N (%)	Rpt	Avg	Corrected N (%) (-0.008%)	$\delta^{13}C_{org}$ (‰)	Rpt	Avg	$\delta^{15}N$ (‰)	Rpt	Avg	C/N	Corrected C/N
369.75	393.75	1578.61	1.07		1.07	0.085		0.08	0.077	-26.31		-26.31	2.51		2.51	12.60	13.91
370.25	394.25	1578.10	0.99		0.99	0.086		0.09	0.078	-26.31		-26.31	2.61		2.61	11.45	12.63
370.75	394.75	1577.60	0.85		0.85	0.059		0.06	0.051	-26.02		-26.02	1.63		1.63	14.49	16.77
371.25	395.25	1577.09	1.05		1.05	0.081		0.08	0.073	-26.25		-26.25	2.25		2.25	12.97	14.40
371.75	395.75	1576.59	1.33		1.33	0.103		0.10	0.095	-26.66		-26.66	2.14		2.14	12.89	13.97
372.25	396.25	1576.09	1.40		1.40	0.119		0.12	0.111	-26.15		-26.15	2.23		2.23	11.71	12.55
372.75	396.75	1575.58	1.39		1.39	0.120		0.12	0.112	-26.17		-26.17	2.30		2.30	11.58	12.41
373.25	397.25	1575.08	1.36		1.36	0.117		0.12	0.109	-26.14		-26.14	2.37		2.37	11.62	12.46
373.75	397.75	1574.57	0.70		0.70	0.061		0.06	0.053	-26.00		-26.00	2.44		2.44	11.55	13.30
374.25	398.25	1574.07	0.73		0.73	0.059		0.06	0.051	-26.01		-26.01	2.75		2.75	12.46	14.42
374.75	398.75	1573.56	0.59		0.59	0.050		0.05	0.042	-26.98		-26.98	2.76		2.76	11.67	13.89
375.25	399.25	1573.06	0.67	0.67	0.67	0.063	0.06	0.06	0.055	-26.02	-26.11	-26.07	2.24	2.33	2.28	10.68	12.24
375.75	399.75	1572.55	0.93		0.93	0.087		0.09	0.079	-26.21		-26.21	2.64		2.64	10.73	11.83
376.25	400.25	1572.05	0.71		0.71	0.056		0.06	0.048	-26.00		-26.00	2.05		2.05	12.65	14.76
376.75	400.75	1571.55	0.74		0.74	0.067		0.07	0.059	-26.08		-26.08	2.54		2.54	11.01	12.50
377.25	401.25	1571.04	0.94		0.94	0.075		0.07	0.067	-26.04		-26.04	2.13		2.13	12.64	14.16
377.75	401.75	1570.54	0.98		0.98	0.083		0.08	0.075	-26.28		-26.28	2.10		2.10	11.76	13.01
378.25	402.25	1570.03	1.15		1.15	0.091		0.09	0.083	-26.11		-26.11	1.97		1.97	12.60	13.81
378.75	402.75	1569.53	1.36		1.36	0.121		0.12	0.113	-26.09		-26.09	2.28		2.28	11.24	12.04
379.25	403.25	1569.02	1.40		1.40	0.131		0.13	0.123	-26.08		-26.08	2.24		2.24	10.63	11.32
379.75	403.75	1568.52	1.40		1.40	0.128		0.13	0.120	-26.79		-26.79	2.39		2.39	10.86	11.59
380.25	404.25	1568.02	0.71		0.71	0.063		0.06	0.055	-26.09		-26.09	2.23		2.23	11.23	12.86
380.75	404.75	1567.51	0.54		0.54	0.047		0.05	0.039	-26.02		-26.02	2.15		2.15	11.41	13.74
381.25	405.25	1567.01	0.62		0.62	0.060		0.06	0.052	-26.26		-26.26	2.01		2.01	10.35	11.96
381.75	405.75	1566.50	0.92		0.92	0.081		0.08	0.073	-27.09		-27.09	2.30		2.30	11.28	12.51
382.25	406.25	1566.00	1.05		1.05	0.094		0.09	0.086	-26.17		-26.17	2.14		2.14	11.21	12.25
382.75	406.75	1565.49	0.69		0.69	0.057		0.06	0.049	-25.98		-25.98	1.99		1.99	11.99	13.94
383.25	407.25	1564.99	0.63		0.63	0.055		0.06	0.047	-25.81		-25.81	2.36		2.36	11.35	13.27
383.75	407.75	1564.48	0.66		0.66	0.065		0.07	0.057	-26.01		-26.01	2.66		2.66	10.12	11.54
384.25	408.25	1563.98	0.91		0.91	0.081		0.08	0.073	-25.94		-25.94	2.49		2.49	11.24	12.48
384.75	408.75	1563.48	1.20		1.20	0.104		0.10	0.096	-25.97		-25.97	2.49		2.49	11.53	12.49
385.25	409.25	1562.97	1.13	1.14	1.13	0.102	0.10	0.10	0.093	-25.83	-25.82	-25.82	2.55	2.55	2.55	11.16	12.12
385.75	409.75	1562.47	0.83		0.83	0.074		0.07	0.066	-25.86		-25.86	2.47		2.47	11.25	12.62
386.25	410.25	1561.96	0.73		0.73	0.065		0.07	0.057	-26.13		-26.13	2.23		2.23	11.11	12.67
386.75	410.75	1561.46	1.40		1.40	0.125		0.12	0.117	-26.50		-26.50	2.56		2.56	11.16	11.92
387.25	411.25	1560.95	1.20		1.20	0.107		0.11	0.099	-26.37		-26.37	2.42		2.42	11.20	12.11
387.75	411.75	1560.45	0.93		0.93	0.084		0.08	0.076	-26.63		-26.63	2.34		2.34	11.06	12.22

PAD 15 VC3 Distal Site																	
Sample mid-depth	*Adjusted mid-depth (+24cm)*	*Year AD*	*C_{org} (%)*	*Rpt*	*Avg*	*N (%)*	*Rpt*	*Avg*	*Corrected N (%) (-0.008%)*	*$\delta^{13}C_{org}$ (‰)*	*Rpt*	*Avg*	*$\delta^{15}N$ (‰)*	*Rpt*	*Avg*	*C/N*	*Corrected C/N*
388.25	412.25	1559.95	0.85		0.85	0.076		0.08	0.068	-26.34		-26.34	2.53		2.53	11.07	12.37
388.75	412.75	1559.44	0.72		0.72	0.067		0.07	0.059	-26.17		-26.17	2.62		2.62	10.75	12.20
389.25	413.25	1558.94	0.70		0.70	0.056		0.06	0.048	-26.10		-26.10	2.73		2.73	12.48	14.55
389.75	413.75	1558.43	0.80		0.80	0.062		0.06	0.054	-25.89		-25.89	2.28		2.28	12.82	14.71
390.25	414.25	1557.93	0.61		0.61	0.056		0.06	0.048	-26.03		-26.03	2.33		2.33	10.93	12.74
390.75	414.75	1557.42	0.61		0.61	0.062		0.06	0.054	-25.80		-25.80	2.45		2.45	9.82	11.27
391.25	415.25	1556.92	0.48		0.48	0.045		0.04	0.037	-25.94		-25.94	2.56		2.56	10.80	13.15
391.75	415.75	1556.41	0.72		0.72	0.062		0.06	0.054	-26.26		-26.26	2.36		2.36	11.64	13.37
392.25	416.25	1555.91	0.78		0.78	0.071		0.07	0.063	-25.89		-25.89	2.57		2.57	10.90	12.28
392.75	416.75	1555.41	0.59		0.59	0.054		0.05	0.046	-25.99		-25.99	2.59		2.59	11.05	12.97
393.25	417.25	1554.90	0.79		0.79	0.073		0.07	0.065	-25.97		-25.97	2.80		2.80	10.94	12.29
393.75	417.75	1554.40	0.73		0.73	0.068		0.07	0.060	-26.30		-26.30	2.49		2.49	10.74	12.17
394.25	418.25	1553.89	0.45		0.45	0.041		0.04	0.033	-25.89		-25.89	2.70		2.70	10.89	13.52
394.75	418.75	1553.39	0.63		0.63	0.059		0.06	0.051	-26.13		-26.13	2.75		2.75	10.78	12.48
395.25	419.25	1552.88	1.07	1.08	1.08	0.103	0.10	0.10	0.095	-26.88	-26.23	-26.55	2.41	2.48	2.44	10.42	11.29
395.75	419.75	1552.38	0.96		0.96	0.090		0.09	0.082	-26.45		-26.45	2.50		2.50	10.68	11.73
396.25	420.25	1551.87	0.62		0.62	0.058		0.06	0.050	-25.96		-25.96	2.69		2.69	10.83	12.57
396.75	420.75	1551.37	0.81		0.81	0.076		0.08	0.068	-26.48		-26.48	2.78		2.78	10.71	11.97
397.25	421.25	1550.87	0.85		0.85	0.082		0.08	0.074	-26.56		-26.56	2.67		2.67	10.42	11.55
397.75	421.75	1550.36	0.52		0.52	0.048		0.05	0.040	-25.89		-25.89	2.67		2.67	10.74	12.90
398.25	422.25	1549.86	0.62		0.62	0.058		0.06	0.050	-25.93		-25.93	2.78		2.78	10.64	12.35
398.75	422.75	1549.35	0.97		0.97	0.084		0.08	0.076	-26.43		-26.43	2.31		2.31	11.56	12.77
399.25	423.25	1548.85	0.95		0.95	0.084		0.08	0.076	-26.17		-26.17	2.53		2.53	11.22	12.40
399.75	423.75	1548.34	0.65		0.65	0.055		0.05	0.047	-26.30		-26.30	2.34		2.34	11.82	13.84
400.25	424.25	1547.84	0.69		0.69	0.060		0.06	0.052	-26.33		-26.33	2.23		2.23	11.35	13.08
400.75	424.75	1547.34	1.11		1.11	0.094		0.09	0.086	-26.03		-26.03	2.25		2.25	11.82	12.91
401.25	425.25	1546.83	1.20		1.20	0.105		0.11	0.097	-26.28		-26.28	2.12		2.12	11.42	12.35
401.75	425.75	1546.33	1.14		1.14	0.097		0.10	0.089	-25.99		-25.99	2.26		2.26	11.78	12.84
402.25	426.25	1545.82	1.23		1.23	0.108		0.11	0.100	-25.82		-25.82	2.32		2.32	11.38	12.28
402.75	426.75	1545.32	0.87		0.87	0.078		0.08	0.070	-26.40		-26.40	2.66		2.66	11.14	12.42
403.25	427.25	1544.81	0.38		0.38	0.037		0.04	0.029	-25.83		-25.83	2.79		2.79	10.34	13.19
403.75	427.75	1544.31	0.49		0.49	0.046		0.05	0.038	-25.92		-25.92	2.39		2.39	10.64	12.87
404.25	428.25	1543.80	0.72		0.72	0.065		0.07	0.057	-26.27		-26.27	2.53		2.53	11.00	12.53
404.75	428.75	1543.30	1.05		1.05	0.095		0.10	0.087	-26.46		-26.46	2.44		2.44	11.03	12.04
405.25	429.25	1542.80	0.93	0.94	0.93	0.085	0.08	0.08	0.076	-26.10	-26.01	-26.06	2.50	2.39	2.45	11.06	12.22
405.75	429.75	1542.29	0.98		0.98	0.087		0.09	0.079	-26.86		-26.86	2.40		2.40	11.24	12.37
406.25	430.25	1541.79	0.68		0.68	0.060		0.06	0.052	-26.38		-26.38	2.23		2.23	11.24	12.95

PAD 15 VC3 Distal Site																	
Sample mid-depth	*Adjusted mid-depth (+24cm)*	*Year AD*	*C_{org} (%)*	*Rpt*	*Avg*	*N (%)*	*Rpt*	*Avg*	*Corrected N (%) (-0.008%)*	*$\delta^{13}C_{org}$ (‰)*	*Rpt*	*Avg*	*$\delta^{15}N$ (‰)*	*Rpt*	*Avg*	*C/N*	*Corrected C/N*
406.75	430.75	1541.28	0.89		0.89	0.078		0.08	0.070	-26.15		-26.15	2.39		2.39	11.42	12.72
407.25	431.25	1540.78	1.16		1.16	0.106		0.11	0.098	-26.27		-26.27	2.29		2.29	10.99	11.89
407.75	431.75	1540.27	0.74		0.74	0.068		0.07	0.060	-26.46		-26.46	2.20		2.20	10.88	12.34
408.25	432.25	1539.77	0.61		0.61	0.058		0.06	0.050	-26.14		-26.14	2.31		2.31	10.54	12.24
408.75	432.75	1539.27	0.96		0.96	0.086		0.09	0.078	-26.52		-26.52	2.35		2.35	11.27	12.43
409.25	433.25	1538.76	1.30		1.30	0.116		0.12	0.108	-26.70		-26.70	2.22		2.22	11.25	12.09
409.75	433.75	1538.26	1.25		1.25	0.116		0.12	0.108	-26.23		-26.23	2.26		2.26	10.79	11.59
410.25	434.25	1537.75	0.34		0.34	0.034		0.03	0.026	-25.71		-25.71	2.94		2.94	10.01	13.06
410.75	434.75	1537.25	0.55		0.55	0.048		0.05	0.040	-26.16		-26.16	2.23		2.23	11.59	13.92
411.25	435.25	1536.74	0.74		0.74	0.061		0.06	0.053	-26.34		-26.34	2.07		2.07	12.17	14.00
411.75	435.75	1536.24	1.37		1.37	0.102		0.10	0.094	-27.07		-27.07	2.01		2.01	13.40	14.54
412.25	436.25	1535.73	1.38		1.38	0.119		0.12	0.111	-26.19		-26.19	2.25		2.25	11.67	12.52
412.75	436.75	1535.23	0.85		0.85	0.076		0.08	0.068	-26.14		-26.14	3.84		3.84	11.17	12.49
413.25	437.25	1534.73	0.77		0.77	0.060		0.06	0.052	-26.03		-26.03	3.67		3.67	12.97	14.98
413.75	437.75	1534.22	1.16		1.16	0.092		0.09	0.084	-26.12		-26.12	2.66		2.66	12.60	13.79
414.25	438.25	1533.72	1.40		1.40	0.118		0.12	0.110	-26.13		-26.13	2.20		2.20	11.88	12.74
414.75	438.75	1533.21	1.18		1.18	0.102		0.10	0.094	-26.10		-26.10	3.07		3.07	11.51	12.49
415.25	439.25	1532.71	0.65	0.65	0.65	0.055	0.06	0.06	0.047	-26.20	-26.11	-26.15	2.35	2.54	2.45	11.75	13.73
415.75	439.75	1532.20	0.90		0.90	0.078		0.08	0.070	-25.83		-25.83	2.80		2.80	11.44	12.75
416.25	440.25	1531.70	1.02		1.02	0.080		0.08	0.072	-25.95		-25.95	2.99		2.99	12.81	14.25
416.75	440.75	1531.19	0.80		0.80	0.070		0.07	0.062	-26.00		-26.00	2.59		2.59	11.49	12.98
417.25	441.25	1530.69	1.35		1.35	0.119		0.12	0.111	-26.03		-26.03	2.16		2.16	11.31	12.13
417.75	441.75	1530.19	1.35		1.35	0.131		0.13	0.123	-25.90		-25.90	2.50		2.50	10.33	11.00
418.25	442.25	1529.68	0.92		0.92	0.090		0.09	0.082	-25.79		-25.79	2.05		2.05	10.20	11.19
418.75	442.75	1529.18	0.37		0.37	0.035		0.03	0.027	-26.21		-26.21	2.72		2.72	10.84	14.11
419.25	443.25	1528.67	0.33		0.33	0.029		0.03	0.021	-26.17		-26.17	2.75		2.75	11.06	15.20
419.75	443.75	1528.17	0.73		0.73	0.070		0.07	0.062	-26.03		-26.03	2.68		2.68	10.43	11.78
420.25	444.25	1527.66	0.63		0.63	0.052		0.05	0.044	-26.08		-26.08	1.44		1.44	12.11	14.31
420.75	444.75	1527.16	0.71		0.71	0.053		0.05	0.045	-25.84		-25.84	2.10		2.10	13.39	15.78
421.25	445.25	1526.66	0.83		0.83	0.070		0.07	0.062	-26.05		-26.05	2.09		2.09	11.83	13.36
421.75	445.75	1526.15	1.16		1.16	0.102		0.10	0.094	-25.18		-25.18	2.34		2.34	11.40	12.37
422.25	446.25	1525.65	1.06		1.06	0.087		0.09	0.079	-25.21		-25.21	2.13		2.13	12.25	13.49
422.75	446.75	1525.14	0.78		0.78	0.063		0.06	0.055	-25.71		-25.71	2.21		2.21	12.31	14.10
423.25	447.25	1524.64	1.06		1.06	0.093		0.09	0.085	-25.80		-25.80	2.21		2.21	11.35	12.42
423.75	447.75	1524.13	1.17		1.17	0.100		0.10	0.092	-25.61		-25.61	2.35		2.35	11.75	12.77
424.25	448.25	1523.63	0.74		0.74	0.069		0.07	0.061	-25.87		-25.87	2.42		2.42	10.77	12.19
424.75	448.75	1523.12	0.61		0.61	0.051		0.05	0.043	-25.99		-25.99	2.15		2.15	12.01	14.24

PAD 15 VC3 Distal Site																	
Sample mid-depth	*Adjusted mid-depth (+24cm)*	*Year AD*	*C_{org} (%)*	*Rpt*	*Avg*	*N (%)*	*Rpt*	*Avg*	*Corrected N (%) (-0.008%)*	*$\delta^{13}C_{org}$ (‰)*	*Rpt*	*Avg*	*$\delta^{15}N$ (‰)*	*Rpt*	*Avg*	*C/N*	*Corrected C/N*
425.25	449.25	1522.62	0.76	0.77	0.77	0.064	0.06	0.06	0.056	-25.98	-25.61	-25.80	2.21	2.16	2.18	11.91	13.60
425.75	449.75	1522.12	0.78		0.78	0.074		0.07	0.066	-26.00		-26.00	2.45		2.45	10.62	11.91
426.25	450.25	1521.61	0.75		0.75	0.060		0.06	0.052	-25.80		-25.80	1.74		1.74	12.43	14.33
426.75	450.75	1521.11	1.05		1.05	0.085		0.08	0.077	-25.50		-25.50	2.24		2.24	12.36	13.65
427.25	451.25	1520.60	1.31		1.31	0.112		0.11	0.104	-25.09		-25.09	2.35		2.35	11.70	12.60
427.75	451.75	1520.10	1.34		1.34	0.115		0.12	0.107	-25.32		-25.32	2.21		2.21	11.59	12.46
428.25	452.25	1519.59	1.34		1.34	0.128		0.13	0.120	-26.02		-26.02	2.24		2.24	10.50	11.21
428.75	452.75	1519.09	1.07		1.07	0.102		0.10	0.094	-25.92		-25.92	2.24		2.24	10.54	11.44
429.25	453.25	1518.59	0.45		0.45	0.042		0.04	0.034	-26.16		-26.16	2.45		2.45	10.78	13.32
429.75	453.75	1518.08	0.77		0.77	0.059		0.06	0.051	-25.90		-25.90	2.35		2.35	12.90	14.90
430.25	454.25	1517.58	1.12		1.12	0.088		0.09	0.080	-25.77		-25.77	2.08		2.08	12.65	13.92
430.75	454.75	1517.07	1.30		1.30	0.113		0.11	0.105	-25.94		-25.94	2.29		2.29	11.54	12.41
431.25	455.25	1516.57	1.15		1.15	0.110		0.11	0.102	-25.85		-25.85	2.48		2.48	10.46	11.28
431.75	455.75	1516.06	0.61		0.61	0.060		0.06	0.052	-26.19		-26.19	2.34		2.34	10.22	11.79
432.25	456.25	1515.56	0.67		0.67	0.059		0.06	0.051	-26.07		-26.07	2.33		2.33	11.39	13.19
432.75	456.75	1515.05	0.60		0.60	0.053		0.05	0.045	-26.08		-26.08	1.83		1.83	11.31	13.34
433.25	457.25	1514.55	0.49		0.49	0.049		0.05	0.041	-26.23		-26.23	1.82		1.82	9.97	11.91
433.75	457.75	1514.05	0.83		0.83	0.072		0.07	0.064	-25.99		-25.99	2.13		2.13	11.45	12.87
434.25	458.25	1513.54	1.08		1.08	0.091		0.09	0.083	-25.63		-25.63	2.18		2.18	11.84	12.98
434.75	458.75	1513.04	1.22		1.22	0.105		0.11	0.097	-25.95		-25.95	2.16		2.16	11.62	12.58
435.25	459.25	1512.53	1.06	1.07	1.07	0.095	0.10	0.10	0.088	-26.98	-26.03	-26.50	2.05	2.06	2.06	11.06	12.06
435.75	459.75	1512.03	0.88		0.88	0.080		0.08	0.072	-26.09		-26.09	2.09		2.09	10.96	12.17
436.25	460.25	1511.52	0.77		0.77	0.069		0.07	0.061	-25.90		-25.90	2.17		2.17	11.11	12.56
436.75	460.75	1511.02	0.99		0.99	0.090		0.09	0.082	-25.42		-25.42	2.23		2.23	11.00	12.07
437.25	461.25	1510.51	0.62		0.62	0.058		0.06	0.050	-25.70		-25.70	2.41		2.41	10.56	12.24
437.75	461.75	1510.01	1.04		1.04	0.090		0.09	0.082	-26.05		-26.05	2.11		2.11	11.57	12.70
438.25	462.25	1509.51	1.29		1.29	0.110		0.11	0.102	-25.95		-25.95	2.16		2.16	11.74	12.66
438.75	462.75	1509.00	1.18		1.18	0.105		0.11	0.097	-26.85		-26.85	2.25		2.25	11.20	12.12
439.25	463.25	1508.50	0.99		0.99	0.090		0.09	0.082	-25.98		-25.98	2.30		2.30	11.02	12.10
439.75	463.75	1507.99	0.37		0.37	0.037		0.04	0.029	-26.15		-26.15	2.55		2.55	10.03	12.82
440.25	464.25	1507.49	0.49		0.49	0.048		0.05	0.040	-26.09		-26.09	2.32		2.32	10.29	12.37
440.75	464.75	1506.98	1.15		1.15	0.101		0.10	0.093	-25.92		-25.92	2.13		2.13	11.36	12.33
441.25	465.25	1506.48	1.18		1.18	0.108		0.11	0.100	-25.88		-25.88	2.05		2.05	10.94	11.82
441.75	465.75	1505.98	0.72		0.72	0.066		0.07	0.058	-25.90		-25.90	2.20		2.20	10.84	12.33
442.25	466.25	1505.47	0.38		0.38	0.038		0.04	0.030	-26.08		-26.08	2.07		2.07	10.05	12.76
442.75	466.75	1504.97	0.41		0.41	0.038		0.04	0.030	-26.17		-26.17	2.27		2.27	10.81	13.67
443.25	467.25	1504.46	0.56		0.56	0.049		0.05	0.041	-26.08		-26.08	2.08		2.08	11.50	13.75

PAD 15 VC3 Distal Site																	
Sample mid-depth	*Adjusted mid-depth (+24cm)*	*Year AD*	*C_{org} (%)*	*Rpt*	*Avg*	*N (%)*	*Rpt*	*Avg*	*Corrected N (%) (-0.008%)*	*$\delta^{13}C_{org}$ (‰)*	*Rpt*	*Avg*	*$\delta^{15}N$ (‰)*	*Rpt*	*Avg*	*C/N*	*Corrected C/N*
443.75	467.75	1503.96	0.61		0.61	0.058		0.06	0.050	-26.05		-26.05	2.39		2.39	10.62	12.33
444.25	468.25	1503.45	0.58		0.58	0.056		0.06	0.048	-26.05		-26.05	2.37		2.37	10.28	11.98
444.75	468.75	1502.95	0.49		0.49	0.046		0.05	0.038	-26.58		-26.58	2.08		2.08	10.62	12.85
445.25	469.25	1502.44	0.69	0.68	0.68	0.065	0.06	0.06	0.057	-26.02	-26.06	-26.04	2.13	2.25	2.19	10.57	12.06
445.75	469.75	1501.94	0.95		0.95	0.089		0.09	0.081	-26.03		-26.03	2.17		2.17	10.65	11.70
446.25	470.25	1501.44	1.23		1.23	0.122		0.12	0.114	-25.69		-25.69	2.26		2.26	10.07	10.78
446.75	470.75	1500.93	1.12		1.12	0.117		0.12	0.109	-26.11		-26.11	2.21		2.21	9.55	10.25
447.25	471.25	1500.43	0.53		0.53	0.056		0.06	0.048	-26.19		-26.19	2.49		2.49	9.43	11.00
447.75	471.75	1499.92	0.55		0.55	0.050		0.05	0.042	-26.13		-26.13	1.99		1.99	10.91	12.98
448.25	472.25	1499.42	0.86		0.86	0.083		0.08	0.075	-26.12		-26.12	2.30		2.30	10.28	11.37
448.75	472.75	1498.91	0.40		0.40	0.041		0.04	0.033	-26.02		-26.02	2.50		2.50	9.64	11.96
449.25	473.25	1498.41	0.52		0.52	0.050		0.05	0.042	-26.09		-26.09	2.50		2.50	10.37	12.35
449.75	473.75	1497.91	0.90		0.90	0.082		0.08	0.074	-26.06		-26.06	2.08		2.08	10.92	12.10
450.25	474.25	1497.40	0.85		0.85	0.088		0.09	0.080	-25.74		-25.74	2.25		2.25	9.69	10.65
450.75	474.75	1496.90	0.28		0.28	0.030		0.03	0.022	-30.19		-30.19	2.41		2.41	9.07	12.31
451.25	475.25	1496.39	0.67		0.67	0.060		0.06	0.052	-26.20		-26.20	2.21		2.21	11.02	12.70
451.75	475.75	1495.89	0.80		0.80	0.075		0.07	0.067	-26.12		-26.12	2.13		2.13	10.70	11.98
452.25	476.25	1495.38	0.92		0.92	0.087		0.09	0.079	-26.00		-26.00	2.37		2.37	10.51	11.57
452.75	476.75	1494.88	0.98		0.98	0.094		0.09	0.086	-26.05		-26.05	2.12		2.12	10.38	11.34
453.25	477.25	1494.37	0.70		0.70	0.070		0.07	0.062	-26.11		-26.11	2.11		2.11	10.07	11.37
453.75	477.75	1493.87	0.43		0.43	0.042		0.04	0.034	-26.57		-26.57	1.95		1.95	10.27	12.69
454.25	478.25	1493.37	1.10		1.10	0.104		0.10	0.096	-25.84		-25.84	2.07		2.07	10.59	11.47
454.75	478.75	1492.86	0.93	1.01	0.97	0.090	0.10	0.09	0.085	-26.10	-26.04	-26.07	2.15	2.35	2.25	10.50	11.49
455.25	479.25	1492.36	1.00		1.00	0.097		0.10	0.089	-26.00		-26.00	2.14		2.14	10.33	11.26
455.75	479.75	1491.85	1.27		1.27	0.112		0.11	0.104	-25.91		-25.91	2.17		2.17	11.30	12.16
456.25	480.25	1491.35	1.32		1.32	0.118		0.12	0.110	-25.28		-25.28	2.29		2.29	11.17	11.98
456.75	480.75	1490.84	1.32		1.32	0.104		0.10	0.096	-24.17		-24.17	2.06		2.06	12.65	13.70
457.25	481.25	1490.34	1.19		1.19	0.105		0.11	0.097	-25.54		-25.54	2.16		2.16	11.33	12.26
457.75	481.75	1489.84	1.23		1.23	0.111		0.11	0.103	-25.78		-25.78	2.45		2.45	11.13	12.00
458.25	482.25	1489.33	1.36		1.36	0.126		0.13	0.118	-26.03		-26.03	2.33		2.33	10.77	11.50
458.75	482.75	1488.83	1.31		1.31	0.125		0.13	0.117	-25.75		-25.75	2.29		2.29	10.47	11.18
459.25	483.25	1488.32	1.22		1.22	0.118		0.12	0.110	-25.92		-25.92	2.25		2.25	10.35	11.10
459.75	483.75	1487.82	0.80		0.80	0.071		0.07	0.063	-25.80		-25.80	2.52		2.52	11.16	12.57
460.25	484.25	1487.31	0.96		0.96	0.087		0.09	0.079	-25.76		-25.76	2.32		2.32	11.07	12.19
460.75	484.75	1486.81	1.15		1.15	0.099		0.10	0.091	-24.95		-24.95	2.62		2.62	11.64	12.67
461.25	485.25	1486.30	0.84		0.84	0.078		0.08	0.070	-26.00		-26.00	2.51		2.51	10.79	12.02
461.75	485.75	1485.80	0.64		0.64	0.059		0.06	0.051	-25.98		-25.98	2.77		2.77	10.86	12.57

PAD 15 VC3 Distal Site																	
Sample mid-depth	Adjusted mid-depth (+24cm)	Year AD	C_{org} (%)	Rpt	Avg	N (%)	Rpt	Avg	Corrected N (%) (-0.008%)	$\delta^{13}C_{org}$ (‰)	Rpt	Avg	$\delta^{15}N$ (‰)	Rpt	Avg	C/N	Corrected C/N
462.25	486.25	1485.30	0.78		0.78	0.068		0.07	0.060	-25.88		-25.88	2.34		2.34	11.49	13.02
462.75	486.75	1484.79	1.27		1.27	0.116		0.12	0.108	-26.00		-26.00	2.60		2.60	10.97	11.78
463.25	487.25	1484.29	1.39		1.39	0.134		0.13	0.126	-26.16		-26.16	2.45		2.45	10.35	11.01
463.75	487.75	1483.78	1.36		1.36	0.139		0.14	0.131	-26.09		-26.09	2.63		2.63	9.75	10.35
464.25	488.25	1483.28	0.71		0.71	0.073		0.07	0.065	-26.08		-26.08	2.81		2.81	9.69	10.89
464.75	488.75	1482.77	0.80		0.80	0.072		0.07	0.064	-26.03		-26.03	2.25		2.25	11.11	12.50
465.25	489.25	1482.27	1.27	1.30	1.29	0.108	0.11	0.11	0.099	-24.22	-23.89	-24.06	2.75	2.56	2.66	12.02	12.99
465.75	489.75	1481.76	1.27		1.27	0.113		0.11	0.105	-26.07		-26.07	2.51		2.51	11.18	12.03
466.25	490.25	1481.26	1.35		1.35	0.120		0.12	0.112	-26.22		-26.22	2.40		2.40	11.21	12.01
466.75	490.75	1480.76	1.43		1.43	0.127		0.13	0.119	-26.13		-26.13	2.40		2.40	11.24	11.99
467.25	491.25	1480.25	1.38		1.38	0.120		0.12	0.112	-25.96		-25.96	2.56		2.56	11.46	12.28
467.75	491.75	1479.75	1.39		1.39	0.128		0.13	0.120	-26.06		-26.06	2.53		2.53	10.80	11.52
468.25	492.25	1479.24	1.43		1.43	0.146		0.15	0.138	-26.12		-26.12	2.73		2.73	9.78	10.34
468.75	492.75	1478.74	1.31		1.31	0.135		0.13	0.127	-26.10		-26.10	2.59		2.59	9.73	10.35
469.25	493.25	1478.23	0.95		0.95	0.095		0.09	0.087	-26.08		-26.08	2.53		2.53	9.98	10.90
469.75	493.75	1477.73	0.93		0.93	0.086		0.09	0.078	-25.90		-25.90	2.43		2.43	10.92	12.05
470.25	494.25	1477.23	1.29		1.29	0.120		0.12	0.112	-25.70		-25.70	2.45		2.45	10.69	11.45
470.75	494.75	1476.72	1.37		1.37	0.134		0.13	0.126	-25.59		-25.59	2.41		2.41	10.20	10.85
471.25	495.25	1476.22	1.44		1.44	0.146		0.15	0.138	-26.11		-26.11	2.45		2.45	9.84	10.41
471.75	495.75	1475.71	1.33		1.33	0.137		0.14	0.129	-25.92		-25.92	2.47		2.47	9.72	10.32
472.25	496.25	1475.21	0.79		0.79	0.079		0.08	0.071	-25.98		-25.98	2.52		2.52	9.97	11.09
472.75	496.75	1474.70	0.62		0.62	0.062		0.06	0.054	-25.92		-25.92	2.46		2.46	10.11	11.62
473.25	497.25	1474.20	0.66		0.66	0.063		0.06	0.055	-25.95		-25.95	2.58		2.58	10.34	11.83
473.75	497.75	1473.69	1.10		1.10	0.111		0.11	0.103	-25.98		-25.98	2.49		2.49	9.92	10.69
474.25	498.25	1473.19	0.44		0.44	0.044		0.04	0.036	-26.06		-26.06	2.79		2.79	10.06	12.31
474.75	498.75	1472.69	0.87		0.87	0.081		0.08	0.073	-25.77		-25.77	2.64		2.64	10.80	11.99
475.25	499.25	1472.18	1.06	1.06	1.06	0.096	0.10	0.10	0.088	-25.70	-25.73	-25.71	2.31	2.39	2.35	10.99	11.99
475.75	499.75	1471.68	1.15		1.15	0.104		0.10	0.096	-25.63		-25.63	2.36		2.36	11.00	11.92
476.25	500.25	1471.17	1.20		1.20	0.109		0.11	0.101	-25.36		-25.36	2.25		2.25	10.99	11.86
476.75	500.75	1470.67	1.28		1.28	0.115		0.11	0.107	-25.48		-25.48	2.42		2.42	11.12	11.95
477.25	501.25	1470.16	1.32		1.32	0.116		0.12	0.108	-25.67		-25.67	2.47		2.47	11.37	12.22
477.75	501.75	1469.66	1.36		1.36	0.121		0.12	0.113	-25.73		-25.73	2.49		2.49	11.25	12.05
478.25	502.25	1469.16	1.33		1.33	0.122		0.12	0.114	-25.89		-25.89	2.33		2.33	10.96	11.73
478.75	502.75	1468.65	1.02		1.02	0.095		0.10	0.087	-25.88		-25.88	2.45		2.45	10.73	11.72
479.25	503.25	1468.15	0.87		0.87	0.080		0.08	0.072	-26.04		-26.04	2.46		2.46	10.92	12.14
479.75	503.75	1467.64	0.78		0.78	0.073		0.07	0.065	-25.91		-25.91	2.46		2.46	10.81	12.14
480.25	504.25	1467.14	0.80		0.80	0.075		0.07	0.067	-25.99		-25.99	2.42		2.42	10.71	12.00

PAD 15 VC3 Distal Site																	
Sample mid-depth	Adjusted mid-depth (+24cm)	Year AD	C_{org} (%)	Rpt	Avg	N (%)	Rpt	Avg	Corrected N (%) (-0.008%)	$\delta^{13}C_{org}$ (‰)	Rpt	Avg	$\delta^{15}N$ (‰)	Rpt	Avg	C/N	Corrected C/N
480.75	504.75	1466.63	0.62		0.62	0.058		0.06	0.050	-26.01		-26.01	2.87		2.87	10.64	12.33
481.25	505.25	1466.13	0.78		0.78	0.077		0.08	0.069	-25.93		-25.93	2.62		2.62	10.17	11.35
481.75	505.75	1465.62	1.11		1.11	0.110		0.11	0.102	-25.75		-25.75	2.44		2.44	10.09	10.88
482.25	506.25	1465.12	0.98		0.98	0.097		0.10	0.089	-25.73		-25.73	2.66		2.66	10.07	10.97
482.75	506.75	1464.62	0.97		0.97	0.097		0.10	0.089	-25.78		-25.78	2.47		2.47	10.01	10.91
483.25	507.25	1464.11	0.92		0.92	0.091		0.09	0.083	-25.99		-25.99	2.54		2.54	10.11	11.08
483.75	507.75	1463.61	1.11		1.11	0.110		0.11	0.102	-26.03		-26.03	2.38		2.38	10.09	10.88
484.25	508.25	1463.10	0.88		0.88	0.092		0.09	0.084	-26.04		-26.04	2.46		2.46	9.59	10.50
484.75	508.75	1462.60	0.60		0.60	0.058		0.06	0.050	-25.94		-25.94	2.40		2.40	10.40	12.06
485.25	509.25	1462.09	0.62	0.65	0.64	0.060	0.06	0.06	0.053	-26.04	-25.98	-26.01	1.94	2.17	2.06	10.45	12.02
485.75	509.75	1461.59	1.00		1.00	0.091		0.09	0.083	-25.76		-25.76	2.39		2.39	11.00	12.06
486.25	510.25	1461.08	1.06		1.06	0.101		0.10	0.093	-25.72		-25.72	2.33		2.33	10.56	11.48
486.75	510.75	1460.58	0.74		0.74	0.072		0.07	0.064	-25.91		-25.91	2.65		2.65	10.21	11.47
487.25	511.25	1460.08	0.86		0.86	0.080		0.08	0.072	-26.05		-26.05	2.39		2.39	10.72	11.91
487.75	511.75	1459.57	0.58		0.58	0.056		0.06	0.048	-25.91		-25.91	2.59		2.59	10.44	12.18
488.25	512.25	1459.07	0.65		0.65	0.061		0.06	0.053	-25.91		-25.91	2.41		2.41	10.60	12.20
488.75	512.75	1458.56	0.56		0.56	0.054		0.05	0.046	-25.96		-25.96	2.55		2.55	10.46	12.29
489.25	513.25	1458.06	0.59		0.59	0.057		0.06	0.049	-25.91		-25.91	2.55		2.55	10.37	12.05
489.75	513.75	1457.55	0.51		0.51	0.049		0.05	0.041	-25.79		-25.79	2.56		2.56	10.35	12.37
490.25	514.25	1457.05	0.49		0.49	0.047		0.05	0.039	-25.85		-25.85	2.34		2.34	10.40	12.54
490.75	514.75	1456.55	0.45		0.45	0.044		0.04	0.036	-25.86		-25.86	2.55		2.55	10.28	12.59
491.25	515.25	1456.04	0.45		0.45	0.044		0.04	0.036	-25.81		-25.81	2.55		2.55	10.20	12.44
491.75	515.75	1455.54	0.44		0.44	0.044		0.04	0.036	-25.93		-25.93	2.60		2.60	9.90	12.07
492.25	516.25	1455.03	0.46		0.46	0.046		0.05	0.038	-25.97		-25.97	2.51		2.51	10.19	12.36
492.75	516.75	1454.53	0.52		0.52	0.049		0.05	0.041	-25.90		-25.90	2.38		2.38	10.51	12.56
493.25	517.25	1454.02	0.66		0.66	0.062		0.06	0.054	-25.97		-25.97	2.60		2.60	10.74	12.33
493.75	517.75	1453.52	0.63		0.63	0.059		0.06	0.051	-25.85		-25.85	2.16		2.16	10.74	12.42
494.25	518.25	1453.01	0.84		0.84	0.073		0.07	0.065	-24.82		-24.82	2.26		2.26	11.45	12.85
494.75	518.75	1452.51	0.92		0.92	0.082		0.08	0.074	-26.01		-26.01	2.23		2.23	11.20	12.41
495.25	519.25	1452.01	1.04		1.04	0.089		0.09	0.081	-24.98		-24.98	2.43		2.43	11.60	12.73
495.75	519.75	1451.50	0.97		0.97	0.085		0.08	0.077	-25.82		-25.82	2.08		2.08	11.45	12.64
496.25	520.25	1451.00	0.93		0.93	0.083		0.08	0.075	-25.85		-25.85	2.04		2.04	11.24	12.44
496.75	520.75	1450.49	1.03		1.03	0.080		0.08	0.072	-23.56		-23.56	2.27		2.27	12.85	14.28
497.25	521.25	1449.99	1.01		1.01	0.088		0.09	0.080	-25.72		-25.72	2.18		2.18	11.49	12.64
497.75	521.75	1449.48	1.15		1.15	0.079		0.08	0.071	-20.35		-20.35	2.06		2.06	14.54	16.17
498.25	522.25	1448.98	1.26		1.26	0.084		0.08	0.076	-19.94		-19.94	2.15		2.15	15.06	16.65
498.75	522.75	1448.48	1.64		1.64	0.087		0.09	0.079	-15.74		-15.74	2.27		2.27	18.77	20.66

PAD 15 VC3 Distal Site																	
Sample mid-depth	*Adjusted mid-depth (+24cm)*	*Year AD*	*C_{org} (%)*	*Rpt*	*Avg*	*N (%)*	*Rpt*	*Avg*	*Corrected N (%) (-0.008%)*	*$\delta^{13}C_{org}$ (‰)*	*Rpt*	*Avg*	*$\delta^{15}N$ (‰)*	*Rpt*	*Avg*	*C/N*	*Corrected C/N*
499.25	523.25	1447.97	1.02		1.02	0.093		0.09	0.085	-25.97		-25.97	2.19		2.19	10.97	12.00
499.75	523.75	1447.47	1.03		1.03	0.092		0.09	0.084	-25.99		-25.99	2.35		2.35	11.15	12.21
500.25	524.25	1446.96	0.99		0.99	0.091		0.09	0.083	-26.14		-26.14	1.84		1.84	10.96	12.02
500.75	524.75	1446.46	0.86		0.86	0.081		0.08	0.073	-26.02		-26.02	2.25		2.25	10.67	11.84
501.25	525.25	1445.95	1.01		1.01	0.092		0.09	0.084	-26.10		-26.10	2.19		2.19	10.96	12.01
501.75	525.75	1445.45	0.95		0.95	0.083		0.08	0.075	-25.91		-25.91	1.94		1.94	11.33	12.53
502.25	526.25	1444.94	0.93		0.93	0.085		0.09	0.077	-25.94		-25.94	2.30		2.30	10.86	11.98
502.75	526.75	1444.44	1.31		1.31	0.088		0.09	0.080	-19.02		-19.02	2.51		2.51	14.95	16.45
503.25	527.25	1443.94	1.30		1.30	0.089		0.09	0.081	-19.36		-19.36	2.51		2.51	14.66	16.11
503.75	527.75	1443.43	1.30		1.30	0.087		0.09	0.079	-19.29		-19.29	2.21		2.21	14.88	16.39
504.25	528.25	1442.93	1.01		1.01	0.096		0.10	0.088	-26.00		-26.00	2.16		2.16	10.57	11.53
504.75	528.75	1442.42	1.04		1.04	0.097		0.10	0.089	-25.44		-25.44	2.30		2.30	10.72	11.67
505.25	529.25	1441.92	1.00	1.00	1.00	0.097	0.10	0.10	0.090	-25.85	-25.93	-25.89	2.26	2.32	2.29	10.24	11.15
505.75	529.75	1441.41	1.02		1.02	0.094		0.09	0.086	-25.36		-25.36	2.24		2.24	10.92	11.94
506.25	530.25	1440.91	1.10		1.10	0.103		0.10	0.095	-26.07		-26.07	2.47		2.47	10.72	11.62
506.75	530.75	1440.41	1.09		1.09	0.097		0.10	0.089	-25.13		-25.13	2.37		2.37	11.24	12.26
507.25	531.25	1439.90	1.15		1.15	0.098		0.10	0.090	-23.43		-23.43	2.16		2.16	11.83	12.89
507.75	531.75	1439.40	1.37		1.37	0.098		0.10	0.090	-19.89		-19.89	2.30		2.30	14.01	15.26
508.25	532.25	1438.89	1.57		1.57	0.094		0.09	0.086	-18.18		-18.18	2.44		2.44	16.60	18.14
508.75	532.75	1438.39	1.27		1.27	0.094		0.09	0.086	-21.52		-21.52	2.25		2.25	13.49	14.74
509.25	533.25	1437.88	1.05		1.05	0.095		0.09	0.087	-26.57		-26.57	2.15		2.15	11.05	12.07
509.75	533.75	1437.38	0.99		0.99	0.091		0.09	0.083	-26.39		-26.39	2.42		2.42	10.91	11.96
510.25	534.25	1436.87	0.90		0.90	0.083		0.08	0.075	-26.65		-26.65	2.54		2.54	10.92	12.09
510.75	534.75	1436.37	0.78		0.78	0.073		0.07	0.065	-26.76		-26.76	2.45		2.45	10.62	11.93
511.25	535.25	1435.87	0.72		0.72	0.070		0.07	0.062	-26.89		-26.89	2.55		2.55	10.22	11.53
511.75	535.75	1435.36	0.50		0.50	0.051		0.05	0.043	-26.90		-26.90	2.76		2.76	9.86	11.69
512.25	536.25	1434.86	0.50		0.50	0.050		0.05	0.042	-26.95		-26.95	2.71		2.71	9.89	11.75
512.75	536.75	1434.35	0.61		0.61	0.061		0.06	0.053	-26.07		-26.07	2.34		2.34	9.91	11.40
513.25	537.25	1433.85	0.64		0.64	0.063		0.06	0.055	-26.09		-26.09	2.25		2.25	10.15	11.62
513.75	537.75	1433.34	0.49		0.49	0.052		0.05	0.044	-26.05		-26.05	2.70		2.70	9.51	11.24
514.25	538.25	1432.84	0.72		0.72	0.074		0.07	0.066	-26.07		-26.07	2.38		2.38	9.69	10.86
514.75	538.75	1432.33	0.94		0.94	0.096		0.10	0.088	-26.08		-26.08	2.40		2.40	9.86	10.76
515.25	539.25	1431.83	0.92	0.93	0.92	0.092	0.09	0.09	0.084	-26.00	-26.06	-26.03	2.51	2.39	2.45	10.08	11.04
515.75	539.75	1431.33	0.92		0.92	0.087		0.09	0.079	-25.17		-25.17	2.33		2.33	10.60	11.68
516.25	540.25	1430.82	x		x	x		x		x		x	x		x	x	
516.75	540.75	1430.32	1.15		1.15	0.097		0.10	0.089	-23.42		-23.42	2.27		2.27	11.80	12.86
517.25	541.25	1429.81	1.41		1.41	0.095		0.09	0.087	-19.72		-19.72	2.21		2.21	14.88	16.25

PAD 15 VC3 Distal Site																	
Sample mid-depth	*Adjusted mid-depth (+24cm)*	*Year AD*	*C_{org} (%)*	*Rpt*	*Avg*	*N (%)*	*Rpt*	*Avg*	*Corrected N (%) (-0.008%)*	*$\delta^{13}C_{org}$ (‰)*	*Rpt*	*Avg*	*$\delta^{15}N$ (‰)*	*Rpt*	*Avg*	*C/N*	*Corrected C/N*
517.75	541.75	1429.31	1.09		1.09	0.100		0.10	0.092	-26.26		-26.26	2.28		2.28	10.89	11.83
518.25	542.25	1428.80	1.07		1.07	0.101		0.10	0.093	-26.29		-26.29	2.14		2.14	10.62	11.53
518.75	542.75	1428.30	0.87		0.87	0.083		0.08	0.075	-26.26		-26.26	2.12		2.12	10.53	11.65
519.25	543.25	1427.80	0.81		0.81	0.076		0.08	0.068	-26.18		-26.18	2.21		2.21	10.71	11.97
519.75	543.75	1427.29	0.77		0.77	0.074		0.07	0.066	-26.19		-26.19	2.33		2.33	10.38	11.63
520.25	544.25	1426.79	0.76		0.76	0.071		0.07	0.063	-26.17		-26.17	2.53		2.53	10.71	12.09
520.75	544.75	1426.28	0.81		0.81	0.077		0.08	0.069	-26.12		-26.12	2.54		2.54	10.59	11.82
521.25	545.25	1425.78	0.96		0.96	0.089		0.09	0.081	-25.78		-25.78	2.38		2.38	10.84	11.91
521.75	545.75	1425.27	0.92		0.92	0.083		0.08	0.075	-25.46		-25.46	2.89		2.89	11.09	12.27
522.25	546.25	1424.77	0.76		0.76	0.073		0.07	0.065	-26.05		-26.05	2.54		2.54	10.49	11.78
522.75	546.75	1424.26	0.75		0.75	0.074		0.07	0.066	-26.28		-26.28	2.62		2.62	10.20	11.43
523.25	547.25	1423.76	0.66		0.66	0.066		0.07	0.058	-26.23		-26.23	2.48		2.48	10.05	11.44
523.75	547.75	1423.26	0.68		0.68	0.068		0.07	0.060	-26.24		-26.24	2.60		2.60	9.97	11.29
524.25	548.25	1422.75	0.66		0.66	0.066		0.07	0.058	-26.37		-26.37	2.20		2.20	10.09	11.49
524.75	548.75	1422.25	0.59		0.59	0.062		0.06	0.054	-26.24		-26.24	2.63		2.63	9.57	10.99
525.25	549.25	1421.74	0.67	0.68	0.67	0.063	0.06	0.06	0.056	-26.14	-26.33	-26.24	2.81	2.06	2.44	10.57	12.09
525.75	549.75	1421.24	0.69		0.69	0.067		0.07	0.059	-26.20		-26.20	2.31		2.31	10.30	11.70
526.25	550.25	1420.73	0.82		0.82	0.081		0.08	0.073	-26.10		-26.10	2.12		2.12	10.08	11.19
526.75	550.75	1420.23	0.89		0.89	0.089		0.09	0.081	-26.02		-26.02	2.24		2.24	10.05	11.05
527.25	551.25	1419.73	1.08		1.08	0.108		0.11	0.100	-25.98		-25.98	2.34		2.34	10.00	10.80
527.75	551.75	1419.22	1.19		1.19	0.121		0.12	0.113	-25.85		-25.85	2.38		2.38	9.84	10.53
528.25	552.25	1418.72	1.28		1.28	0.129		0.13	0.121	-25.91		-25.91	2.43		2.43	9.95	10.61
528.75	552.75	1418.21	1.29		1.29	0.127		0.13	0.119	-25.79		-25.79	2.44		2.44	10.13	10.81
529.25	553.25	1417.71	0.97		0.97	0.095		0.09	0.087	-26.14		-26.14	2.40		2.40	10.21	11.15